30982

LAPORAN AKHIR PROJEK PENYELIDIKAN JANGKA PANJANG (IRPA R&D)

(Project Number : 08-02-05-2185 EA006)

TAJUK PROJEK

PROCESS FOR HIGH VALUE PRODUCTS FROM PYROLYSIS OF SCRAP TIRES USING FLUIDIZED BED

NAMA PENYELIDIK

DR RIDZUAN ZAKARIA

DR MOHAMAD ZAILANI ABU BAKAR

PROF ABDUL RAHMAN MOHAMED

LAMPIRAN-LAMPIRAN
DAN KEPUTUSAN-KEPUTUSAN
DARIPADA PENYELIDIKAN

The 17th Symposium of Malaysian Chemical Engineers
(SOMChE 2003)

PROCEEDINGS:
SOMChE 2003

THEME:

Roles of Chemical Engineers for Sustainability of Small Medium Industries (SMI)

The Copthorne Orchid Hotel
Tanjung Bungah, Penang, Malaysia

29 – 30th December 2003

Jointly Organised:

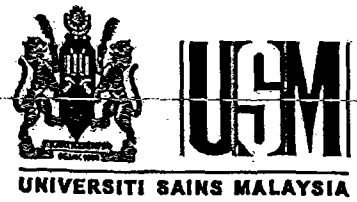

School of Chemical Engineering
Engineering Campus
Universiti Sains Malaysia

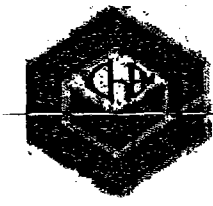

Institution of Chemical
Engineers Malaysia

PROCEEDINGS

The 17th Symposium of Malaysian Chemical Engineers

SOMChE 2003

"Role of Chemical Engineers for Sustainability of Small Medium Industries (SMI)"

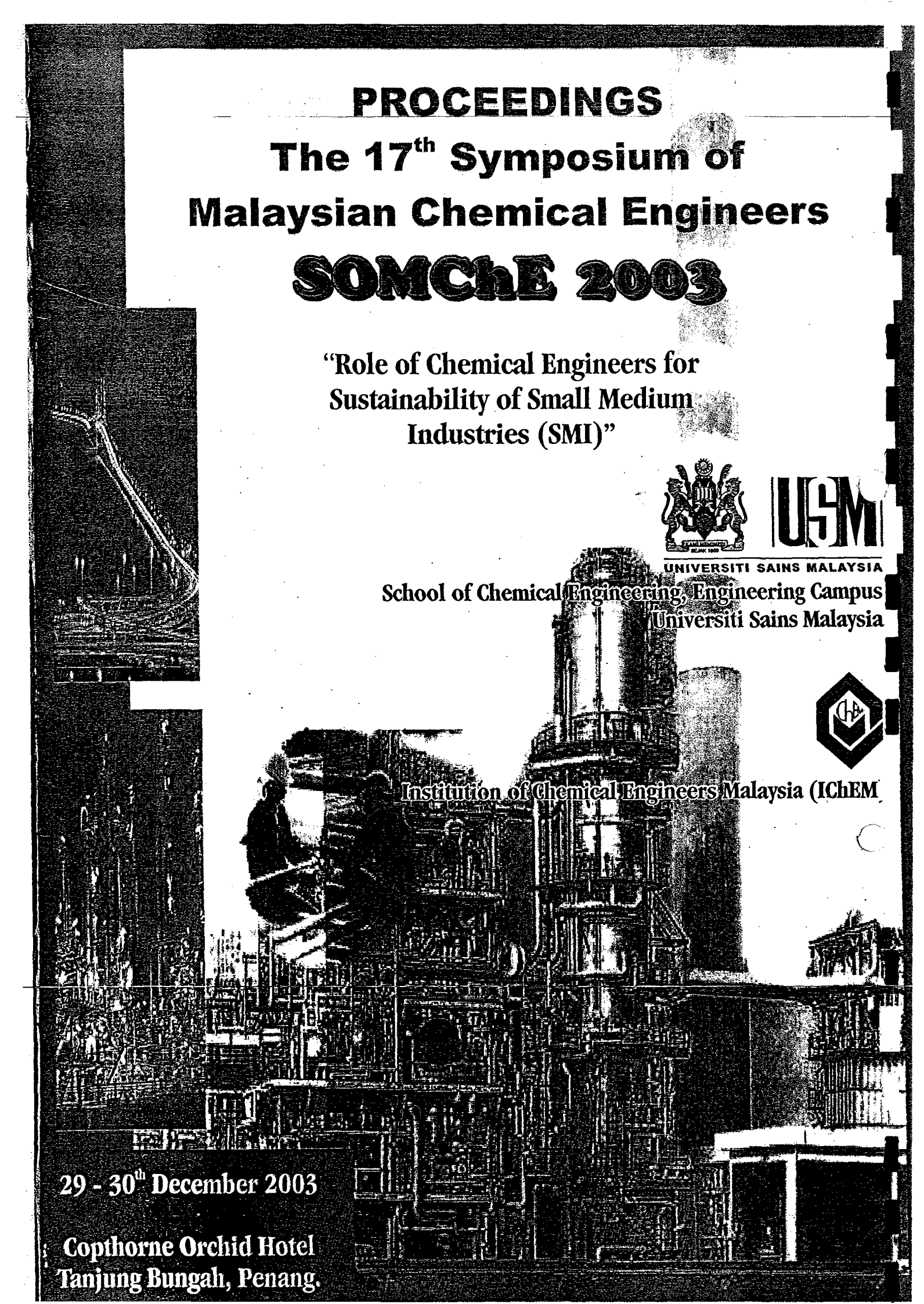

UNIVERSITI SAINS MALAYSIA

School of Chemical Engineering, Engineering Campus
Universiti Sains Malaysia

Institution of Chemical Engineers Malaysia (IChEM)

29 - 30th December 2003

Copthorne Orchid Hotel
Tanjung Bungah, Penang.

A Review on Pyrolysis of Scrap Tire.

Nurul Fakhri Osman[1], Dr. C. Srinivasakannan[1], Dr. Mohamad Zailani Abu Bakar[1], Dr. Ridzuan Zakaria[1], and Dr. Abdul Rahman Bin Mohamed[1]

[1]School of Chemical Engineering, Engineering Campus, University Sains Malaysia, 14300 Nibong Tebal Seberang Perai Selatan, Penang, Malaysia.

ABSTRACT

The disposal of scrap tires is a growing problem throughout the world. Globally about 17 million tires are discarded every year and accumulated over the years in different countries. The need for the special treatment method and disposal for the tire waste has been recognized globally. Along the years, different alternatives for tire recycling such as retreading, reclaiming, incineration, grinding etc., have been used. However all these have significant drawbacks and limitations [1,4]. The negative environmental impact caused by disposal of scrap tires (non biodegradable) in landfills is understood and European union landfill directive bans land-filling tires effective from 2003. Therefore, pyrolysis method has been introduced. Pyrolysis is an established process method, but its use in the tire pyrolysis is in laboratory scale. This process presents an alternative to scrap tire disposal and it can result in the recovery of useful products in an environmentally friendly manner. This process could be carried out in a fluidized bed, shaft furnace, an extruder and a rotary kiln etc. Each type of pyrolysis has the advantages and disadvantages, depends on the material used to pyrolysed. The products recovered by a typical pyrolysis process are usually 33-38 wt% pyrolytic char, 38-55% wt% oil and 10-30 wt % gas fraction [1]. Pyrolytic oil contains many valuable hydrocarbons such as limonene, benzene, toluene, xylene etc, which can be source of chemical feedstock. Moreover the high calorific value of ~43 MJ/kg, the oil can be used as fuel [4]. The pyrolysis gases are composed of hydrogen, methane, and other hydrocarbons, which have sufficient energy value. The solid carbon char has potential to be converted in to activated carbon or directly as a low-grade carbon black. Number of works on pyrolysis of tire waste reported in literature address to characterization and the effect of operating variables on product distribution. The effect of the operating variables such as the temperature, the heating rate, the residence time, and the particle size on the product distribution and the quality of the product on its optimum conditions were reported. The present work envisages to thoroughly review the literature to identify the area that require for further research.

1.0 INTRODUCTION

Pyrolysis involves the decomposition of organic wastes at high temperature in absence of air by using inert gas such as Nitrogen or Helium. This process presents an alternative to scrap tire disposal and it can result in the recovery of useful products in environmentally manner. Commercially, pyrolysis process can be done in a fluidized bed, shaft furnace, an extruder and a rotary klin, etc.

Tires are complex mixtures of very different materials, which include several rubbers, carbon black, steel cord, and other organic and inorganic minor components. Tires are composed of very different components (rubbers, carbon blacks, steel, fillers, etc.), which additionally are heterogeneously distributed along the tires.

1.1 Problems in Tire Disposal.

The complex nature of tires makes it difficult to recycle them. One one hand, the main component of tires, rubber, is a chemically cross link polymer and therefore is neither fusible nor soluble and consequently cannot be remolded into other shapes without serious degradation. Land filing of tires is declining as a disposal option since tires do not degrade easily in landfills, they are bulky, taking up landfill space and preventing waste compaction. Open dumping may result in accidental fires with high pollution emissions and tires can be breeding ground for insects and a home for vermin. Alternative waste management options to landfilling and open dumping have included, tire retreading, crumbing to produce rubber for applications such as carpets, sports surfaces and children's' playgrounds. Incineration of tires with energy recovery is also a growing option since it utilizes the high calorific value of tires [19]. Along the years, different alternatives for tire recycling, such as retreading, reclaiming, incineration, grinding, etc. have been used. However, all of them have significant drawbacks and/or limitations [1,4].

In the past several laboratory, pilot plant and even commercial attempts have been made to economical units for pyrolysis of tires (e.g. Kobe Steel in Japan, Tosco in USA, Tyrolysis in However the economics of the process were not cost-effective. At present, economics is not the considered, but the rapid increase in discarded tyre legislation that is being produced in many [1,21]. For instance, the new European Union Landfill Directive bands landfilling whole effective date is 2003.Therefore, an advance in the knowledge of the characteristics and potential the products obtained in tire pyrolysis is, at present, of the most interest [20].

1.2 Potential of Yield Products.

Pyrolysis of scrap tire produces an oil, char and gaseous product. The oil can be used directly as fu since it has properties similar to apetroleum derived light fuel oil or gas oil. The char can be used as low-grade carbon or as a solid fuel. However, the char may be upgraded using either steam or carbon dioxide gasification to produce an activated carbon. The activated carbon has a high surface area of over $600m^2/g$ and maybe acid washed to reduce the ash content. The high concentrations of aromatic hydrocarbons present in the tire oils have been suggested as a potential high value products, which could offset the costs of, tire disposal. For example, xylenes are regarded as major industrial chemicals which have applications in the plastics industry [19]. o-Xylene is used to produced phthalic anhydride which is used to produce plasticisers, dyes and pigments, m-xylene derivatives have applications in the resin and fibre industries and p-xylene derivatives are used in the production of polyester fibres [19]. Toluene has a wide range of applications as a chemical feedstock and is used for example in the production of pesticides, dyestuffs, surfactants and solvents. Styrene is one of the most important building blocks used in the production of plastic materials and is also used to make synthetic rubber and other polymers [17]. Also, indene is regarded as being of particular technical importance since it is used to produce indene/coumarone resins which find extensive application, especially in the production of adhesives, as reinforces and tackifiers in the production of commercial rubber products, and in paint manufacture [17].

1.3 Characteristics of Waste Tire

Table 1.0
The main component of the tire section

Organic Compounds		Inorganic Compound	
Volatile (mainly rubbers)	Nonvolatile (mainly carbon blacks)	Steel	Others
58.8	27.7	9.6	3.9

Table 1.0 shows components of the tire section (%) obtained by Isabel et al [20] by using cryogenic pieces of 2 – 3cm wide (175g) of a commercial car tire Firestone 155R13, F-570.From the table above one can clearly see that most of the tire composition are organic compound. This organic compound can be divided into two groups, volatile (mainly rubber) and nonvolatile (mainly carbon blacks). The major component in tire is volatile organic compounds, 58.8wt% followed by nonvolatile organic compounds (mainly Carbon Blacks), 27.7 wt%. Inorganic compounds of the tire contain in a small amount of steel (9.6%) and others 3.9%.

Table 2.0
Typical composition of the scrap tires feedstock rubber

Elemental composition (%)	**Proximate analysis (%)**	**Gross calorific value ($MJkg^{-1}$)**
C (86.4)	Volatiles (62.2) Fixed Carbon (29.4) Ash (7.1) Moisture (1.3)	40.0
H (8.0)		
N (0.5)		
S (1.7)		
O (3.4)		
Ash (2.4)		

Table 2.0 shows the proximate and ultimate analysis on steel and fabric free basis, and the calorific value of tire tread obtained by Williams et al. [19]. The tire sample used in the experiment was shredded into

passenger car tires in narrow strips approximately 3cm x 1.5cm thick and between 50 to 150cm maximum dimension retaining both steel and fabric cords were kept in dry conditions prior to pyrolysis [19]. From the table above, the major element in tire is Carbon, followed by Hydrogen, Nitrogen, Sulphur, Oxygen and ash. Volatile compound is a major component in proximate analysis (62.2%) and higher than volatile compound obtained by Isabel et al. [19]. The gross calorific value for tire obtained by Williams et al. [19] is 40.0 $MJkg^{-1}$.

2.0 RESULTS AND DISCUSSIONS

2.1 Char

Table 3.0
A review on the Char yield obtained by other researchers

Author	Condition Temperature	Heating rate	Residence Time	% Char Remarks	Equipment used
Kawakimi et al. [8]	540°C - 750°C	–	–	Char yield increased from 38wt% to 40wt% as the temperature increased.	Rotary Klin reactor
Teng et al.[2]	–			Small influence of temperature in char yield.	
Wlliams et al.[6]	420°C – 600°C	5$Kmin^{-1}$	Shorter gas residence.	Decreased char yield from 56.6wt% to 40.2wt% as the temperature increased.	Smaller scale fixed bed reactor with shorter gas residence hot zone.
		20K/min – 80K/min		The char yield decreased as the heating rate increased	
Kaminsky and Sinh [7]	640°C – 840°C	–	–	Increased of char yield as the temperature increased.	Fluidised bed pyrolysis
Wlliams et al [19]	450°C – 600°C		120s	Char nearly constant at mean value 37.8wt% as the temperature increased.	Static bed reactor
TGA analyzer [19]	500°C - 900°C	450°C/min	–	Char yield decreased from 40wt% to 36wt% as the temperature increased.	TGA analyzer in Helium as an inert gas.

Pyrolysis of scrap tire produced a solid product, char composed of Carbon, Nitrogen, Hydrogen, Sulphur and ash as major components. From the table above it has been observed that some of the researchers found that the yield of char remains constant or only a small change with the pyrolysis parameters. For example, Williams et al.[19] reported that the yield of char remains constant at 37.8wt%, while Teng et al.[11] reported only a small influence of temperature yield of the char. Kawakimi et al. [8] obtained char yield between 38wt% to 40wt% in the temperature range of 540°C - 750°C by using rotary klin.

On the other hand, some of the researchers found that the yield of char decreased with the the pyrolysis parameters i.e. temperature, heating rate, residence time and etc. Williams smaller scale fixed bed reactor with shorter gas residence time in hot zone found a signific in char yield from 56.6wt% to 40.2wt% as the temperature of pyrolysis was in 420°C - 600°C at constant heating rate, 5Kmin^{-1}. A decreased of char yield also obser heating rate increased from 20Kmin^{-1}- 80Kmin^{-1}.

In commercial scale, i.e. 1 tonne of batch pyrolysis of tires has been done. The yield of ch from 59.4wt% at 59.4°C to 46.8wt% at 950°C, final temperature of pyrolysis [13]. But, K Sinh [7] using fliuidised bed pyrolysis unit, found an increased in char yield as the f temperature increased from 640°C to 840°C. Pyrolysis by using TGA analyzer [19] showe decreased from 40wt% to 36wt% when the temperature increased from 500°C to 900°C at 30°C/min in Helium. Williams et al. [19] suggests that the decreased of char yield was increasing devotilisation of solid hydrocarbon in char and partial gasification of char for temperature maybe because of the long residence time of oil hydrocarbons in the hot zone [19

2.2 Oil Yield

2.2.1 High oil yield.

Table 3.0
A review on the high oil yield obtained by other researchers

Author	Temperature	Residence Time	Equipment	Results
Williams et al. [19]	450°C – 600°C	120 s	Static bed reactor	Maximum y 58wt% at T after that d with in temperature.
Roy and Unsworth [5]	415°C	–	Vacuum pyrolysis to pyrolysed tyres.	Maximum oil 56.6wt%.
Kawakimi [8]	540°C – 640°C	–	Rotary Klin Reactor	Obtained m oil yield at 53
Williams et al. [6]	–	–	Small scale 50g, Nitrogen purge bed reactor	Maximum O obtained = 58
Lucchesi and Mashio [10]	500°C	–	Continously-fed vertical reactor woth rotating grate purged by a counter current of Nitrogen.	Obtained m 47wt% of oil y

2.2.2 Low Oil Yield

Table 5.0
A review on the low oil yield obtained by other researchers

Author	Temperature	Equipment	Results
Kaminsky and Sinh [7]	640°C – 840°C	Fluidised bed reactor	Obtained oil yi 40wt% at T= 640 and 27wt% at t 840°C.
Colin [11]	740°C	Rotary klin reactor	Obtained maximu 23wt% oil.
Williams et al. [13]		Large scale 1 tonne batch tire pyrolysis unit	Obtained maximu oil yield at 32.5wt%

From Table 4.0 and 5.0 above, it has been observed that 5 research obtained high oil yield. Will [19] has reached maximum 58.2wt% of oil yield at T = 475°C by using Nitrogen purge static b .Roy and Unsworth [5] reported maximum oil yield, 56.6wt% at T = 415°C in vacuum pyro Williams et al. [19] obtained maximum oil yield at 58.8wt% by using small scale Nitrogen p

static bed reactor while Lucchesi and Mashio[10] obtained 47wt% at T = 500°C by using continuously-fed vertical reactor with rotating grate purged by counter-current Nitrogen gas.

Three authors reported that they obtained a low oil yield. Kaminsky and Sinh [7] reported that they obtained maximum oil yield 40wt% at temperature 640°C and decreased to 27wt% at temperature 840°C (final temperature) in Fluidized bed reactor. Colin [11] reported 23wt% oil yield by using rotary klin reactor operated at 740°C. Finally, Williams et al. [13] obtained oil yield of maximum 32.5wt% for large-scale 1 tonne batch tire pyrolysis unit.

Williams et al. [19] mentioned that higher heating rates with short hot zone residence time and rapid quenching of the products regarded as favoring the formation of liquid products. This statement is supported other authors findings. Roy and Unsworth [5] obtained 56.6wt% of oil yield by rapid removal of the gasses by the vacuum process reactor.Cypress and Bettens [12] increased the removal pyrolysis vapors from scrap tires from secondary hot zone by increasing the flow of Nitrogen carrier. The result shoes that by reducing the secondary reaction, the yield of oil increased.

The decreased in oil yield with increasing temperature and corresponding increased in gas yield observed by Williams et al. [19]. Other workers, such as, Williams et al. [6,13], Kaminsky and Sinh, Luches and Mashio [10] all found significant decreased in oil yield and increased of gas yield as the temperature of pyrolysis is increased.

2.2.3 Polycyclic Aromatic Hydrocarbon

Williams et al. [19] has reported the composition of polycyclic aromatic hydrocarbon (PAH) and lighter aromatic hydrocarbons determine in pyrolytic oil. The composition of PAH obtained by Williams et al. [19] is showed at Table 6.0

Table 6.0
Concentration of polycyclic aromatic hydrocarbons (PAH) in tire derived pyrolysis oils in relation to pyrolysis temperature (ppm)

PAH	Tire pyrolysis temperature (°C)					
	450	475	500	525	560	600
Naphtalene	465	420	725	1115	665	1630
2-Methylnaphtalene	650	570	730	770	1005	2365
1-Methylnaphtalene	460	490	625	645	895	1570
Biphenyl	1030	1040	1630	885	1320	3000
1-Ethylnaphtalene	430	510	690	830	745	1335
2,6-Dimethylnaphtalene	565	565	885	755	995	1990
1,7-Dimethylnaphtalene	550	440	365	1020	700	560
1,6-Dimethylnaphtalene	275	600	595	715	485	1085
1,5-Dimethylnaphtalene	190	305	375	1440	635	880
1,2-Dimethylnaphtalene	770	405	600	450	460	1385
Acenapthalene	560	580	635	700	620	1070
Trimethylnaphtalene	765	470	670	1050	605	825
Trimethylnaphtalene	665	515	425	330	830	1570
Trimethylnaphtalene	155	175	220	695	430	710
Fluorene	280	210	325	290	295	605
Methylfluorene	65	180	135	90	240	585
2-Methylfluorene	115	245	220	175	335	745
1-Methylfluorene	260	340	370	310	450	555
Methylfluorene	135	200	170	320	195	280
Phenanthrene	95	230	200	125	195	315
Anthracene	85	160	125	135	225	295
Dimethlfluorene	215	425	425	165	320	465
2-Methylphenanthrene	595	495	315	470	815	1240
2-Methylanthracene	455	640	500	1010	720	1140
4-Methylphenanthrene	355	200	140	275	605	730

1-Methylphenanthrene	595	890	470	585	600	555
Dimethlphenanthrene	745	1200	520	650	760	1290
2,7-Dimethlphenanthrene	1255	1300	1740	525	1060	1075
Dimethlphenanthrene	105	120	455	350	1260	540
Fluoranthrene	120	325	325	355	790	1100
Dimethlphenanthrene	730	<5	490	445	1490	1210
Dimethlphenanthrene	440	385	305	615	5195	370
Pyrene	530	105	120	425	225	115
Trimethylphenanthrene	530	400	600	470	520	940
Tetramethlyphenanthrene	30	35	65	35	30	150
Chrysene	30	15	35	<5	30	60
Total %	1.53	1.52	1.72	192	2.67	3.43

The results obtained by Williams et al. [19] showed that the influence of pyrolysis temp an increased on the aromatic content of the oils as the temperature increased. But, the content of the oil is decreased as the temperature increased. It is observed from the table PAH content of the oils were found increased from 1.5wt% to 3.5wt% of the total o temperature increase from 450 ° C to 600 ° C [19]. Williams et.al [19] also obtain compounds such as methylfluorenes, tri-and tetra-methylphenanthrene and chrys identified in significant concentrations. Table 6.0 also indicated that the alkylated c increased with temperature. Other authors support this result. For example, Williams a [21] using a batch pyrolysis reactor with post-pyrolysis heating of the tire vapors increased of PAH content of tire derived oil from 1.4wt % at 500°C to 10wt% at 72 pyrolysis temperature. Cypers and Bettens [12] also found the similar trends as Wil Taylor [21]. Williams et al. [19] mentioned that the increased of residence time of vapors in the hot zone of reactor will lead to increased secondary reaction such as the of PAH. Williams et al. [19] suggested that a Diels – Alder reaction mechanism respon the increased in aromatic content with temperature.

2.2.4 Volatile Hydrocarbons in Pyrolytic Oils

The derived pyrolysis oil also contains light aromatic hydrocarbons as reported by Williams et a

Table7.0
Concentration of light aromatic hydrocarbons in tire derived pyrolysis oils (ppm)

Volatile Hydrocarbon	Tire pyrolysis temperature (°C)					
	450	**475**	**500**	**525**	**560**	**60**
Benzene	<5	55	770	2950	70	60
Toluene	2250	3200	6095	17 740	7770	50
Ethylbenzene	250	235	120	405	370	19
1,2-Dimethylbenzene	2780	3190	3345	5710	5875	35
1,4- Dimethylbenzene	2750	2665	3620	6880	8350	31
Styrene	1205	1705	1950	3545	3635	19
1,3-Dimethylbenzene	920	1020	1325	2450	2570	10
Trimethylbenzene	840	825	1255	1085	1285	82
Trimethylbenzene	1050	1265	1670	1240	1530	12
Trimethylbenzene	1550	1350	2370	2320	3210	14
Methlystyrene	730	570	1090	1145	1590	71
Trimethylbenzene	1075	1070	1325	1295	1395	10
4-Methylstyrene	730	570	1090	1145	1590	71
Trimethylbenzene	370	440	490	675	320	33
Methylstyrene	6020	6025	7630	8865	9030	69
Limonene	31 320	30 330	29010	28 965	4 590	25
Indene	2190	2630	3175	3090	3105	15

show the concentration of Volatile Aromatic Hydrocarbon (VAH). The concentrations of VAH significant concentrations, [19]. This statement is supported by other researchers, such as, Williams [16] reported 0.47 wt% toluene, 1.78wt% xylene/limonene up to 7.43wt% of pyrolysis oil in a small scale purge static batch reactor at 420°C. The table indicated that the concentration of VAH increased with increasing temperature from 525°C to 560°C, but at higher temperature, 600°C the concentration of VAH decreased. When the temperature of pyrolysis increased, the concentration of limonene decreased but concentration of benzene, toluene and styrene increased. Similarly, Pakdel et al. pyrolysed tires in a 3.5kg/h found that increasing temperature of the hearts in the vacuum pyrolysis from 226°C to 510°C result an increase in the concentration of benzene, toluene and xylenes but, reduced the concentration of limonene. Cypres and Bettens [12] obtained higher concentration of volatile compound from the pyrolysis of tires with post-pyrolysis vapors. Wolfson et al. [9] used fixed bed batch pyrolysis of tires obtained significant concentration of benzene,toluene xylene and styrene in oil derived was influenced by temperature. In addition, Kaminsky and Sinh [7] reported high concentration of volatile aromatic compounds by using fluidized bed pyrolysis unit at temperature range from 640°C to 740°C. Williams et al. [19] suggested that above the pyrolysis temperature 525 - 560°C, the degradation of limonene occur, results the consequent decreased in concentration of Limonene in oil. The degradation of Limonene at higher temperature has reported by other researchers [14,16,18].

4.0 GAS

Williams et al. [19] analysed gas yield in packed column gas chromatography and indicated H_2, CH_4, CO and CO_2 and minor concentration of other hydrocarbon gasses. Butadiene, C_4H_6 was the main gas evolved and is formed from the thermal degradation of the polymer butadiene-styrene rubber used in the manufacture of tires [19]. This findings is supported by other authors, for example, Cypress and Bettens [12] suggested that methane and ethane result from secondary aromatization reactions which produce aromatic hydrocarbons. Roy and Unsworth [5] and Kaminsky and Sinh [7] have also shown the gas phase to consist mainly of H_2, CO, CO_2, and hydrocarbons including CH_4, C_2H_6, C_2H_4, C_2H_4, C_3H_8, C_3H_6, C_4H_{10}, C_4H_8 and C_4H_6. Other authors' detected the presence of other product such as SO_2 and NH_3 detected by Teng et al. [2] and H_2S detected by Wolfson and co-workers. The gasses generated have a significant calorific value in the order of 40MJ/m^3 and it has been suggested that the gasses may be used to provide the total energy requirement of the pyrolysis plant, [19].

4.0 CONCLUSION

The formation of char involve in several factor, such temperature, heating rate, residence time, size of reactor, efficiency of heat transfer from hot surfaces within tire mass and gas residence time in hot zone. Higher heating rates with short hot zone residence time and rapid quenching of the products regarded as favoring the formation of liquid products. Increasing the temperature of pyrolysis caused decreased in concentration of Limonene, but increasing concentration of benzene, toluene and styrene.

5.0 REFERENCES

1. J.W.Jang, T.S.Yoo, J.H.Oh, I. Iwasaki, Conser.Recycl. 22(1998) 1-14.
2. H.Teng, M.A. Serio, R.Bassilakis, P.W. Morrison, P.R. Solomon, Am.Chem.Soc.Div.Fuel Chem. 27, (1992) 533-554.
3. P.T.Williams, S.Besler, T.D. Taylor, Fuel 69 (1990) 1474-1482.
4. C. Roy, J. Unsworth, Pilot plant demonstration of used tyres vacuum pyrolysis, in: G.L. Ferrero,K. Maniatis, A. Buekens, A.V. Bridgwater (Eds.), Pyrolysis and Gasification, Elsevier AppliedScience, London, UK, 1989.
5. W. Kaminsky, H. Sinn, Pyrolysis of plastic waste and scrap tyres using a fluidised bed process, in: J.L. Jones, S.B. Radding (Eds.), Thermal Conversion of Solid Wastes and Biomass, ACS SymposiumSeries 130, American Chemical Society Publishers, Washington DC, 1980.

6. S. Kawakami, K. Inoue, H. Tanaka, T. Sakai, Pyrolysis process for scrap tyres, in: S.B.Radding (Eds.), Thermal Conversion of Solid Wastes and Biomass, ACS Symposium 130,American Chemical Society Publishers, Washington DC, 1980.

7. D.E. Wolfson, J.A. Beckman, J.G. Walters, D.J. Bennett, Destructive distillation of USDept. of Interior, Bureau of Mines Report of Investigations 7302 (1969).

8. G. Collin, Pyrolytic recovery of raw materials from special wastes, in: J.L. Radding(Eds.), Thermal Conversion of Solid Wastes and Biomass, ACS Symposium AmericanChemical Society Publishers, Washington DC, 1980.

9. R. Cypres, B. Bettens, Production of benzoles and active carbon from waste plasticmaterials by means of pyrolysis with simultaneous post-cracking, in: G.L. Maniatis, A.Buekens, A.V. Bridgwater (Eds.), Pyrolysis and Gasification, Elsevier London,UK, 1989.

International Conference on Environment 2006 (ICENV 2006)
13-15 November 2006, Penang, Malaysia.

30984

ADSORPTION OF METHYLENE BLUE DYE USING ACTIVATED CARBON ADSORBENT FROM WASTE TIRES

NURULHUDA AMRI, RIDZUAN ZAKARIA* and MOHAMAD ZAILANI ABU BAKAR
School of Chemical Engineering. Engineering Campus, Universiti Sains Malaysia,
14300 Nibong Tebal, Penang, Malaysia
*Corresponding author. Fax: +604-5941013
Email address: chduan@eng.usm.my

ABSTRACT

The adsorption of methylene blue dye from aqueous solutions on activated carbon from waste tires was studied in a batch system at initial concentration (100-500mg/L) at temperature 30°C. The activated carbon was prepared using two-step chemical activation with potassium hydroxide (KOH) at ratio KOH/char = 3. The carbonization process is at 600°C for 1 hour with nitrogen flowrate 100ml/min followed by activation with the same nitrogen flowrate at 760°C for 1 hour. The adsorption isotherms were determined by shaking 0.1g of activated carbon with 100ml methylene blue dye solutions. The initial and final concentrations of methylene blue in aqueous solution were analyzed by UV-Visible Spectrophotometer (Shimadzu, UV-1601) at wavelength of 665nm. The experimental isotherm data were analyzed using Langmuir and Freundlich isotherm models. The results show that Langmuir isotherm describes the experimental data well. Adsorption capacity of the adsorbent obtained from Langmuir model up to 227.27 mg/g.

Keywords : Methylene blue dye; Activated carbon; Chemical activation; Adsorption isotherms.

INTRODUCTION

The disposal of tires represents a major environmental issue throughout the world. Globally more than 330 million tires are discarded every year and accumulated over the years in different countries [1]. The disposal and reprocessing tires are difficult since they contain complex mixture of different materials such as rubber, carbon black, steel cord and other organic and inorganic minor components [2].

Waste tires that have been increasingly taking up large amount of valuable landfill space have been considered as an alternative precursor for activated carbons [3-8]. Generally there are two processes for preparation of activated carbon: physical activation and chemical activation. Physical activation involves carbonization of carbonaceous materials followed by activation of the resulting char in the presence of activating agents such as CO_2 or steam. While, chemical activation is known as a single or two step method of preparation of activated carbon in the presence of chemical agents. The chemical activation usually takes place at a temperature lower than that used in physical activation, therefore it can improve the pore development in the carbon structure because the effect of chemicals. The carbon yields of chemical activation are higher than physical one [9].

The adsorption process is used for the removal of colors, odors, biological matter and organic matter from process or waste effluents [10]. Activated carbons are the most widely used adsorbents due to their adsorption abilities for organic pollutants. The high adsorption capacities of activated carbons are usually related to their high surface area, pore volume and porosity. Microporous carbons are generally used in gas-phase adsorption because of the

small gas molecules, whereas mesoporous carbons are mostly used in liquid-phase adsorption [11]. With the existence of mesopores in carbon the diffusion in large or hydrated molecules to the carbon interior would be less obstructive, hence the equilibrium capacity of the carbon would be high [12].

Aqueous adsorption tests were conducted on produced activated carbon with the aim of producing further evidence about their porous structure and also for assessing potential applications in the water treatment industry. The adsorption properties of active carbon are generally estimated by determining the isotherm of adsorption from liquid phase. Adsorbates can serve as a model compound for checking the adsorption of medium size organics molecules from aqueous solutions.

The aim of this work was to investigate the adsorption of dye on prepared activated carbon using methylene blue as a model component. Laboratory batch isotherm studies were conducted to evaluate the adsorption capacity of activated carbon. The effects of contacts time and initial adsorbate concentration were studied. The Langmuir and Freundlich isotherm models were tested for their applicability. The results intend to offer the tire derived carbons a potential application in the field of wastewater treatment.

EXPERIMENTAL PROCEDURE

Preparation of the activated carbon by KOH activation. The experiments will be carried out initially by carbonization process. A certain amount of waste tires (diameter = 0.425 mm) was put on the tray and placed inside the batch muffle furnace. The temperature was ramped from the ambient temperature to 600°C and kept for 1 hour under nitrogen flow rate. The char product then was cooled down to room temperature and stored in an air tight container.

The next step is impregnation procedure. The tire char was well dispersed in KOH solutions in a stainless steel beakers with water:KOH:char equal to 3:3:1 by mass, denoted as the KOH/char ratio = 3. The beaker was immersed in a constant temperature shaker bath. The mixing will be performed at 30°C and lasted 3 hr to make sure the potassium hydroxide pellets were completely dissolved. Then the beaker was placed inside an oven at temperature 110°C for 24 hour for dehydrating purpose.

The chemically treated char was placed inside a batch muffle furnace reactor and heated to 760°C under nitrogen flow of 100 ml/min for 1 hour. The activated product was cooled under the nitrogen flow to room temperature and washed with deionized water. The sample was then poured to a beaker containing 0.1M HCl (250cm^3) and stirred for 1 hour. They were finally washed with hot water until the conductivity of the filtrate is less than 10μs. This is to ensure that all the KOH used for activation is removed before the carbon is taken for characterization. The carbon will be dried at 105°C until it is bone dry and stored in air tight sample holder.

Procedures for adsorption experiments. The activated carbon was characterized for its adsorption capacity using methlene blue dye. A methylene blue solution of 1500mg/m^3 concentration was prepared in appropriate volumetric flask. The stock solution will be diluted to the desired initial concentrations (100-500 mg/L) for batch equilibrium studies. An amount of 0.1g of activated carbon will be introduced into a 100ml of 100 to 500mg/L of methylene blue solution, and kept in a laboratory shaker for 48 hours at 30°C. The samples will be withdrawn at appropriate time interval using a glass syringe to determine the residual concentration of the solutions. For high concentrations, 0.1 cm^3 of the solution will be withdrawn and diluted to 50 cm^3 using deionized water before determining the residual concentration using UV-Spectrophotometer at 665nm wavelength for methylene blue dye.

The amount of adsorbates adsorbed at time, q_t and at equilibrium condition, q_e will be calculated according to the Equation (1) and (2) below.

$$q_t = \frac{(C_o - C_t)V}{w} \quad (1)$$

$$q_e = \frac{(C_o - C_e)V}{w} \quad (2)$$

Where C_o and C_e are initial and equilibrium adsorbate concentration, mg/L. C_t is adsorbate concentration at time, mg/L. V is volume of solution, L and w is weight of adsorbent, g.

RESULTS AND DISCUSSION

The adsorption of methylene blue on prepared activated carbon at 30°C and various initial concentrations were studied as a function of contact time in order to determine the equilibrium time for adsorbate. The results are presented in Figure 1. The time profiles of methylene blue uptake at various concentrations shown by activated carbons were single, smooth and continuous curve leading to the saturation. The shape of the plots can be explained by dividing the whole adsorption process into three different time-based regimes. The first regimes characterized very fast sorption process due to rapid attachment of the adsorbates to the carbon surface. As the second regime described slower process due to intra-particle diffusion and the third regime, the adsorption process was ceased as the equilibrium was almost reached. The equilibrium state was achieved faster at lower concentration range because the adsorption process just took place on the carbon surface. The fastest removal was showed at initial concentration 100 mg/L which is within 1 hour to reach equilibrium. For initial concentration 200 and 300 mg/L, equilibrium was achieved within 6 hours. While for high initial concentration 400 and 500 mg/L, it gradually increased to attain equilibrium at 48 hour.

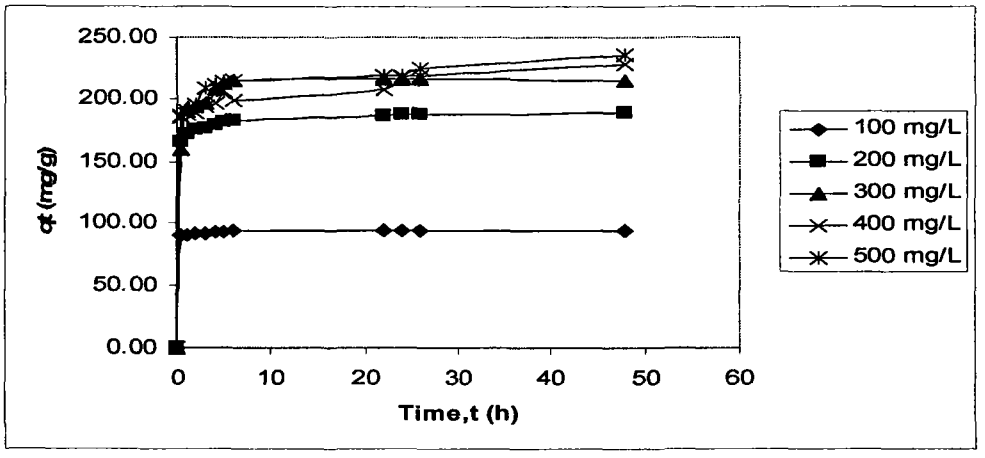

Figure 1 : Adsorption of methylene blue on activated carbon as a function of time at different initial concentrations at 30°C.

ADSORTION ISOTHERM

The relationship between the amount of a substance adsorbed at constant temperature and its concentration in the equilibrium solution is called adsorption isotherm. Figure 2 show the adsorption isotherm of methylene blue at 30°C using prepared activated carbon. Methylene blue uptake of prepared activated carbon was 224.67 mg/g.

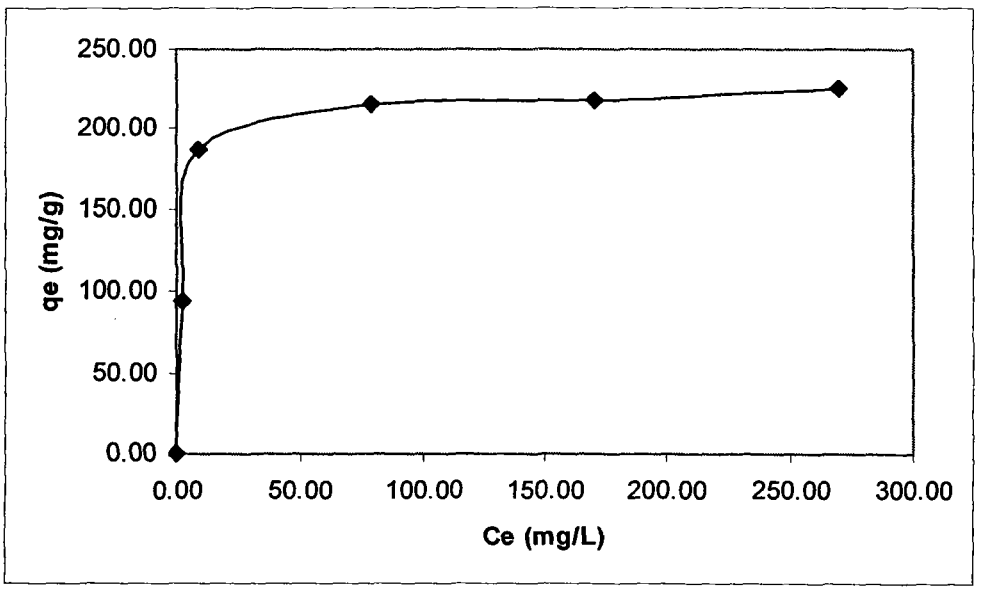

Figure 2: Adsorption isotherm of methylene blue using activated carbon at 30°C.

Several models have been published in the literature to describe experimental data of adsorption isotherms. The Langmuir and Freundlich are the most frequently employed models. In this work, both models were used to describe the relationship between the amount of methylene blue adsorbed and its equilibrium concentration.

LANGMUIR ISOTHERM

The Langmuir adsorption isotherm is often used for adsorption of the solute from a liquid solution. The Langmuir adsorption isotherm is perhaps the best known of all isotherms describing adsorption and is often expressed as:

$$q_e = \frac{Q^o K_L C_e}{(1 + K_L C_e)} \tag{4}$$

Where:

q_e = adsorption capacity at equilibrium solute concentration, C_e (mg/g)

C_e = concentration of adsorbate in solution (mg/L)

Q^o = maximum adsorption capacity corresponding to complete monolayer coverage (mg/g)

K_L = Langmuir constant related with affinity of the points of union (L/mg)

The above equation can be rearranged to the following linear form:

$$\frac{C_e}{q_e} = \frac{1}{Q^o K_L} + \frac{C_e}{Q^o} \tag{5}$$

The linear form can be used for linearization of experimental data by plotting C_e/q_e against C_e. The Langmuir constant X_m and K can be evaluated from the slope and intercept of linear equation, respectively as shown in Figure 3.

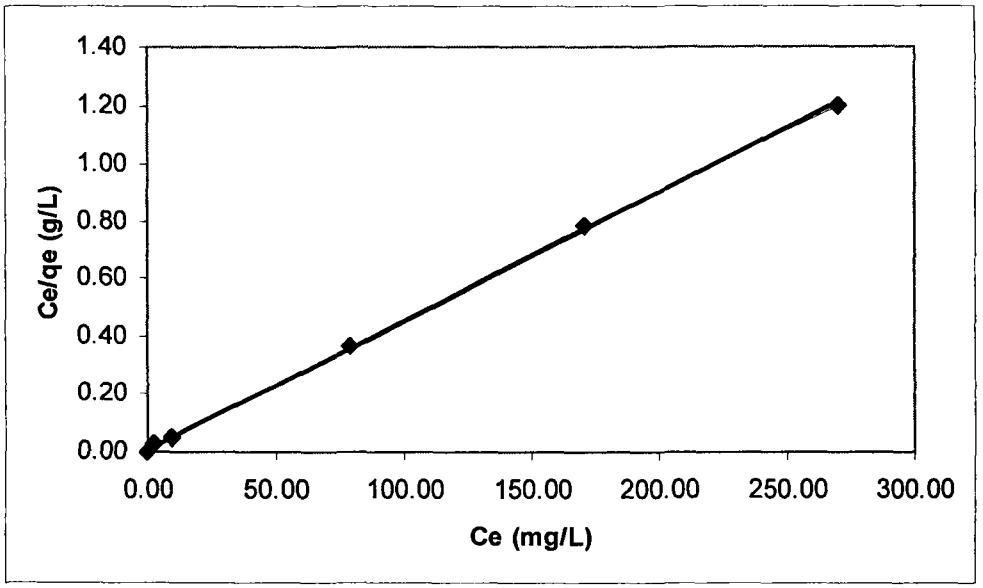

Figure 3: Langmuir isotherms for the removal of methylene blue by adsorption on prepared activated carbon at 30°C.

The essential characteristics of Langmuir equation can be expressed in terms of dimensionless separation factor, R_L, defined as:

$$R_L = \frac{1}{(1 + K_L C_o)} \tag{6}$$

Where C_o is the highest initial solute concentration.

The R_L value implies the adsorption to be favourable (R_L>1), linear (R_L=1), favourable (0<R_L<1), or irreversible (R_L=0). Value of R_L for prepared activated carbon was found to be 0.0046. Therefore the present adsorption systems reveal favourable.

FREUNDLICH ISOTHERM

The freundlich isotherm is the earliest known relationship describing the adsorption equation an often expressed as:

$$q_e = K_f C_e^{1/n} \tag{7}$$

Where:

q_e = adsorption capacity at equilibrium solute concentration, C_e (mg/g)
C_e = concentration of adsorbate in solution (mg/L)
K_f = empirical constants depending on several environmental factors
n = greater than one.

The equation is conveniently used in the linear form by taking the logarithmic of both sides as:

$$\log q_e = \log K_f + \frac{1}{n}\log C_e \tag{8}$$

A plot of $(\log q_e)$ against $(\log C_e)$ yielding a straight line indicates the confirmation of the Freundlich isotherm for adsorption. The constant can be obtained from the slope and intercept of the linear plot of experimental data as shown in Figure 4. The value of n indicates favourable adsorption when $1<n<10$. Value of n was found to be 6.2696. Therefore the present adsorption systems reveal favourable.

The Langmuir constants K and X_m and Freundlich constants K_F and n are given in the Table 1. Correlation coefficient, R^2 values show that Langmuir isotherm model was found to fit the adsorption data of the prepared activated carbon very well. Adsorption capacity of the adsorbent obtained from Langmuir model up to 227.27 mg/g. This result was similar with the work done by Lin et al., [12]. In his work, the adsorption capacity of tire char at 30°C was 227 mg/g.

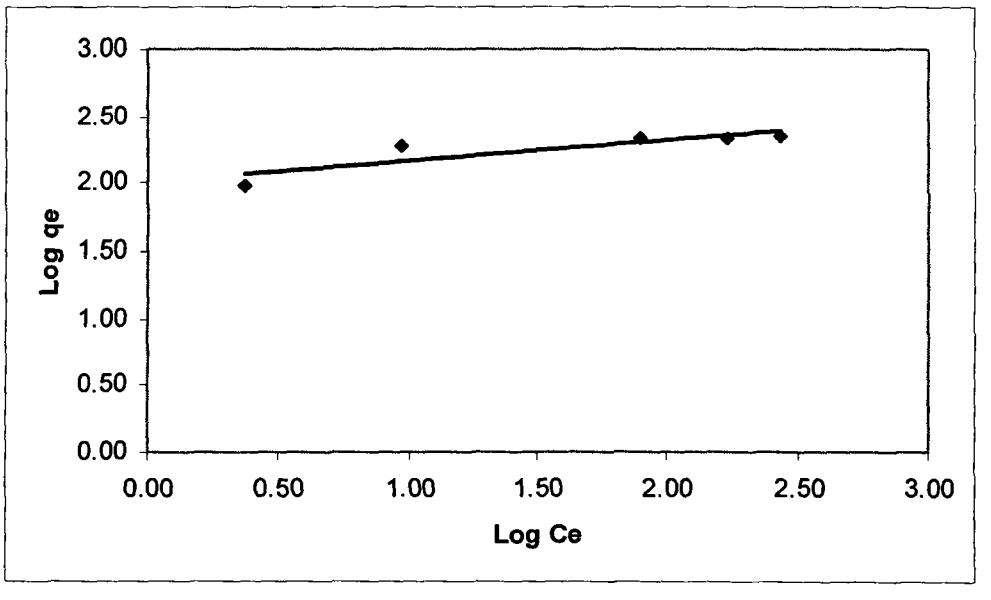

Figure 4: Freundlich isotherms for the removal of methylene blue by adsorption on prepared activated carbon at 30°C.

Table 1: Langmuir and Freundlich constants for the adsorption methylene blue on the prepared activated carbon.

	Langmuir isotherm model				Freundlich isotherm model		
Type of adsorbent	Q^o (mg/g)	K_L (L/mg)	Correlation Coefficient, R^2	R_L	K_F (mg/g)(L/mg)$^{1/n}$	n	Correlation Coefficient, R^2
Activated carbon	227.27	0.4314	0.9997	0.0046	7.4038	6.2696	0.7679

CONCLUSION

The experimental data of adsorption studies on methylene blue using prepared activated carbon was described well to Langmuir adsorption isotherm model. This indicates that adsorption of methylene blue from aqueous solutions shows monolayer coverage of the adsorbate on the carbon surface and a full access of the adsorbate to all pores [12]. Adsorption capacity of the adsorbent obtained from Langmuir model up to 227.27 mg/g. The present study concludes that the production of activated carbon adsorbents from waste tire rubber can provide a two-fold environmental and economic benefit: A recycling path is created for waste vehicles tires and new low-cost adsorbents are produced for commercial use in wastewater treatment.

ACKNOWLEGDEMENT

The authors acknowledge the Long-term IRPA grant provided by MOSTI for this present work. The authors also very thankful to the school of Chemical Engineering, Universiti Sains Malaysia for providing the facilities and constant encouragement.

REFERENCES

[1] Cunliffe A.M. and Williams P.T., Influence of process conditions on the rate of activation of chars derived from pyrolysis of used tyres, *Energy Fuels,* Vol 13(1), 1999, pp166-75.

[2] Rodriguez Isabel, D.M., M.F. Laresgoiti, M.A. Cabrero, A. Torres, M.J. Chomon, B. Caballero, Pyrolysis of scrap tyres, *Fuel Proc.Tech*, Vol 92, 2001, pp. 9-22.

[3] Merchant, A.A. and M.A. Petrich, Pyrolysis of scrap tires and conversion of chars to activated carbon, *AIChE J*, Vol 39(8), 1993, pp. 1370-1376.

[4] Sun, J., T.A. Brady, M.J. Rood, C.M. Lehman, M. Rostam-Abadi and A.A. Lizzi , Adsorbed natural gas storage with activated carbons made from Illinois coals and scrap tires, *Energy Fuels,* Vol 11, 1997, pp. 316-322.

[5] Allen, J.L., J.L. Gatz and P.C. Eklund, Applications for activated carbons from used tires; butane working capacity, *Carbon*, Vol 37, 1999, pp.1485-1459.

[6] Teng, H., Y.C. Lin and L.Y. Hsu, Production of activated carbons from pyrolysis of waste tires impregnated with potassium hydroxide, *Journal Air Waste Management Assoc,* Vol 50, 2000, pp. 1940-1946.

[7] Ariyadejwanich, P., W. Tanthapanichakoon, K. Nakagawa, S.R. Mukai and H Tamon, Preparation and characterization of mesoporous activated carbon from waste tires, *Carbon*, Vol 40-41, 2003, pp. 157-164.

[8] Stavropoulos, G.G., Precursor materials suitability for super activated carbons production, *Fuel Processing Technolog,* Vol 86, 2005, pp. 1165-1173.

[9] Ahmadpour, A., Do and D.D, The preparation of activated carbon from macadamia nutshell by chemical activation, *Carbon*, Vol 35, 1997, pp. 1723-1732.

[10] Wu, F.C. and R.L. Tseng, Preparation of highly surface area carbon from fir wood by KOH etching and CO2 gasification for adsorption of dyes and phenols from water, *Colloids and Interface Science*, Vol 294, 2006, pp. 21-30.

[11] Srinivasakannan, C. and M.Z.A. Bakar, Production of activated carbon from rubber wood sawdust, *Biomass & Bioenergy,* Vol 27, 2004, pp. 89-96.

[12] Lin, Y.R. and H. Teng, Mesoporous carbons from waste tire char and their application in wastewater discoloration, *Microporous and Mesoporous Materials,* Vol 54, 2002, pp. 167-174.

Symposium of Malaysian Chemical Engineers (SOMChE) 2007,
11 – 13th of December 2007, Selangor, Malaysia

30985

ADSORPTION OF PHENOL USING ACTIVATED CARBON ADSORBENT FROM WASTE TYRES

NURULHUDA AMRI, RIDZUAN ZAKARIA* and MOHAMAD ZAILANI ABU BAKAR

School of Chemical Engineering. Engineering Campus, Universiti Sains Malaysia,
14300 Nibong Tebal, Penang, Malaysia
*Corresponding author. Fax: +604-5941013
Email address: chduan@eng.usm.my

ABSTRACT

The adsorption of phenol from aqueous solutions on activated carbon from waste tyres was studied in a batch system at initial concentration (100-500mg/L) at temperature 30°C. The activated carbon was prepared using two-step physiochemical activation with potassium hydroxide (KOH) at ratio KOH/char = 5. The carbonization process is at 800°C for 1 hour with nitrogen flowrate 150ml/min followed by activation with the carbon dioxide flowrate 150ml/min at 850°C for 2 hour. The adsorption isotherms were determined by shaking 0.1g of activated carbon with 100ml phenol solutions. The initial and final concentrations of phenol in aqueous solution were analyzed by UV-Visible Spectrophotometer (Shimadzu, UV-1601) at wavelength of 270nm. The experimental isotherm data were analyzed using Langmuir and Freundlich isotherm models. The equilibrium data for phenol adsorption was fit well to both isotherm models with R^2 value 0.9911 and 0.9907 respectively. The rates of adsorption were found to conform to the pseudo-second-order kinetics with good correlation. Adsorption capacity of the adsorbent obtained from Langmuir model up to 238.095 mg/g.

1.0 Introduction

Phenol and related compounds are toxic to human and aquatic life, creating an oxygen demand in receiving waters. Phenolic pollutants occur in wastewater of a number of industries, such as petroleum refineries, petrochemical, steel mills, coke oven plants, coal gas, synthetic resins, pharmaceuticals, paints, plywood industries, and mine discharge [Patterson, 1975]. Chronic toxic effects due to the phenol pollution reported in humans include vomiting, anorexia, difficulty in swallowing, liver and kidney damage, headhache, fainting and other mental disturbances [Fawell, 1988]. The demand for the removal of organics compounds including phenol has been increased by the increasing the industrial wastewaters. The Department of Environment (DOE) of Malaysia has set the maximum concentration of phenol as 0.001mg/L for standard A and 1.0mg/L for standard B in the industrial effluent discharge to Malaysia inland waters (Environment Quality Act, 2001).

These organics compounds are considered as priority pollutants since they are harmful to organisms at low concentrations and can be toxic when present elevated levels and are suspected to be carcinogens [Ozkaya, 2006]. Therefore, it is necessary to remove phenol from industrial effluents before discharging into the water stream.

Various treatment methods are available for removal of phenol including adsorption, reverse osmosis, chemical oxidation, ion exchange, distillation, precipitation, gas stripping, solvent extraction, complexation, and bio-remediation [Mukherjee et al, 2006]. Among all these methods, adsorption by activated carbon (AC) is the best and most frequently used treatment method for separation toxic pollutant from water environment.

The use of activated carbon for adsorption treatment was first recorded more than two hundred years ago [ ]. In waste water treatment, activated carbon is powerful adsorbent because it has a large surface area and pore volume, which allows the removal of organics compounds, heavy metal ions and colors [Hsieh and Teng, 2000]. Although activated carbon adsorption is considered as the best available technologies for the

removal of organic compounds, but it is still considered highly expensive according to the market price of commercial activated carbon available. Therefore, more inexpensive and effective activated carbon adsorbent need to be found for removal of phenol in wastewater treatment so that the strict regulation on the concentration of phenol in wastewater can be implemented.

Recently, there has been an increasingly amount of literature devoted to the study of preparation activated carbon from agricultural and solid wastes for the cheaper adsorbent which can be used for the removal organics compounds such as phenol [(Kennedy et, al, 2007), (Mukherjee et, al, 2006), (Wu et, al, 2006), (Tseng et, al, 2006), (Wu et, al, 2005), (Srivastava et, al, 2006), (Tanthapanichakoon et. al, 2005), (Ariyadejwanich et. al, 2003), (Miguel et. al, 2003), (Rengaraj et. al, 2002), (Helleur et. al, 2001)]. Regarding to the literature studies, it was proved that, among several solid wastes, activated carbons prepared from waste tyres are considered highly mesoporous and have remarkably high adsorption capacity for large molecules (Nakagawa et. al., 2004). In some applications, especially those involving large molecules or macromolecules which cannot easily penetrate into the micropores (<2 nm diameter) and adsorb onto them, the activated carbons should possess not only micropores but also interconnecting mesopores (Hsieh and Teng, 2000; Tamai et. al., 1999).

The purpose of this work was to determine the adsorption potential of prepared activated carbon from waste tyres for removal of phenol from wastewater. Laboratory batch isotherm studies were conducted to evaluate the adsorption capacity of the activated carbon adsorbent. Effects of contacts time and initial phenol concentration have been investigated. Langmuir and Freundlich isotherm models were tested for their applicability with the experimental data. The kinetics of adsorption of phenol on the adsorbent has also been studied using pseudo-first order and pseudo-second order kinetic models.

2.0 Experimental

2.1 Experimental rig

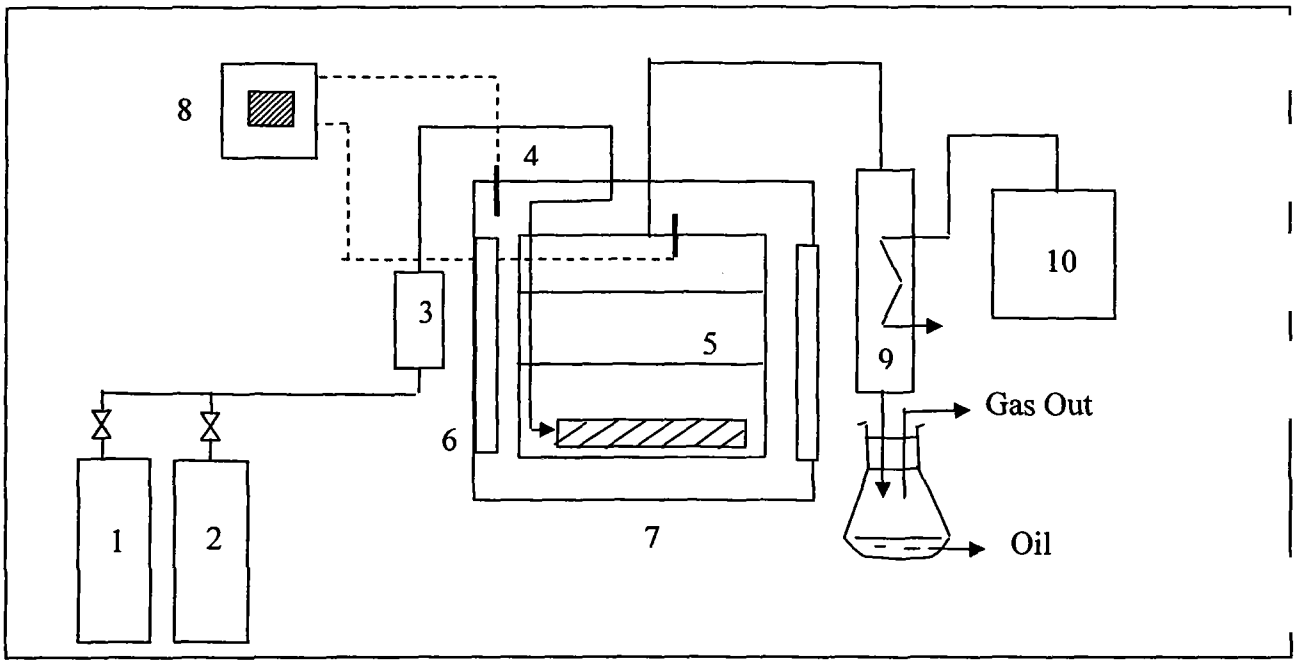

Figure 1 : Schematic diagram of the pyrolysis unit. (1) N_2 source, (2) CO_2 source, (3) gas rotameter, (4) Type-K thermocouple, (5) Tray, (6) Heating element, (7) Furnace, (8) Digital thermometer, (9) Condenser and (10) Circulator.

Experiments in the present work were carried out in a batch muffle furnace which can heat up to a temperature of 1000°C with in a temperature accuracy of ± 2°C. The muffle furnace is suitably modified with a small internal chamber dimension of 110mm length, 110mm breadth and 150mm height. The pyrolytic product (gas) during pyrolysis is removed out of the chamber immediately using a gas exit pipe from the top of the internal chamber. The heating rate of the muffle furnace could be varied from 5°C/min to 80°C/min. The gaseous product leaving the pyrolytic chamber is sent through a sequence of condensers kept at different temperatures to collect the liquid product.

2.2 Preparation of the activated carbon by physiochemical activation method

The experiments will be carried out initially by carbonization process. A certain amount of waste tires (diameter = 0.425 mm) was put on the tray and placed inside the batch muffle furnace. The temperature was ramped from the ambient temperature to 800°C and kept for 1 hour under nitrogen flow rate. The char product then was cooled down to room temperature and stored in an air tight container.

The next step is impregnation procedure. The tire char was well dispersed in KOH solutions in a stainless steel beakers with water:KOH:char equal to 5:5:1 by mass, denoted as the KOH/char ratio = 5. The beaker was immersed in a constant temperature shaker bath. The mixing will be performed at 30°C and lasted 3 hr to make sure the potassium hydroxide pellets were completely dissolved. Then the beaker was placed inside an oven at temperature 110°C for 24 hour for dehydrating purpose.

The chemically treated char was placed inside a batch muffle furnace reactor and heated to 850°C under nitrogen flow of 150 ml/min. After the temperature reached the setting point, the gas flow will be switched to carbon dioxide at flow rate of 150 ml/min for 2 hour. The activated products were then will be cooled under the nitrogen flow to room temperature. The sample was then poured to a beaker containing 0.1M HCl ($250cm^3$) and stirred for 1 hour. They were finally washed with hot water until the conductivity of the filtrate is less than 10μs. This is to ensure that all the KOH used for activation is removed before the carbon is taken for adsorption study. The carbon will be dried at 105°C until it is bone dry and stored in air tight sample holder.

2.3 Procedures for adsorption experiments

The activated carbon was characterized for its adsorption capacity using phenol. A phenol solution of $1500mg/m^3$ concentration was prepared in appropriate volumetric flask. The stock solution will be diluted to the desired initial concentrations (100-500 mg/L) for batch equilibrium studies. An amount of 0.1g of activated carbon will be introduced into a 100ml of 100 to 500mg/L of phenol solution, and kept in a laboratory shaker for 48 hours at 30°C. The samples will be withdrawn at appropriate time interval

using a glass syringe to determine the residual concentration of the solutions. For high concentrations, 0.1 cm^3 of the solution will be withdrawn and diluted to 50 cm^3 using deionized water before determining the residual concentration using UV-Spectrophotometer at 270nm wavelength for phenol.

The amount of adsorbates adsorbed at time, q_t and at equilibrium condition, q_e will be calculated according to the Equation (1) and (2) below.

$$q_t = \frac{(C_o - C_t)V}{w} \tag{1}$$

$$q_e = \frac{(C_o - C_e)V}{w} \tag{2}$$

Where C_o and C_e are initial and equilibrium adsorbate concentration, mg/L. C_t is adsorbate concentration at time, mg/L. V is volume of solution, L and w is weight of adsorbent, g.

3.0 Results and discussion

3.1 Effect initial concentration of phenol

Effect of initial concentration phenol, C_o on the adsorption capacity, q_t as a function of time is shown in Fig. 1. The amount of phenol adsorbed per unit weight of adsorbent increased with increase in phenol concentration. When the initial concentration increased from 100 to 500 mg/L, the adsorption capacity increased from 58.65 mg/g to 163.21 mg/g. It is because the initial concentration plays an important role which provides the necessary driving force to overcome the resistances to the mass transfer of phenol between the aqueous and the solid phases [Srivasta, et. al, 2006]. The interaction between phenol and the prepared activated carbon adsorbent also enhances with the increasing of the initial concentration. Thus, it can be concluded higher initial concentration enhances the adsorption uptake of phenol.

3.3 Effect of contact time

Aqueous phenol solutions with different initial concentration ranging from 100 to 500 mg/L were kept in contact with the adsorbents for 48 hour. Available adsorption results reveal that the uptake of the adsorbate is fast at the initial stage of the contact period, and then it become slower near to the equilibrium. The rate of adsorption is nearly constant in the between of these two stages of the uptake. [Srivasta, et. al, 2006]. It is because at the initial stage of contact time, number of adsorption sites available is higher and the driving force for the mass transfer is greater. Therefore, it is much easier for the adsorbate to reach the adsorption site. After a lapse of time, number of active sites becomes less and the adsorbent becomes crowded inside the particles, thus impeding the movement of the adsorbate [Kennedy et. al, 2007]. This fact is agreed with the results presented in Fig. 1. The fastest removal was showed at initial concentration 100 mg/L which is within 1 hour to reach equilibrium. For initial concentration 200mg/L, equilibrium was achieved within 6 hours. While for high initial concentration 300, 400 and 500 mg/L, it gradually increased to attain equilibrium at 48 hour.

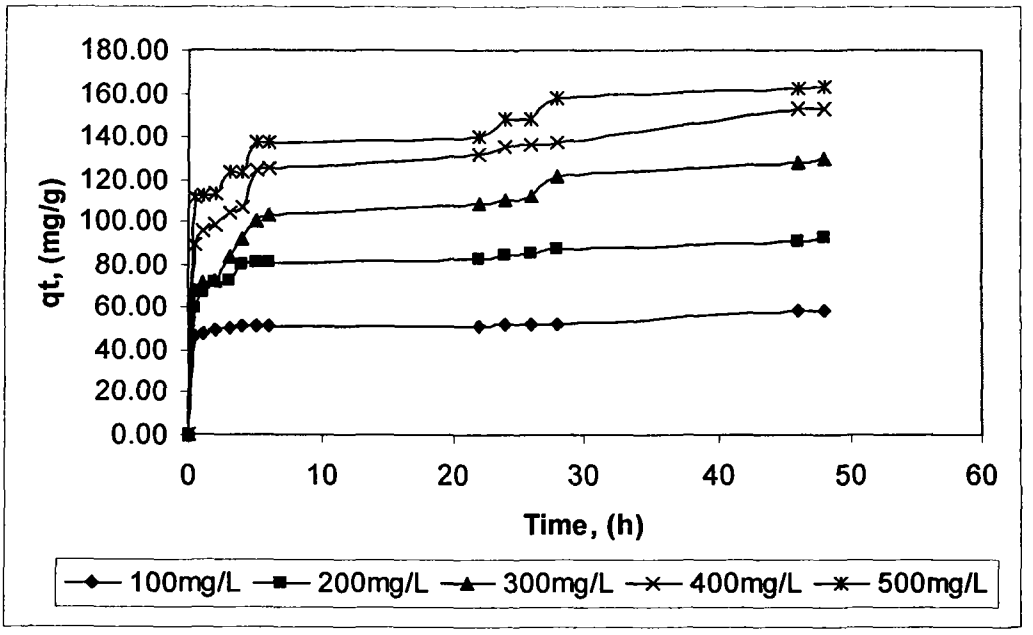

Figure 1: Effect of initial phenol concentration on the adsorption of MB onto the prepared activated carbon.

3.3 Adsorption isotherms

An adsorption isotherm describes the relationship between the amount of adsorbate that is adsorbed on the adsorbent and the concentration of dissolved adsorbate in the liquid at equilibrium [Roostaei and Tezel, 2004]. The equilibrium adsorption isotherm is fundamentally important in the design of adsorption systems. The amount of phenol adsorbed at equilibrium, q_e has been plotted against the equilibrium condition, C_e as shown in Fig. 2. As a result, the value of q_e is increased with the increase in phenol concentration.

The adsorption isotherm of phenol onto prepared activated carbon was fitted by several well-known isotherms models which is Langmuir and Freundlich models to assess their utility. The Langmuir model is obtained under the ideal consumption of a totally homogeneous adsorption surface, whereas the Freundlich model is suitable for a highly heterogenous surface. In this work, both models were used to describe the relationship between the amount of phenol adsorbed and its equilibrium concentration.

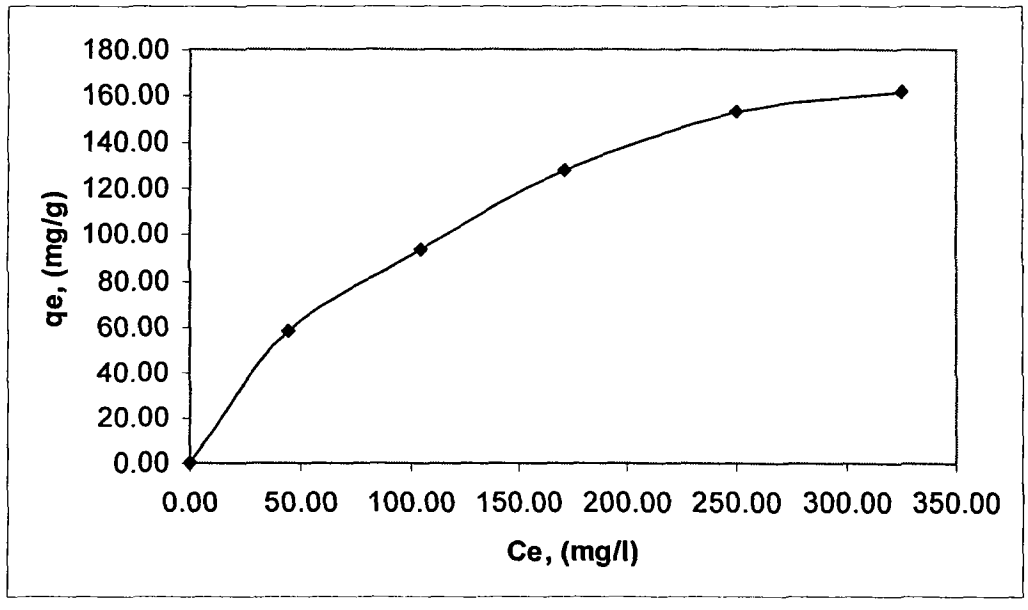

Figure 2: Equilibrium adsorption isotherm of phenol onto prepared activated carbon at 30°C

3.3.1 Langmuir isotherms

The Langmuir adsorption isotherm is often used for adsorption of the solute from a liquid solution. The Langmuir adsorption isotherm is perhaps the best known of all isotherms describing adsorption and is often expressed as:

$$q_e = \frac{Q^o K_L C_e}{(1 + K_L C_e)} \tag{4}$$

Where:

q_e = adsorption capacity at equilibrium solute concentration, C_e (mg/g)

C_e = concentration of adsorbate in solution (mg/L)

Q^o = maximum adsorption capacity corresponding to complete monolayer coverage (mg/g)

K_L = Langmuir constant related with affinity of the points of union (L/mg)

The above equation can be rearranged to the following linear form:

$$\frac{C_e}{q_e} = \frac{1}{Q^o K_L} + \frac{C_e}{Q^o} \tag{5}$$

The linear form can be used for linearization of experimental data by plotting C_e/q_e against C_e. The Langmuir constant Q^o and K can be evaluated from the slope and intercept of linear equation, respectively as shown in Figure 3.

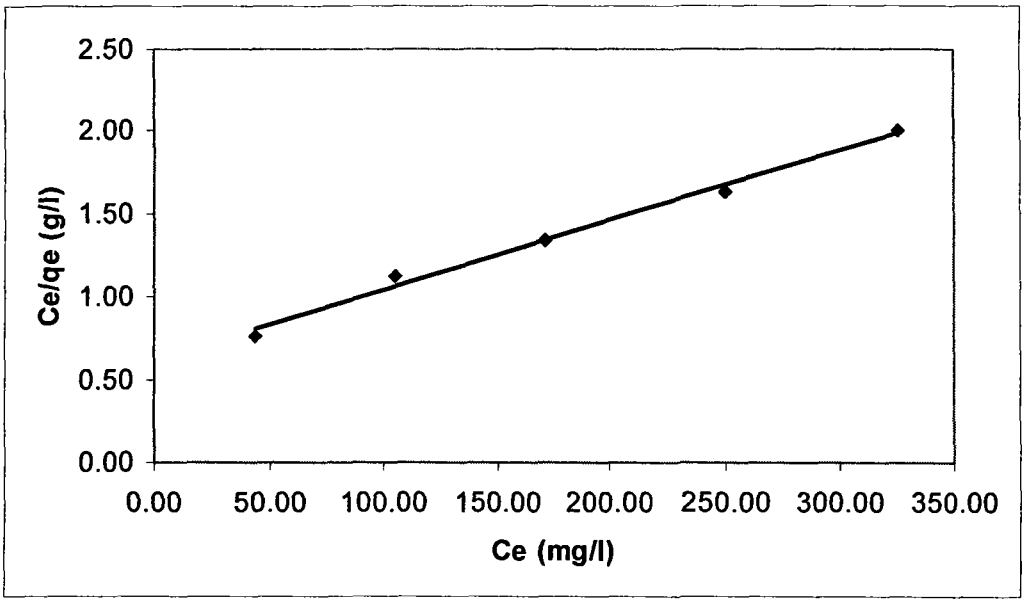

Figure 3 : Langmuir adsorption isotherm of phenol onto activated carbon at 30°C

The essential characteristics of Langmuir equation can be expressed in terms of dimensionless separation factor, R_L, defined as:

$$R_L = \frac{1}{(1 + K_L C_o)} \tag{6}$$

Where C_o is the highest initial solute concentration.

The R_L value implies the adsorption to be favourable (R_L>1), linear (R_L=1), favourable (0<R_L<1), or irreversible (R_L=0). Value of R_L was found to be 0.2271 and this confirmed that prepared activated carbon is favourable for adsorption of phenol under conditions used in this present study [Aktas and Cecen, 2007].

3.3.2 Freundlich isotherms

The freundlich isotherm is the earliest known relationship describing the adsorption equation an often expressed as:

$$q_e = K_f C_e^{1/n} \tag{7}$$

Where:

q_e = adsorption capacity at equilibrium solute concentration, C_e (mg/g)

C_e = concentration of adsorbate in solution (mg/L)

K_f = empirical constants depending on several environmental factors

n = greater than one.

The equation is conveniently used in the linear form by taking the logarithmic of both sides as:

$$\log q_e = \log K_f + \frac{1}{n} \log C_e \tag{8}$$

A plot of $(\log q_e)$ against $(\log C_e)$ yielding a straight line indicates the confirmation of the Freundlich isotherm for adsorption. The constant can be obtained from the slope and intercept of the linear plot of experimental data as shown in Figure 4. The value of n indicates favourable adsorption when $1<n<10$. Value of n was found to be 1.8699. Therefore the present adsorption systems reveal favourable [Ozkaya, 2006].

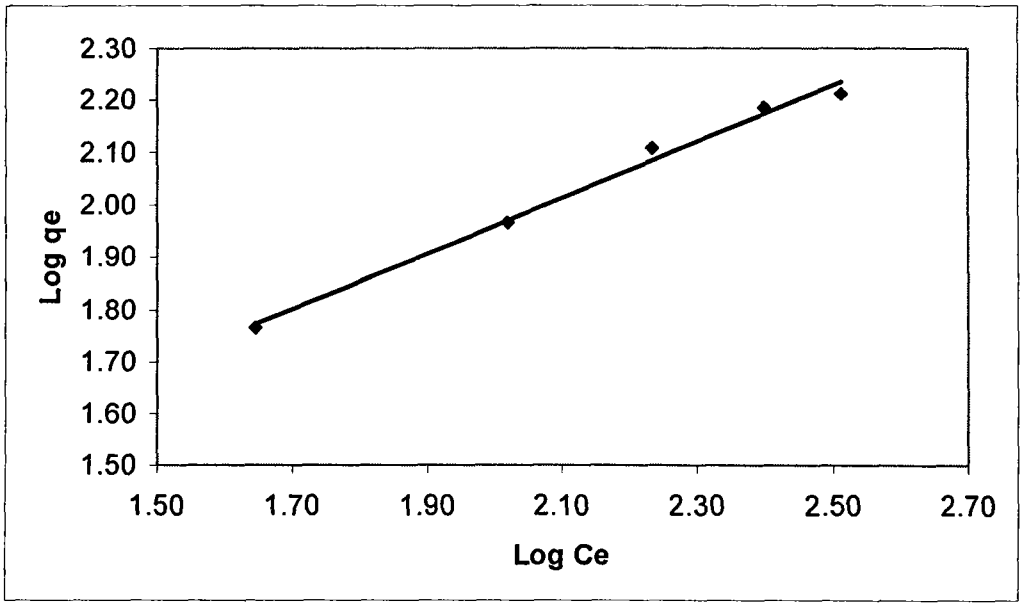

Figure 4 : Freundlich adsorption isotherm of phenol onto activated carbon at 30°C

The Langmuir constants Q^o and K_L and Freundlich constants K_F and n are given in the Table 1. Correlation coefficient, R^2 values show that Langmuir and Freundlich isotherm model was found to fit the adsorption data of the prepared activated carbon very well with R^2 value 0.9911 and 0.9907 respectively. Adsorption capacity of the adsorbent obtained from Langmuir model up to 238.095 mg/g. This result show that the prepared activated carbon in this study has a very high adsorption capacity compare to the other works listed in the Table 2. This is may be due to the different of the activation method used, which eventually results in different surface characteristics [Aktas and Cecen, 2007].

Table 1: Langmuir and Freundlich isotherm constants for phenol on the prepared activated carbon at 30°C.

	Langmuir isotherm model				Freundlich isotherm model		
Type of adsorbent	Q^o (mg/g)	K_L (1/mg)	Correlation Coefficient, R^2	R_L	K_F (mg/g)(L/mg)$^{1/n}$	n	Correlation Coefficient, R^2
Activated carbon	238.095	0.0068	0.9911	0.2271	2.4376	1.8699	0.9907

Table 2: Comparison of the maximum monolayer adsorption of phenol on activated carbon adsorbents from waste tyres.

Adsorbent	Maximum monolayer adsorption capacity, (mg/g)	Method of Activation	Reference
Activated carbon	238.095 mg/g	Physiochemical activation	Present work
Tyre rubber-derived carbon	106.00 mg/g	Physical activation	Miguel et. al (2003)

3.4 Adsorption kinetic studies

In order to investigate the adsorption process onto prepared activated carbon, the frequently used kinetics models such as the linearised form of pseudo-first-order and pseudo-second-order models were used to determine the mechanism of adsorption process.

3.4.1 The Pseudo-first order and Pseudo-second order kinetic model

The linearised pseudo-first order and pseudo-second order kinetic equation by Lagergren and Svenka [ ] are generally expressed as Eqs (4) and (5) respectively:

$$\ln(q_e - q_t) = \ln q_e - k_1 t \tag{4}$$

$$\frac{1}{q_t} = \frac{1}{k_2 q_e^{\,2}} + \left(\frac{1}{q_t}\right) t \tag{5}$$

Where;

q_e = Amount of adsorbate adsorbed at equilibrium, (mg/g)

q_t = Amount of solute adsorb per unit weight of adsorbent at time, (mg/g)

k_1 = Rate constant of pseudo-first order sorption (1/hr)

k_2 = Rate constant of pseudo-second order sorption (g/hr.mg)

The pseudo-first order and pseudo-second order rate constants were evaluated from the linear plots of $\ln(q_e - q_t)$ versus t and t/q_t versus t respectively and are shown in Figs. (5) and (6). The correlation coefficient (R^2) calculated from these plots were used to evaluated the applicability of these models and the value of R^2 were listed in the table 3.

The correlation coefficient (R^2) values for the pseudo-first-order was slightly lower ranging from 0.38 to 0.89. This phenomenon agree with Mckay and Ho, 1999 that suggest the first order equation of Lagergren does not fit well with the whole range of contact time and is generally applicable over the initial stage of the adsorption process in many cases. The experimental equilibrium adsorption capacity data, $q_{e,exp}$ was also do not agree with the calculated ones, $q_{e,cal}$ that obtained from the linear plots in the Fig. 5. This result proved that the adsorption of phenol onto prepared activated carbon was not a pseudo-first-order kinetic.

On the other hand, the experimental data was found to fit well to the pseudo-second-order model with R^2 values greater than 0.99. Similar observation was reported by adsorption of phenol from aqueous solution using mesoporous carbon prepared by two-stage process [Kennedy et. al, 2007] and adsorptive removal of phenol by bagasse fly ash and activated carbon [Srivasta et. al, 2006]. More over, the calculated equilibrium adsorption capacity, $q_{e,cal}$ for this second-order model is consistent with the experimental ones, $q_{e,exp}$. Therefore, the sorption reaction can be approximated more favourably by the pseudo-second-order model for the prepared activated carbon.

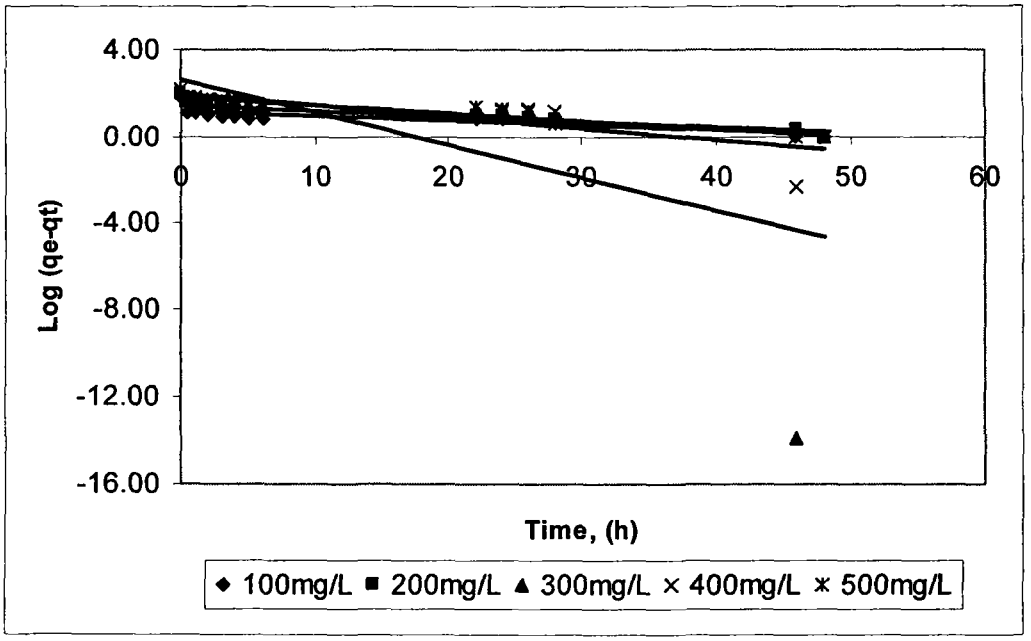

Figure 5 : Pseudo-first order kinetics for adsorption of phenol by prepared activated carbon at 30°C

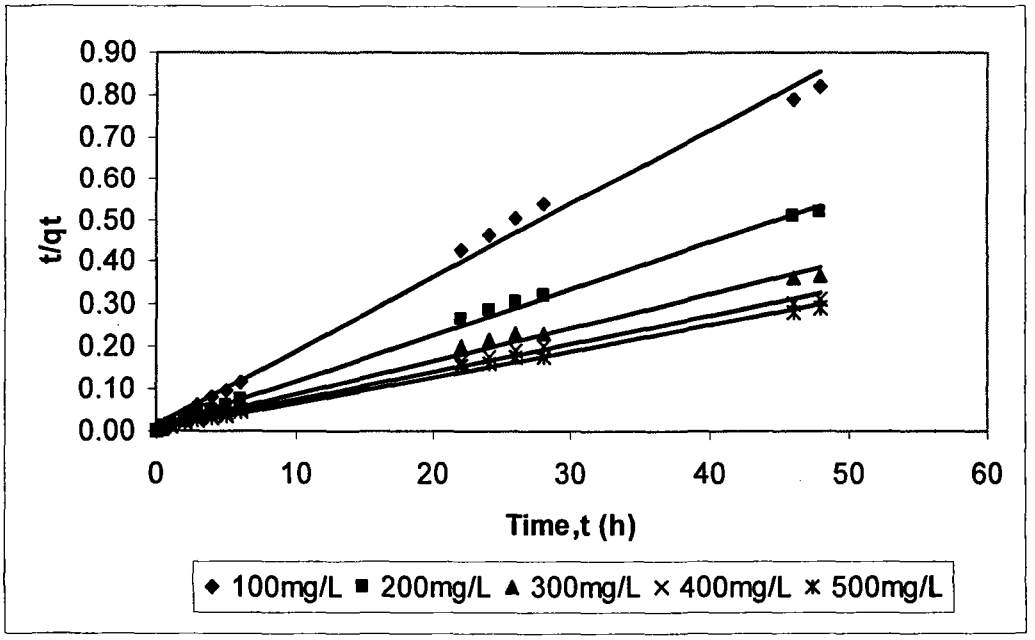

Figure 6 : Pseudo-second order kinetics for adsorption of phenol by prepared activated carbon at 30°C.

Table 3 : Comparison of the pseudo first and second-order kinetics for adsorption of phenol for different initial concentration.

Initial Conc. (mg/L)	$q_{e,exp}$ (mg/g)	Pseudo first-order				Pseudo second-order			
		k_1 (h^{-1})	$q_{e,cal}$ (mg/g)	R^2	SSE (%)	k_2 (g/h.mg)	$q_{e,cal}$ (mg/g)	R^2	SSE (%)
100	58.14	0.0479	13.81	0.6795	12.30	0.0224	57.14	0.9942	0.28
200	93.08	0.0603	29.45	0.8329	17.65	0.0141	90.91	0.9974	0.60
300	127.86	0.3443	392.55	0.3795	73.41	0.0051	128.21	0.9928	0.10
400	153.36	0.1244	102.05	0.6662	14.23	0.0049	151.52	0.9941	0.51
500	162.23	0.0827	63.96	0.8920	27.26	0.0061	161.29	0.9960	0.26

3.5 Validity of kinetic models

The adsorption kinetics of phenol onto prepared activated carbon was verified at different initial concentration. The validity of the pseudo-first and second-order kinetics model was determined by the sum of error squares (SSE, %) given by Eqs. (6):

$$SSE(\%) = \sqrt{\frac{\sum\left(q_{e,\exp} - q_{e,cal}\right)^2}{N}} \qquad (6)$$

Where N is the number of data points.

The goodness of the fit can be determined by the highest value of correlation coefficient, R^2 and the lowest value of SSE, (%). The results show in the Table 3 proved that the adsorption of phenol using prepared activated carbon can be best described by the second order model.

ACKNOWLEGDEMENT

The authors acknowledge the Long-term IRPA grant provided by MOSTI for this present work. The authors also very thankful to the school of Chemical Engineering, Universiti Sains Malaysia for providing the facilities and constant encouragement.

References :

[1] J.W. Patterson, Industrial Wastewater Treatment Technology, Wastewater Treatment Technology , Ann Arbor Science Inc. 1975..

[2] J.K Fawell, S. Hunt, Environmental Toxicology: Organic Pollutants, Halstd Press, John Wiley & Sons, NY, 1988, 398.

[3] Environmental Quality Act, Sewage and Industrial Effluent in Environment Quality Act and regulations, laws of malysia.12th Ed. MDC Publisher Printers Sdn. Bhd., Malysia, 61.

[4] Ozkaya, B., Adsorption and Desorption of phenol on activated carbon and a comparison of isotherm models, Journal of Hazardous Materials B129 (2006) 158-163.

[5] Mukherjee, S., Kumar, S., Misra, A.K., Fan, M., Removal of phenols from water environment by activated carbon, bagasse ash and wood charcoal, Chemical Engineering Journal , 2006.

[6] Hsieh, C.T. and Teng, H., Influence of mesopore volume and adsorbate size on adsorption capacities of activated carbons in aqueous solutions, Carbon 38 (2000)863-869.

[7] Nakagawa, K., Namba, A., Mukai, S.R., Tamon, H., Ariyadejwanich, P., Tanthapanichakoon, W., Adsorption of phenol and reactive dye from aqueous solution on activated carbons derived from solid wastes, Water Research 38 (2004) 1791-1798

[8] Tamai, H., Yoshida, T., Sasaki, M., Yasuda, H.,Dye adsorption on mesoporous activated carbon fiber obtained from pitch containing yttrium complex, Carbon 37 (1999) 983-989.

[9] Tanthapanichakoon, W., Ariyadejwanich, P., Japthong, P., Nakagawa, K., Mukai, S.R., Tamon, H., Adsorption-desorption characteristics of phenol and reactive dys from aqueous solution on mesoporous activated carbon prepared from waste tires, Water Research 39 (2005) 1347-1353.

[10] Helleur, R., Popovic, N., Ikura, M., Stanciulescu, M. and Liu, D., Characterization and potential applications of pyrolytic char from ablative pyrolysis of used tire, Journal of Analytical and Applied Pyrolysis, Vol 58-59, pp 813-824, 2001.

[11] Ariyadejwanich, P., Tanthapanichakoon, W., Nakagawa, K., Mukai, S.R. and Tamon, H., Preparation and characterization of mesoporous activated carbon from waste tires, Carbon, Vol 40-41, pp 157-164, 2003.

[12] Miguel, G.S., Fowler, G.D. and Sollars, C.J., A study of the characteristics of activated carbons produced by steam and carbon dioxide activation of waste tyre rubber, Carbon 41, pp 1009-1016, 2003.

[13] Tseng, R.L., Tseng, S.K. and Wu F.C, Preparation of high surface area carbons from corncob with KOH etching plus CO2 gasification for the adsorption of dyes and phenols from water, Colloids and Surfaces, Vol 279, pp 69-70, 2006.

[14] Wu, F.C. and Tseng, R.L., Preparation of highly porous carbon from fir wood by KOH etching and CO2 gasification for adsorption of dyes and phenols from water, Colloids and Interface Science, Vol 294, pp 21-30, 2006.

[15] Wu, F.C., Tseng, R.L. and Juang, R.S., Preparation of highly microporous carbons from fir wood by KOH activation for adsorption of dyes and phenols from water, Separation purification Technology, Vol 47, pp 10-19, 2005.

[16] Srivastava, V.C., Swamy, M.M., Mall, I.D., Prasad, B., Mishra, I.M., Adsorptive removal of phenol by bagasse fly ash and activated carbon: Equilibrium, kinetics and thermodynamics, Colloids and Surfaces, Vol 272, pp 89-104, 2006.

[17] Roostaei, N. and Tezel, F.H.,Removal of phenol from aqueous solutions by adsorption, Journal of Environment Management 70 (2004) 157-164.

[18] Rengaraj, S., Moon, S.H., Sivabalan, R., Arabindoo, B., Murugesan, V., Agricultural solid waste for the removal of organics: adsorption of phenol from water and wastewater by palm seed coat activated carbon, Waste Management 22 (2002) 543-548.

[19] Kennedy, L.J., Vijaya, J.J., Kayalvizhi, K., Sekaran, G., Adsorption of phenol from aqueous solutions using mesoporous carbon prepared by two stage process, Chemical Engineering Journal , 2007.

[20] Aktas, O. and Cecen, F., Adsorption, Desorption and bioregeneration in the treatment of 2-chlorophenol with activated carbon, Journal of Hazardous Materials 141 (2007) 769-777.

PRODUCTION OF ACTIVATED CARBONS FROM PYROLYSIS OF WASTE TYRES IMPREGNATED WITH POTASSIUM HYDROXIDE (KOH) AND INFLUENCE OF OPERATING VARIABLES

By

LEE FOO LOON

Thesis submitted in partial fulfillment of the requirements for the degree of Bachelor of Chemical Engineering

May 2006

ABSTRACT

Activated carbons are prepared from many carbonaceous materials such as biomass and organic wastes. Pyrolysis is an established technique for the disposal different kinds of solid wastes including the tire, polymer and rubber wastes. Since very limited work pertaining to the utilization of the waste tires into activated carbon has been reported in literature especially by using the chemical activation method with potassium hydroxide (KOH) acts as activating agent, the present work is to study the influence of activation temperature (500 – 800°C) and activation time (60, 90 and 120 min) at a fixed impregnation ratio (KOH : tire) of 4 on the production of activated carbon from scrap tires by pyrolysis impregnated with potassium hydroxide. Experiments were conducted in a lab scale muffle furnace under the purging of pure nitrogen. The precursor material with impregnation agent is pyrolyzed under a prescribed condition. A yield of activated carbon of 86.7% is obtained for pyrolysis temperature of 800°C. This resulted the activation temperature of 800°C is the optimum temperature for production of activated carbon. The adsorption capacity in methylene blue and phenol are estimated by using spectrophotometer. It was found that maximum methylene blue number of 146 was obtained while the maximum adsorption capacity of phenol was 20.9 mg/g AC. The adsorption of adsorbates is found to increase with increase in activation temperature or with decrease in the yield of activated carbon. Adsorption Isotherms of activated carbons prepared from waste tires are then determined. Based on the adsorption tests conducted by adsorption of activated carbons on methylene blue and phenol solution, it follows Langmuir adsorption Isotherm with favorable adsorption effectiveness.

CHAPTER 5

RESULTS AND DISCUSSION

5.1 CHARACTERISTICS OF THE SAMPLE PYROLYSED

Tires are composed of variety of components such as rubbers, carbon blacks, steel, minor inorganic compounds, volatile and non-volatile organic compounds. These components are heterogeneously distributed along the tire **[31]**. Besides that, tires contain vulcanized rubber and various reinforced materials. For example, a styrene–butadiene copolymer (SBR) or a mixture of natural rubber and SBR are most commonly used as the vulcanized rubber **[32]**. In order to dispose of invariable and representative samples of the whole tire, cross-section pieces of 1-2 cm wide of a commercial car tire were used for this pyrolysis experiments. A typical composition for the tire used in this experiment is shown in Table 5.1.

Table 5.1: Typical composition of tire which is used throughout this pyrolysis experiment.

Component	**Weight %**
Styrene-butadiene copolymer (SBR)	62.1
Carbon black	31.0
Extender oil	1.9
Zinc oxide	1.9
Stearic acid	1.2
Sulfur	1.1
Accelerator	0.7
Total	99.9

In order to study the characteristics and properties of the tire pieces (samples) used for the experiments, thermogravimetric analyses were carried out with the prepared samples using thermogravimetric analyzer (TGA) model Perkin Elmer from USA. In a

thermogravimetric analysis, the mass of sample is recorded continuously as its temperature is increased linearly from ambient to as high as 850°C. A platinum pan was used to hold the sample. Oxygen was flowed through the analyzer which was heated from 30°C to 850°C at a rate of 20°C/min. A plot of mass as a function of temperature (a thermogram) provides both qualitative and quantitative information. Figure 5.1 and Appendix A show a recorded thermogram obtained by increasing the temperature of 5.213 mg tire in a flowing stream of oxygen at a rate of 20°C/min.

It can be observed from Figure 5.1 that a significant weight loss from ~90 wt% to ~35 wt% which corresponding to the temperature changes from 370°C to 520°C and finally stopped at 850°C. Hence, the yield of tire carbonization is approximately equal to 33.3%. The observation implies that the tires are pyrolysed effectively in the temperature range from 370°C to 850°C. However, it has been proved that the pyrolytic char obtained at 300°C and 400°C is not fully pyrolysed which is based on the observation that the product is still rubbery **[31]**.

On the contrary, a char yield of 35% has been reported by previous researches **[17]** at 500°C and activation time of 120 minutes. Previous studies **[33]** reported fraction of char yield ranges between 38.6% to 36.7% for corresponding temperature ranges from 500°C to 700°C. All the activation pyrolysed for 120 minutes. Another study **[34]** reported char yield ranges from 25 wt% to 60 wt% for corresponding temperature ranges between 500°C and 800°C, while the pyrolysis time was not mentioned. In addition, previous work **[31]** has been proved that tire decomposition at 500°C, 600°C and 700°C is complete and that ≈ 34% of char and carbonaceous material has been formed. This pyrolysis experiments were carried out in nitrogen atmosphere, using an unstirred stainless steel autoclave and the system was maintained for 30 minutes.

To compensate for the above phenomenon, temperature ranges from 500°C to 800°C were used to study the effects of different pyrolysis temperatures on the production of activated carbon throughout the experiment.

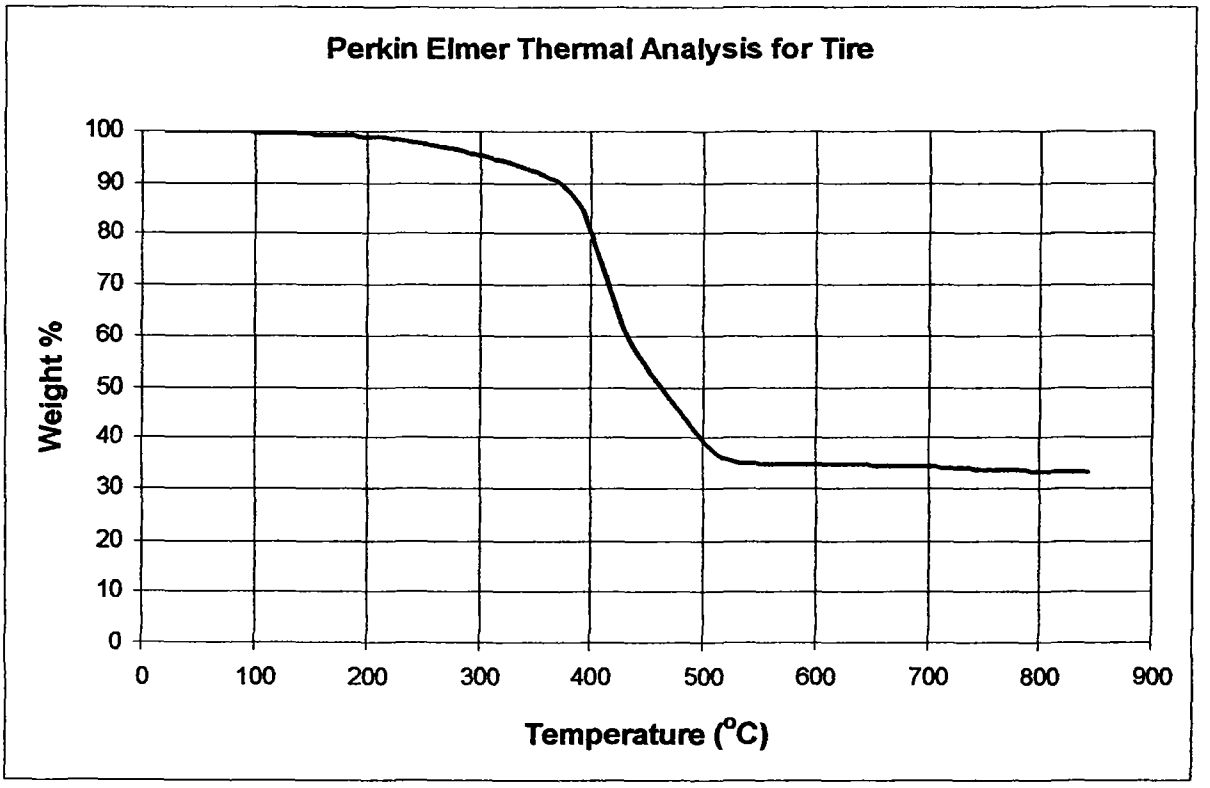

Figure 5.1: Thermogram for carbonization of 5.213 mg tire. Thermogravimetric analyzer (TGA) model Perkin Elmer was used (oxygen flow rate = 20°C/min) to heat sample from 30°C to 850°C.

In the first part of the experiment, preparation of activated carbons was conducted. In order to study the effects of pyrolysis activation temperature and effects of activation time on the production of activated carbons impregnated by potassium hydroxide (KOH) with the fixed KOH/tire mass ratio of 4, twelve samples were prepared at different temperature and activation time. Pyrolysis experiments were carried out in nitrogen atmosphere, using batch muffle furnace. The nitrogen is passed through at a rate of 100

ml/min and the system is heated at a rate (ranging from 5°C/min to 80°C/min) to the desired temperature and then to the desired activation time. Table 5.2 summarizes preparation of the sample at different conditions.

Table 5.2: Preparation of samples at different conditions impregnated by potassium hydroxide (KOH) with the fixed KOH/tire mass ratio of 4 (tire diameter 1-2 cm).

Sample no.	Experimental conditions			
	Weight of tire (g)	Weight of KOH pellet (g)	Activation temperature (°C)	Activation time (min)
1	7	28	500	60
2	7	28	500	90
3	5	20	500	120
4	7	28	600	60
5	5	20	600	90
6	5	20	600	120
7	7	28	700	60
8	5	20	700	90
9	5	20	700	120
10	7	28	800	60
11	5	20	800	90
12	5	20	800	120

5.2 YIELD OF ACTIVATED CARBON

Activated carbon was obtained after pyrolysis of scrap tires by using potassium hydroxide (KOH) as activating agent. A fixed amount of tires and pellet KOH was prepared to be placed in the batch muffle furnace. Pyrolysis was carried out at 500°C, 600°C, 700°C and 800°C in nitrogen atmosphere. Nitrogen was passed through at a rate of 100 ml/min and the sample was heated to the desired temperature and desired activation time (60 min, 90 min and 120 min). The pyrolysed samples were washed repeatedly (filtration) with distilled water until free of chloride ions (determined by the conductivity reading of the filtrate). Once the activating agent was removed (if the conductivity of the filtrate is less than 10 μs), the sample was dried at 105°C until it was bone-dried.

The purpose of washing the pyrolysed sample was to ensure that all the KOH used for activation was removed before the carbon was taken for characterization. Previous study **[13]** has shown that the unwashed sample does not show any N_2 adsorption. This happened due to the porosity created in the carbon samples was blocked by the potassium compounds that must be removed to obtain an accessible microporosity.

The washing step is the last stage in the preparation of a chemically activated carbon. Most of the study **[13, 14, 16, 35, 36]** has the common washing stage, which is the pyrolysed mixture was leached in water and acid solutions to remove the chemical activating agent. In the present study, the pyrolysed mixture only washed several times by distilled water as previous study **[13]** has concluded that an acid washing could be avoided because the results are not very different from those obtained with water washing.

To discuss the effects of activation temperature on the yield of activated carbon, a correlation has to be set up. In conjunction with that, the yield of activated carbon was estimated according to the correlation below:

$$\text{Activated carbon yield (\%)} = \left(\frac{W_{ac}}{W_{tire}}\right) \times 100 \qquad (6)$$

where W_{ac} and W_{tire} are the weights of the activated carbon produce and weight of tires, respectively. Figure 5.2 shows the effects of activation temperatures on the yield of activated carbon obtained at different activation time at impregnation ratio of 4. In addition, Appendix B shows the tabulated data collected to produce Figure 5.2 during the experiments were conducted. It also shows the sample of calculation of the yield of activated carbon by using correlation (6).

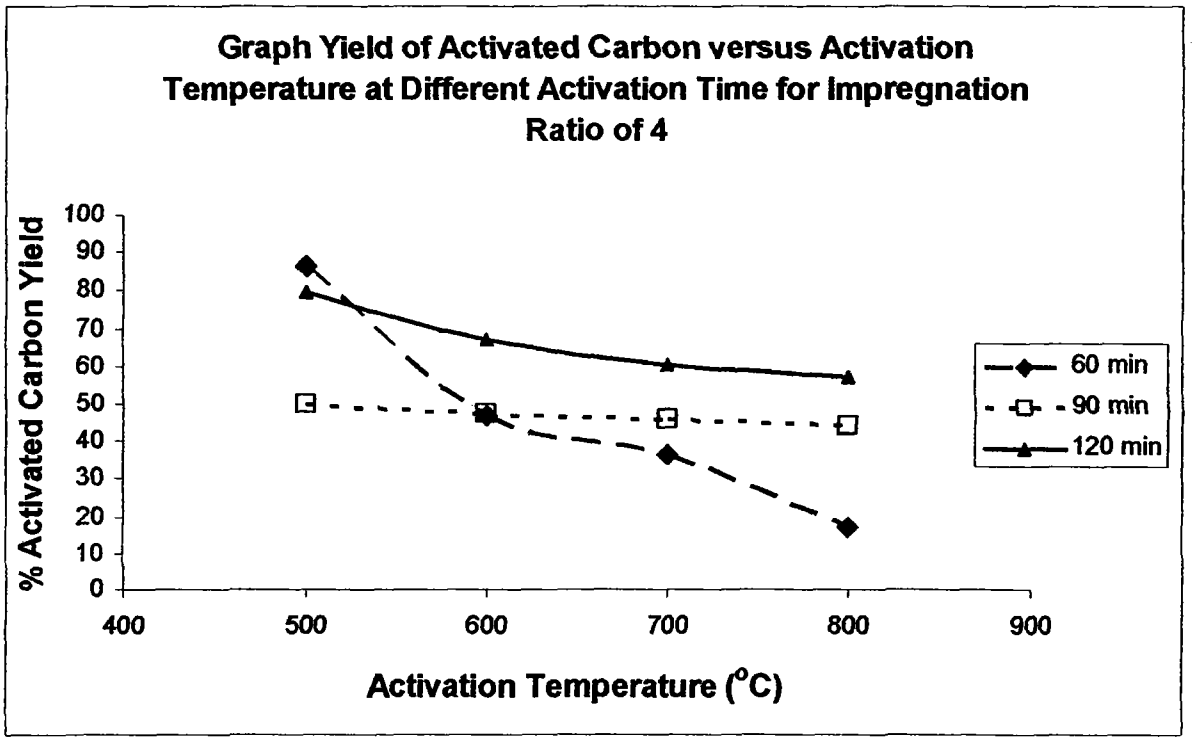

Figure 5.2: Effect of activation temperatures on the yield of activated carbon for different activation time at impregnation ratio of 4.

Figure 5.2 shows that the activated carbon yield is a decreasing function of the activation temperature. For 60 minutes activation time, the yield of activated carbon is decreased from 86.7% to 17.3% when the activation temperature is increased from 500°C to 800°C. While the yield of activated carbon for 90 minutes activation time is decreased from 50.0% to 44.4% and the yield of activated carbon for 120 minutes activation time is decreased from 79.5% to 57.5% when the activation temperature is decreased from 500°C to 800°C. This is expected as the carbon consumption and amount of volatiles released is increased with increasing activation temperature due to the C-KOH reaction **[9]**. Previous research **[36]** has proved that the increased of carbon gasification by CO_2 or oxygen in the alkali was attributed to the decrease in carbon yield with temperature. It also has been reported that at high temperatures the release of CO_2 from K_2CO_3 formed during carbonization becomes significant **[37]**. Previous researches **[14]** have stated that the evolved CO_2 can react with carbon atoms to open up closed pores and enlarge existing micropores, resulting in the increase in porosity.

Apart from the gasification by CO_2, at a temperature higher than 700°C, the potassium-containing compounds (such as K_2O and K_2CO_3) can be reduced by carbon to form K metal **[36]**, thus causing the carbon gasification and the oxidation. Based on the previous work, previous researches **[14]** have summarized that alkaline surface salt complexes can be formed through the interaction between KOH and carbonaceous materials at low temperatures. These complexes are the active sites in gasification.

5.3 ADSORPTION CHARACTERISTICS OF ACTIVATED CARBON

Adsorption tests were conducted on the activated carbon produced from various activation time and activation temperatures with the aim of producing further evidence about their porous structure and also for assessing potential applications in the water treatment industry. Phenol and methylene blue are commonly used to characterize the adsorption capacity of activated carbons.

5.3.1 Adsorption of Methylene Blue and Phenol Solution

To study the adsorptive behaviors of the activated carbons on methylene blue, the equilibrium adsorption capacities (q_e) at different adsorbate concentrations were determined according to the mass balance on the adsorbate by using Equation (2) in Section 3.5. In the present study, the porosity or the adsorption capacity of the activated carbon is measured using methylene blue number in terms of milligrams of methylene blue adsorbed by gram of carbon (mg/g AC).

Figure 5.3 and Figure 5.4 show the effect of activation temperatures on the methylene blue number and adsorption of phenol for different activation time at impregnation ratio of 4, respectively. Appendix C and Appendix D show calibration data and curves for methylene blue and phenol, respectively. Appendix E shows the tabulated data and sample of calculation that is used to obtain Figure 5.3 and Figure 5.4.

Figure 5.3 and Figure 5.4 exhibit a common trend of the effect of activation temperatures on the adsorbates, which is an increasing trend from 500°C to 800°C for activation time of 60 min, 90 min and 120 min. It is expected that the increasing trend was observed.

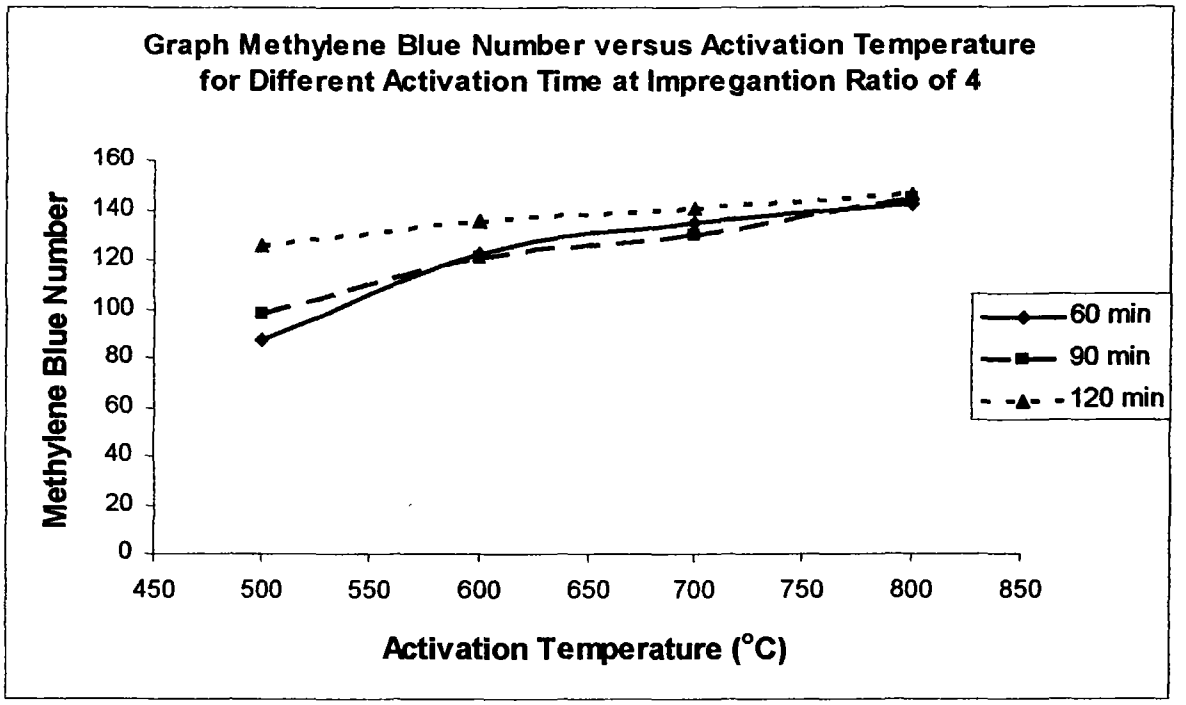

Figure 5.3: Effect of activation temperatures on the methylene blue number for different activation time at impregnation ratio of 4.

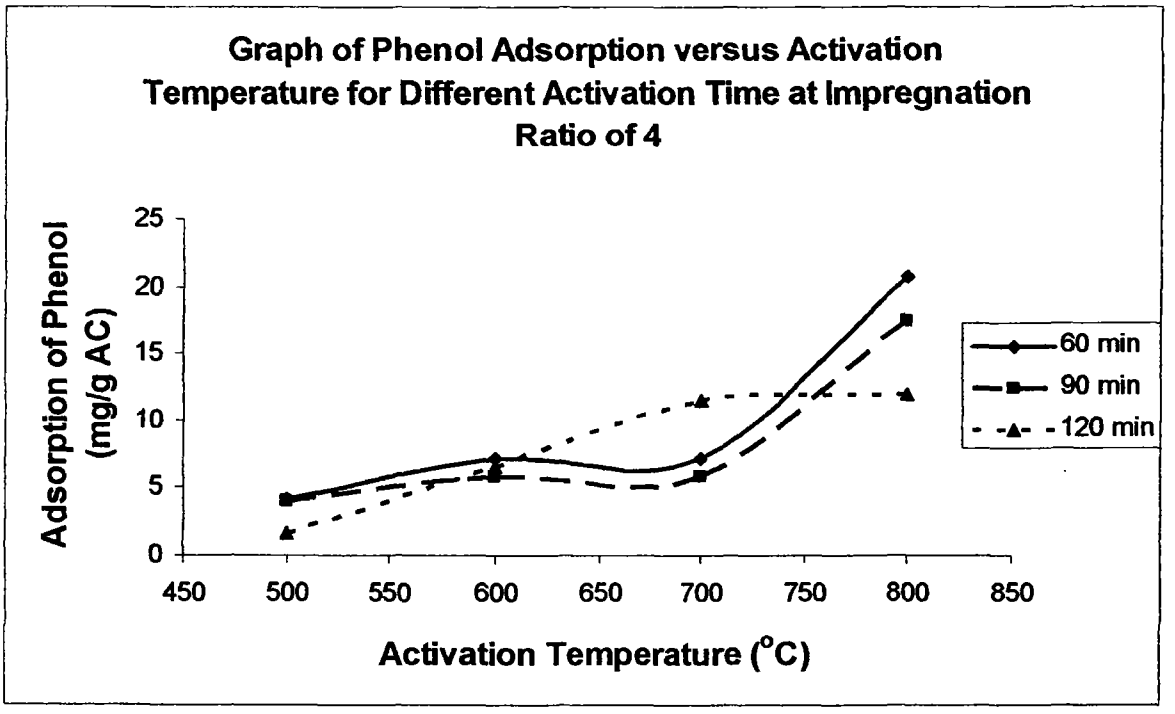

Figure 5.4: Effect of activation temperatures on the adsorption of phenol for different activation time at impregnation ratio of 4.

If refer to Figure 5.2 which showed a decrease in yield of activated carbon with increase in the activation time, it can be interpreted that with decrease in the yield of activated carbon the adsorption capacity of the adsorbates is found to increase.

From Figure 5.3, it is observed that at activation temperature of 800°C, the methylene blue number is increased when the activation time is increased. It can be expected that quality of the carbon produce was improved with further increase in the activation time. However, this increasing trend does not show in Figure 5.4 for activation temperature of 800°C. This could happen mainly due to the impurities found in the activated carbon especially the broken pieces of porcelain bowl.

In a nutshell, a maximum methylene blue number of 146 at activation temperature of 800°C and activation time of 120 minutes are obtained while the maximum adsorption capacity of phenol is 20.9 mg/g AC for at activation temperature of 800°C and activation time of 60 minutes. A methylene blue number in excess of 200 mg/g of carbon in commercial market is regarded as carbon with good adsorption capacity and it has good market demand.

5.3.2 Adsorption Equilibrium

Methylene blue and phenol are commonly used to characterize the adsorption capacity of activated carbons. Figure 5.5 (a), (b) respectively show the sorption isotherms for methylene blue and phenol on activated carbons for different temperature at activation time of 60 minutes. Figure 5.6 (a), (b) respectively show the sorption isotherms for methylene blue and phenol on activated carbons for different temperature at activation time of 90 minutes. Figure 5.7 (a), (b) respectively show the sorption isotherms for methylene

blue and phenol on activated carbons for different temperature at activation time of 120 minutes.

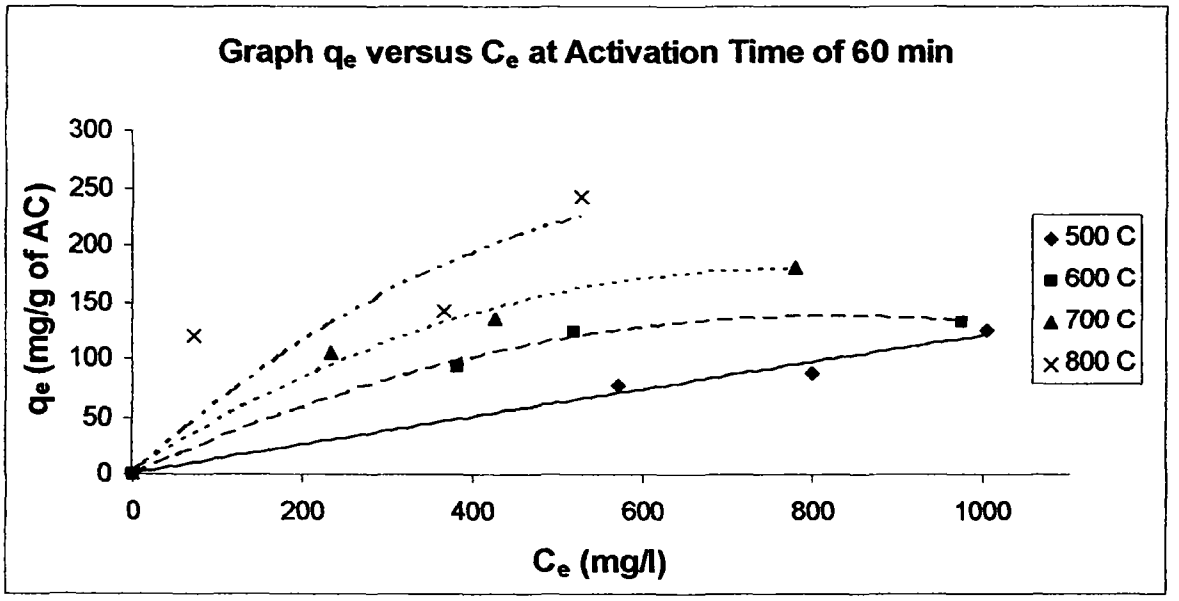

Figure 5.5 (a): Adsorption isotherms of methylene blue for different activation temperature at activation time of 60 minutes.

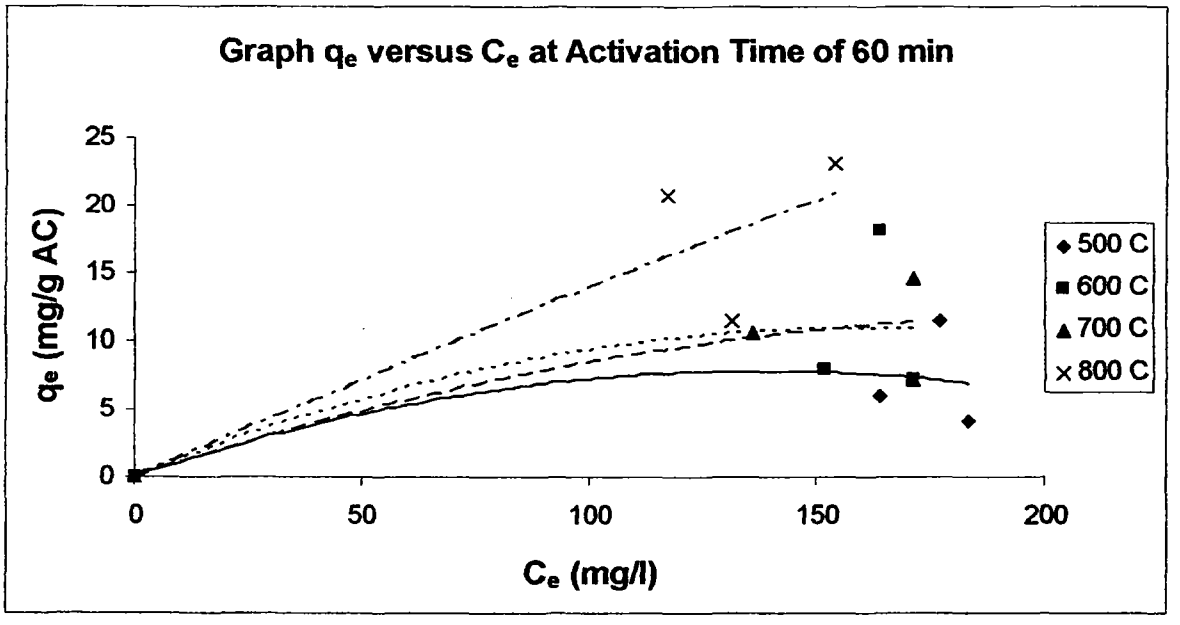

Figure 5.5 (b): Adsorption isotherms of phenol for different activation temperature at activation time of 60 minutes.

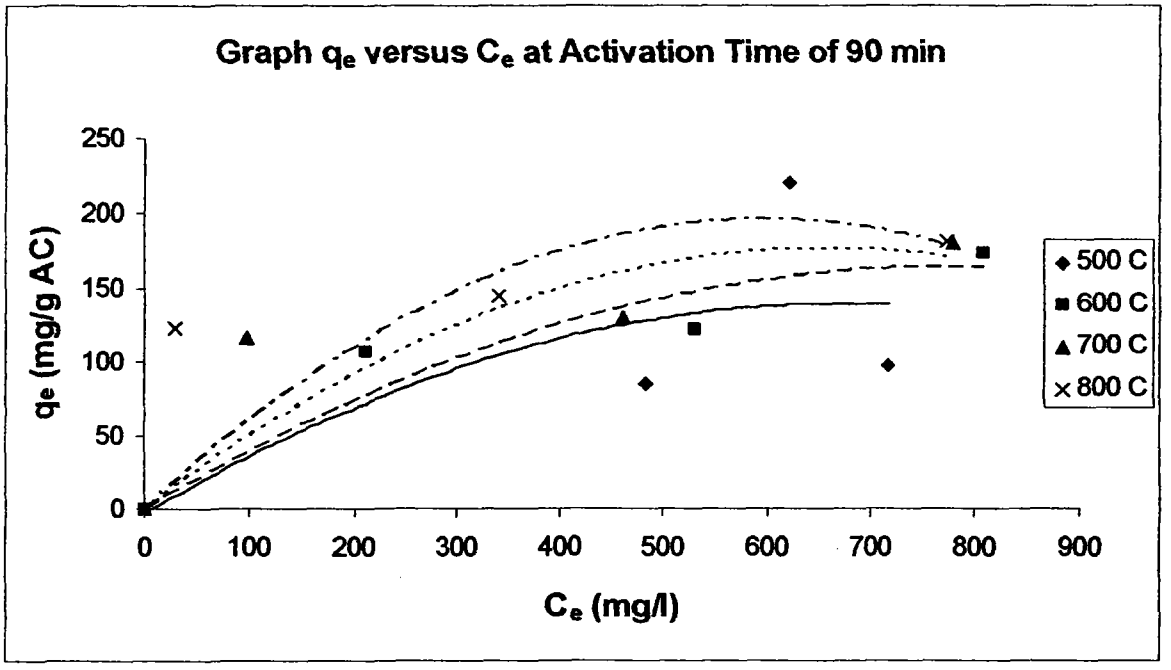

Figure 5.6 (a): Adsorption isotherms of methylene blue for different activation temperature at activation time of 90 minutes.

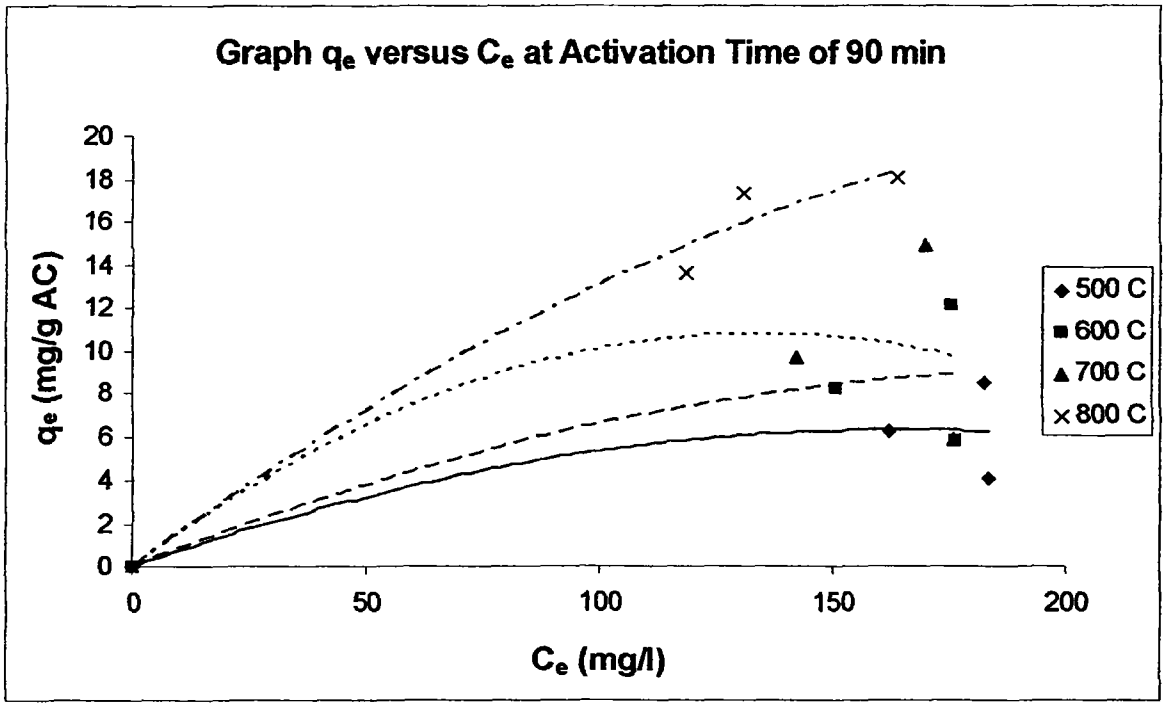

Figure 5.6 (b): Adsorption isotherms of phenol for different activation temperature at activation time of 90 minutes.

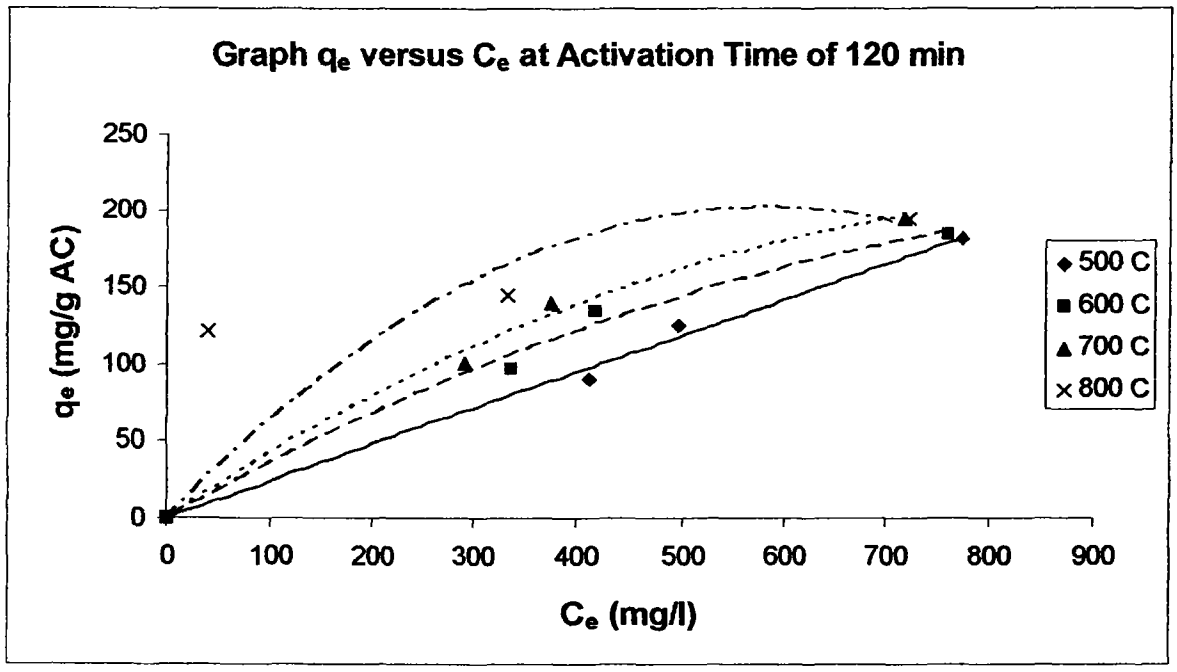

Figure 5.7 (a): Adsorption isotherms of methylene blue for different activation temperature at activation time of 120 minutes.

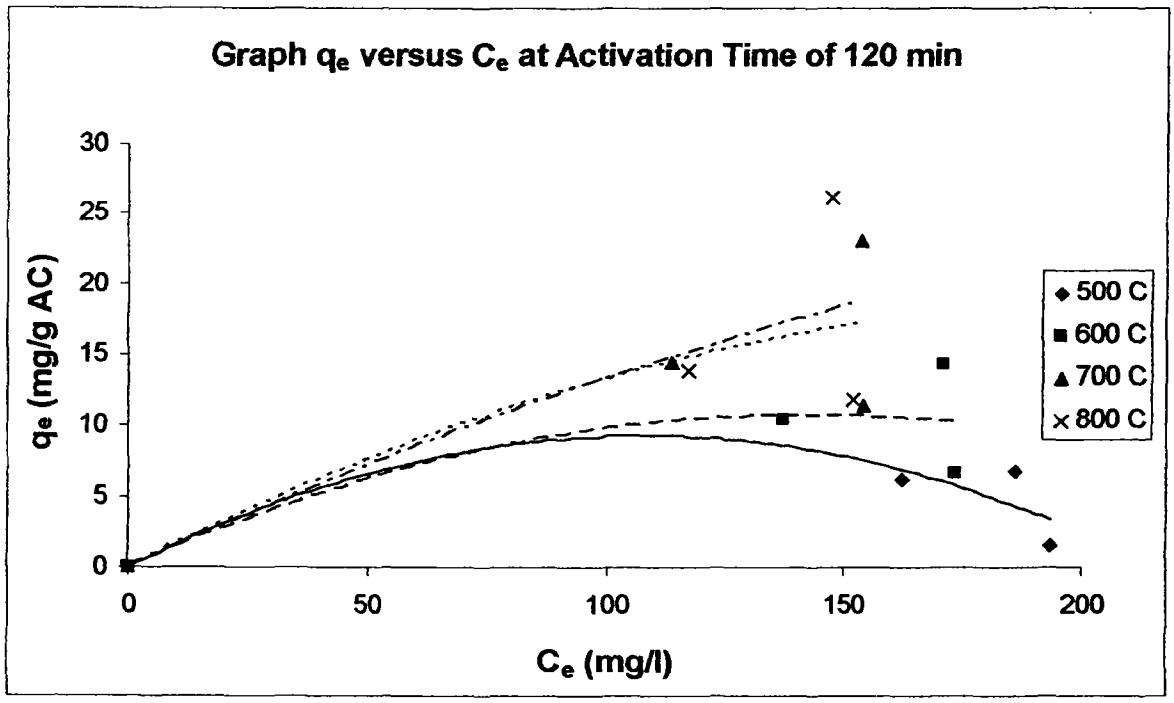

Figure 5.7 (b): Adsorption isotherms of phenol for different activation temperature at activation time of 120 minutes.

From Figure 5.5, 5.6 and 5.7, they show L-type which the shape of the isotherm is a gradual positive curve that flattens to a constant value. However, the L-type was not exactly shown by some of the curves. This is mainly due to only three samples were taken for adsorption isotherms test. Generally, the adsorption isotherms of methylene blue and phenol onto carbon surfaces are of Langmuir type. Because of the strong interaction between the heteroatom-containing groups on the carbon surface and the positive charges on the methylene blue molecules **[32]**, it is possible that the adsorption is site-specific and thus a monolayer is formed.

In the range of equilibrium concentrations shown in Figure 5.5, 5.6 and 5.7, the equilibrium adsorption capacity, q_e at each activation time is generally increases.

After linearization of these isotherms as described above, all the coefficients of the models of Langmuir and Freundlich have been evaluated by linear regression and reported in Tables 5.3 and 5.4. The plots of linearization of these isotherms are shown in Appendix F. In addition, it shows a sample of calculation of the isotherms constants by using Equations in Section 3.5.

Table 5.3 (a): Values of constants for the models of Langmuir and Freundlich. These values were obtained from adsorption of methylene blue in aqueous solution for different activation temperature at activation time of 60 minutes.

Activation temperature (°C)	Langmuir constants				Freundlich constants		
	Q_0 (mg/g)	b (l/mg)	R_L	r^2	$1/n$	k	r^2
500	588.24	0.00025	0.728	0.1838	0.8071	0.442	0.8686
600	169.49	0.00383	0.148	0.9659	0.3302	14.013	0.7507
700	263.16	0.00269	0.199	0.9868	0.4432	9.341	0.9969
800	263.16	0.00693	0.088	0.7230	0.2806	34.381	0.6457

Table 5.3 (b): Values of constants for the models of Langmuir and Freundlich. These values were obtained from adsorption of methylene blue in aqueous solution for different activation temperature at activation time of 90 minutes.

Activation temperature (°C)	Langmuir constants				Freundlich constants		
	Q_0 (mg/g)	b (l/mg)	R_L	r^2	$1/n$	k	r^2
500	196.08	0.00230	0.225	0.0678	0.7450	1.040	0.0835
600	217.39	0.00353	0.159	0.8600	0.3213	18.392	0.7827
700	192.31	0.00866	0.071	0.9279	0.1770	50.039	0.7132
800	188.68	0.02129	0.030	0.9847	0.1080	83.421	0.8698

Table 5.3 (c): Values of constants for the models of Langmuir and Freundlich. These values were obtained from adsorption of methylene blue in aqueous solution for different activation temperature at activation time of 120 minutes.

Activation temperature (°C)	Langmuir constants				Freundlich constants		
	Q_0 (mg/g)	b (l/mg)	R_L	r^2	$1/n$	k	r^2
500	362.54	0.00640	1.073	0.0285	1.0438	0.179	0.9660
600	526.32	0.00074	0.475	0.7095	0.7369	1.434	0.9215
700	454.55	0.00106	0.387	0.8447	0.6882	2.167	0.9355
800	204.08	0.01525	0.042	0.9708	0.1450	69.519	0.8506

Table 5.4 (a): Values of constants for the models of Langmuir and Freundlich. These values were obtained from adsorption of phenol in aqueous solution for different activation temperature at activation time of 60 minutes.

Activation temperature (°C)	Langmuir constants				Freundlich constants		
	Q_0 (mg/g)	b (l/mg)	R_L	r^2	$1/n$	k	r^2
500	1.64	0.00786	0.389	0.1748	-1.4269	10428.524	0.0255
600	7.14	0.02563	0.163	0.0330	0.4368	1.097	0.0027
700	6.97	0.02121	0.191	0.1905	-0.1839	26.293	0.0048
800	163.93	0.00085	0.854	0.0013	0.6360	0.782	0.0527

Table 5.4 (b): Values of constants for the models of Langmuir and Freundlich. These values were obtained from adsorption of phenol in aqueous solution for different activation temperature at activation time of 90 minutes.

Activation temperature (°C)	Langmuir constants				Freundlich constants		
	Q_0 (mg/g)	b (l/mg)	R_L	r^2	$1/n$	k	r^2
500	2.68	0.01067	0.319	0.1308	-0.6223	149.830	0.0140
600	5.43	0.01898	0.209	0.1033	-0.0126	8.845	0.0000
700	5.43	0.01058	0.321	0.2553	0.1072	9.047	0.0012
800	60.61	0.00267	0.652	0.2279	0.7465	0.413	0.6618

Table 5.4 (c): Values of constants for the models of Langmuir and Freundlich. These values were obtained from adsorption of phenol in aqueous solution for different activation temperature at activation time of 120 minutes.

Activation temperature (°C)	Langmuir constants				Freundlich constants		
	Q_0 (mg/g)	b (l/mg)	R_L	r^2	$1/n$	k	r^2
500	0.42	0.00641	0.438	0.4779	-5.6420	217.20	0.3974
600	5.27	0.01898	0.260	0.2354	-0.4656	105.731	0.0249
700	17.95	0.03687	0.119	0.1299	0.3704	2.509	0.0340
800	21.60	0.01821	0.215	0.0601	0.6665	0.609	0.0524

From Table 5.3 and Table 5.4, the coefficients Q_0 and b of the Langmuir model were obtained with low regression coefficient. However, if compared to Freundlich model which have lower regression coefficients, it can be conclude that the Langmuir model yields a better fit than the Freundlich model for adsorption tests of methylene blue and phenol solution. Generally, the Langmuir model has low regression coefficient for the above adsorption tests. This is mainly due to human errors when preparing the solution of methylene blue and phenol. Besides that, the consistency in preparation and conduction the adsorption test was low.

From Table 5.3 and 5.4, it is observed that the entire sample tested at all activation temperature show the favorable effectiveness of an adsorption as $0 < R_L < 1$. In addition,

most of the sample tested show the situation $1/n < 1$. As mentioned in Section 3.5, this is the most common and corresponds to a normal Langmuir isotherm i.e. of L-type. Previous study **[12]** has reported that the slope $1/n$, ranging between 0 and 1 is a measure of adsorption intensity or surface heterogeneity, becoming more heterogenous as its value gets closer to zero.

5.3.3 Activation Mechanism

A lot of studies have been carried out in the area of chemical activation using potassium hydroxide. Previous researchers **[9]** studied the effect of KOH on different cokes and stated that the presence of oxygen in the alkali resulted in the removal of cross-linking and stabilizing of carbon atoms in the crystallites. Potassium metal liberated at the reaction temperatures may intercalate and force apart the separate lamellae of the crystallite. Removal of these potassium salts (by washing) and carbon atoms (by activation reaction) from the internal volume of the carbon creates the micropores in the structure.

Previous researchers **[38]** studied the activation mechanism of high surface area carbon from petroleum coke by KOH activation. They found that considerable amounts of K_2CO_3 and hydrogen were formed and only a small amount of CO_2 was contained in the effluent gas. Also, they concluded that high temperature would cause several atomic layers of carbon being widened and hence, forming large pores. Some possible reactions were proposed:

$$2\,KOH \rightarrow K_2O + H_2O \text{ (dehydration)} \quad (7)$$

$$C + H_2O \rightarrow H_2 + CO \text{ (water-gas reaction)} \quad (8)$$

$$CO + H_2O \rightarrow H_2 + CO_2 \text{ (water-gas shift reaction)} \quad (9)$$

$$K_2O + CO_2 \rightarrow K_2CO_3 \text{ (carbonate formation)} \quad (10)$$

When the activation temperature exceeds 700°C, a considerable amount of metallic potassium is formed due to the following possible reactions:

$$K_2O + H_2 \rightarrow 2\,K + H_2O \text{ (reduction by hydrogen)} \quad (11)$$

$$K_2O + C \rightarrow 2\,K + CO \text{ (reduction by carbon)} \quad (12)$$

Dr Ridzuan

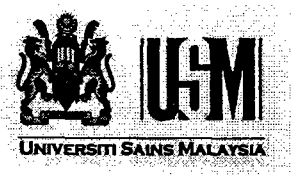

UNIVERSITI SAINS MALAYSIA
SCHOOL OF CHEMICAL ENGINEERING
ENGINEERING CAMPUS

THE STUDY ON THE INFLUENCES OF OPERATING VARIABLES IN THE PRODUCTION OF ACTIVATED CARBON FROM WASTE SCRAP TYRES

CATHERINE LIM
Matric No.: **70471**

April 2006

ABSTRACT

This final year project presents a study on the influences of activation time and impregnation ratio in the production of activated carbon from waste scrap tyres. The activated carbons were produced from waste scrap tyres and potassium hydroxide (KOH) was used as an activating agent. Chemical activation was used to produce the activated carbons under the temperature of 800°C. In this project, three series were produced using different activation time: 60min, 90min and 120min. Every series contains fives impregnation ratios from 1 to 5. The adsorption capacity of the activated carbons were tested by using methylene blue and phenol. The influences of different operating variables during chemical activation such as activation time and impregnation ratio on the carbon yield and the adsorption characteristics were explored and the optimum preparation conditions were recommended. A carbon yield ranging from 12.63% to 75.58% was obtained for activation time ranging from 60min to 120min. The highest amount adsorbed for phenol and methylene blue were 30.47mg/g AC and 173.45mg/g AC respectively. The optimum operating condition for preparing the activated carbon is 800°C, 60min and a impregnation ratio of 4. BET surface areas could not be determined and presented in this report because the Autosorb Surface Area Analyzer is out of order.

CHAPTER 4

RESULTS AND DISCUSSION

The activated carbon was obtained from waste scrap tyre by chemical activation and potassium hydroxide (KOH) pellet was used as the activating agent. The waste scrap tyre was activated at 800°C covering different activation time: 60min, 90min and 120 min for the impregnation ratio of 1 to 5. Table 4.1 and Figure 4.1 shows the percent yield of activated carbon produced at 800°C, 60min, 90min and 120min for different impregnation ratio.

Table 4.1. Percent yield of the activated carbon produced at 800°C, 60min, 90min and 120min for different impregnation ratio.

Impregnation Ratio (KOH/Tyre)	Weight of Activated Carbon (g) at 800°C, 60min	Percent Yield (%) at 800°C, 60min	Weight of Activated Carbon (g) at 800°C, 90min	Percent Yield (%) at 800°C, 90min	Weight of Activated Carbon (g) at 800°C, 120min	Percent Yield (%) at 800°C, 120min
1	0.884	12.63	1.312	26.24	1.874	37.48
2	2.739	39.13	2.430	48.60	1.948	38.96
3	3.054	43.63	2.955	59.10	2.608	52.16
4	1.214	17.34	2.221	44.42	2.876	57.52
5	2.829	40.41	2.551	51.02	3.779	75.58

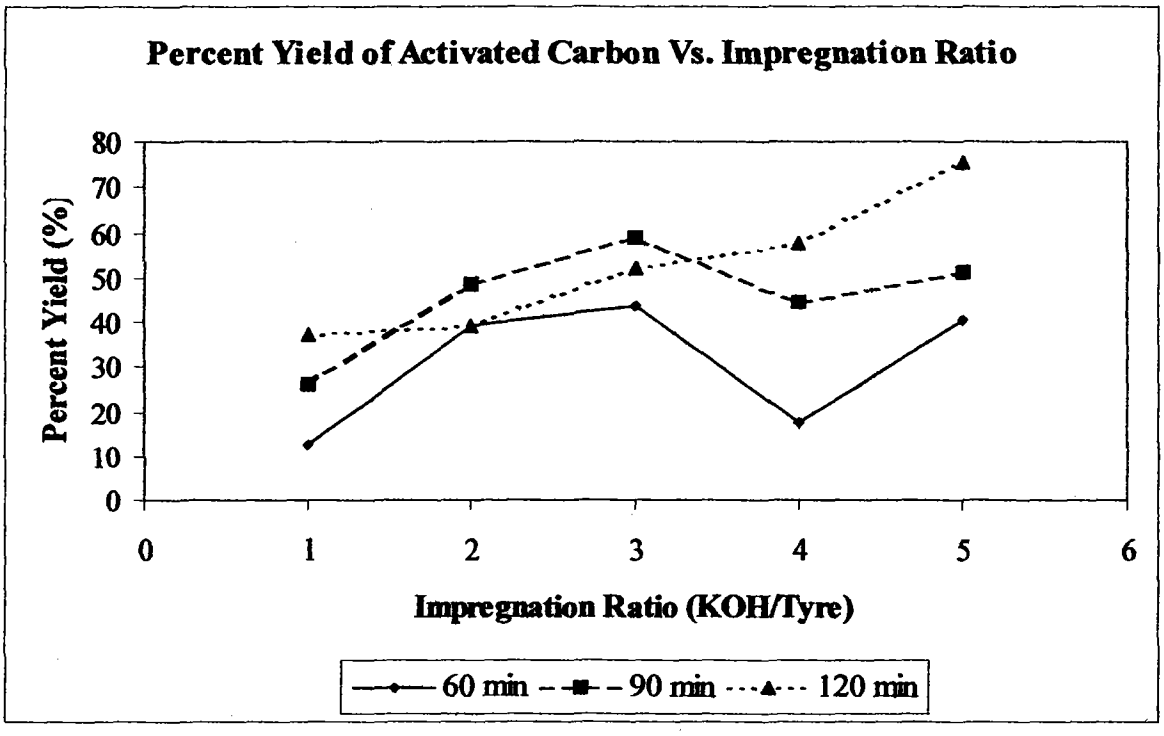

Figure 4.1. Percent yield of activated carbon produced at 800°C, 60min, 90min and 120min versus impregnation ratio (KOH/Tyre).

4.1 Yield of the Activated Carbon Produced from KOH and Tyre

From Table 4.1 and Figure 4.1, the percent yield of activated carbon produced at 800°C at all activation time was found to increase from impregnation ratio of 1 to 5 except for 60min and 90min, the yield decreases from ratio 3 to 4. From Table 4.1 and Figure 4.1 also, the percent yield of all the impregnation ratios were found to increase as the activation time increases from 60min to 120 min except for 90 min where ratio 2 and 3 reported the highest percent yield among the three activation times. However, Teng *et al* (2000) reported that for chemical activation, the carbon yield was found to decrease with the increase in chemical ratio and in activation time. The results obtained were different from literature because some errors occurred during this experiment was carried out like the KOH is a corrosive agent and the porcelain bowl was corroded or broken after it is heated to high

temperature. Some of the pieces of porcelain bowl will be mixed with the activated carbon when the activated carbon is transferred from the porcelain bowl to conical flask and it is hard to be separated from the activated carbon. As a consequence, this will contribute to the percent yield of the activated carbon produced. On the other hand, some of the activated carbon could not be completely taken out from the porcelain bowl and some of it was stuck on the filter paper and hard to be taken out. Ariyadejwanich *et al* (2002) reported a carbonization yield of around 35% for physical activation. From the results of this experiment and the results from journal, it is clearly shown that the carbon yield from chemical activation is more than the yield from physical activation. Besides that, the activated carbon with a much more ordered structure is produced from chemical activation and once the chemical agent is eliminated after the heat treatment, the porosity is so much developed.

4.2 Aqueous Adsorption Capacity of Activated Carbon Produced from KOH and Tyre.

Aqueous adsorption tests were conducted on activated carbon produced at 800°C, 60min, 90min and 120min for different impregnation ratio with the aim of producing further evidence about its porous structure and also for assessing potential applications in the water treatment industry. Phenol is preferentially adsorbed in small and medium sized micropores while methylene blue is mainly adsorbed in medium and large micropores. Table 4.2-4.3 and Figure 4.2-4.3 shows the adsorption capacity for phenol and methylene blue by 0.2g of activated carbon produced at 800°C, 60min, 90min and 120min for different impregnation ratio.

Table 4.2. Concentration of adsorbate (Phenol) for activated carbon produced at 800°C, 60min, 90min and 120min for different impregnation ratio.

Impregnation Ratio (KOH/Tyre)	Concentration of the Adsorbate, q_e at 60min	Concentration of the Adsorbate, q_e at 90min	Concentration of the Adsorbate, q_e at 120min
1	30.47	23.57	5.32
2	27.85	15.86	2.26
3	20.63	6.14	2.16
4	20.68	17.34	11.92
5	13.41	16.98	8.19

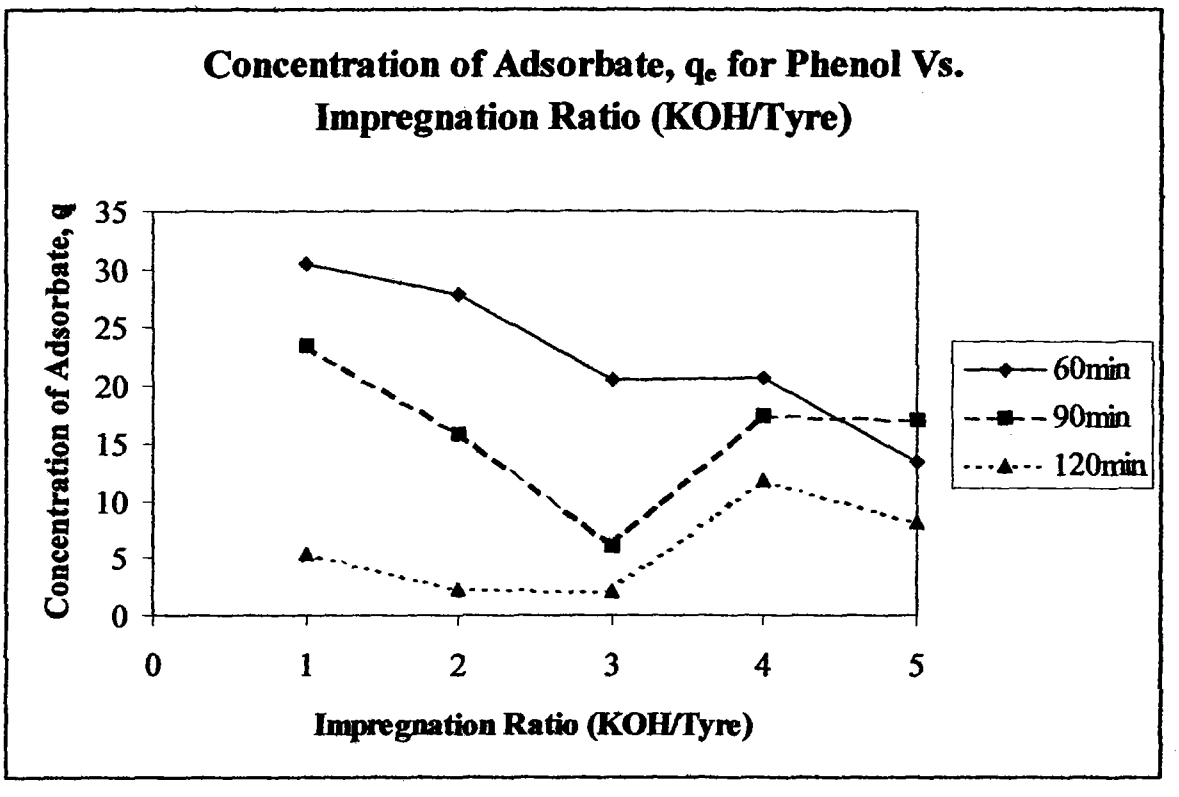

Figure 4.2. Adsorption capacity for phenol by 0.2g of activated carbon produced at 800°C, 60min, 90min and 120min versus impregnation ratio (KOH/Tyre).

Table 4.3. Concentration of adsorbate (Methylene Blue) for activated carbon produced at 800°C, 60min, 90min and 120min for different impregnation ratio.

Impregnation Ratio (KOH/Tyre)	Concentration of the Adsorbate, q_e at 60min	Concentration of the Adsorbate, q_e at 90min	Concentration of the Adsorbate, q_e at 120min
1	132.06	127.29	117.69
2	125.45	117.29	112.34
3	121.14	120.04	105.71
4	141.74	144.76	141.54
5	103.90	173.45	140.17

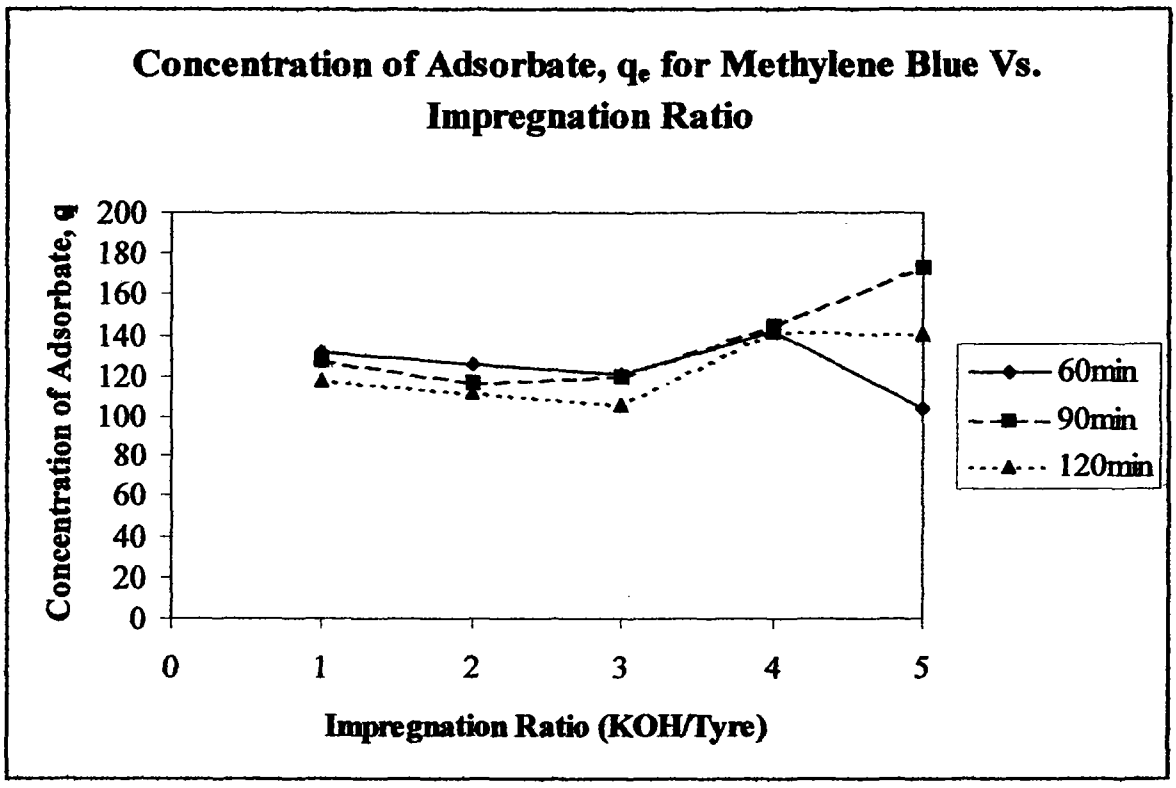

Figure 4.3. Adsorption capacity for methylene blue by 0.2g of activated carbon produced at 800°C, 60min, 90min and 120min versus impregnation ratio (KOH/Tyre).

From Table 4.2-4.3 and Figure 4.2-4.3, it was found that for all the three activation time, the amount adsorbed by both phenol and methylene blue decreased from impregnation ratio of 1 to 3 and then increased from ratio 3 to 4 and then decreased again from ratio 4 to 5. For the activation time of 90min, the amount adsorbed by methylene blue increased from impregnation ratio of 4 to 5 instead of decreased. For both the phenol and methylene blue adsorption, the amount adsorbed was found to decrease with activation time except for the activation time of 90min where ratio 4 and 5 reported the highest amount adsorbed among the three activation times. Phenol adsorption depends not only on the porous properties of the adsorbent but also on its surface properties. Due to its higher ash content, it is reasonable to assume that the surface of the prepared activated carbon was somewhat hydrophilic in nature, leading to a lower phenol adsorption if compare to methylene blue adsorption. The high ash content interfered in filtration thus causing the final conductivity for the ratio of 3 to be the highest among the 5 ratios. As a consequence, the amount adsorbed for impregnation ratio of 3 always reported the lowest among the 5 ratios for both phenol and methylene blue test. This indicates that the porosity created in the activated carbon is blocked by the potassium compounds that must be removed to obtain an accessible microporosity. For phenol test, ratio 1 always reported the highest amount adsorbed by phenol because the KOH is thoroughly removed in washing stage.

4.3 Adsorption Equilibrium

The adsorption isotherms of phenol at 45°C are shown in Figure 4.5-4.7 and the adsorption isotherms of methylene blue at 30°C are shown in Figure 4.11-4.13. There is a widely used two-parameter Langmuir equation given as follows:

$$\frac{C_e}{q_e} = \left(\frac{1}{K_L q_{mon}}\right) + \left(\frac{1}{q_{mon}}\right) C_e \qquad (1)$$

Where q_{mon} = The amount of adsorption corresponding to monolayer coverage

K_L = The Langmuir constant

Based on equation (1), linear plots of $\frac{C_e}{q_e}$ against C_e will give K_L and q_{mon}. On the other hand, a widely used empirical Freundlich equation is shown as follows:

$$\log q_e = \log K_F + \frac{1}{n} \log C_e \qquad (2)$$

where n and K_F are the constants for a given solute-adsorbent system. Both parameters can be obtained from a linear plot of $\log q_e$ against $\log C_e$ from equation (2).

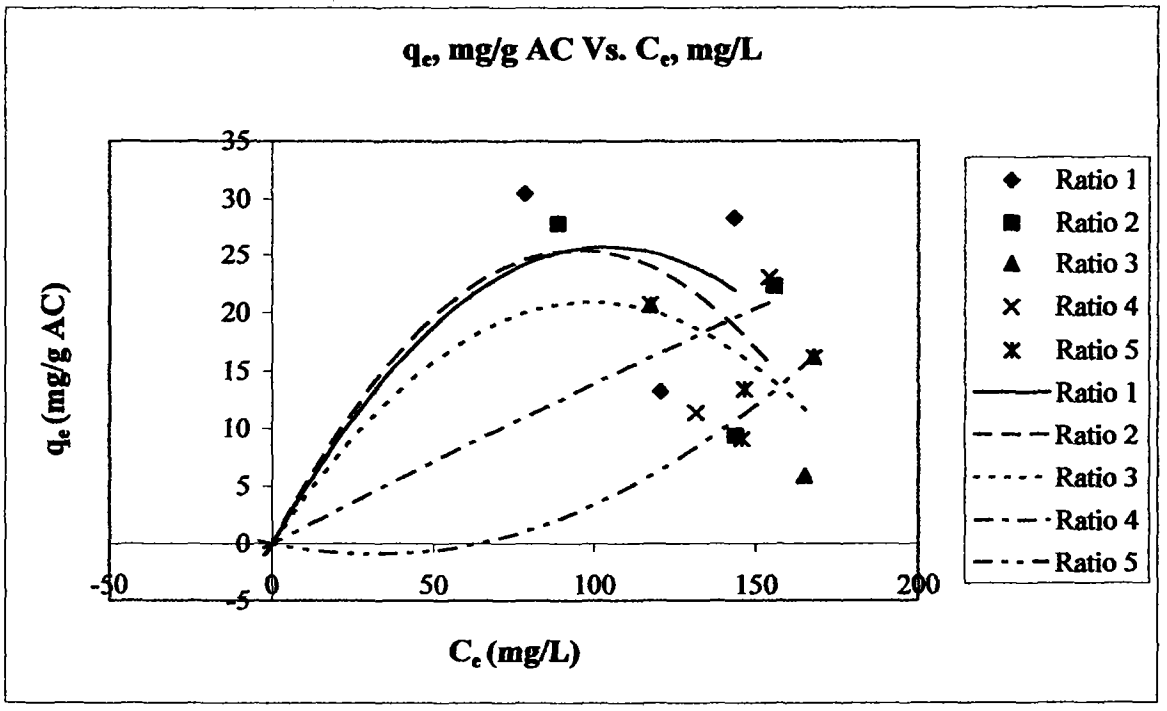

Figure 4.4. Adsorption isotherms of phenol by activated carbon produced at 800°C, 60min of different impregnation ratio (KOH/Tyre).

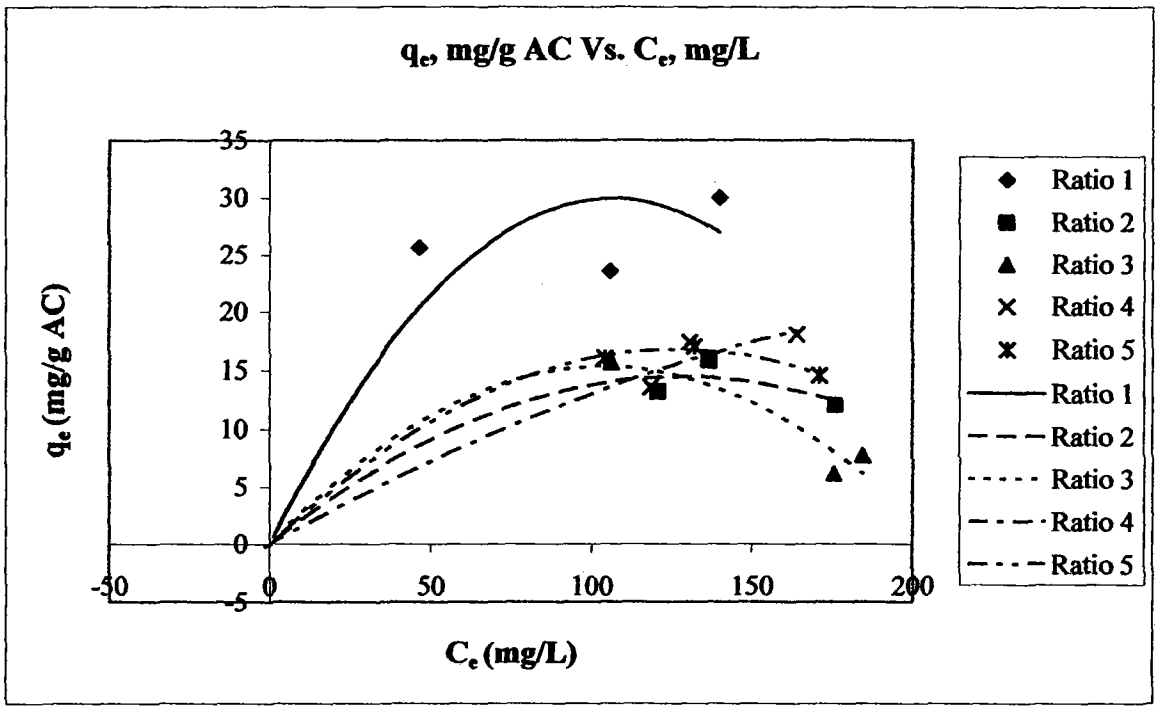

Figure 4.5. Adsorption isotherms of phenol by activated carbon produced at 800°C, 90min of different impregnation ratio (KOH/Tyre).

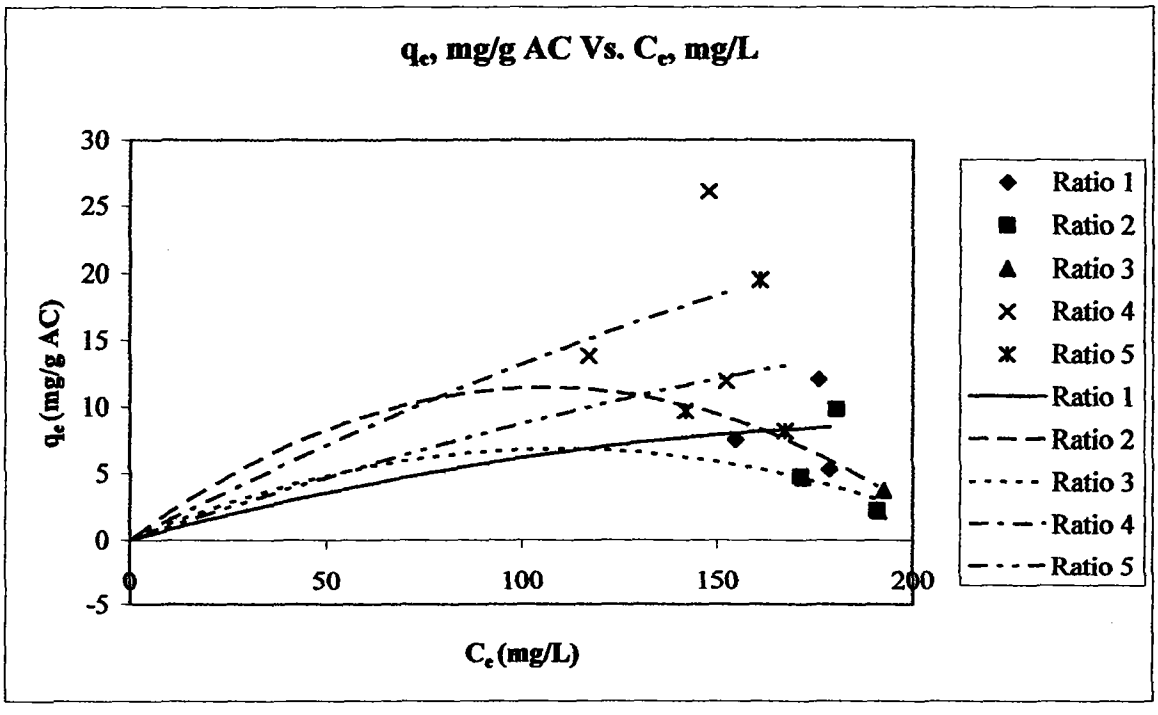

Figure 4.6. Adsorption isotherms of phenol by activated carbon produced at 800°C, 120min of different impregnation ratio (KOH/Tyre).

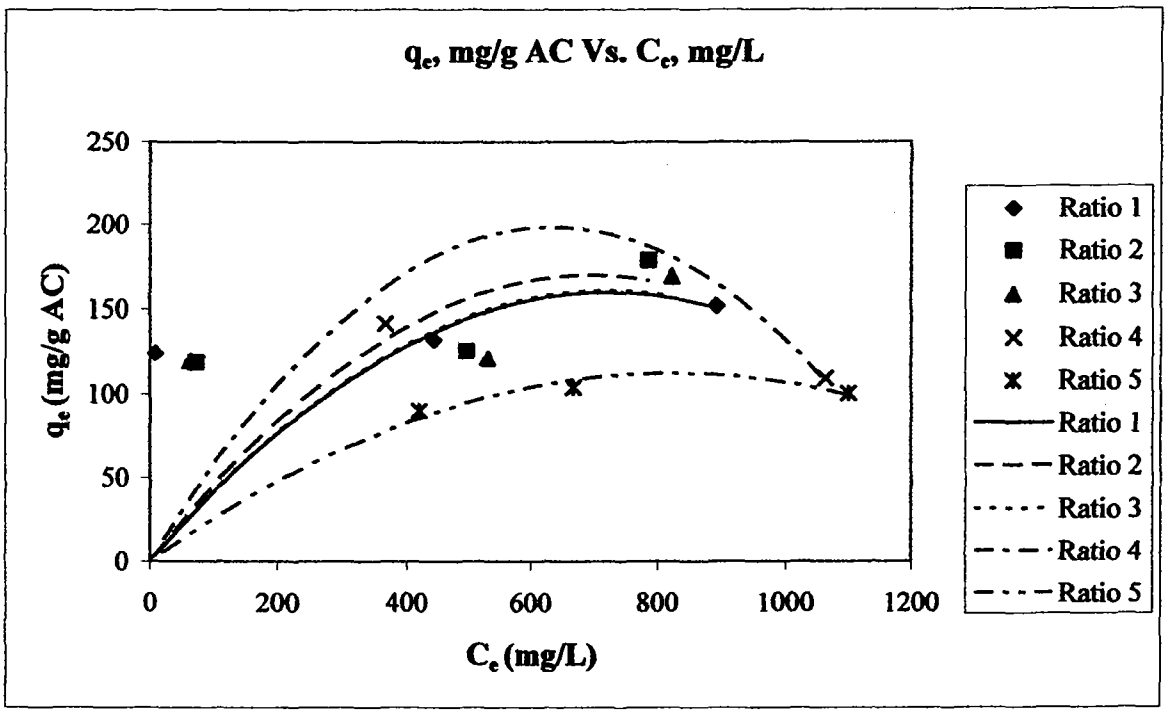

Figure 4.7. Adsorption isotherms of methylene blue by activated carbon produced at 800°C, 60min of different impregnation ratio (KOH/Tyre).

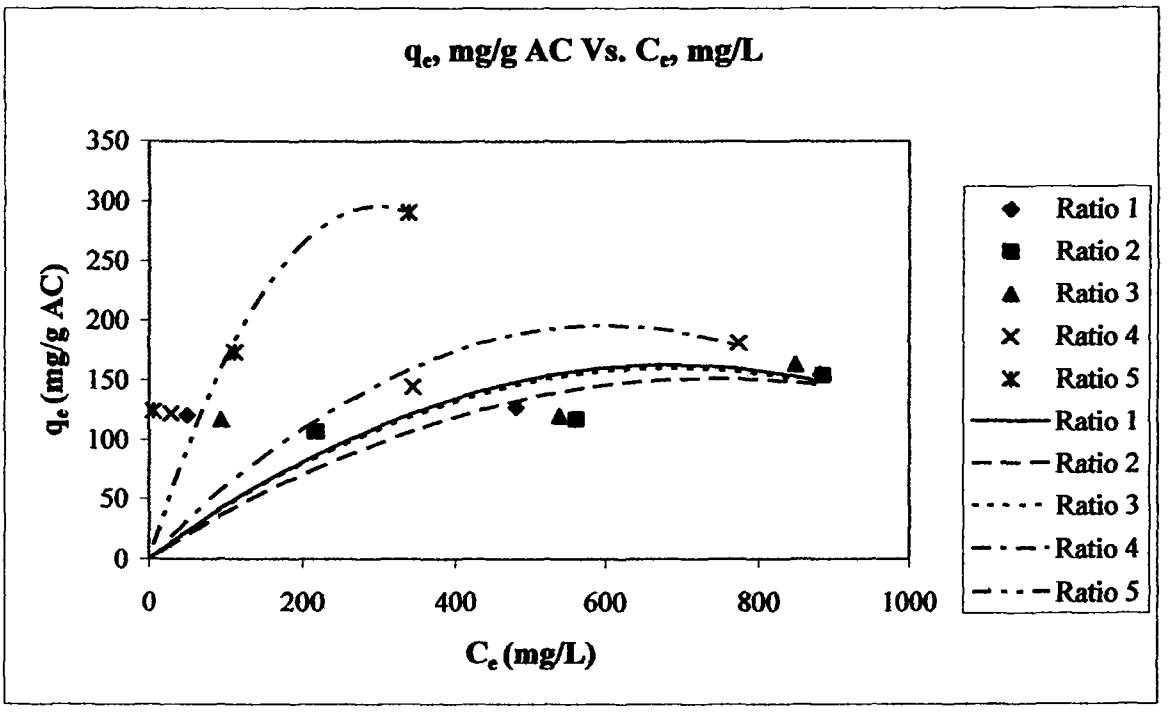

Figure 4.8. Adsorption isotherms of methylene blue by activated carbon produced at 800°C, 90min of different impregnation ratio (KOH/Tyre).

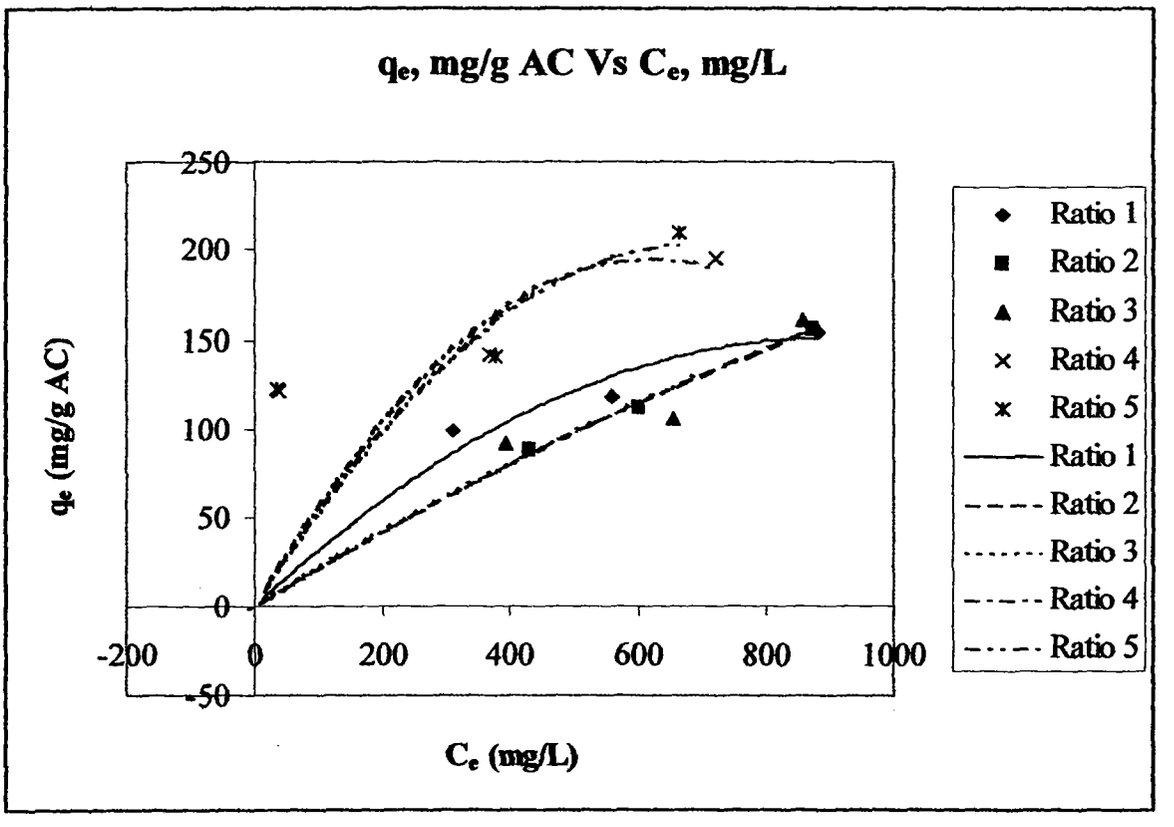

Figure 4.9. Adsorption isotherms of methylene blue by activated carbon produced at 800°C, 120min of different impregnation ratio (KOH/Tyre).

The adsorption of the adsorbate is very dependent on pore size distribution and will depend on the number of micro-, meso- and macropores in the structure. Adsorbates of different molecular size will be adsorbed to varying extent depending on the availability of pores of appropriate size. The rate of adsorption of a specific molecule will depend on its mobility in the solution phase, the pore structure and particle size of the adsorbent and the hydrodynamics of contact between the solution and particle phase.

Dr. Ridzuan

UNIVERSITI SAINS MALAYSIA
SCHOOL OF CHEMICAL ENGINEERING
ENGINEERING CAMPUS

PREPARATION OF ACTIVATED CARBON FROM WASTE TIRE BY CHEMICAL ACTIVATION AND ADSORPTION PERFORMANCE

CHIN SIOW TENG
Matric No.: **73109**

April 2007

ABTRACT

A sand fluidized bed reactor is used for pyrolysis of waste tires in producing char and chemical activation of char to prepare activated carbon. Waste tire is an abundant and non-biodegradable material was used to prepare activated carbon by chemical activation with potassium hydroxide (KOH) as the activating agent at various parameters. The parameters include activation temperature, activation time and impregnation ratio. The yield of activated carbon is increased when both of the activation temperature and activation time is decreased. However, the yield of activated carbon is decreased when the impregnation ratio is increased except for impregnation ratio 4. The adsorption equilibrium and kinetics of phenol on such carbon were then studied at 30℃ for 48 hours. The equilibrium data for phenol adsorption well fitted to Langmuir isotherm equation, with a maximum monolayer adsorption capacity of 238.10 mg/g. The best quality of activated carbon was obtained at an activation time, temperature and impregnation ratio of 2 h, 850 and 4 respectively. The characteristics of typical commercial activated carbon were measured and compared. The adsorption kinetics shows that pseudo-second-order rate fitted the adsorption kinetics better than pseudo-first-order rate equation.

Keywords: Activated carbon; Waste tires; Pyrolysis; Phenol Adsorption; Isotherms; Kinetics

CHAPTER 5: RESULTS AND DISCUSSION

5.1 PROPERTIES AND CHARACTERIZATION OF WASTE TIRES

The composition of scrap tires varies with different manufacturing companies and formulation, so a typical elemental analysis and composition of scrap tire are presented in Table 5.1 and Table 5.2, respectively. The pore structure of waste tires which analyzed by Scanning Electron Micrographs (SEM) is shown in Fig.5.1. From the Table 5.1, it can be observed that the carbon content in waste tire is high which 86.03 %.

Table 5.1: Elemental analysis of waste tire

Element	Percentage (%)
Carbon	86.03
Hydrogen	6.60
Nitrogen	0.95
Sulfur	2.11
Unknown	4.31

Table 5.2: Component of waste tire from Thermogravimetric analysis (TGA)

Component	Percentage (%)
Moisture	0.69
Volatile	69.51
Fixed Carbon	25.10
Ash	4.70

From Figure 5.1, it can be observed that the surface of waste tire is rough and there is no pore is shown..

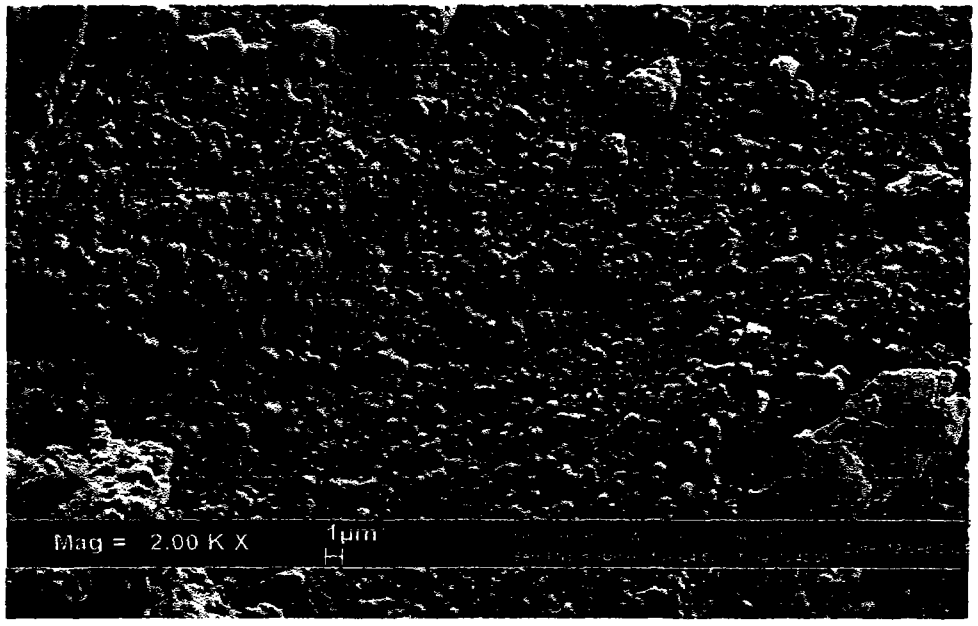

Fig. 5.1: Scanning electron micrographs at a magnification of x2000 of waste tire

5.2 PROPERTIES OF CHAR FROM PYROLYSIS IN FLUIDIZED BED

The chemical composition of the pyrolytic char produced by fluidized bed reactor pyrolysis unit is given in Table 5.3.The pore structure of the char is shown in Fig.5.2.

From Table 5.3, it has shown that the percentage of carbon, hydrogen, nitrogen and sulfur is reduced after pyrolysis in fluidized bed compared with waste tire. This is due to reaction is occurred during pyrolysis of waste tire. The main chemical reaction could be described as:

$$\text{Waste Tires} \longrightarrow \text{Char} + \text{Oil} + \text{Gas}\ (CO_2, CO, CH_4, C_mH_n, H_2) \quad (1)$$

In this work, only the char is analyzed. The char is analyzed by SEM (Scanning electron micrographs) to observe the surface pore morphology while the composition of char produced can be analyzed by Elemental analysis. It is important to analysis the properties of char because char is used for further activation process to produce activated carbon.

Further activation process for pyrolytic char is necessary because it contains almost all the inorganic compounds present in tires and a significant amount of condensed by products formed during pyrolysis process.

Table 5.3: Elemental analysis of Pyrolytic Char

Element	Percentage (%)
Carbon	80.97
Hydrogen	0.78
Nitrogen	0.43
Sulfur	1.32
Unknown	16.50

From Fig.5.2, it can be observed that the pore is available in char that produced from pyrolysis at 800℃ for 1 hour in fluidized bed. The pore size of the char is 10.68 μm. It also can be observed that the char has rather smooth surface areas with long ridges, resembling a series of parallel lines. Based on the outward appearance, it can be said that the pores are not cross-linked. Pore was observed in char is due to the decomposition of organic wastes that presented in waste tire which is blocked the surface pore of the carbon in waste tires.

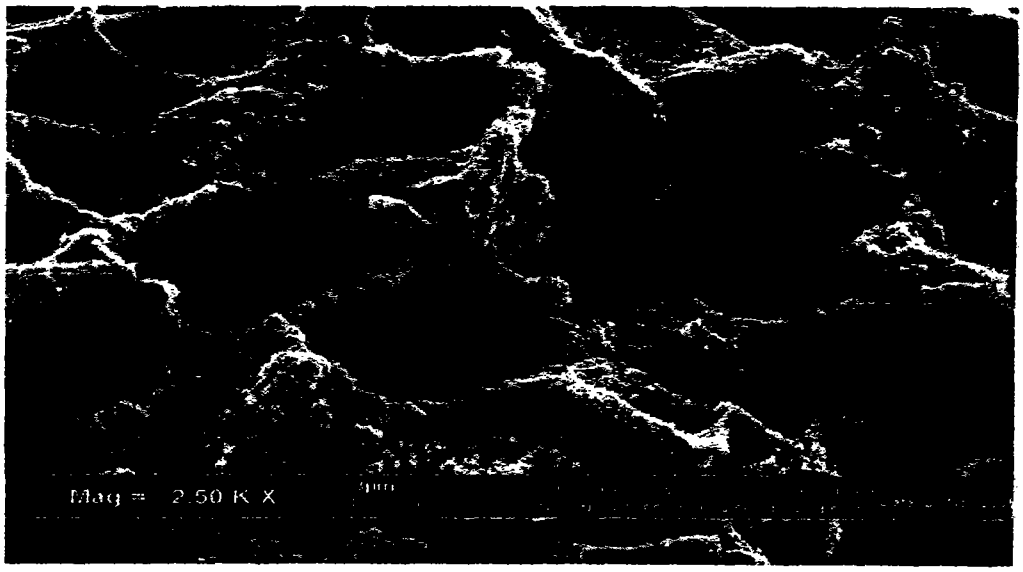

Fig.5.2: Scanning electron micrographs at a magnification of x2500 of Char

The yield of char that produced from pyrolysis of waste tire is 25.26% which comparable with the yield of char that shown in literature of *(Dai et.al., 2001)* is 27%.

The yield of char (%) is calculated by based on the formula that shown as below:

$$\text{Yield of Char} = \frac{Weight\_char\_produce(g)}{Weight\_tire\_feed(g)} \times 100 \qquad (2)$$

5.3 YIELD OF ACTIVATED CARBON

5.3.1 Yield of activated carbon at various condition of activation

Table 5.4 shows the yield of activated carbon at various conditions that included activation temperatures, impregnation ratio and activation time. The yield of activated carbon (%) can be calculated by:

$$\text{Yield of Activated Carbon} = \frac{Activated\_Carbon(g)}{Char(g)} \times 100 \qquad (3)$$

Table 5.4: Yield of activated carbon at different condition

Temperature (℃)	Activation Time (hour)	Impregnation Ratio	Yield (%)
850	1	3	40.619
		4	45.357
		5	42.043

	2	3	35.864
		4	39.803
		5	38.291
800	1	3	39.564
		4	56.415
		5	47.934
	2	3	33.299
		4	49.731
		5	42.653

5.3.2 Yield of activated carbon at different impregnation ratio

The overall yields of activated carbons prepared at various impregnation ratios of KOH to mass waste tires are shown in Fig. 5.3. Activated carbon used in this part were prepared by impregnating chars with various amounts of KOH and then activated at 850 and 2 hours. From the Fig. 5.3, the yield of activated carbon is decreased when the increased of impregnation ratio. This is due to the oxidation reaction is predominant, and therefore the yield decreases with increasing impregnation ratio as a result of burn-off of carbon and the release of volatiles. *(Yang and Lua, 2003)*

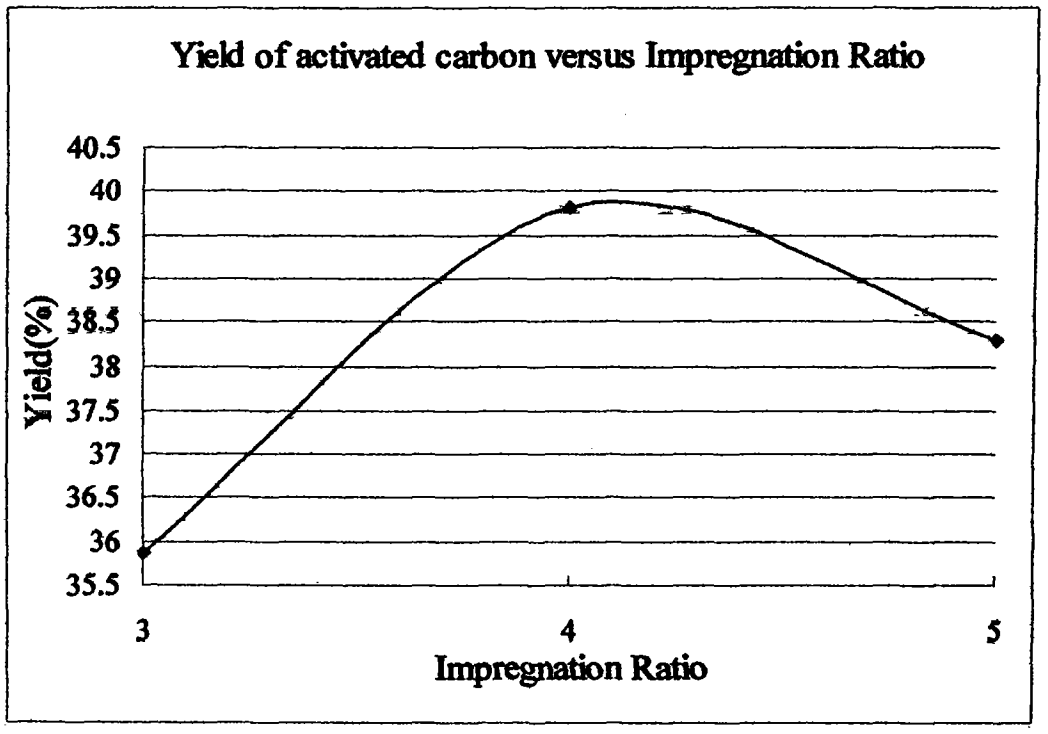

Fig. 5.3: Yield of Activated Carbon at activation temperature of 850℃ and activation time of 2 hours

5.3.3 Yield of Activated Carbon at different Activation Time

Based on the various activation condition of activated carbon, a graph which yields of activated carbon versus impregnation is plotted. It is to identify the effect of each parameter to the yield of activated carbon that produced from chemical activation in a furnace. The yield of activated carbon for vary activation time versus impregnation ratio is plotted and shown in Fig. 5.4 and Fig.5.5.

From the Fig.5.6 and Fig.5.7, the yield of activated carbon is decreased with the increasing of activation time at the same activation temperatures that are 850℃ and 800℃. This is due to a complete burn-off of carbon is occurred. Furthermore, the extent of oxidation reaction increases proportionally when activation time increases. Thus, the yield of activated carbon is deceased with the increased of activation time.

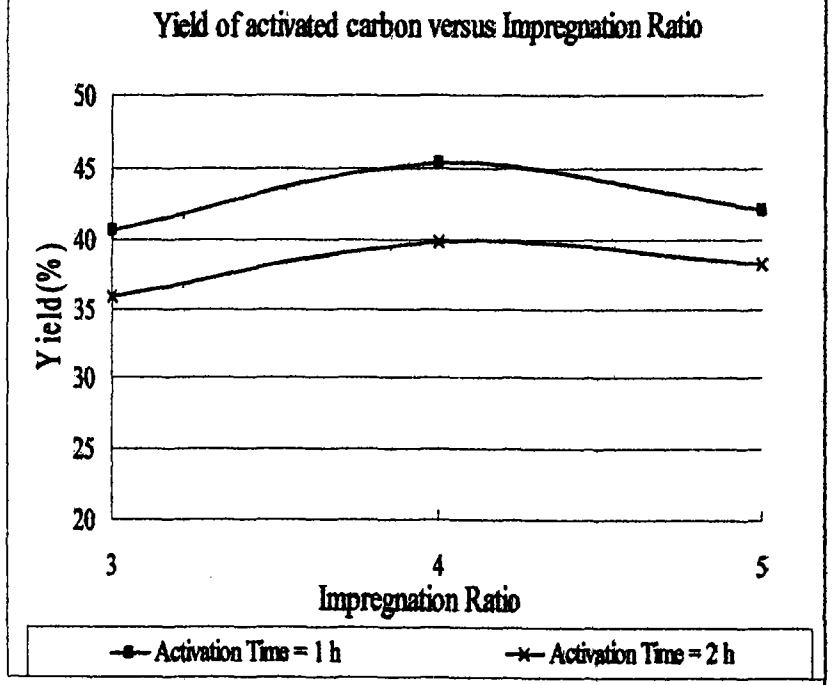

Fig. 5.4: Yield of Activated Carbon at temperature 850℃ with various activation hold time.

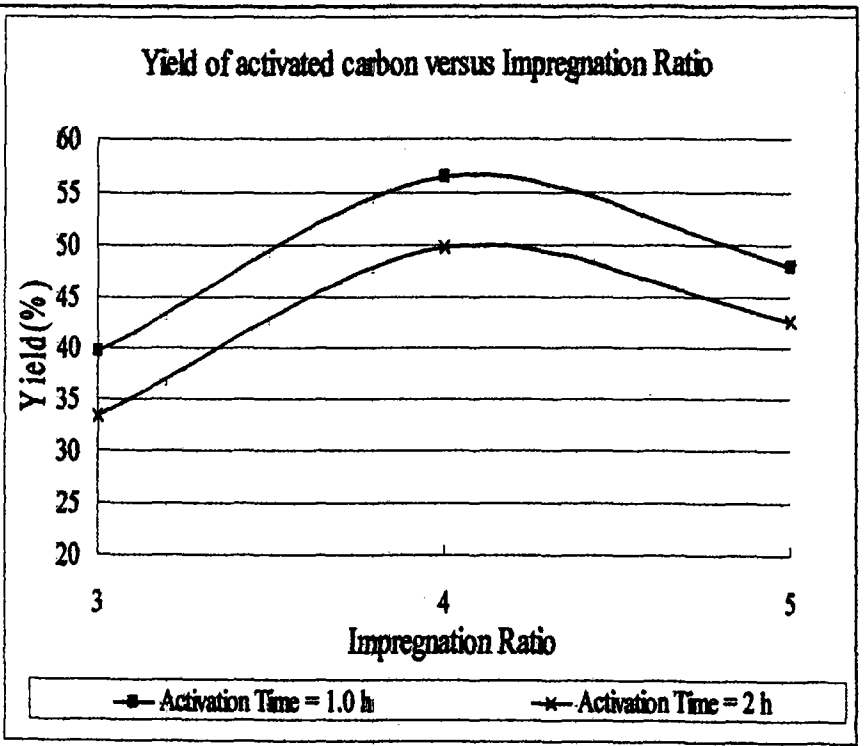

Fig.5.5: Yield of Activated Carbon at temperature 800℃ with various activation hold time.

5.3.4 Yield of Activated Carbon at different Activation Temperature

For vary activation temperature, a yield of activated carbon versus impregnation ratio is plotted and shown in Fig.5.6 and Fig.5.7.Both Fig.5.6 and Fig.5.7 has shown that the increasing of activation temperature reduced the yield of activated carbon at the same activation time of 1 hour and 2 hours respectively. This is due to an increasing amount of volatiles is released during the increasing activation temperature from 800-850℃. Besides, the carbon consumption is increased due to the C-KOH reaction. These phenomena are also manifested in the decreasing volatile content and increasing fixed carbon for increasing activation temperature. These two opposing trends are due to predominance of the loss in volatiles over carbon consumption for increasing activation temperature (*Yang and Lua; 2003.)*

However, for the impregnation ratio of 3, the increased of activation temperature has slightly increased the yield of activated carbon for both activation time of 1 hour and 2 hour. . Yield is increased is due to the amount of KOH is not sufficient to cover and distribute the carbons. Therefore, the increased of activation temperature at impregnation ratio 3 promotes the more pyrolysis and evaporation occurred. As a result, the yield of activated carbon is increased. *(Tseng et.al., 2006)*

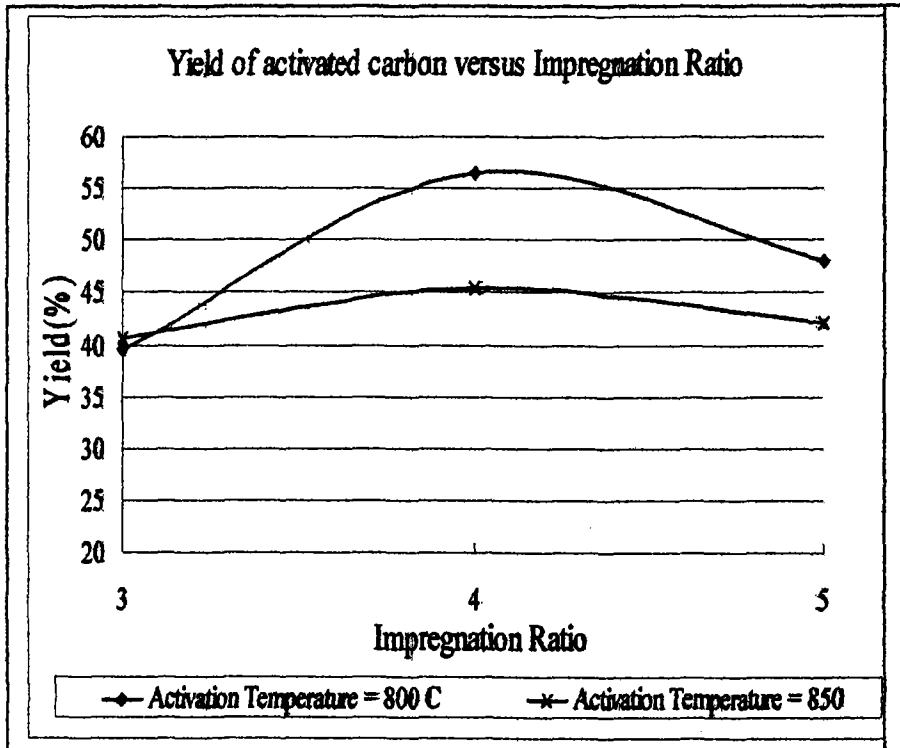

Fig 5.6: Yield of Activated Carbon at activation time of 1 hour with various activation temperatures.

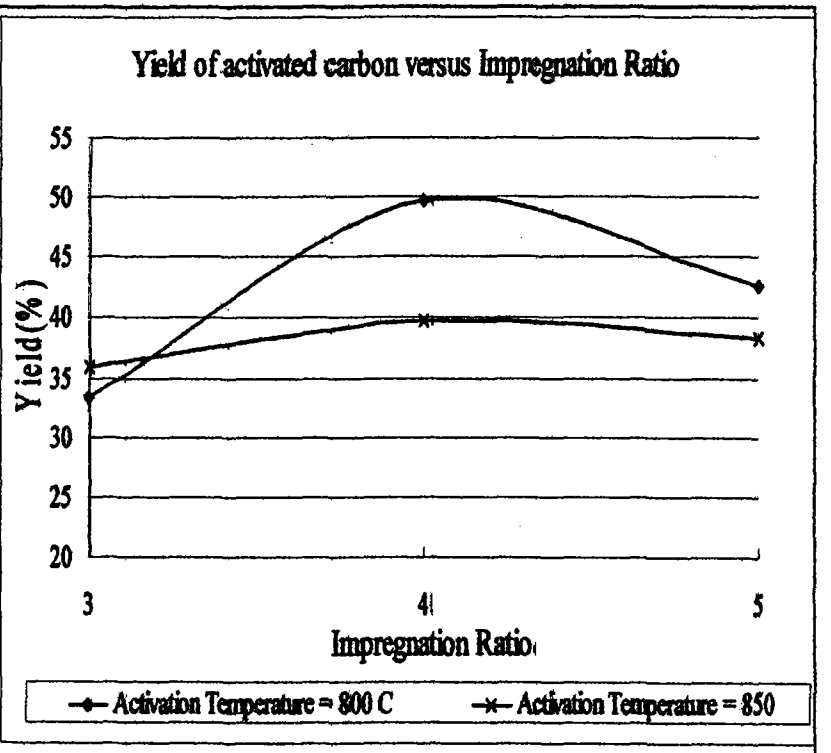

Fig 5.7: Yield of Activated Carbon at activation time of 2 hours with various activation temperatures.

5.4 PROPERTIES OF ACTIVATED CARBON

The composition of each activated carbon for various condition analyzed by elemental analyzer was shown in Table 5.5. From the Table 5.5, AC850-2-3 has the highest carbon content compared to others. Besides, the sulfur content of activated carbon in average can be considered low compare to waste tire and char. Thus, the activated carbon that produced from chemical activation in furnace can be categorized as an environmental friendly product which preferable to industry treatment process.

Table 5.5: Elemental analysis of Activated carbon at different condition

Element	Carbon (%)	Hydrogen (%)	Nitrogen (%)	Sulfur (%)	Unknown (%)
AC800-2-3	51.65	0.70	0.30	1.51	45.84
AC800-2-4	56.78	0.03	0.80	2.18	59.79
AC800-2-5	72.98	0.10	0.79	0.67	25.46
AC850-2-3	84.31	0.10	0.59	0.15	14.85
AC850-2-4	80.70	0.47	0.00	0.10	18.73
AC850-2-5	77.58	0.58	0.15	0.05	21.64
Commercial	74.42	2.24	0.85	0.20	22.29

Note: a-b-c denotes activation temperature (℃)-activation hold time (h)-ratio of KOH/char

From the Fig 5.8, it can be observed that the percentage of carbon for AC850-2-3 is the highest. At the average, the carbon content for activated carbon produced from experiment is comparable with the commercial activated carbon. Besides, it also can be discovered that the sulfur content is low and negligible compared to the carbon and unknown content. Thus, activated carbon that produced is an environmental friendly product. The components of the unknown are gas (CO_2, CO, CH_4, C_mH_n, H_2) and oil.

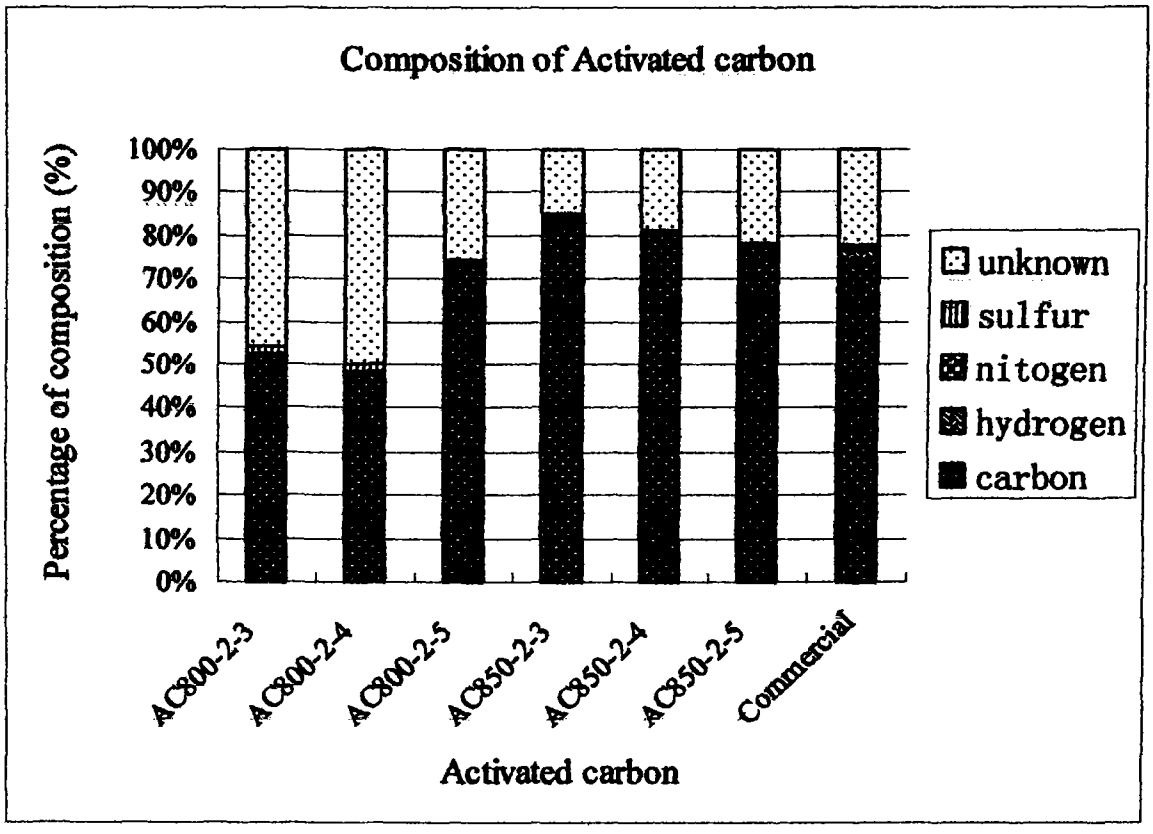

Fig.5.8: Percentage composition of activated carbon from different condition.

5.5 ADSORPTION PHENOL PERFORMANCE

5.5.1 Adsorption Isotherm

Adsorption isotherm study is carried out on two well-known isotherms which are Langmuir and Freundlich.

Langmuir Isotherm is a monolayer adsorption which means the surface of the adsorbent is uniform that is all the adsorption sites are equal. Besides, the adsorbed molecules do not interact and occurs through the same mechanism. At the maximum adsorption, only a monolayer is formed which is molecules of adsorbate (phenol) only on the free surface of the adsorbent (activated carbon).

However, for Freundlich Isotherm, the surface of the activated carbon particles was heterogeneous, non-specific and non-uniform in nature.

The applicability of the isotherm equation is compared by judging the linear regression co-efficient R^2.

5.5.2 Langmuir Isotherm

The linear form of Langmuir's isotherm model is given by the following equation:

$$\frac{C_e}{q_e} = \left(\frac{1}{Q_o b}\right) + \left(\frac{1}{Q_o}\right) C_e \quad (4)$$

where C_e is the equilibrium concentration of the adsorbate (phenol) (mg/L), q_e the amount of adsorbate adsorbed per unit mass of adsorbent (mg/g), and Q_o and b are Langmuir constants related to adsorption capacity and rate of adsorption, respectively. When C_e/q_e is plotted against C_e, straight line with the slope of $1/Q_o$ was obtained (Fig. 5.13 or Fig.5.14), indicating the adsorption of phenol on activated carbon follows the Langmuir Isotherm. The Langmuir constant b and Q_o were calculated from this isotherm and the values are given in Table 5.6.

Besides, the essential characteristics of the Langmuir isotherm can be expressed in terms of a dimensionless equilibrium parameter (R_L), which is defined by:

$$R_L = \frac{1}{1 + bC_o} \quad (5)$$

where b is the Langmuir constant and C_o is the highest phenol concentration (mg/L). The value of R_L indicates the type of the isotherm to be either unfavorable ($R_L > 1$), linear ($R_L = 1$), favorable ($0 < R_L < 1$) or irreversible ($R_L = 0$). From the Table 8, value of R_L was found to be 0.1841 (maximum) and 0.0026 (minimum) which are in the range of $0 < R_L < 1$. Therefore, the activated carbon is favorable for adsorption of phenol under adsorption temperature of 30℃ for 48 hours.

5.5.3 Freundlich Isotherm

The well-known logarithmic form of Freundlich model is given by the following equation:

$$\log q_e = \log K_F + (\frac{1}{n}) \log C_e \quad (6)$$

where q_e is the amount adsorbed at equilibrium (mg/g), C_e the equilibrium concentration of adsorbate (phenol) (mg/L) and K_F and n are Freundlich constants, n giving an indication of how favorable of the adsorption process and K_F (mg/g(L/mg)^n) is the adsorption capacity of the adsorbent. Besides, K_F also can be defined as the adsorption or distribution coefficient and represents the quantity of phenol adsorbed onto activated carbon adsorbent for a unit equilibrium concentration. The slope 1/n ranging between 0 and 1 is a measure of adsorption intensity or surface heterogeneity.

From the Table 8, the slope 1/n which calculated from the plot of log q_e versus log C_e (Fig.5.15 or Fig.5.16) is below 1 indicates a normal Langmuir isotherm and show that the adsorption phenol also follows the Freundlich isotherm.

From the Table 5.6, it can be observed that the adsorption capacity of AC850-2-4 is the highest which is 238.10 mg/g. The order for adsorption phenol capacity is AC850-2-4 > AC850-2-3 > Commercial > AC850-2-5 > AC800-2-5. Both AC850-2-4 and AC850-2-3 that produced from experiment have a higher adsorption capacity compared to commercial.

At the same temperature of 850℃, the activated carbon with impregnation ratio of 4 has the highest adsorption capacity. However, for the same impregnation ratio of

activated carbon, the increased of temperature is increased the adsorption phenol capacity.

Moreover, it also can be discovered that all the activated carbon accept AC800-2-5 that produced from chemical activation is best fitted with both Langmuir and Freundlich Isotherm due to the value of linear regression co-efficient $R^2 > 0.90$. From the result, it can be concluded that the adsorption capacity for most of the activated carbon that produced from experiment is contributed by both monolayer and heterogeneity adsorption.

However, AC800-2-5 is just best fitted to Langmuir Isotherm which indicates the homogeneous nature of the surface AC800-2-5 that only the formation of monolayer coverage of phenol molecule at the outer surface of activated carbon of AC800-2-5.

Table 5.6: Adsorption Capacity of activated carbon

Adsorbent	Langmuir Isotherm				Freundlich Isotherm		
	Q_o (mg/g)	b (1/mg)	R^2	R_L	$\frac{1}{n}$	K_F (mg/g)(L/mg)^a	R^2
AC850-2-4	238.10	0.0089	0.8750	0.1841	0.4112	3.3831	0.9212
AC850-2-3	232.56	0.0141	0.9607	0.1240	0.3372	4.2207	0.8918
Commercial	222.22	0.0146	0.9807	0.1206	0.3361	4.1766	0.9763
AC850-2-5	188.68	0.0246	0.9944	0.0752	0.3182	4.2875	0.9463
AC800-2-5	117.65	0.7658	0.9845	0.0026	0.1574	5.4970	0.6989

Note: a-b-c denotes activation temperature (℃)-activation hold time (h)-ratio of KOH/char

5.5.4 Adsorption Curve

5.5.4.1 Adsorption Capacity Curve

From the Figure 5.9 and Figure 5.10 below, there is a little cross between the different initial concentrations for both commercial and AC850-2-4. However, the equilibrium adsorption is achieved earlier for AC850-2-4 compared to Commercial. AC850-2-4 achieved the equilibrium at around 28 hours of adsorption while the Commercial achieved equilibrium at around 46 hours of adsorption. Amount of phenol adsorbed increased when the initial concentration increased due to the increased of driving force concentrations.

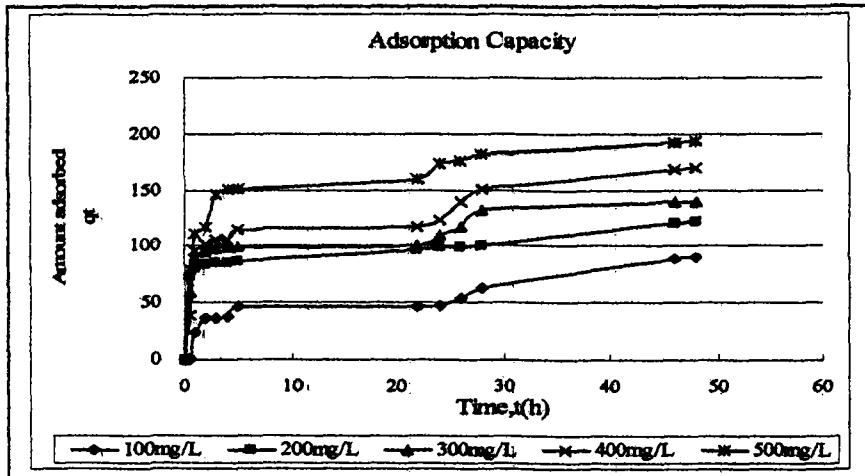

Fig.5.9: Variation of Adsorption capacity with adsorption time at various initial phenol concentration at 30℃ (commercial activated carbon)

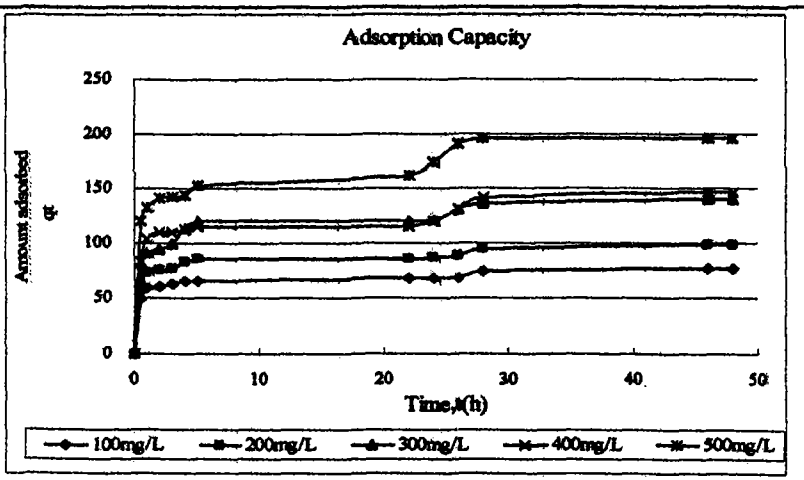

Fig.5.10: Variation of Adsorption capacity with adsorption time at various initial phenol concentration at 30℃ (AC850-2-4)

5.5.4.2 Equilibrium Adsorption Isotherm Curve

From the figure 5.11 & 5.12 below, the adsorption isotherm curve of AC850-2-4 is comparable to the curve of Commercial. The equilibrium adsorption phenol is increased when the equilibrium concentration is increased. However, the equilibrium curve for AC850-2-4 does not increased smoothly as the Commercial.

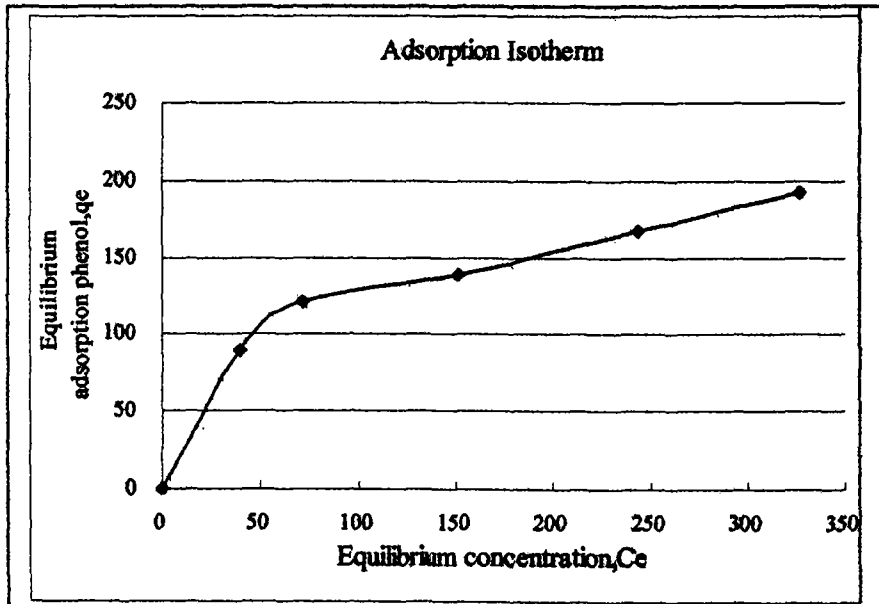

Fig.5.11: Equilibrium Adsorption Isotherm of phenol onto commercial activated carbon at 30℃

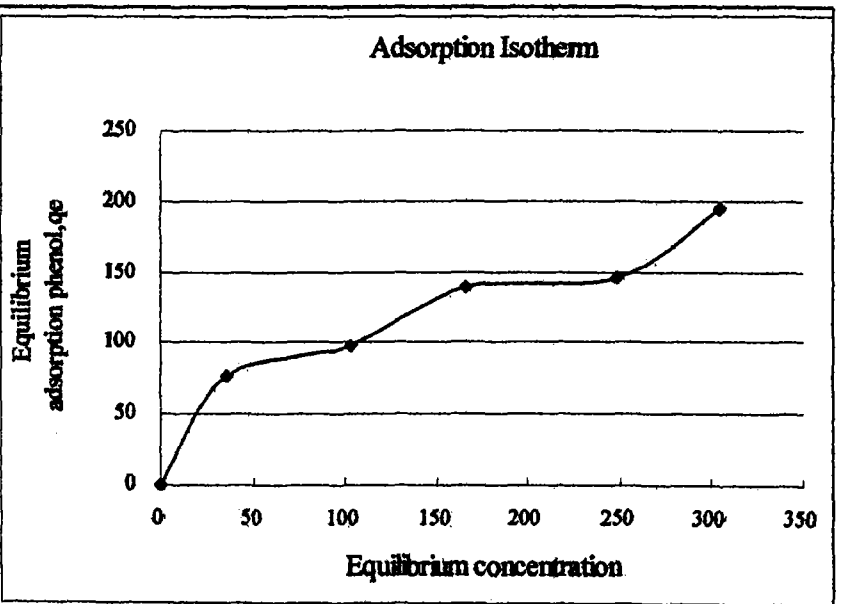

Fig.5.12: Equilibrium Adsorption Isotherm of phenol onto AC850-2-4 at 30℃

5.5.4.3 Langmuir Isotherm Curve

From the figure below, both activated carbons is fitted to the Langmuir isotherm due to the high value of linear regression co-efficient, R^2. The Commercial had the higher R^2= 0.9807 which is higher than AC850-2-4. This can be concluded that Commercial is more favorable to the monolayer adsorption.

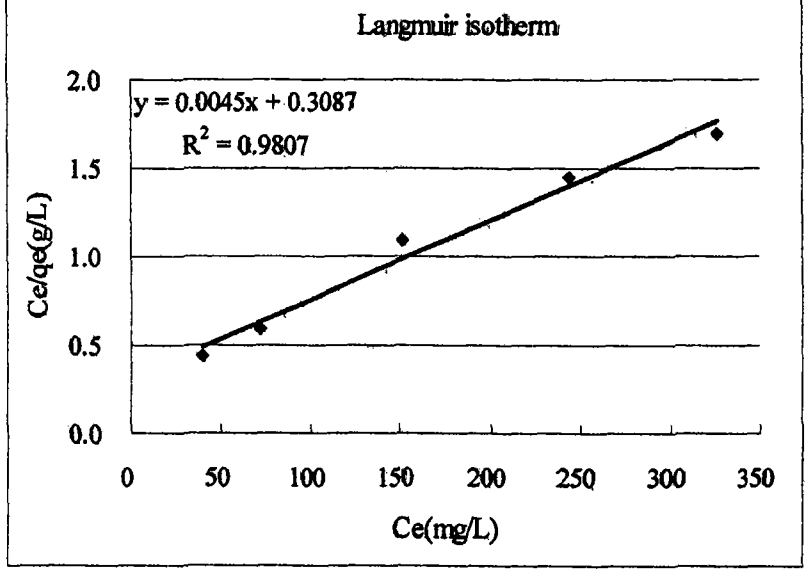

Fig.5.13: Langmuir adsorption Isotherm of phenol-commercial activated carbon adsorption at 30℃

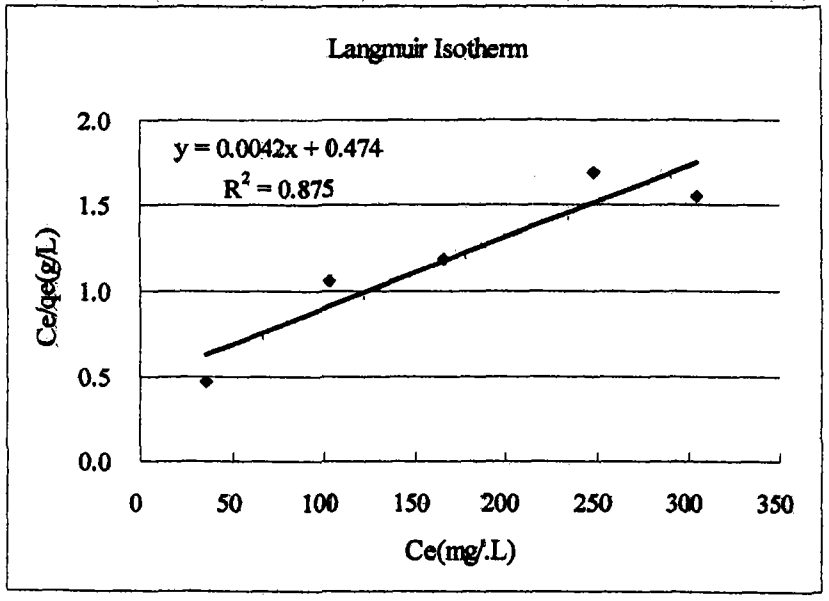

Fig.5.14: Langmuir adsorption Isotherm of phenol-AC850-2-4 adsorption at 30℃

5.5.4.4 Freundlich Isotherm Curve

From the figure below, it can be observed that Commercial is more favorable to multilayer adsorption compared to AC850-2-4 due to the higher value of linear regression co-efficient, R^2 for Commercial. However, from the Table 5.6, the adsorption capacity for AC850-2-4 is higher than commercial. This may because of the pore structure and the high carbon content in AC850-2-4. Besides, from Fig.5.15 and Fig.5.6, it showed that the R^2 for Freundlich isotherm is higher than Langmuir isotherm which caused the AC850-2-4 more favorable to the multilayer adsorption. Thus, the adsorption capacity for AC850-2-4 is the highest.

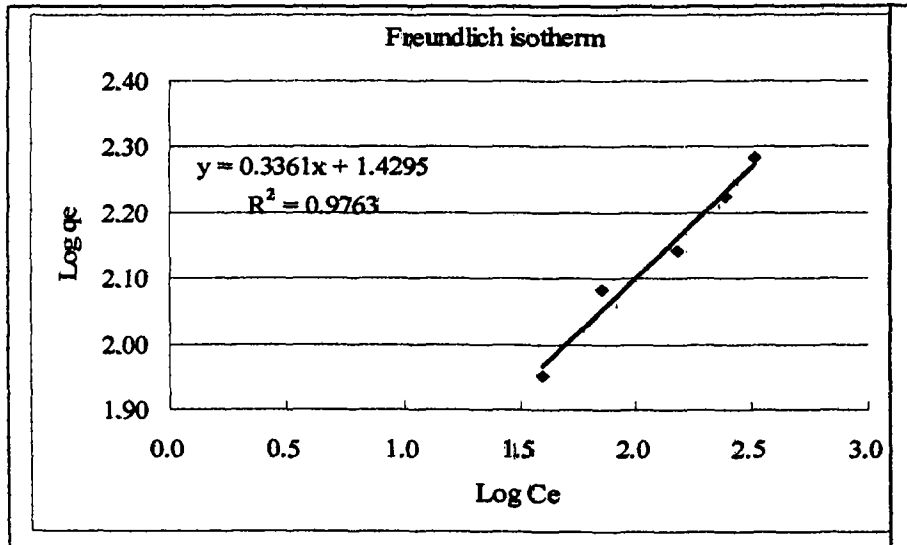

Fig.5.15: Freundlich adsorption Isotherm of phenol-commercial activated carbon adsorption at 30℃

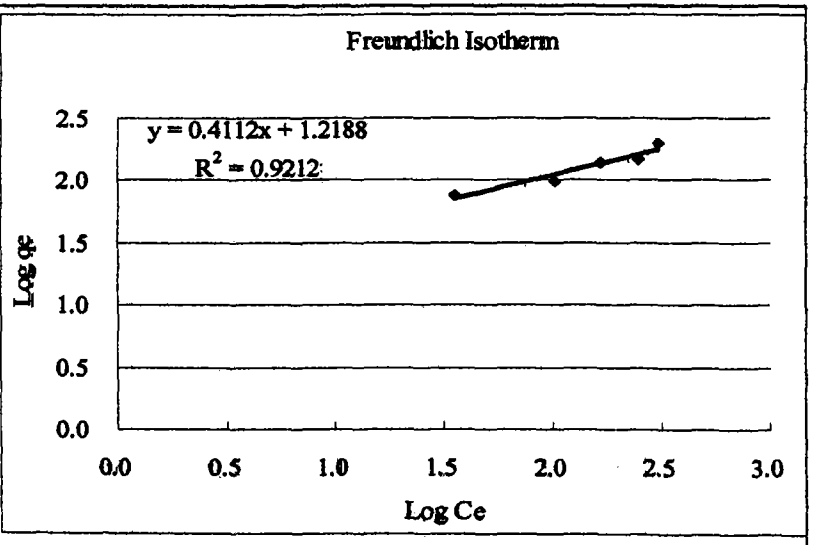

Fig.5.16:Freundlich adsorption Isotherm of phenol-AC850-2-4 adsorption at 30℃

5.6 SURFACE MORPHOLOGIES OF RAW MATERIAL AND PRODUCTS

From figure 5.17 to 5.20 below, development of pore structure from waste tire (raw material) to activated carbon AC850-2-4 (Product) can be observed. The waste tire does not present any pore. After pyrolysis, the char with pore is found. Finally, a micropore structure of AC850-2-4 was obtained from chemical activation of char in furnance. It can be concluded that chemical activation is benefit to the development of a microporous structure. Due to the microporous structure of AC850-2-4 compared to commercial, the adsorption capacity of AC850-2-4 is higher than commercial showed in Table 5.6.

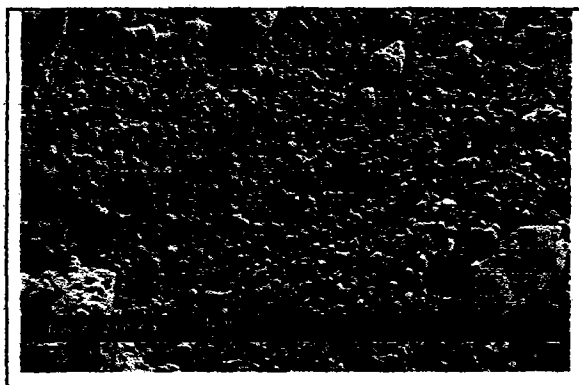

Fig 5.17. : SEM for Waste tire

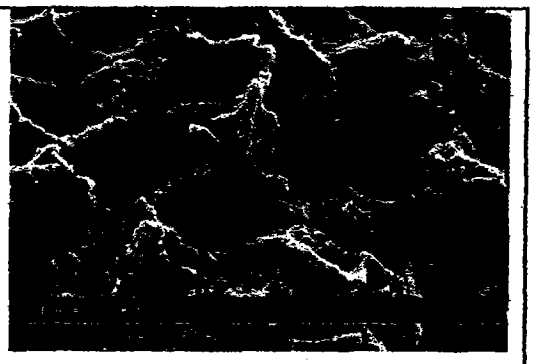

Fig.5.18: SEM for Char

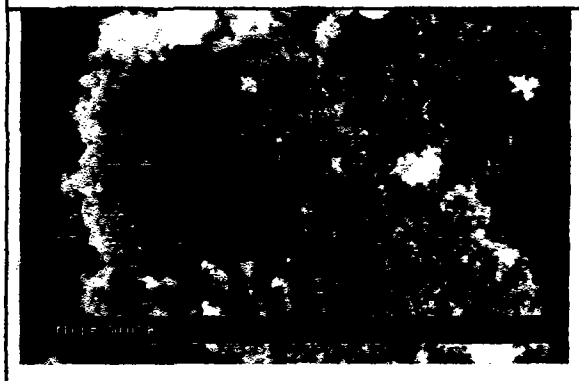

Fig. 5.19: SEM for AC850-2-4

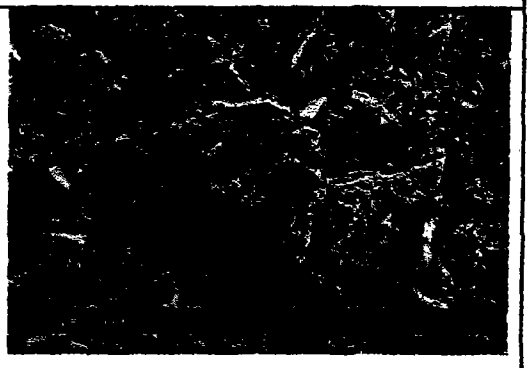

Fig. 5.20: SEM for Commercial

Note: a-b-c denotes activation temperature (℃)-activation hold time (h)-ratio of KOH/char

5.7 COMPARISON ADSORPTION CAPACITY OF PHENOL FOR WASTE TIRE DERIVED ACTIVATED CARBON FROM VARIOUS METHOD OF ACTIVATION

Table 5.7 shows the adsorption capacity for different method activation for the same material which is waste tires. From the Table 9, it can be observed that the waste tire derived activated carbon (AC850-2-4) from chemical activation showed the highest adsorption capacity compared to activated carbon that produce from steam activation and gas carbon dioxide activation. Besides, the adsorption capacity of AC850-2-4 is comparable with the commercial activated carbon. The adsorption capacity of AC850-2-4 is 238.10 mg/g.

Table 5.7: Adsorption capacity for activated carbon from different activation method

Adsorbent	**Monolayer of adsorption capacity (Langmuir Isotherm) (mg/g)**	**Method of Activation**	**References**
AC850-2-4 (experiment)	238.10	Chemical Activation	Present Work
Commercial	222.22	-	-
Activated carbon	99.00	Carbon Dioxide	Miguel et.al., 2003
Activated Carbon	106.00	Steam Activation	Miguel et.al., 2003

5.8 KINETICS OF ADSORPTION

There are two type of kinetics adsorption which is Pseudo first order and Pseudo second order. From the study of kinetics, the important information can be obtained is to find out the best fitted of activated carbon on either Pseudo first order or Pseudo second order.

The rate constant of adsorption is determined from the pseudo first order equation given by Langergren and Svenska:

$$\log(q_e - q) = \log q - \frac{k_1 t}{2.303} \quad (7)$$

where q_e and q are the amounts of phenol adsorbed (mg/g) at equilibrium and at time t (min), respectively, k_1 the rate constant adsorption (h^{-1}). Values of k_1 is calculated from the plot of log (q_e -q) versus t (Fig.5.21 or Fig.5.22) for different initial concentration of phenol. The result of the calculation is shown in Table 5.8. Although the linear regression coefficient value R^2 at high concentration is higher than 0.80, the experimental q_e do not agree with the calculated q_e that obtained from the linear plot (Table 5.8). As a result, the adsorption of phenol onto activated carbon is not a pseudo first order kinetics.

Table 5.8: Kinetics (Pseudo First Order) for various condition of Activated Carbon

Adsorbent	C_0 (mg/L)	First Order Kinetics Model				
		qe,experiment (mg/g)	qe,calculated (mg/g)	k_1 (h^{-1})	R^2	Sum of error squares, SSE (%)
AC850-2-4	100	76.55	45.20	0.1550	0.7832	8.69
	200	98.30	45.79	0.1128	0.6405	14.56
	300	139.70	60.62	0.0827	0.8837	21.93
	400	146.40	128.62	0.1704	0.7685	4.93
	500	195.76	76.90	0.1145	0.4882	32.97
Commercial	100	89.74	129.06	0.1207	0.5940	10.91
	200	120.88	87.80	0.1170	0.6064	9.17
	300	139.08	78.58	0.0811	0.8431	16.78
	400	167.73	117.06	0.0843	0.8342	14.05
	500	192.55	150.56	0.1338	0.6925	11.65

Note: a-b-c denotes activation temperature (℃)-activation hold time (h)-ratio of KOH/char

A pseudo second order equation based on equilibrium adsorption is expressed as:

$$\frac{t}{q} = \frac{1}{k_2 q_e^{\,2}} + \frac{t}{q_e} \qquad (8)$$

where q_e and q are the amounts of phenol adsorbed (mg/g) at equilibrium and at time t (min), respectively, k_2 (g/mg h) is the rates constant of second order adsorption. If

second order kinetics is applicable, the plot of t/q versus t should show a linear relationship. q_e and k_2 can be determined from the slope and intercept of the plot. The value of k_2 and q_e is calculated and shown in Table 11.

Moreover, the applicability of both kinetic models are verified through the sum of error squares (SSE,%). The sum of error squares (SSE, %) given by:

$$SSE(\%) = 100 \times \sqrt{\frac{\sum[(q_{t,exp} - q_{t,cal})]^2}{N}} \quad (9)$$

where N is the number of data points.

The higher is the value of R^2 and the lower value of SSE, the better will be the goodness of fit. The calculated value of SSE was listed in Table 5.8 and Table 5.9

From the Table 5.8 and Table 5.9, the results show that the Pseudo Second Order rate equation agrees well with experimental data for all the activated carbons due to the linear regression co-efficient of 0.99 and the sum of error squares is less when compared to the Pseudo First Order rate equation.

The sum of error squares are less for the linear plots of Pseudo Second Order which show a good agreement between experimental and calculated q_e values (Table 5.9). The linear regression co-efficient of 0.99 which indicating the applicability of the kinetic equation and the second order nature of the adsorption process of phenol on activated carbon.

From the results, it is found that the adsorption of phenol on activated carbon can be best described by second order kinetic model.

Table 5.9: Kinetics (Pseudo Second Order) for various condition of Activated Carbon

Adsorbent	C_0 (mg/L)	Second Order Kinetics Model				
		qe,experiment (mg/g)	qe,calculated (mg/g)	k_2 (g/mg h)	R^2	Sum of error squares, SSE (%)
AC850-2-4	100	76.55	75.76	0.0166	0.9959	0.22
	200	98.30	97.09	0.0117	0.9954	0.33
	300	139.70	138.89	0.0066	0.9946	0.22
	400	146.40	144.93	0.0053	0.9880	0.41
	500	195.76	196.08	0.0044	0.9934	0.09
Commercial	100	89.74	72.99	0.0156	0.6713	4.64
	200	120.88	117.65	0.0051	0.9832	0.90
	300	139.08	136.99	0.0040	0.9775	0.58
	400	167.73	163.93	0.0027	0.9679	1.05
	500	192.55	192.31	0.0031	0.9877	0.07

Note: a-b-c denotes activation temperature (℃)-activation hold time (h)-ratio of KOH/char

5.8.1 Kinetics Pseudo First Order curve

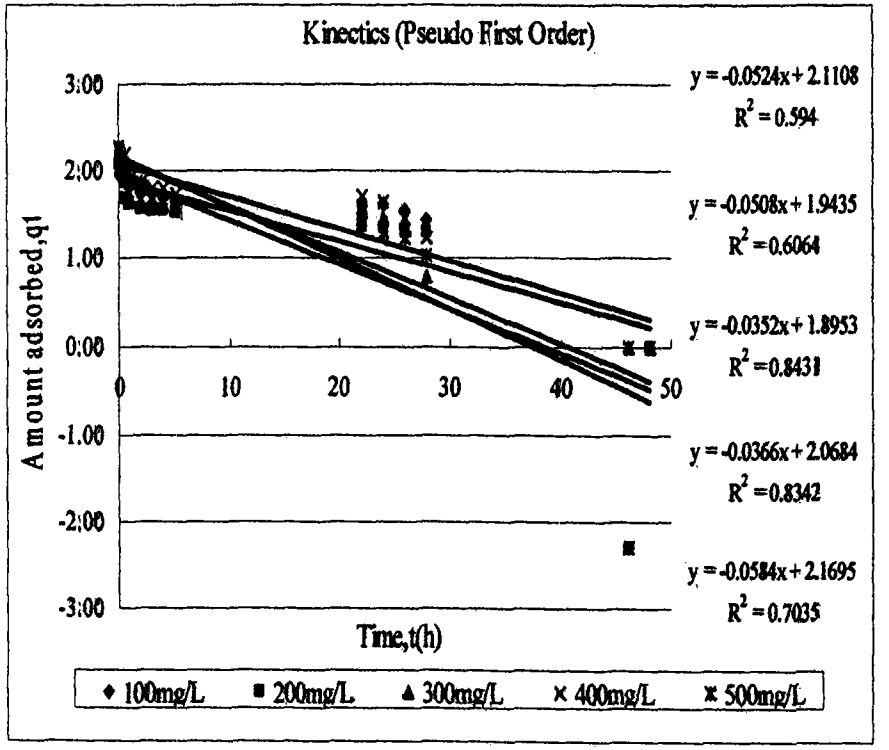

Fig.5.21: Kinetics Pseudo First Order for adsorption of phenol adsorption by commercial activated carbon at 30℃

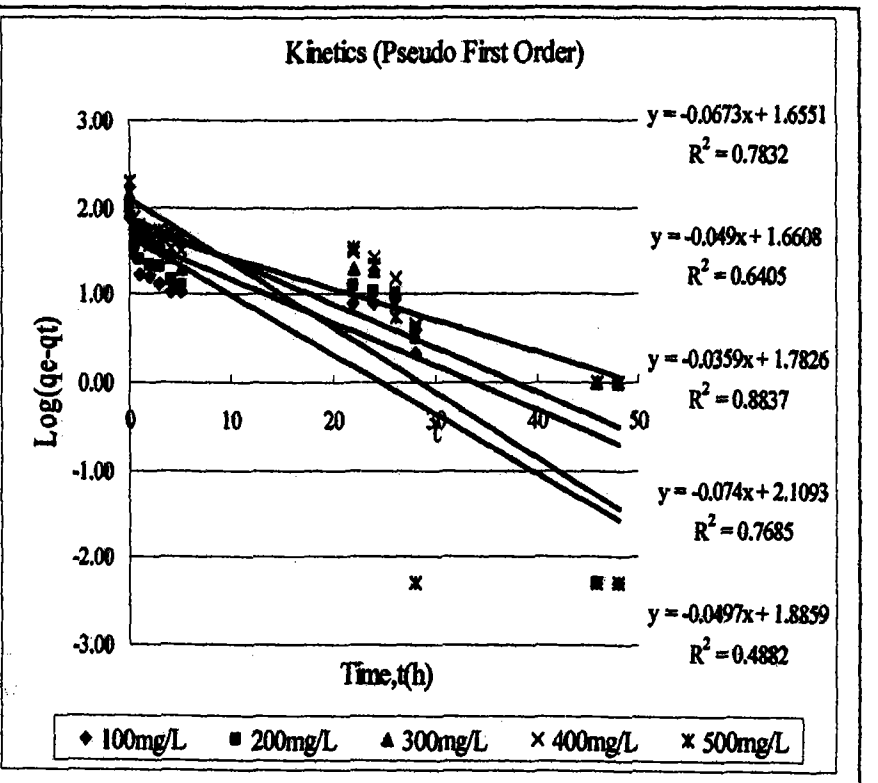

Fig.5.22: Kinetics Pseudo First order for adsorption of phenol adsorption by AC850-2-4 at 30℃

5.8.2 Kinetics Pseudo Second Order curve

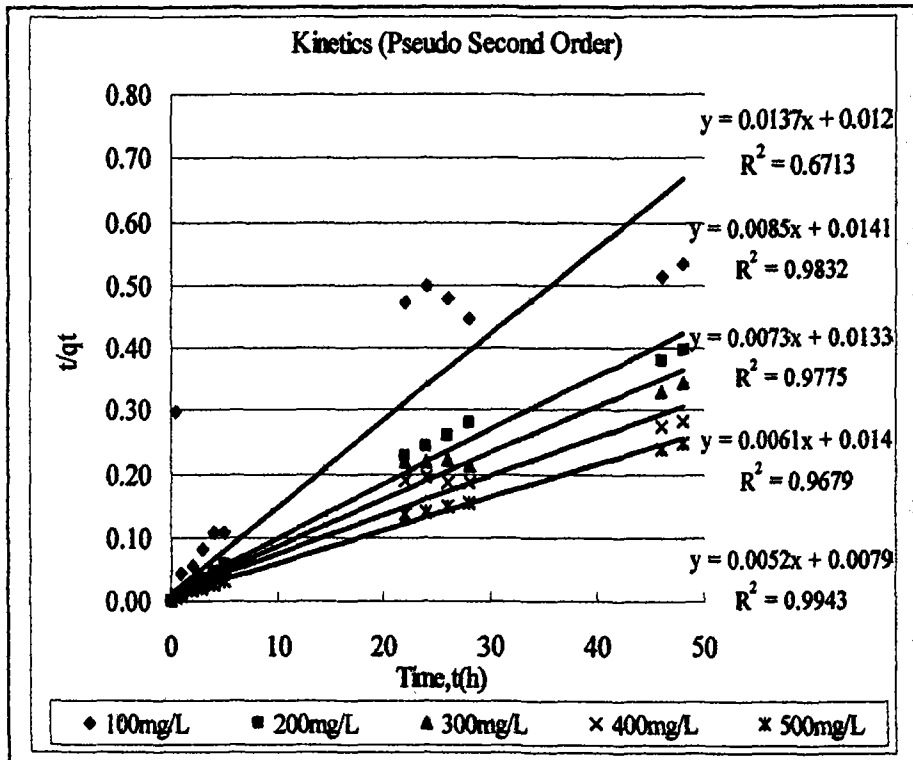

Fig.5.23: Kinetics Pseudo Second Order for adsorption of phenol adsorption by commercial activated carbon at 30℃

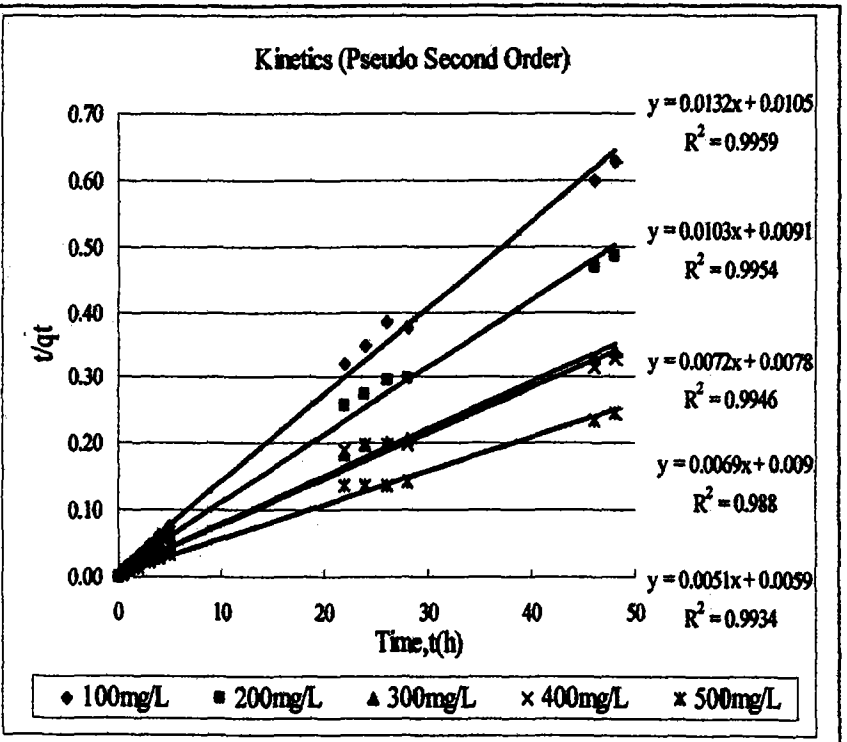

Fig.5.24: Kinetics Pseudo Second order for adsorption of phenol adsorption by AC850-2-4 at 30℃

Dr. Ridzuan

UNIVERSITI SAINS MALAYSIA
SCHOOL OF CHEMICAL ENGINEERING
ENGINEERING CAMPUS

STUDY OF PHYSICAL AND CHEMICAL CHARACTERISTICS OF CHAR PRODUCED FROM WASTE TYRE

KAMARUL HASNAN BIN ABDUL HALIM
Matric No.: **73128**

April 2007

ABSTRACT

Waste tyre was combusted for about 40 to 60 minutes until the combustion temperature turns out to be constant, respectively in fluidized bed. Combusted waste tyre (i.e. char) was fed through varying raw material diameter from 250 to 500 micron and above with feed rate at 0.8 and 2 kg/h. Scanning electron microscopy (SEM) results will show the surfaces in these carbons significant different. Thermal gravimetric analyzer (TGA) results showed moisture, volatile, fixed carbon and ash content meanwhile elemental analyzer (EA) mentioned carbon, hydrogen, nitrogen and sulfur percentage. This work facilitated the preparation of char by effectively controlling pore structures for the adsorption performance of the activated carbon on adsorbates of different molecular forms.

Keyword: Char; Waste tyre; Physical and Chemical characteristics

CHAPTER 5

RESULTS AND DISCUSSION

This chapter presents the experimental results together with the discussion. For convenience, the results have been grouped into two parts. The first part presents the experimental data for the preparation of char from different parameters. The second part gives results of char characterization characterized by SEM, TGA and EA.

5.1 Experimental Data

The five attempted parameters are listed as follow:

- Parameter 1

  Feed rate = 0.8 kg/h

  Waste tyre size = 250 to 355 micron

- Parameter 2

  Feed rate = 0.8 kg/h

  Average waste tyre size = 425 micron

- Parameter 3

  Feed rate = 0.8 kg/h

  Waste tyre size = above 500 micron

- Parameter 4

  Feed rate = 2.0 kg/h

  Average waste tyre size = 425 micron

- Parameter 5

  Feed rate = 2.0 kg/h

  Waste tyre size = above 500 micron

According to experimental procedures heater 1 is set at 450 °C and heater 2 is set at 450 °C. Hot air temperature is set at 393 °C. The waste tyre is fed when the bed or sand temperature is reaching 450 °C indicated by Indicator 1. Indicator 3 showed the temperature of waste tyre combusted at.

From Table 5.1, the combustion temperature constant at 590 °C indicated by Indicator 3.

Table 5.1 Data for Parameter 1

Time (min)	0	10	20	30	40	50	60
Hot Air (°C)	395	395	394	396	393	395	395
Heater 1 (°C)	398	415	417	439	435	434	451
Heater 2 (°C)	433	457	461	454	443	447	462
Indicator 1 (°C)	464	483	495	524	525	524	538
Indicator 2 (°C)	323	335	392	481	519	534	547
Indicator 3 (°C)	280	296	427	529	563	589	588
Indicator 4 (°C)	236	249	350	441	469	470	488

From Table 5.2, the maximum combustion temperature is 650 °C.

Table 5.2 Data for Parameter 2

Time (min)	0	10	20	30	40	50	60
Hot Air (°C)	397	396	393	396	394	395	394
Heater 1 (°C)	420	419	431	442	446	437	445
Heater 2 (°C)	442	460	460	451	439	463	450
Indicator 1 (°C)	491	495	514	528	537	531	535
Indicator 2 (°C)	342	349	404	470	476	489	492
Indicator 3 (°C)	300	303	534	604	613	616	653
Indicator 4 (°C)							

From Table 5.3, the combustion temperature maintain at 610 °C.

Table 5.3 Data for Parameter 3

Time (min)	0	10	20	30	40	50	60
Hot Air (°C)	394	394	393	394	392	391	395
Heater 1 (°C)	378	395	420	424	437	436	435
Heater 2 (°C)	435	438	461	460	446	458	463
Indicator 1 (°C)	443	446	499	512	522	525	525
Indicator 2 (°C)	300	321	427	454	459	473	478
Indicator 3 (°C)	259	279	525	605	608	613	609
Indicator 4 (°C)	216	234	427	486	504	512	516

From Table 5.4, Indicator 3 indicated the combustion temperature constant at 800 °C.

Table 5.4 Data for Parameter 4

Time (min)	0	10	20	30	40	50	60
Hot Air (°C)		251	171	240	275	375	399
Heater 1 (°C)		386	369	390	379	422	420
Heater 2 (°C)		358	331	353	441	437	445
Indicator 1 (°C)		455	419	463	449	516	508
Indicator 2 (°C)		625	672	689	734	730	735
Indicator 3 (°C)		812	811	797	803	803	797
Indicator 4 (°C)		690	707	693	690	684	687

Yield of char obtained after carbonization process under atmosphere according to Parameter 4 at 800 °C. Yields of char and light char were 25.56 and 0.22%, respectively. Yields of char and light char were calculated according to equations 5.1 and 5.2 below:

$$\text{Yield of char, \%} = \frac{w_c}{w_{wt}} \times 100 \qquad (5.1)$$

$$\text{Yield of light char, \%} = \frac{w_{lc}}{w_{wt}} \times 100 \qquad (5.2)$$

w_c = weight of char, g

w_{lc} = weght of light char, g

w_{wt} = weight of waste tyre fed, g

From Table 5.5, the maximum combustion temperature is 840 °C.

Table 5.5 Data for Parameter 5

Time (min)	0	10	20	30	40
Hot Air (°C)	395	394	393	398	393
Heater 1 (°C)	405	412	435	441	446
Heater 2 (°C)	441	441	446	463	451
Indicator 1 (°C)	473	493	533	535	539
Indicator 2 (°C)	333	450	610	619	612
Indicator 3 (°C)	295	691	810	810	838
Indicator 4 (°C)		513	677	696	698

5.2 Char Characterization Results

5.2.1 SEM Observations

Plate 5.1 shows SEM photographs (×1000, ×2000 and ×4000) of waste tyre. The photographs showed rough surface of waste tyre.

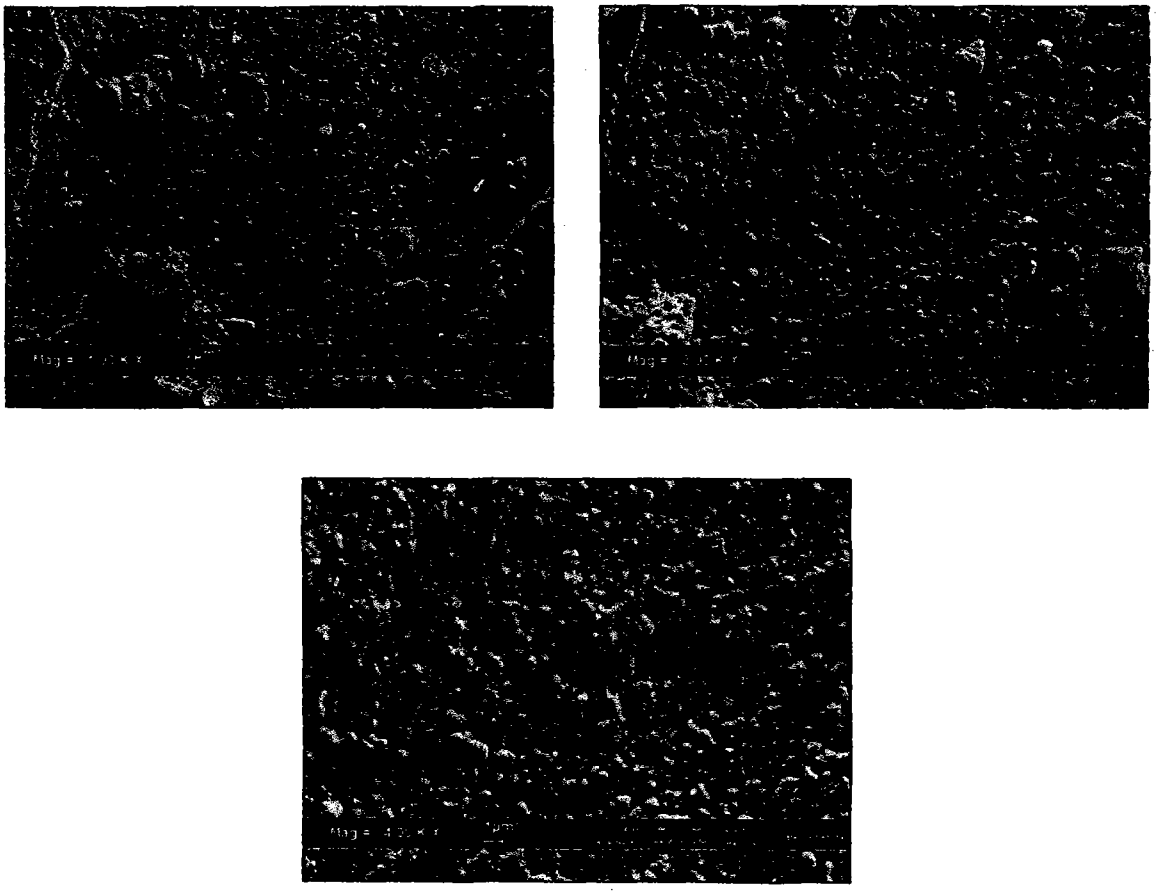

Plate 5.1 SEM photographs of waste tyre

Plate 5.2 shows SEM photographs (×1000) of char outcomes for Parameter 2. The voids formed not developed well. The formation of pore not completed part of them. The photographs showed the formation of pore not identical in diameter.

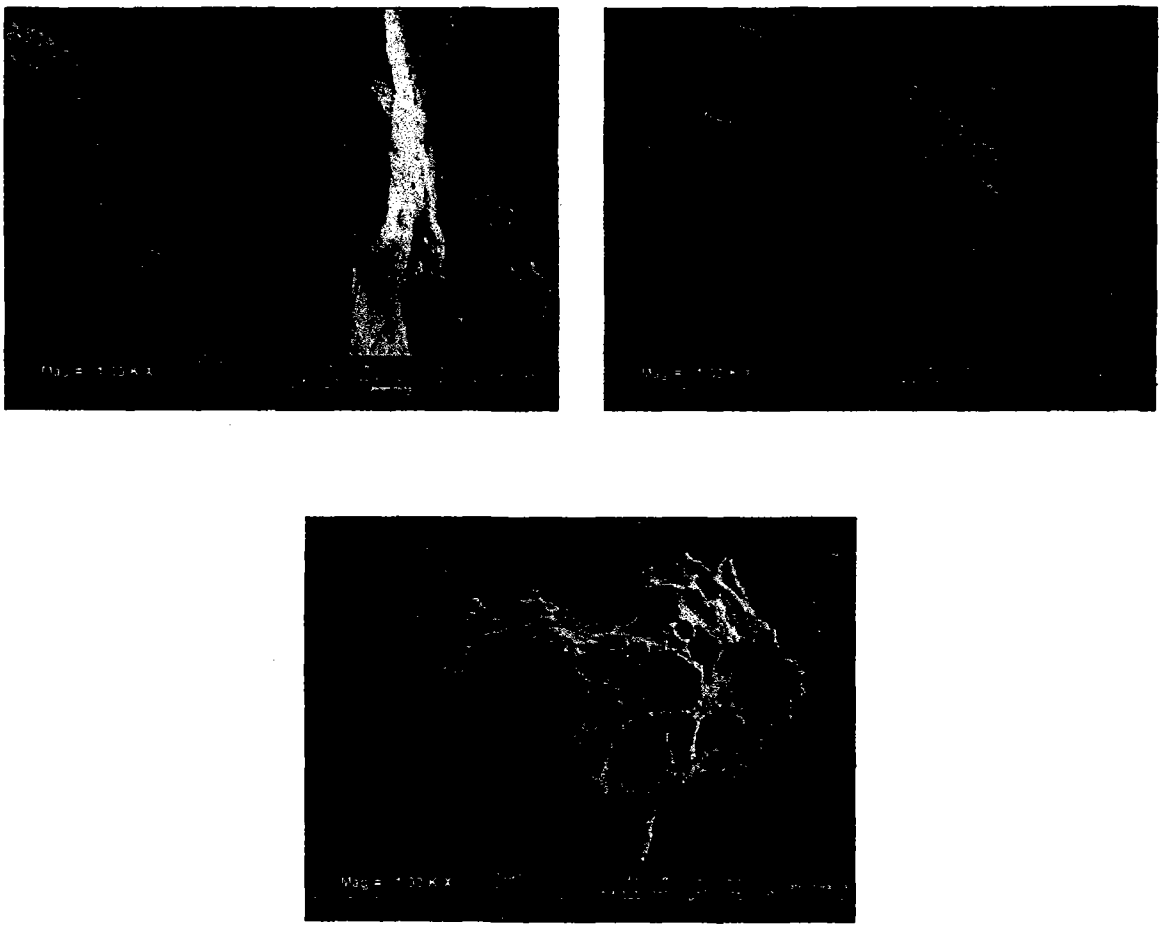

Plate 5.2 SEM photographs of char produced for Parameter 2

Plate 5.3 show SEM photographs of char produced from waste tyre for Parameter 4 collected in first cyclone of fluidized bed pilot plant. The photograph clearly showed honeycomb voids. Honeycomb holes of char-based carbon fully developed and the corner lines of the hole openings not clearly observed. The photographs showed the formation of pore almost identical in diameter.

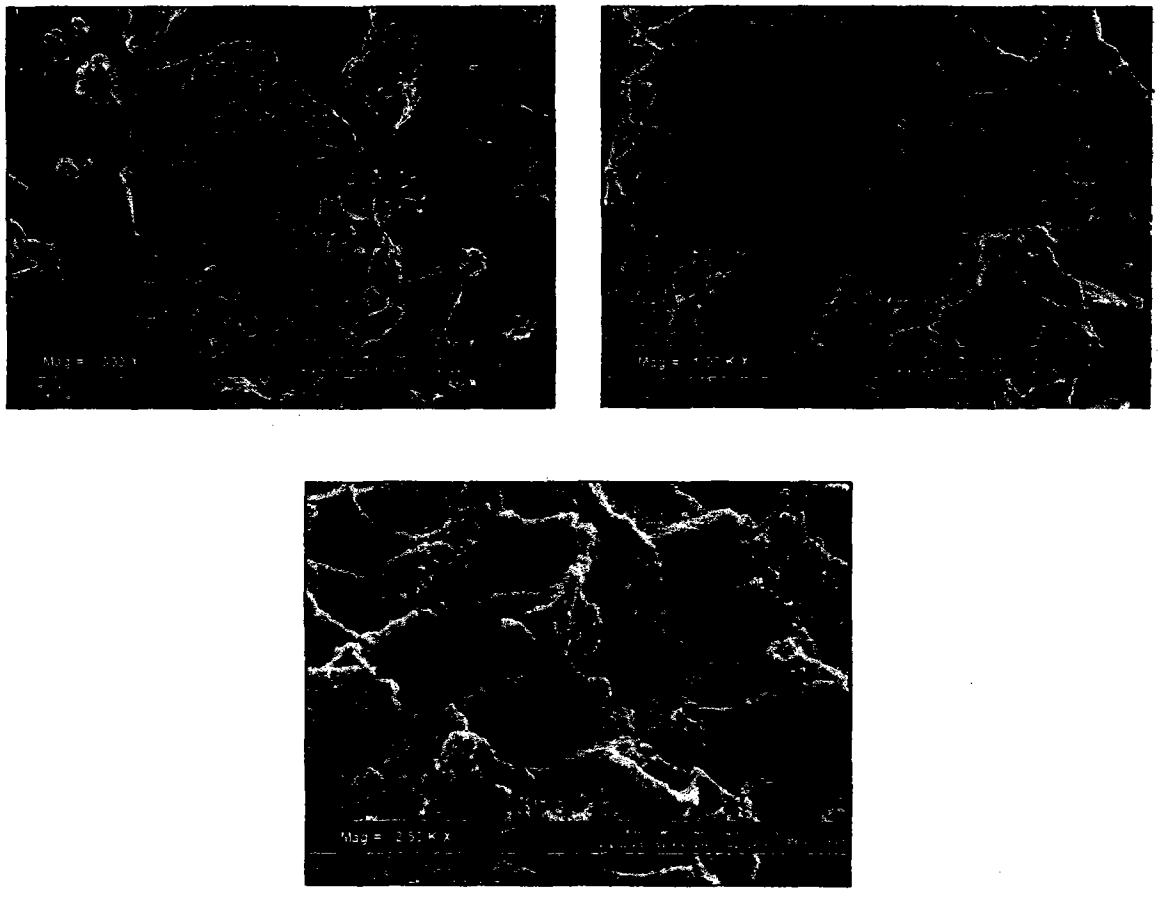

Plate 5.3 SEM photographs (×300, ×1000 and ×2500) of char produced for Parameter 4

Plate 5.4 showed SEM photographs (×500, ×1000 and ×2000) of light char for Parameter 4 collected in second cyclone. The voids formed not developed well. The light char structure look like cotton or sheep fur.

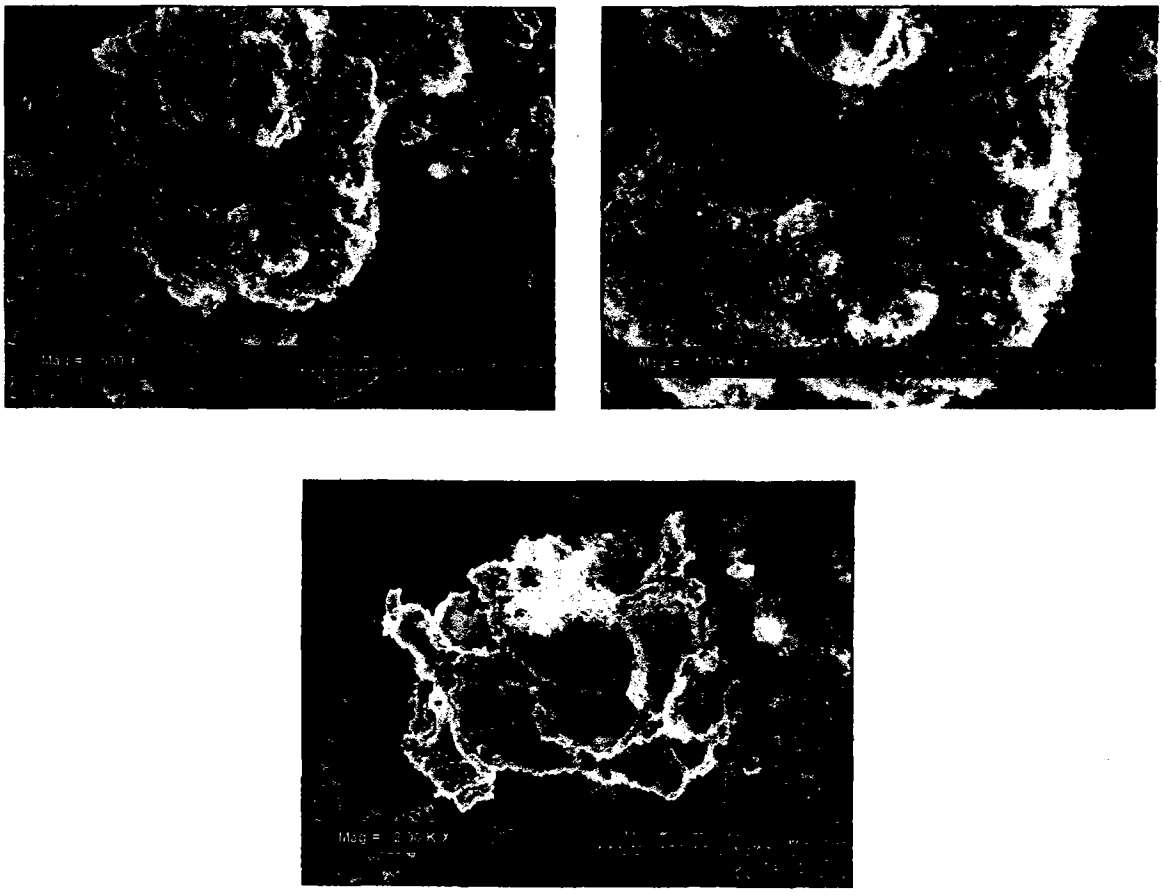

Plate 5.4 SEM photographs of light char for Parameter 4

Plate 5.5 show SEM photographs of char produced from waste tyre for Parameter 5. The photograph clearly showed pores formation. Holes of char-based carbon developed and the corner lines of the hole openings not clearly observed. The photographs showed the formation of pores scattered.

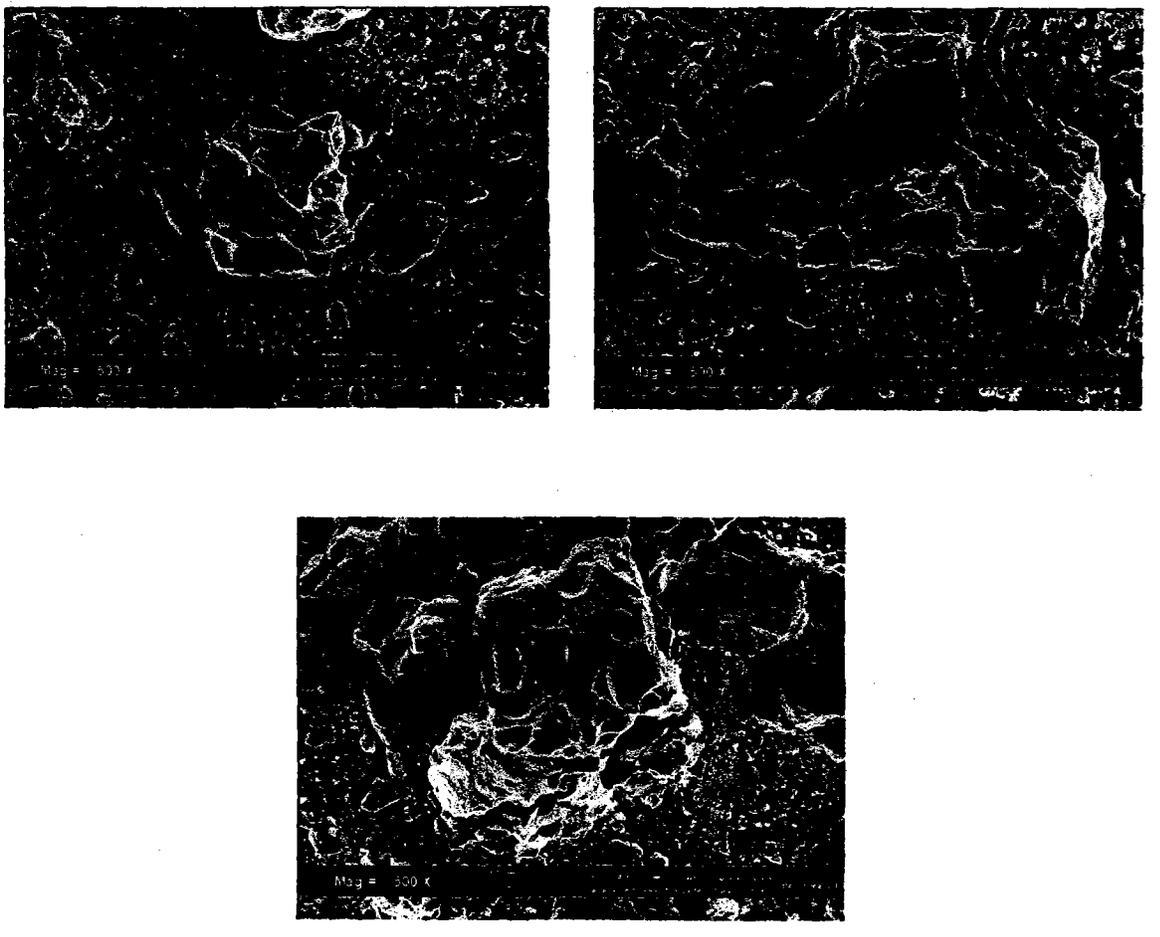

Plate 5.5 SEM photographs of char (×500) for Parameter 5

5.2.2 PROXIMATE ANALYSIS

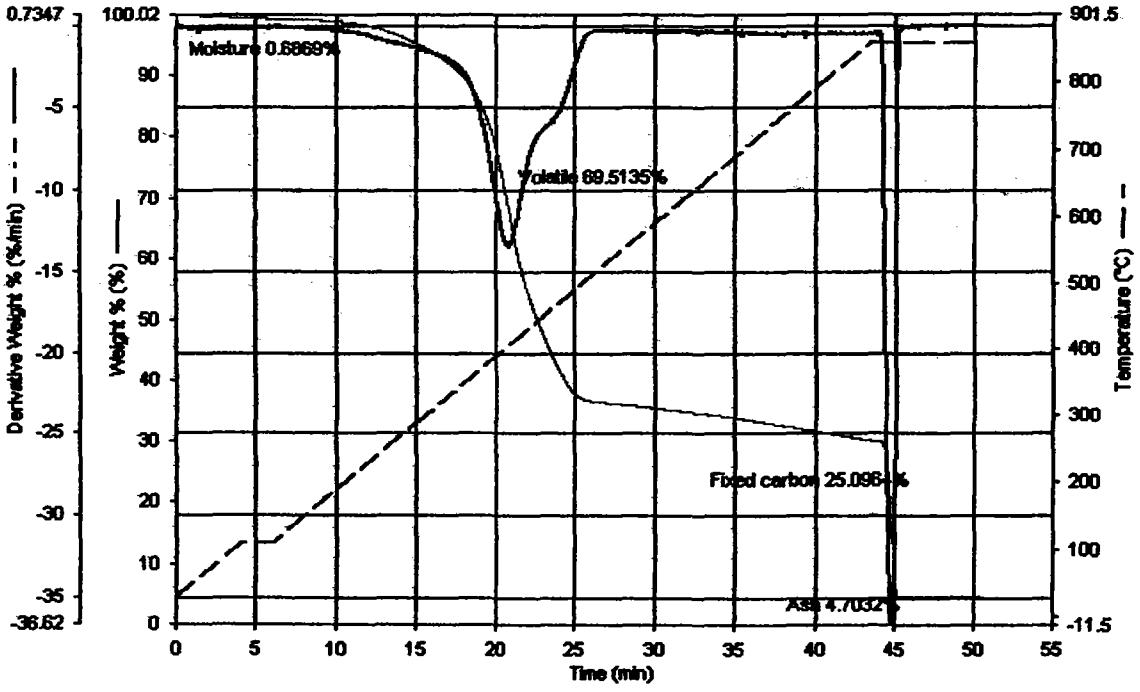

Figure 5.1 TGA analysis of waste tyre (raw material)

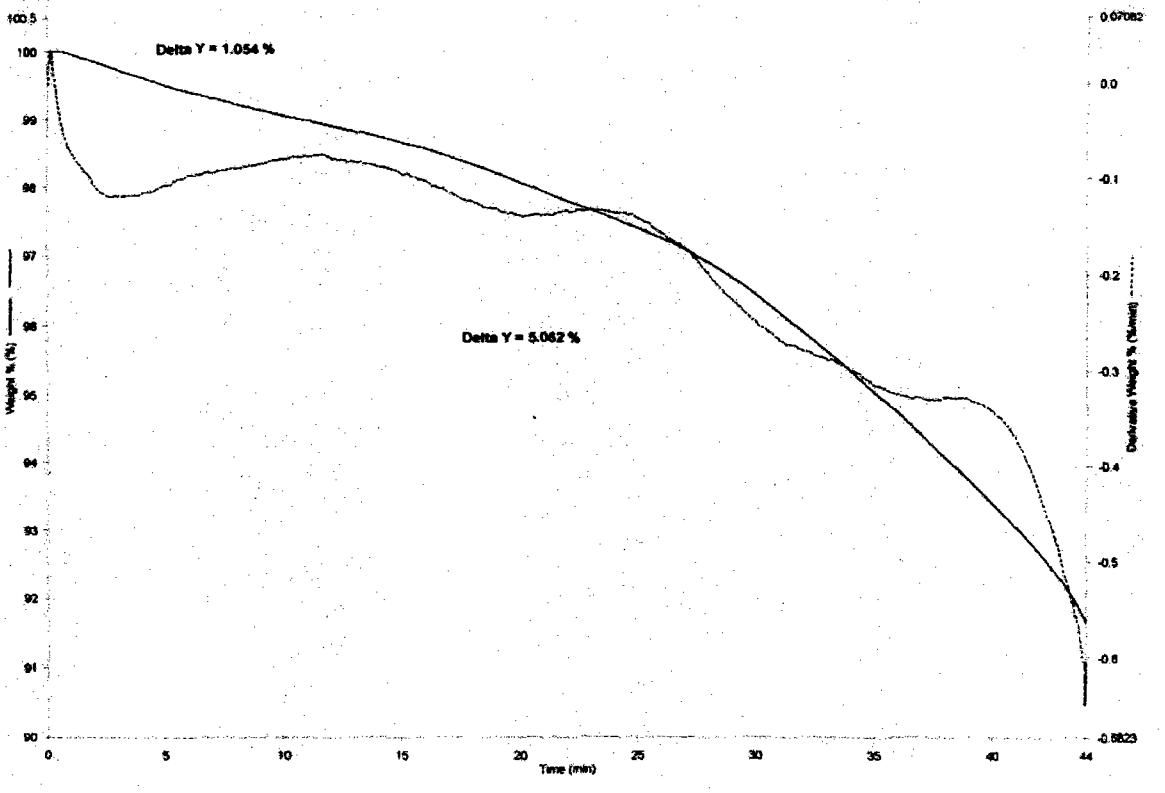

Figure 5.2 TGA analysis of char for Parameter 2

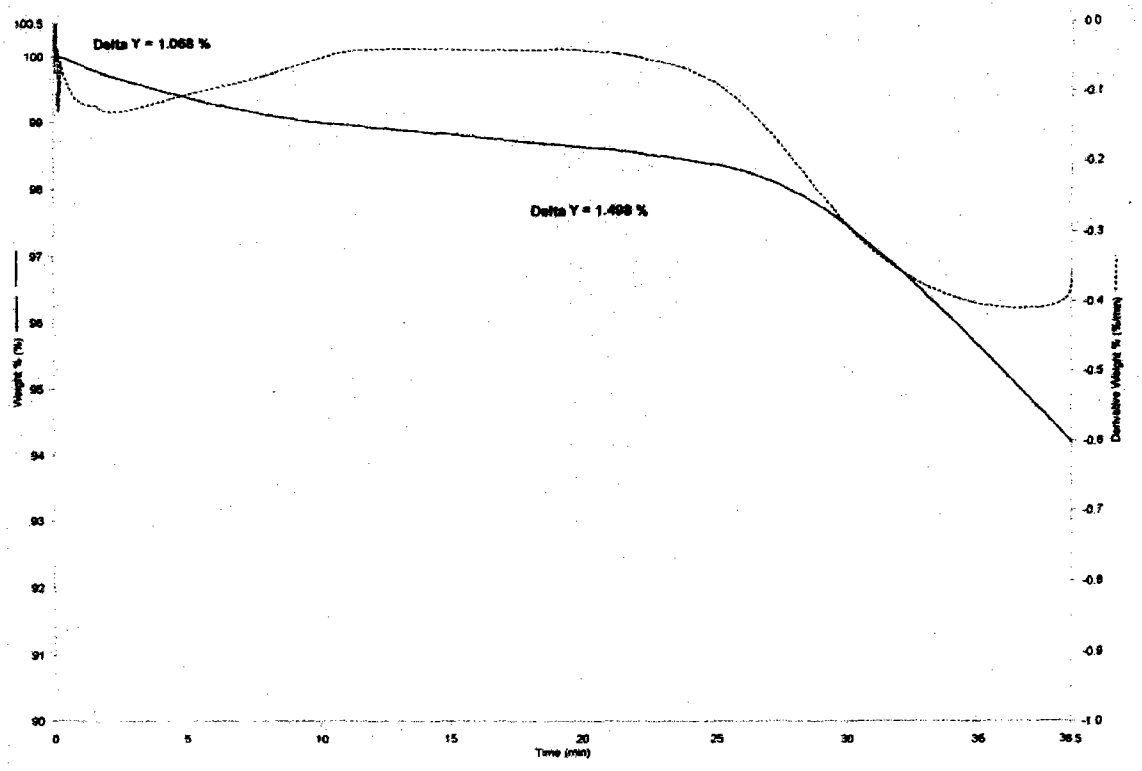

Figure 5.3 TGA analysis of char produced for Parameter 4

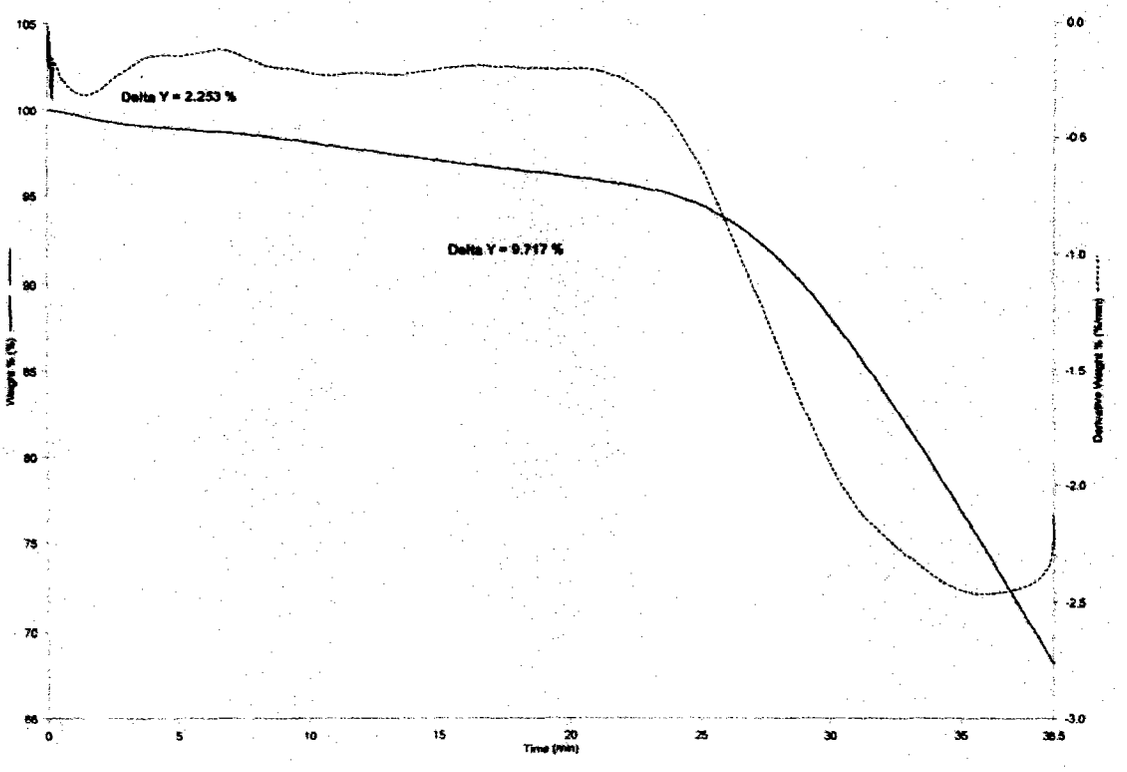

Figure 5.4 TGA analysis of light char outcome for Parameter 4

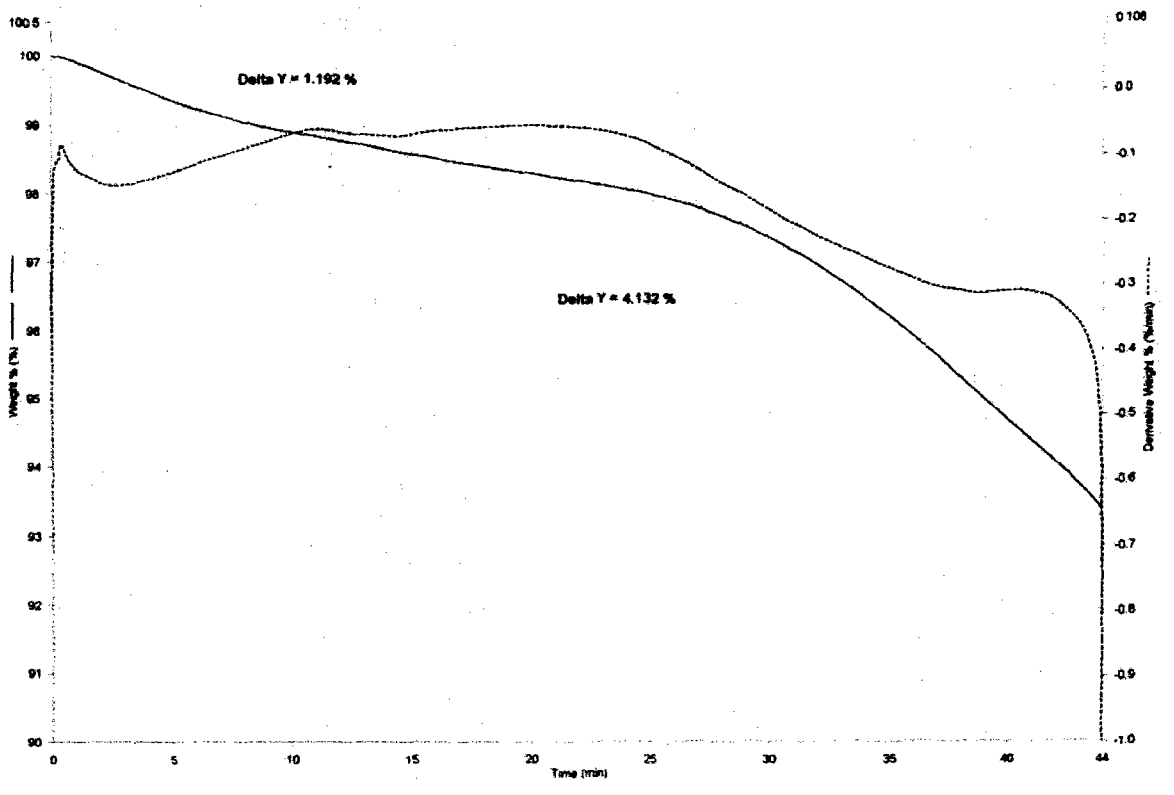

Figure 5.5 TGA analysis of light char for Parameter 5

Proximate analysis of the prepared waste tyre, chars and light char are presented in Table 5.6. Fixed carbon content is 25% in waste tyre was encouraging. The raw material also found to be rich in volatile (69%) but very low in ashes (5%). The low ash content resulted in minimal effects of organic impurities on pore development during combustion process.

The changes of moisture and volatile content in the samples were observed when the raw material was exposed to high temperature during combustion. The moisture content approximately the same for each Parameter while volatile content very low for Parameter 4 char.

Fixed carbon content to each char produced in the range 75 – 83 %. Although light char having high content of fixed carbon, the yield from combustion is low. The fixed carbon content of char for Parameter 4 and 5 give better result for further activation.

Table 5.6 Proximate analysis of waste tyre, chars and light char

	Proximate analysis, %			
	Moisture	**Volatile**	**Fixed Carbon**	**Ash**
Waste tyre	0.687	69.514	25.096	4.703
Char (Parameter 2)	1.054	4.008	*77.621*	*16.531*
Char (Parameter 4)	1.068	0.430	*82.238*	*16.264*
Light char (Parameter 4)	2.253	7.464	*75.192*	*15.091*
Char (Parameter 5)	1.192	2.94	*81.105*	*14.763*

* *Italic* value determined manually (correction).

5.2.3 Ultimate Ananlysis

Table 5.7 presents ultimate analysis of waste tyre, chars and light char. Raw material already possessed higher carbon (86%) for the reason carbon content in synthetic rubber indeed high. Heat supplied during combustion initiates combustion reaction, a thermal degradation process. Decomposition occurs because impurities like organics and volatile compounds cannot maintain their stability at high temperature. A sign of organics and volatile compounds decomposition is shown by decreasing amount of hydrogen in char samples. Combustion reaction becomes slower as most of the volatiles are being completely removed during carbonization and leaving only a portion of stable carbon as residues. Sulfur content in waste tyre and char less 2.2%. Higher feed rate and size of raw material results in higher carbon element.

Table 5.7 Ultimate analysis of waste tyre, chars and light char

	Ultimate analysis, %				
	C	H	N	S	Others
Waste Tyre	86.03	6.6	0.95	2.11	4.31
Char (Parameter 2)	75.14	0.76	0.15		
Char (Parameter 4)	80.97	0.78	0.43	1.32	
Char (Parameter 5)	78.67	0.32	0.15		

5.3 Error During Characterization

The sample was heated up from 30 °C to temperature of 850 °C at 20 °C/min. The sample supposed to be heated up to temperature of 110 °C until complete dehydration and followed by decomposition at 850 °C for 7 minutes to determine volatile matters. The atmosphere then was changed to be oxidizing. The sample was cooled to 800 °C and maintained at this temperature until the weight is remained unchanged for proximate analysis.

5.4 Correction

1 g sample is weighted and put on crucible. Then, crucible containing sample put in furnace that heated up to 750 °C for one hour. After that, sample is weighted again to determine ash content for proximate analysis.

PYROLYSIS OF WASTE TIRE: A KINETIC STUDY

By

CHEW SOON SIONG

Thesis submitted in partial fulfillment of the requirements

for the Bachelor's Degree of Chemical Engineering

April 2007

ABSTRACT

The use of waste tire as a source of raw materials for different applications is a great solution considering that waste tire is presently disposed of by incineration or land filling. The reuse of waste tire is beneficial in economy and environmental point of view. Isothermal thermogravimetric analysis (TGA) was used to study the effect of initial sample weight and temperature on the pyrolysis of waste tire. The effect of heating rate was studied with dynamic TGA. Derivative thermogravimetric (DTG) was employed to assist the studies. The sample weight was varied from 5 to 15 mg and it was found that no other rate-controlling step exists other than chemical reaction. The heating rate was varied from 5 to 20°C/min to study its effect on pyrolysis and to obtain the kinetic parameters. Three regions exist in the DTG curves indicating that there are three independent reactions occurring throughout the pyrolysis. The pyrolysis rate is assumed to be first order and Arhenius equation is applied to obtain the activation energy and pre-exponential factor for all the regions. The temperature was varied from 600°C to 800°C in the isothermal runs and the activation energy and pre-exponential factor obtained is 81.75 kJ/mol and 51.05min^{-1} respectively.

Keywords: Pyrolysis; Waste tire; Thermogravimetric analysis; Activation energy

CHAPTER 4

RESULTS & DISCUSSION

The data from the thermogravimetric analysis were analyzed and is attached in the appendix. The influence of the three factors namely initial sample weight, heating rate and temperature are studied and will be presented accordingly in this report. The influence of heating rate can be studied from the non-isothermal data while the influence of initial sample weight and temperature are to be studied from the isothermal data.

4.1 INFLUENCE OF INITIAL SAMPLE WEIGHT

By varying the initial sample weight, the weight loss rate of the samples can be used to determine whether heat or mass transport affect the pyrolysis rate. Besides, the range of operating conditions in which the reaction is the rate-controlling step can be determined. In order to find the kinetic parameters, the reaction must not be governed by mass or heat transport. Instead, the reaction kinetics must be the only rate-controlling step for Arrhenius equation to hold true.

The initial sample weights were varied from 5 to 15mg to study its effect on the pyrolysis. The weight percent, W obtained from TGA were converted to percent conversion by this simple formula:

$$\text{Percent Conversion} = 100 - W \qquad \text{(Eq. 4.1)}$$

The plot of percent conversion of waste tire for the three initial sample weights is shown in Figure 4.1. The data of the 5, 10 and 15mg of sample weight is obtained from Run 4, 7 and 8 respectively.

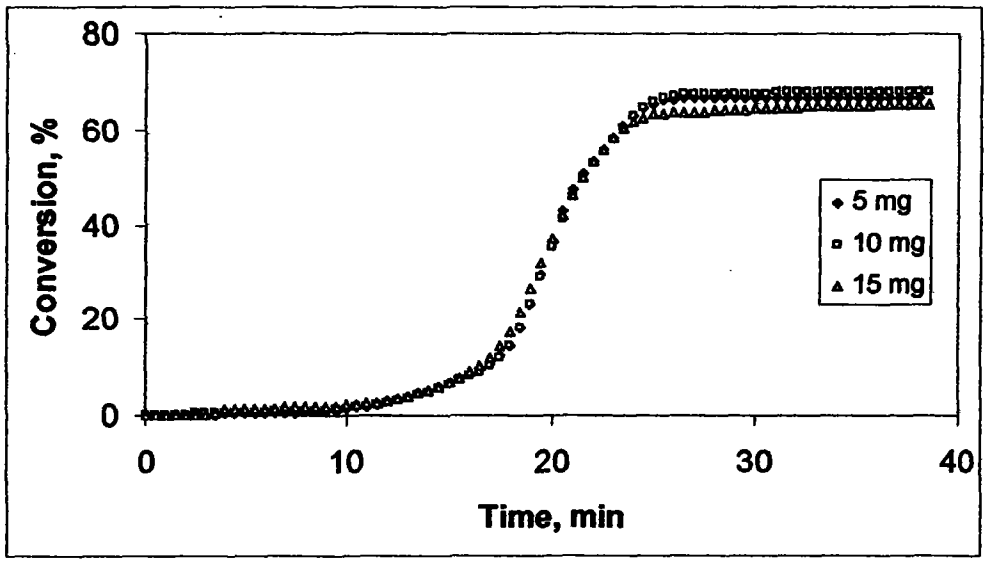

Figure 4.1: Influence of initial sample weight to the percent conversion versus time.

Gonzalez et. al.(2000) performed isothermal pyrolysis of shredded automobile tires at 600°C with initial sample weight of 10 to 100mg. There are three transport processes that may influence the global rate. They are the intra-particle transport, particle-to-fluid transport and inter-particle transport. The intra-particle transport is affected by particle size while the particle-to-fluid transport is affected by nitrogen flow rate and particle size. The inter-particle transport can be studied with fixed particle size and varies the number of layers of particles. Varying the initial sample weight does this.

Since nitrogen flow rate and the sample size are kept constant in all the runs, it can be deduced that intra-particle transport and particle-to-fluid transport do not affect the global rate of pyrolysis. Figure 4.1 shows that the three curves of initial sample weight of 5, 10 and 15 mg are super-imposable from the start until about 23 minutes of the reaction. From that time onwards, there exist differences especially for the run with 15mg initial sample weight. However, these differences are only due to the heterogeneity of the sample

composition. Therefore it is concluded that there is no inter-particle transport that is influencing the pyrolysis rate. This result is similar to Gonzalez et. al.

When only a small amount of sample is used (i.e. 5 mg), all the three transport processes, namely intra-particle, particle-to-fluid and inter-particle transport will be eliminated. The only rate-controlling step present would be the chemical reaction. The heat and mass transfer limitations are minimized. Therefore, 5mg of initial sample weight is used for all the other runs in determining the kinetic parameters.

4.2 INFLUENCE OF HEATING RATE

The heating rates were varied between 5 to 20°C/min and the activation energy and pre-exponential factor were calculated. Figure 4.2 and Figure 4.3 are the thermogravimetric (TG) curves for Run 1, 2 and 3. Figure 4.2 shows the weight percent curve versus temperature for the three heating rates. All the three curves give similar trend along the temperature range indicating that the three samples have the same composition, as in expectation. As the heating rate is increased, from 5 to 20°C/min, the curve moves slightly to a higher temperature range. Figure 4.3 plot the weight percent curve against a time axis. The weight of the sample reduces quicker for a higher heating rate. This is because the decomposition rate of the tire is higher at high temperature.

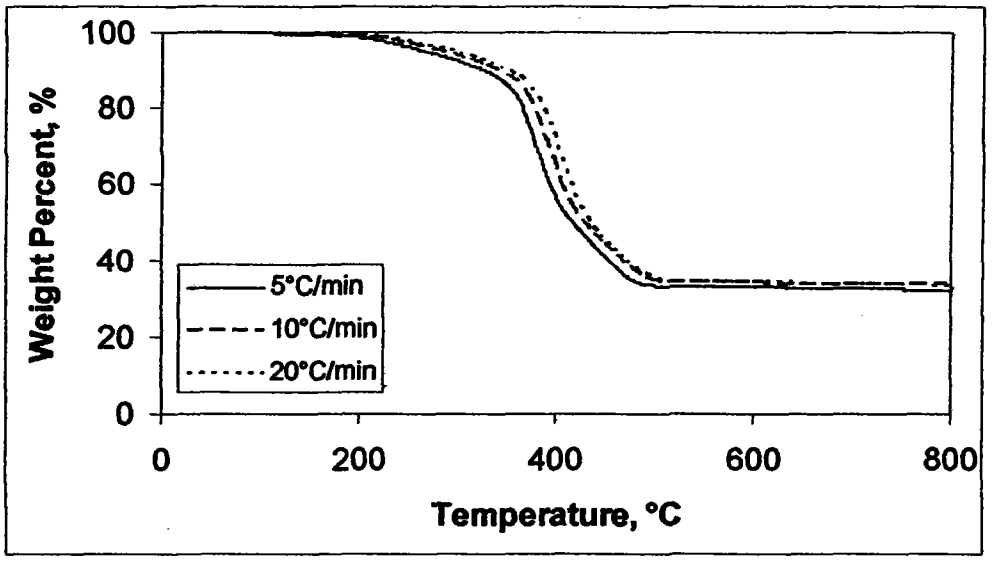

Figure 4.2: Influence of heating rate on the pyrolysis of waste tire.

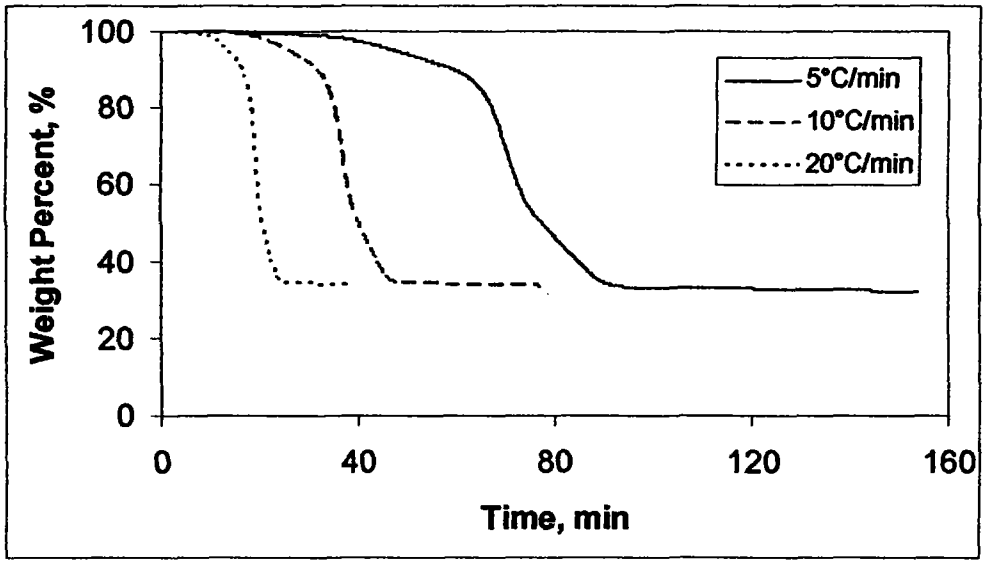

Figure 4.3: Influence of heating rate on the weight percent versus time.

The characteristic temperatures such as the start and final temperatures of pyrolysis are difficult to determine from TG curves. Derivative thermogravimetric (DTG) curves as shown in Figure 4.4 are more useful in displaying subtle changes in mass, which are not

easily discernable on the TG curves. The temperatures of the start, peak and final of the weight loss can be obtained from the DTG and are tabulated in Table 4.1.

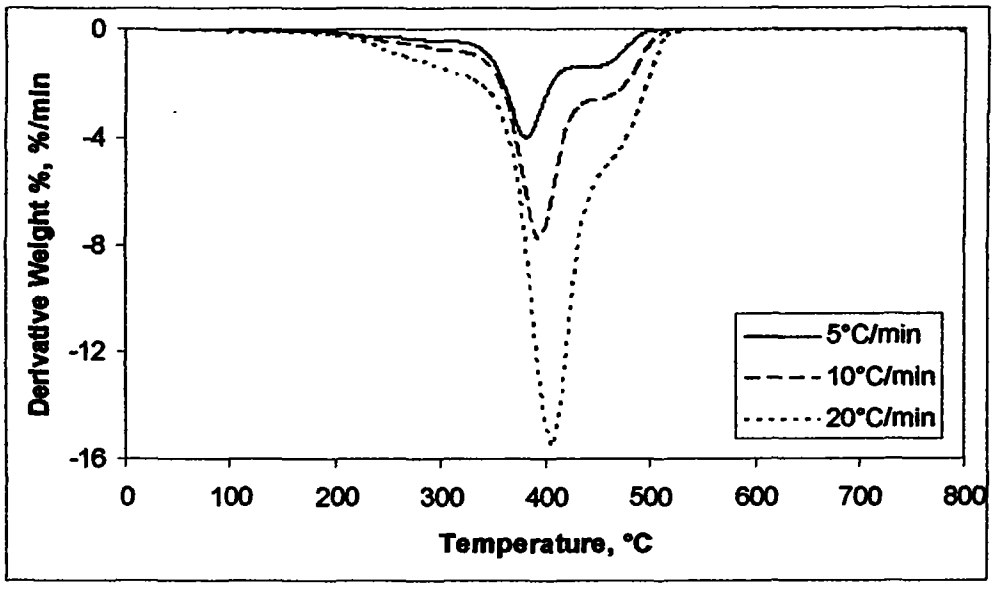

Figure 4.4: Derivative thermogravimetric curves to study the influence of heating rate.

Table 4.1: Characteristic temperatures of the DTG curves.

Heating rate °C/min	Temperature, °C			Derivative Weight % at peak % / min	Weight Loss %
	Starting T_o	At peak T_1	Final T_f		
5	150	382	505	3.9985	68.0
10	170	394	520	7.8092	66.8
20	180	406	525	15.5015	66.9

The reaction zones shift to a higher temperature range when the heating rate is increased. The major weight loss starts at 150°C, 170°C and 180°C for the heating rate of 5, 10 and 20°C/min respectively. The weight loss ends at 505°C, 520°C and 525°C when the heating rate is increased from 5, 10 to 20°C/min respectively. In general, the starting and final temperatures of the weight loss increase with increasing heating rate. Leung and

Wang (1998) reported the same finding. The finding of increased starting temperature with the increased of heating rate is contradictory to the result reported by Chen et. al. (2001). However they reported the same finding of increased T_f with increasing heating rate. The comparison can be seen in Table 4.2. Accurate assignment of T_o and T_f are difficult because it is not easy to decide when the major weight loss begins and ends.

Table 4.2: Comparison of the starting temperature, T_o and final temperature, T_f in °C.

Heating rate	**This work**		**Leung et. al.(1998)**		**Chen et. al.(2001)**	
°C/min	**T_o**	**T_f**	**T_o**	**T_f**	**T_o**	**T_f**
5	150	505	-	-	247	501
10	170	520	185	500	219	503
20	180	525	-	-	213	522
30	-	-	250	520	209	548
45	-	-	260	545	-	-

On the other hand, the temperature for the maximum weight loss rate is relatively easy to decide as indicated by the peak of the DTG curve. The DTG values are negative because it is a measure of weight loss rate. Figure 4.4 shows a dominant peak for the three DTG curves. The increase of heating rate causes the peak to shift to a higher temperature, from 382°C to 406°C for heating rate of 5°C/min and 20°C/min respectively. In addition, the peak height also increases dramatically indicating a higher maximum weight loss rate. The peak height increased from 4.0 to 15.5 %/min. These results are similar to other reports.

The total weight loss for Run 1, 2 and 3 are 68.0%, 66.8% and 66.9 % respectively. These final weight losses only vary slightly due to heterogeneity of the waste tire samples,

(i.e. the initial amount of samples used are not exactly 5mg). The remaining residue of about 33% of initial weight is carbon black or char that would only decompose at a higher temperature in the presence of oxygen.

There is a smaller second peak especially for the low heating rate of 5°C/min. This second peak becomes less pronounce at high heating rate. Williams and Besler (1995), Senneca et. al. (1999) and Gonzalez et. al. (2001) reported that at higher heating rate, the second peak would become less pronounce and eventually become a single peak at a high heating rate. On the contrary, Chen et. al. found that a second peak appears at high heating rate in their studies of pyrolysis of scrap automotive tires of passenger car and truck. However, they concluded that the smoothness of the both TG curves suggested that degradations of two tires might be accounted for or approximated by one lumped reaction.

Figure 4.5 represents the typical DTG curves of the non-isothermal operation runs. Three regions can be distinguished over a temperature range of 200°C to 500°C. This means that the volatiles in tires might be divisible into three non-interacting groups that evolve by three independent parallel reactions. The reactions are assumed to be first order reactions. The existence of these regions suggests that the waste tire sample contains natural rubber (NR), polybutadiene rubber (PBR), styrene butadiene rubber (SBR) and other constituents such as moisture, oil, plasticizers and additives. These constituents would be decomposed at different rates and at different temperature regions when subjected to pyrolysis.

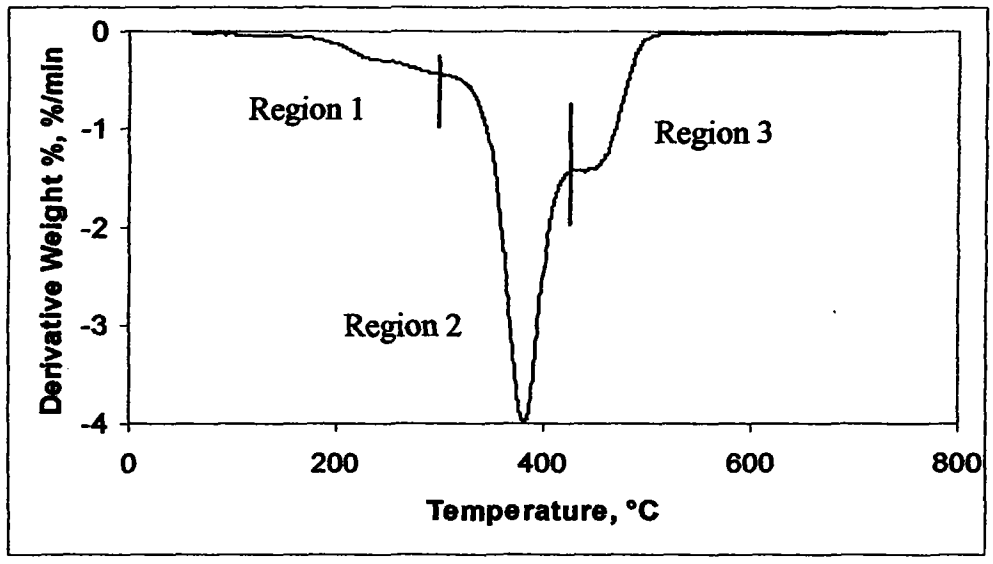

Figure 4.5: DTG curve for heating rate of 5°C/min

Region 1 is the thermal decomposition of a mixture of oil, moisture, plasticizers and additives as well as other low boiling compounds. These volatiles cause the weight loss detected in the range of 150°C to 300°C. Region 2 and 3 are the decomposition of the three rubber materials. Region 2 is in the temperature range of 320°C to 420°C and the weight loss is attributed to NR and PBR. The weight loss rates reach maximum at an average temperature of 394°C as shown in the DTG curves. This shows that the sample contains mainly of natural rubber because the area under the DTG curve is proportional to the amount of weight loss. Region 3 is a second peak and is in temperature range of 420°C to 500°C. This second peak is overlapping with the main peak especially at high heating rate where there exists only one peak. This region 3 is the decomposition of PBR and SBR. The relatively low peak height suggested that the sample has only a small amount of SBR and PBR compared to NR.

Williams and Besler found that NR largely decomposes at a lower temperature than SBR and PBR. PBR shows a tendency to two-stage decomposition, but the secondary decomposition is much less prominent. Bhowmick et. al. (1987) have also shown that thermal degradation of NR in nitrogen at a heating rate of 10°C/min starts at about 330°C and is complete by 485°C. Liu et. al. (1992) investigated the pyrolysis of NR, BR and SBR and found that the maximum weight loss rate of NR occurs at a temperature of 373°C, BR at 372°C and 460°C, SBR at 372°C and 429 - 460°C.

In order to determine the kinetic parameters, the three regions are calculated separately and are assumed to be first order reactions. The decomposition rate can be expressed as:

$$\frac{dW}{dt} = -k\left(W - W_f\right) \qquad \text{(Eq. 4.2)}$$

where W = weight of sample at time t (%)

W_f = weight of the residue at the end of the reaction (%)

k = rate constant (min^{-1})

The rate constant, k can be defined by Arrhenius equation as:

$$k = k_o e^{-\frac{E_a}{RT}} \qquad \text{(Eq. 4.3)}$$

where k_o = pre-exponential factor (min^{-1})

E_a = activation energy (kJ/mol)

R = ideal gas constant = 8.314×10^{-3} kJ/mol·K

T = absolute temperature (K)

Therefore,

$$\frac{dW}{dt} = -k_o e^{\frac{E_a}{RT}} (W - W_f) \qquad \text{(Eq. 4.4)}$$

$$-\frac{1}{(W - W_f)} \frac{dW}{dt} = k_o e^{\frac{E_A}{RT}} \qquad \text{(Eq. 4.5)}$$

$$\ln\left(-\frac{1}{(W - W_f)} \frac{dW}{dt}\right) = \ln k_o - \frac{E_a}{RT} \qquad \text{(Eq. 4.6)}$$

Temperature, $T = T_o + \beta t$ where β is the heating rate (°C/min)

$$\frac{dT}{dt} = \beta \qquad \text{(Eq. 4.7)}$$

Therefore,

$$\ln\left(-\frac{1}{(W - W_f)} \frac{dW}{dT}\right) = \ln \frac{k_o}{\beta} - \frac{E_a}{RT} \qquad A = \frac{k_o}{\beta} \qquad \text{(Eq. 4.8)}$$

$$\ln\left(-\frac{1}{(W - W_f)} \frac{dW}{dT}\right) = \ln A - \frac{E_a}{RT} \qquad \text{(Eq. 4.9)}$$

Arrhenius plot is a straight line

$$\ln\left(-\frac{1}{(W - W_f)} \frac{dW}{dT}\right) \text{ versus } \frac{1}{T}$$

with slope $= -\frac{E_a}{R}$

intercept $= \ln A$

These plots are applied separately to the three regions for each heating rate and the results are as shown in Table 4.3. The least square fit method is used to obtain the best straight line and the correlation coefficient, r^2 were above 0.98 for all the regions.

Table 4.3: Activation energies and Arrhenius pre-exponential factors.

Heating rate	Activation energy, E_a (kJ/mol)			Pre-exponential factor, A (min^{-1})		
°C /min	Region 1	Region 2	Region 3	Region 1	Region 2	Region 3
5	20.06	145.16	95.22	2.07	3.85×10^{10}	1.22×10^{6}
10	28.42	157.92	97.13	3.21	5.20×10^{11}	2.66×10^{6}
20	28.46	139.08	87.71	9.48	2.11×10^{10}	9.81×10^{5}
Average	**25.65**	**147.39**	**93.36**	**4.92**	**1.93×10^{11}**	**1.62×10^{6}**

Refer Appendix for the Arrhenius plots of all regions.

The activation energy and pre-exponential factors do not show any specific trend when the heating rate is being increased. Region 1 has the lowest activation energy and pre-exponential factor whereas region 2 has the highest values. The average activation energy, E_a are 25.6 kJ/mol, 147.4 kJ/mol and 93.4 kJ/mol; and the pre-exponential factor, A are 4.92 min^{-1}, 1.93×10^{11} min^{-1} and 1.62×10^{6} min^{-1} for region 1, 2 and 3 respectively. Gonzalez et. al. also reported the activation energy, E and pre-exponential factor, A in three regions. However, the E and A values reported are much smaller and have a declining trend from region 1 to 3. Leung and Wang has reported a slightly greater values of E = 164.5 kJ/mol and 136.1 kJ/mol; and A = 6.29×10^{13} min^{-1} and 2.13×10^{9} min^{-1} for lower and higher temperature range respectively when the heating rate is 10°C/min. The report concluded that when heating rate is increased, the kinetic parameters would increase, hence increasing the difficulties of pyrolysis reaction. On the other hand, Williams and

Besler reported a decrease in activation energy with increasing heating rate. Bhowmick et. al. calculated E of 225 kJ/mol for the degradation of NR while Brazier and Schwartz (1989) calculated E of 251 kJ/mol for the first stage degradation of PBR. The kinetic parameters are different when being compared to other authors because the samples used are different.

Mechanism for pyrolysis of waste tire is proposed:

Process	**Mechanism**	**Reaction**
Primary Pyrolysis (Region2)	C* ⟶ Volatiles	Main chain scission and depolymerization
Cyclization	C ⟶ Residue	Cyclization and cross-linking
Secondary Pyrolysis (Region3)	Residue ⟶ Volatiles	Degradation of cyclization products

* C represents an organic chain molecule such as NR, PBR and SBR.

Ref: Brazier and Schwartz.

Kinetic models of the pyrolysis rate are proposed:

The rate equations can be written in the form,

$$\frac{dW}{dt} = -Ae^{-\frac{E_a}{RT}}(W - W_f) \qquad \text{or} \qquad \ln k = \ln A - \frac{E_a}{RT}$$

The rate equations for the three regions are as follow:

Region 1: $$\frac{dW}{dt} = -4.92e^{-\frac{3,085}{T}}(W - W_f) \qquad \text{or} \qquad \ln k = 1.59 - \frac{3,085}{T}$$

Region 2: $\frac{dW}{dt} = -1.93 \times 10^{11} e^{-\frac{17,728}{T}} (W - W_f)$ or $\ln k = 25.99 - \frac{17,728}{T}$

Region 3: $\frac{dW}{dt} = -1.62 \times 10^{6} e^{-\frac{11,229}{T}} (W - W_f)$ or $\ln k = 14.30 - \frac{11,229}{T}$

4.3 INFLUENCE OF TEMPERATURE

Isothermal experiments at 600°C, 700°C and 800°C were carried out in Run 4, 5 and 6 respectively. The TGA and DTG curves are shown in Figure 4.6 and Figure 4.7.

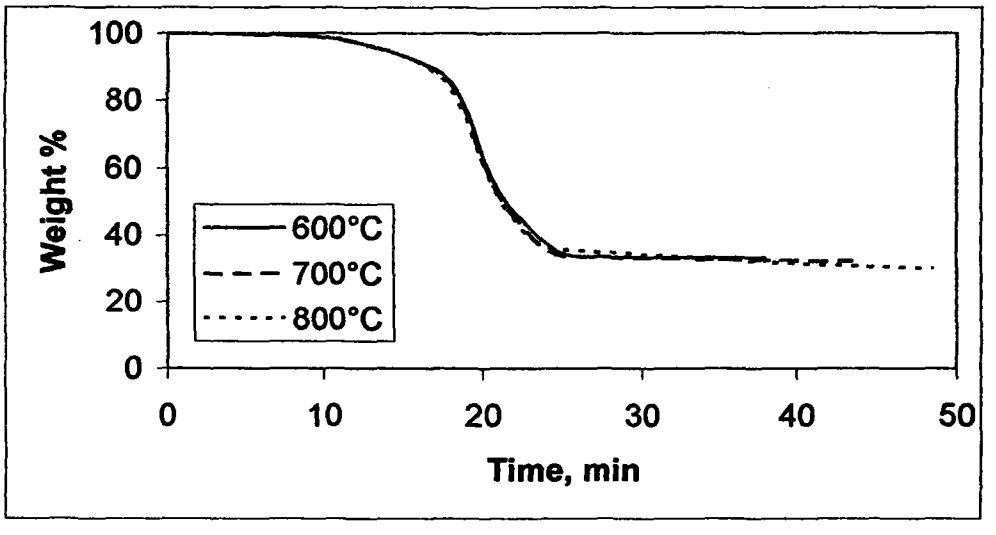

Figure 4.6: The influence of temperature on the weight loss.

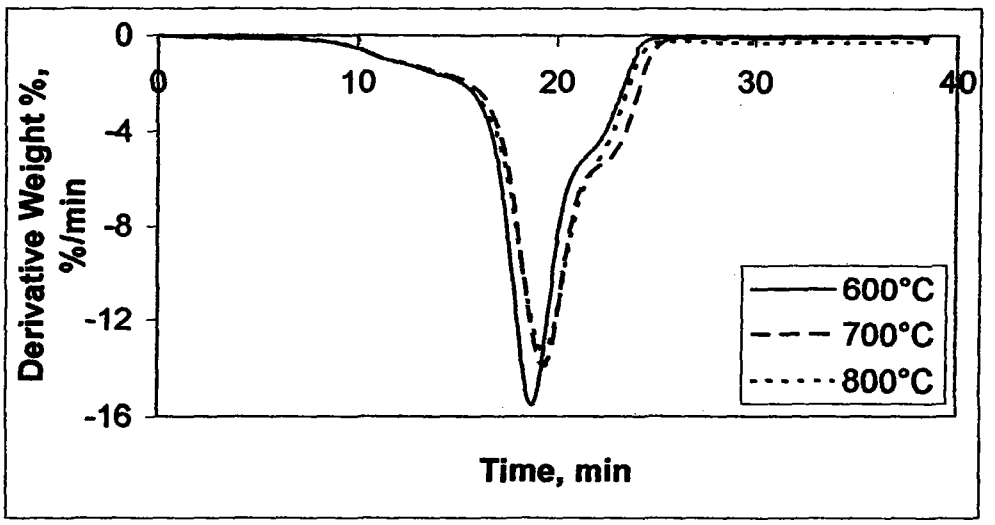

Figure 4.7: Derivative thermogravimetric for the influence of temperature.

Generally there is no difference in the TG curves when the temperature is varied as shown in Figure 4.6. This is contradictory to Gonzalez et. al. that shows greater weight loss rate with increase of temperature. However Gonzalez et. al. run the isothermal experiments at 400°C to 600°C. Their report shows that the TG curves would move towards each other at high temperature (i.e. 550°C curve is very near 600°C curve). Therefore it can be concluded that weight loss rate increase with temperature up to 600°C and further increase of temperature will not affect the weight loss rate.

The DTG curves exhibit single peak at high temperature of 800°C but smaller second peak can be observed at lower temperatures as shown in Figure 4.7. The peaks displaced to a greater times when the temperature of the process is increased. Besides, higher temperature process creates lower dominant peak. These results derived from the DTG curves are all contradictory to Gonzalez et. al. This may be due to the different temperature range used.

In order to find the kinetic parameters, a one-step mechanism with a first order reaction was assumed. The pyrolysis rate is:

$$\frac{dX}{dt} = k(1-X) \qquad \text{(Eq 4.10)}$$

where X = conversion or the ratio between the solid weight loss to the initial solid weight

k = kinetic constant (min^{-1})

t = time (min)

Integrating the equation,

$$\int_0^X \frac{1}{1-X} dX = \int_0^t k\, dt \qquad \text{(Eq. 4.11)}$$

$$\left[-\ln(1-X)\right]_0^X = \left[kt\right]_0^t \qquad \text{(Eq. 4.12)}$$

$$-\ln(1-X) = kt \qquad X = \frac{100-W}{100} \qquad \text{(Eq. 4.13)}$$

$$\ln\left(1-\frac{100-W}{100}\right) = -kt \qquad \text{(Eq. 4.14)}$$

$$\ln W = -kt + \ln 100 \qquad \text{(Eq. 4.15)}$$

The plots of ln W versus time will yield straight lines with a slope of –k. Figure 4.8, 4.9 and 4.10 shows the plots for pyrolysis temperature of 600°C, 700°C and 800°C respectively. Table 4.4 gives the resulting kinetic constants, k and the correlation coefficients, r^2 from the straight line least square fit. The values of r^2 of over 0.98 for all the plots indicate that the fits are good. This indicates that the assumed first order reaction is indeed correct.

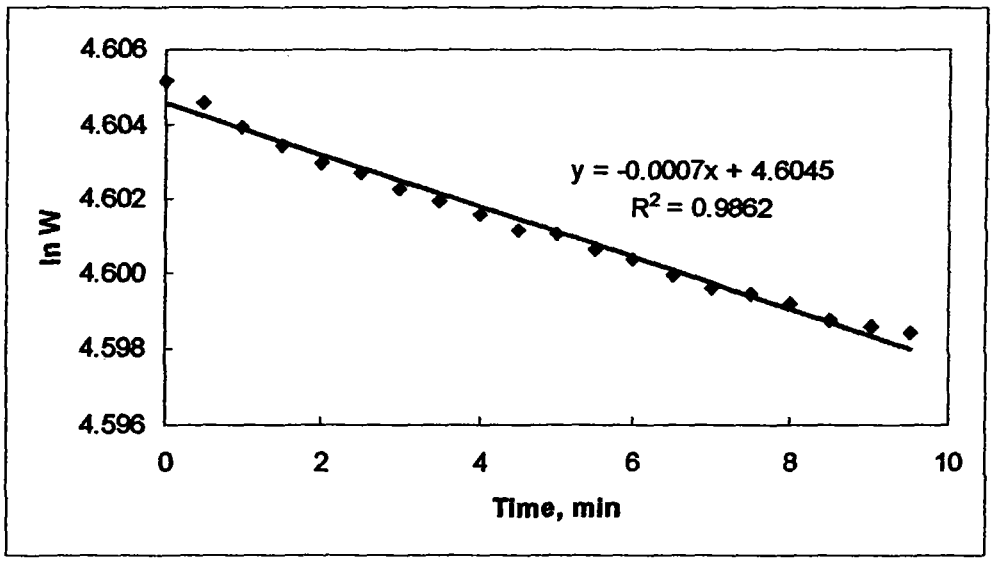

Figure 4.8: Plot of ln W versus time for pyrolysis temperature of 600°C.

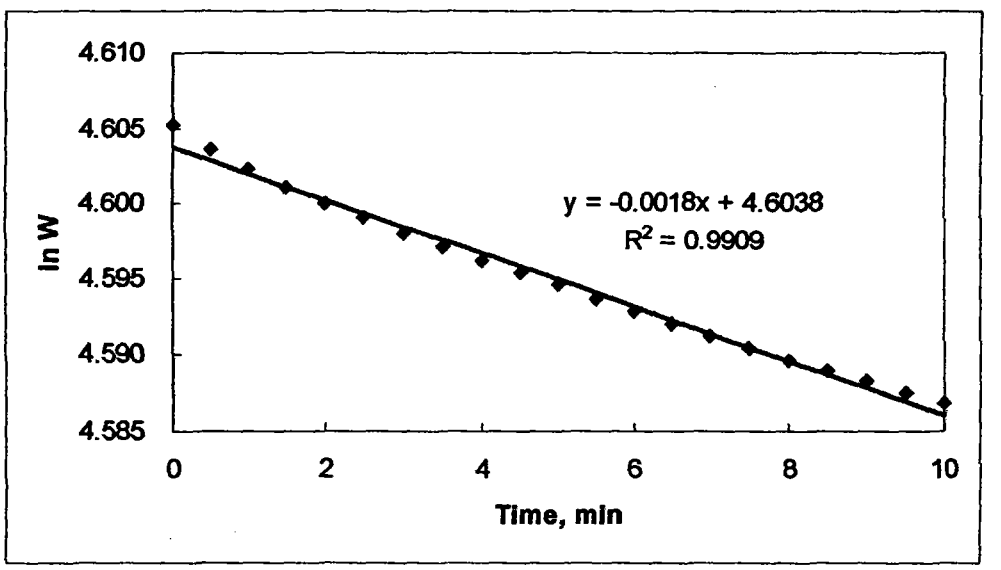

Figure 4.9: Plot of ln W versus time for pyrolysis temperature of 700°C.

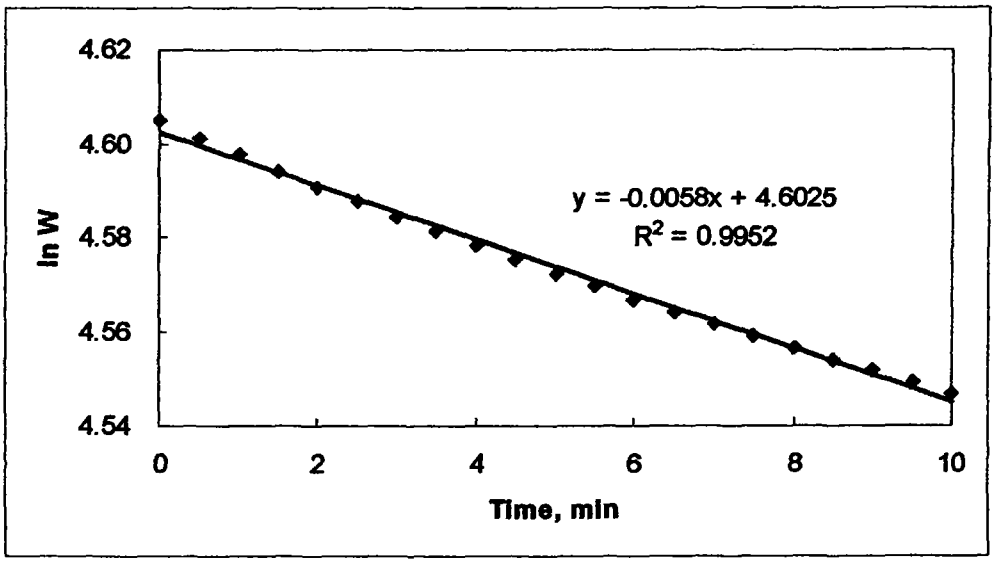

Figure 4.10: Plot of ln W versus time for pyrolysis temperature of 800°C.

Table 4.4: Kinetic constants and correlation coefficients for the isothermal runs.

Run	Temperature, T °C	Kinetic constant, k min^{-1}	Correlation Coefficient, r^2
4	600	0.0007	0.986
5	700	0.0018	0.991
6	800	0.0058	0.995

The values of k can be described as an Arrhenius function:

$$k = Ae^{-\frac{E_a}{RT}} \qquad \text{(Eq. 4.16)}$$

$$\ln k = \ln A - \frac{E_a}{RT} \qquad \text{(Eq. 4.17)}$$

The plot of ln k versus 1/T will yield a straight line with a slope of $-E_a/R$ and an intercept of ln A.

Figure 4.11 shows the plot. The activation energy can be calculated from the slope while the pre-exponential factor is obtained from the intercept of the plot.

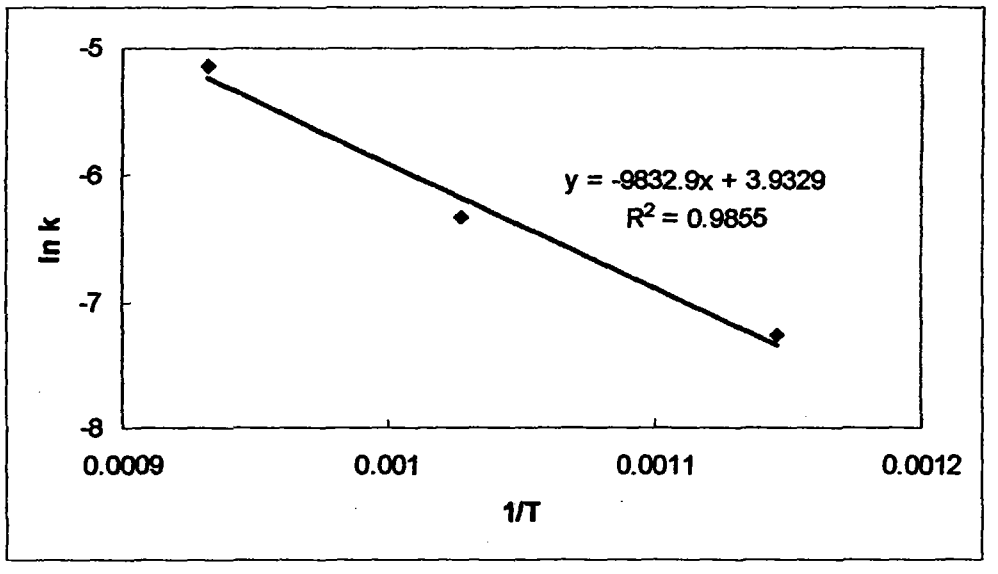

Figure 4.11: Plot of ln k versus 1/T.

The activation energy, E_a obtained is 81.75 kJ/mol and the pre-exponential factor, A is 51.05 min^{-1} or 3,060 s^{-1}. These kinetic parameters are slightly higher when compared to the work of Gonzalez et. al. as shown in Table 4.5.

Table 4.5: The comparison of the kinetic parameters between this work and others.

Kinetic Parameters	**Activation Energy, E_a kJ/mol**	**Pre-exponential factor, A s^{-1}**
This work	81.75	3,060
Gonzalez et. al.	67.20	1,800

PREPARATION OF ACTIVATED CARBON FROM WASTE TIRES BY PYSIOCHEMICAL ACTIVATION AND ADSORPTION PERFORMANCE

NADIA BINTI ISA

UNIVERSITI SAINS MALAYSIA
2007

ABSTRACT

Accumulation of waste tires are increasing every year as the number of vehicles increases. It has contributed to health and environment problems. Therefore, in this work it is converted to activated carbon that is beneficial. High value of carbon content in char produced from waste tires through pyrolisis in the fluidized bed pilot plant was activated with KOH etching followed by carbon dioxide, CO_2 gasification (physiochemical activation). Phenol is applied as the adsorbate to investigate the adsorption capacity. Further study being conducted to determine total fixed carbon and compositions inside waste tire, char and produced activated carbon. The best condition of activated carbon obtained from this work is at activation temperature 850°C, KOH to char ratio 5 and activation time 2 hours where the adsorption capacity obtained is 200mg/g which is higher compared to other works.

Keywords : Waste tires, Activated carbon, Physiochemical activation, Phenol, Adsorption.

CHAPTER 5 : RESULTS AND DISCUSSION

5.1 Raw Material: Waste Tire

The structures of tire are shown according to Figure 5.1 and Figure 5.2. The tire's pore structures could not be seen as the tire is not being combust or undergo the pyrolysis process. Based on Figure 5.3, the proximate result for the waste tires are tabulated in Table 5.1. The amount of fixed carbon in the waste tire is quite high which is 25.0964% where as the amount of ash is low which about 4.7032%. The same result can be obtained from elemental analysis where the highest value is for carbon content which is 86.03%. Therefore, waste tire is suitable to be converted to activated carbon as the amount of carbon is quite reasonable.

Table 5.1 : Elemental composition and proximate analysis of waste tire.

Elemental Composition, %		**Proximate Analysis, % (TGA)**	
Composition	**Value**	**Analysis**	**Value**
Carbon	86.03	Fixed Carbon	25.0964
Sulfur	2.11	Volatiles Matters	69.5135
Nitrogen	0.95	Ash	4.7032
Hydrogen	6.6	Moisture	0.6869
Others	4.31		

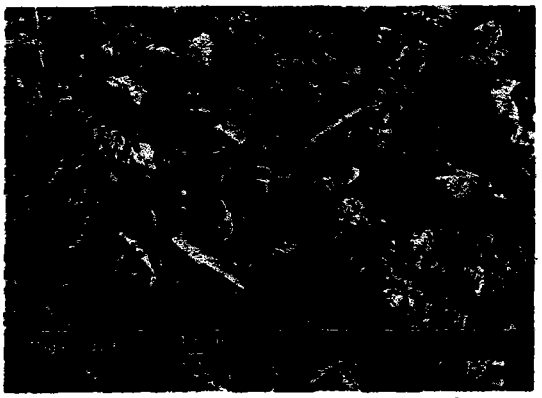

Figure 5.1 : Waste tire magnified 50 X.

Figure 5.2 : Waste tire magnified 4000 X.

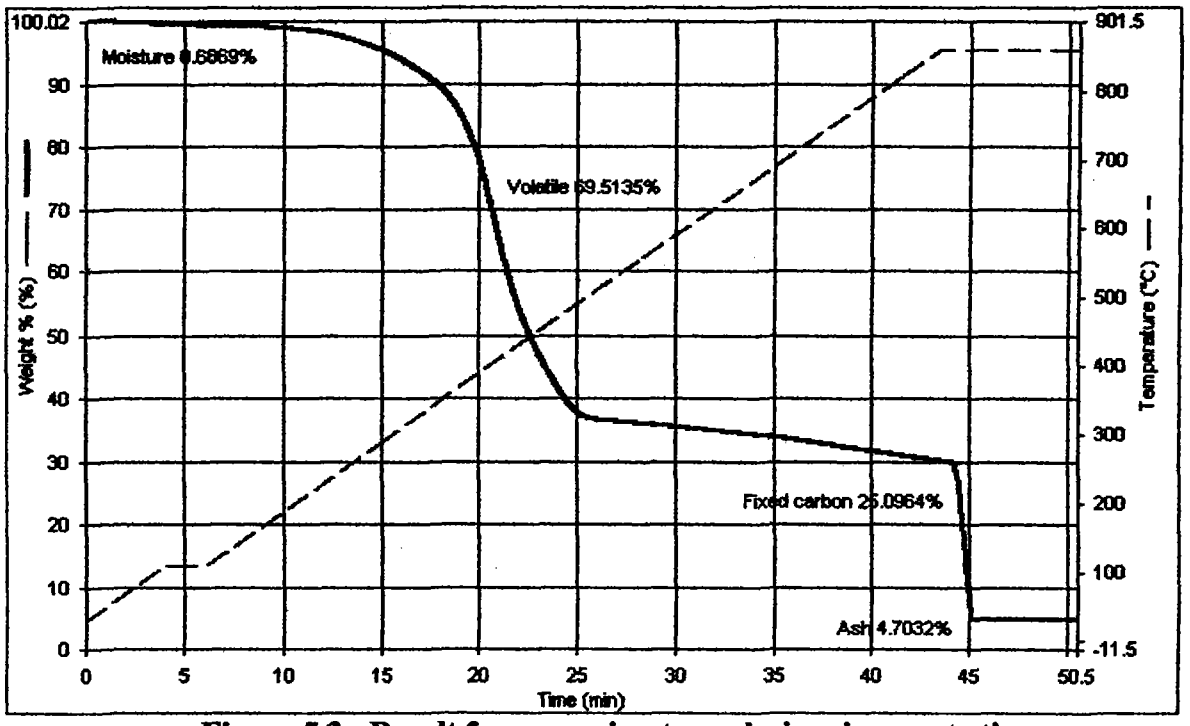

Figure 5.3 : Result from proximate analysis using waste tire

5.2 Production of char using fluidized bed pilot plant

The temperature used to produce char is about 800°C and the time for pyrolysis reaction is about 30 minutes. After 30 minutes reaction of 500 gram waste tires, the yield of char is about 26% and yield of light hydrocarbon is about 22%. Another 52% is collected as water, oil and gaseous that released to the atmosphere. Therefore, the production of char from this work is comparable with pyrolysis result using fluidized bed gasifier where the yield of char is in the range of 24% to 37% [Leung and Wang, 2003] and using batch tubular fixed bed reactor where the yield of char is 33% to 38% [Brady et al., 1995]. The percentage yield of char is calculated based on equation 1.

$$\text{Yield of char} = \frac{\text{Weight of char produced}}{\text{Weight of tire fed}} \times 100 \qquad (1)$$

According to Figure 5.4 (*as indicated by white arrow*), the structure of char from waste tire is highly porous and the pores are distributed uniformly. The size of each pore is about 10.68 micron meter. The smaller the pore size, the higher the surface area and adsorption can occur effectively.

Light hydrocarbon is collected from the second cyclone (Figure 4.2) and the pore structures being tested. The structures of light hydrocarbon are fluffy and very light (Figure 5.5). The probability of high pore structure is too low because the hydrocarbon produced is nearly formed into ash. Therefore, it is not suitable to be further activated to form activated carbon.

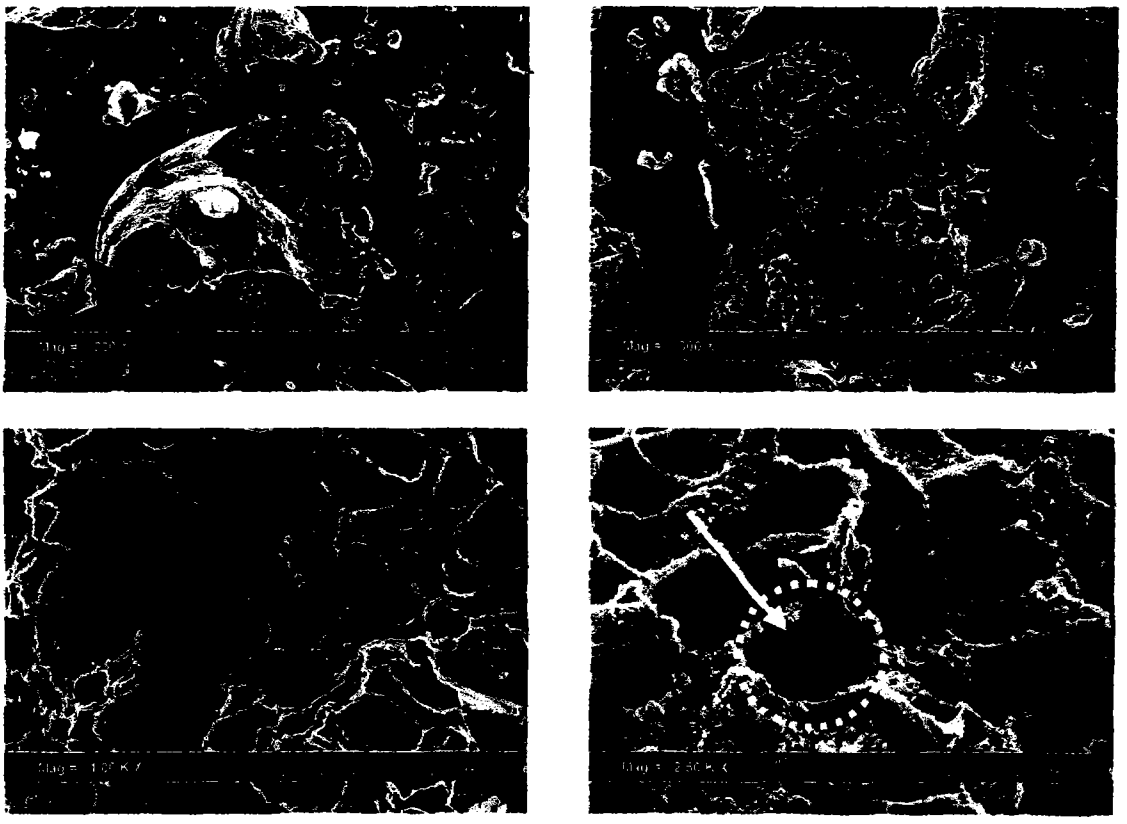

Figure 5.4 : Pore structures of char magnified 200 X, 300 X, 1000 X and 2500 X respectively.

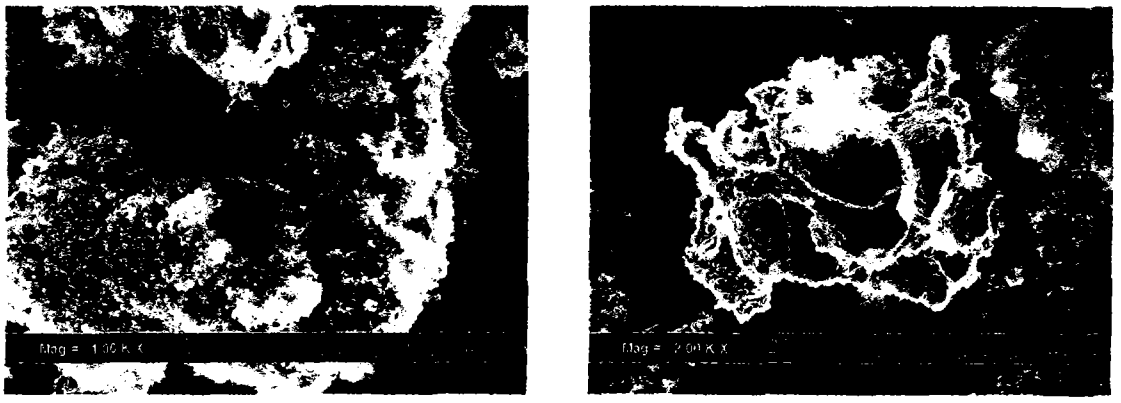

Figure 5.5 : SEM analysis of light hydrocarbon magnified at 1000 X and 2000 X respectively.

According to Table 5.2, the value of carbon analyzed from elemental analyzer (EA) is the highest compared to sulfur, nitrogen, hydrogen and other compositions. Therefore, the higher the carbon content a better quality of activated carbon can produce.

Table 5.2 : Elemental composition of char.

Elemental Composition, %	
Composition	**Value**
Carbon	80.97
Sulfur	1.32
Nitrogen	0.43
Hydrogen	0.78
Others	16.5

5.3 Production of activated carbon and adsorption performance

5.3.1 Yield of activated carbon

Figure 5.6 shows the result of pore structures (morphology) of activated carbon with KOH to char ratio 5 activated at 850°C for 2 hours activation time. The structures of produced activated carbon are not distributed uniformly and the pores are in micron size *(as indicated by white arrow in Figure 5.6)*. However, as the smaller the pore size, the higher the surface area and adsorption capacity is high.

The SEM results for the produced activated carbon are comparable with previous work [Zabaniotou et al., 2004; Hamadi et al., 2001 and Helleur et al., 2001].

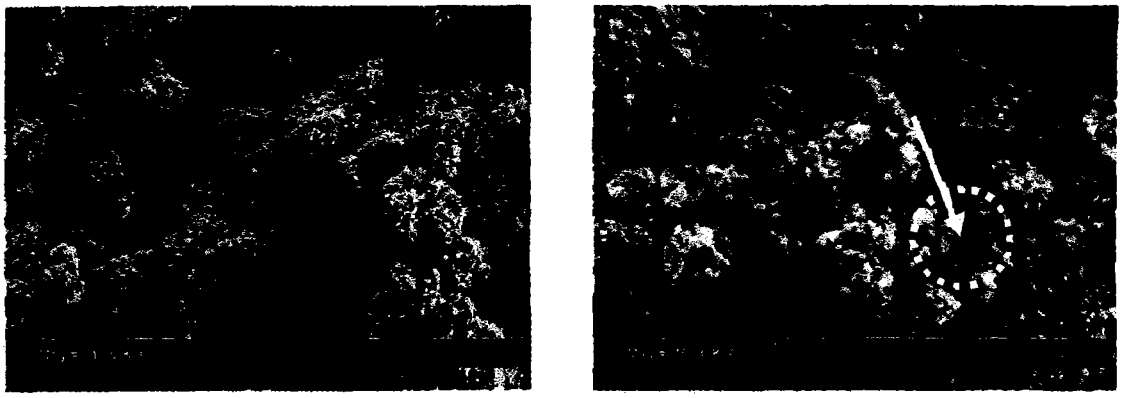

Figure 5.6 : SEM analysis for activated carbon AC850(5)2 at 1000 X and 10000 X respectively.

Equation 2 shows the percentage yield of activated carbon. For this paper, the yield of activated carbon is between 30 percent until 50 percent as shown on Table 5.3.

$$\text{Yield of activated carbon} = \frac{\text{Weight of activated carbon produced}}{\text{Weight of char (precursor)}} \times 100 \qquad (2)$$

Table 5.3 : Yield of activated carbon after washing step in gram.

KOH/char Ratio	Activation 850°C		Activation 800°C	
	1 hr	2 hr	1 hr	2 hr
3	4.6458	3.6942	4.5316	3.9408
4	3.8525	4.1145	5.9391	5.2502
5	3.6396	4.5237	5.3359	4.9508

The yield of activated carbon for 850°C is low compared to activated carbon produced at 800°C for activation time 1 hour and 2 hours (Figure 5.8). However, at ratio 3 of KOH and char, the yield of activated carbon for 850°C is higher than for 800°C. This result occurred because during physiochemical activation some of the activated carbon at 800°C spilt from the tray causing the deviation (Figure 5.7). The longer the activation time, the lesser activated carbon produced. This result is shown in Figure 5.10. Similar problem as Figure 5.7 occurred for Figure 5.9.

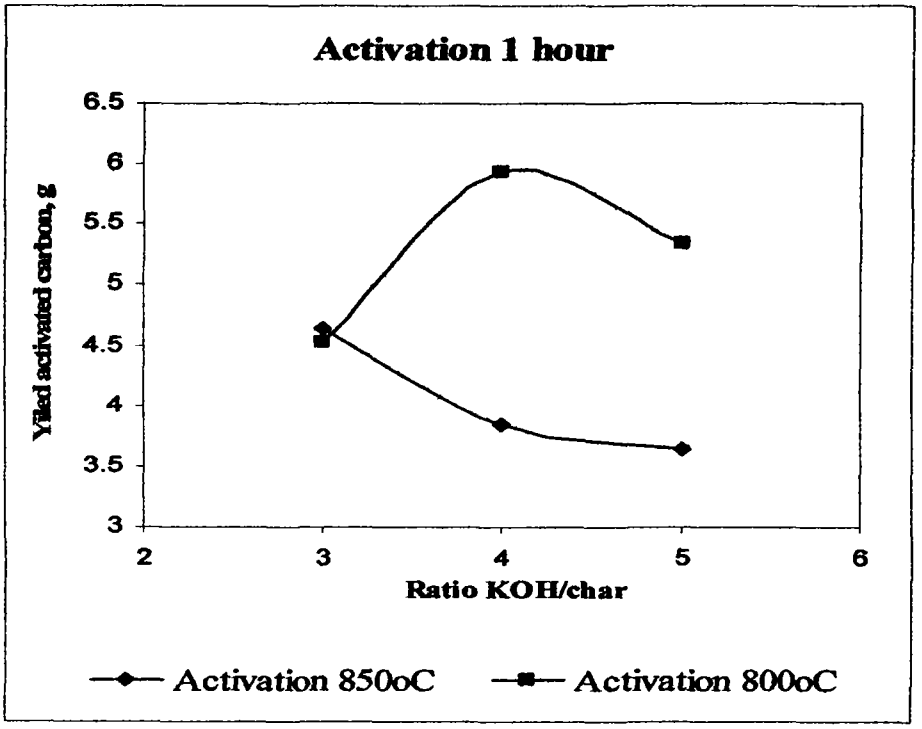

Figure 5.7 : Yield of activated carbon for 1 hour activation at 800°C and 850°C.

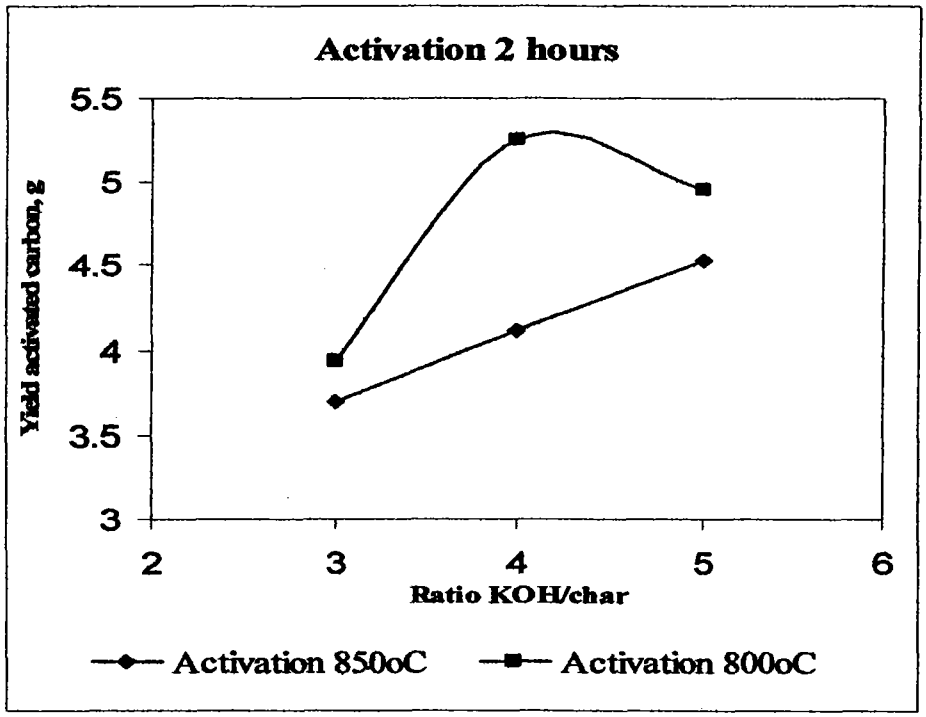

Figure 5.8 : Yield of activated carbon for 2 hours activation at 800°C and 850°C.

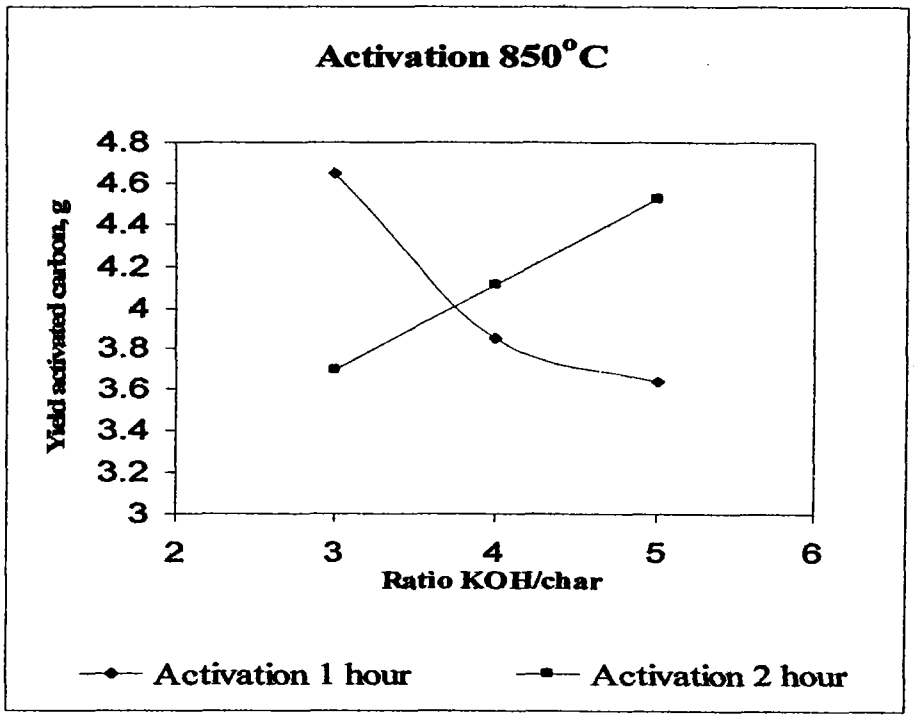

Figure 5.9 : Yield of activated carbon at 850°C activation for activation time 1 hour and 2 hours respectively.

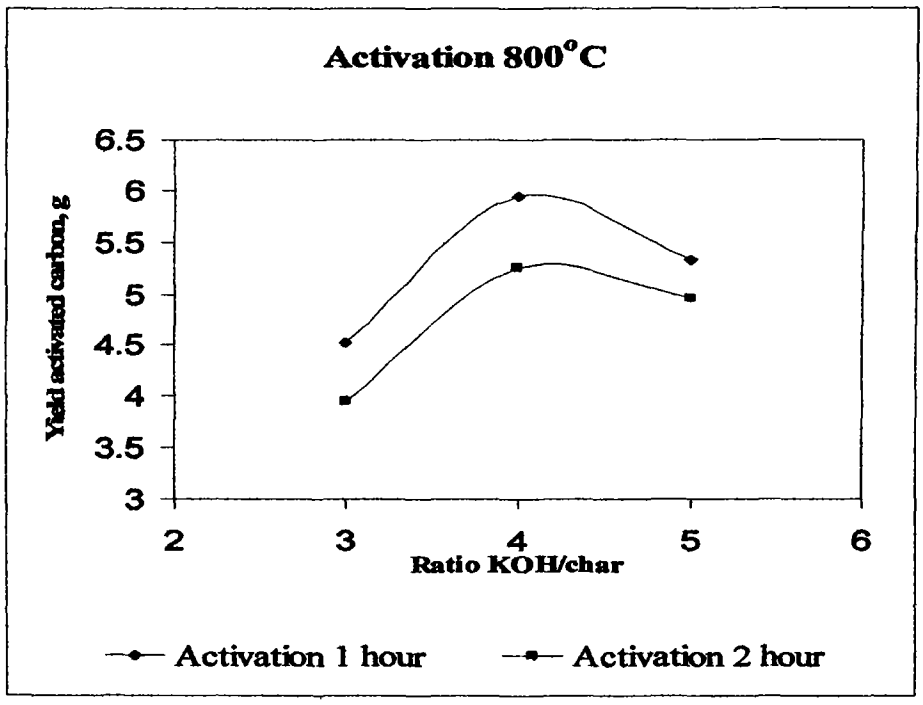

Figure 5.10 : Yield of activated carbon at 800°C activation for activation time 1 hour and 2 hours respectively.

The results of the elemental composition for activated carbon at various temperature, KOH/char ratio and activation used in this study are shown in Table 5.4. The elemental composition result for commercial activated carbon also shown for comparison purposes. The amount of carbon plays a major role in producing a high quality of activated carbon. As the temperature rise, the amount of carbon increases and the highest carbon content is for AC850(5)2 followed by AC800(3)2 based on Table 5.4. Moreover, the highest carbon content is nearly similar to the amount of carbon for commercial activated carbon. Therefore, the probability to commercialize AC850(5)2 is quite high.

However, the percentage of sulfur is also quite high. Nevertheless, it can be consider harmless to the environment because the amount of sulfur is less than 2%.

Table 5.4 : Elemental composition for activated carbon at various activation temperature, KOH/char ratio and activation time.

Type	Percentage, %				
	Carbon content	Sulfur content	Nitrogen content	Hydrogen content	Others
AC commercial	74.42	0.2	0.85	2.24	22.29
AC850(5)2	74.18	1.08	0.49	0.26	23.99
AC800(5)2	65.01	1.28	0.6	0.23	32.88
AC850(4)2	71.42	1.54	0.35	0.29	26.4
AC800(4)2	72.26	1.07	0.53	0.18	25.96
AC850(3)2	60.54	1.27	0.92	0.18	37.09
AC800(3)2	73.61	0.72	0.35	0.35	24.97

5.3.2 Adsorption Capacity

The amount of adsorption at equilibrium, q_e (mg/g) was calculated by:

$$q_e = \frac{(C_o - C_e)V}{W} \qquad (3)$$

where C_o and C_e (mg/L) are the liquid phase concentrations at initial and equilibrium respectively. V is the volume of solution (L) and W is the mass of activated carbon (g).

The procedures of kinetic experiments were basically identical to those of equilibrium tests. The aqueous samples were taken at present time intervals and the concentrations of

phenol were similarly measured. The amount of adsorption at time t, q_t (mg/g) is expressed by:

$$q_t = \frac{(C_o - C_t)V}{W} \quad (4)$$

where C_o and C_e (mg/L) are the liquid phase concentrations at initial and any time t respectively. V is the volume of solution (L) and W is the mass of activated carbon (g).

(Please refer to the Appendix for raw data and sample calculations for activated carbon produced and commercial activated carbon)

Adsorption isotherms are usually determined under equilibrium conditions [Hameed et al,. 2006]. A series of contact time experiments for phenol have been carried out at different initial concentration from 100mg/L until 500mg/L. The results that been shown are based on AC850(5)2 and commercial activated carbon. Figure 5.11 shows the contact time necessary for phenol with concentration 100mg/L to reach equilibrium is about 3 hours. However for higher phenol concentration, to achieve its equilibrium is at 48 hours (2 days).

As can be seen from Figure 5.11, the amount of phenol adsorbed by activated carbon increases with time and at some point reaches a constant. This means as the time passes by, the activated carbon is saturated with phenol and no more phenol can be removed from the solution and sometimes caused desorption.

The higher the initial phenol concentration leads to an increase in the adsorption capacity of phenol onto activated carbon (Figure 5.11 and 5.12). This is due to the increase in the driving force of the concentration gradient as an increase in the initial phenol concentration [Liang et al., 2005].

Different situation occur for commercial activated carbon. According to Figure 5.12, the contact time necessary for concentration to achieve equilibrium is about 46 hours for every phenol concentration.

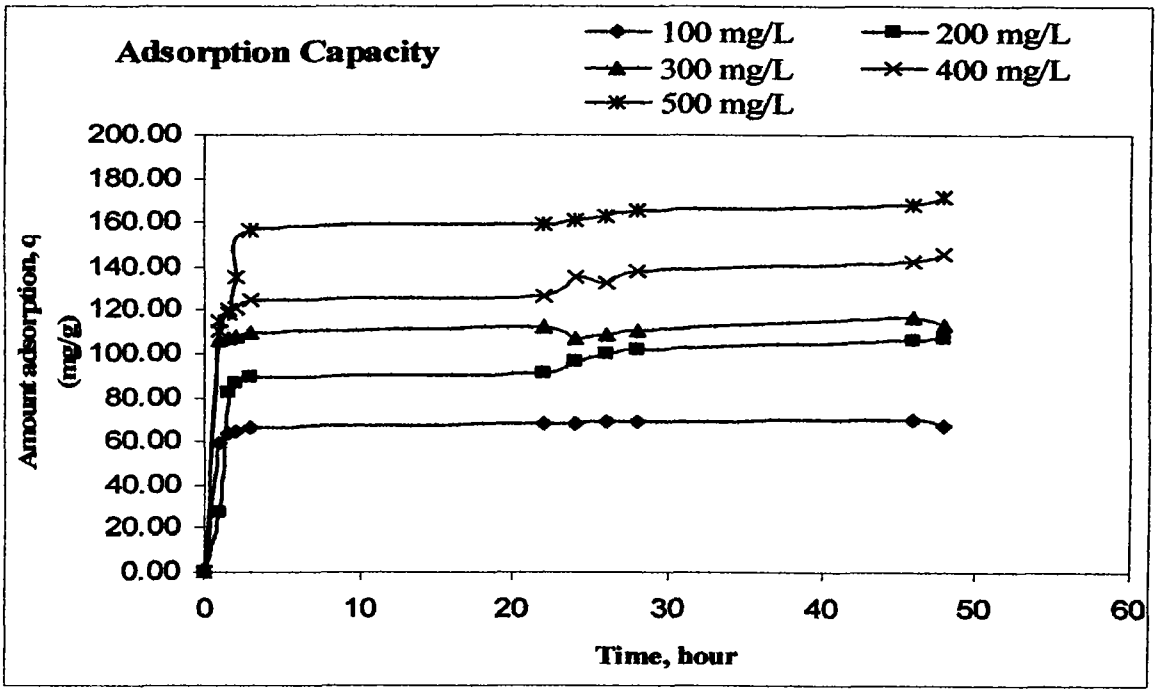

Figure 5.11 : The variation of adsorption capacity with adsorption time at various initial phenol concentration for AC850(5)2.

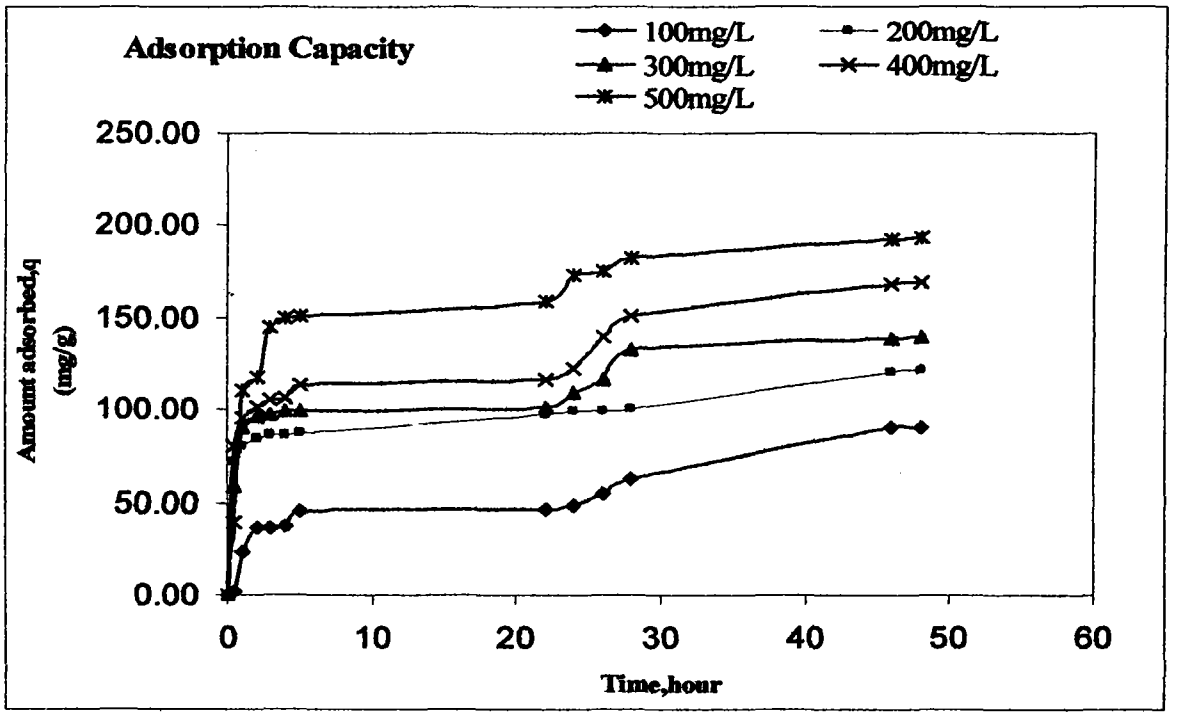

Figure 5.12 : The variation of adsorption capacity with adsorption time at various initial phenol concentration for commercial activated carbon.

5.3.3 Adsorption Isotherms

Adsorption isotherm indicates how the adsorption molecules distribute between the liquid phase and solid phase when the adsorption process reaches an equilibrium state. Adsorption isotherm is basically important to describe how solutes interact with adsorbents and is critical in optimizing the use of adsorbents [Hameed et al., 2006]. Figure 5.13 shows the equilibrium adsorption isotherms of phenol at 850°C for 2 hours activation time on activated carbon from waste tire and Figure 5.14 shows the trend for equilibrium adsorption isotherms for commercial activated carbon.

For this project, adsorption isotherm study is carried out based on Langmuir isotherm and Freundlich isotherm. Langmuir isotherm is predicted on the assumptions that adsorption energy is constant and independent of surface coverage that adsorption occurs on localized sites with no interaction between adsorbate molecules and that maximum adsorption occurs when the surface is covered by a monolayer adsorbate [Slejko, 1985]. Freundlich isotherm is derived by assuming a heterogenous surface with a non-uniform distribution of the heat of adsorption over the surface [Seader and Henley, 1998]. The applicability of the isotherm equation is compared by judging the correlation coefficients, R^2.

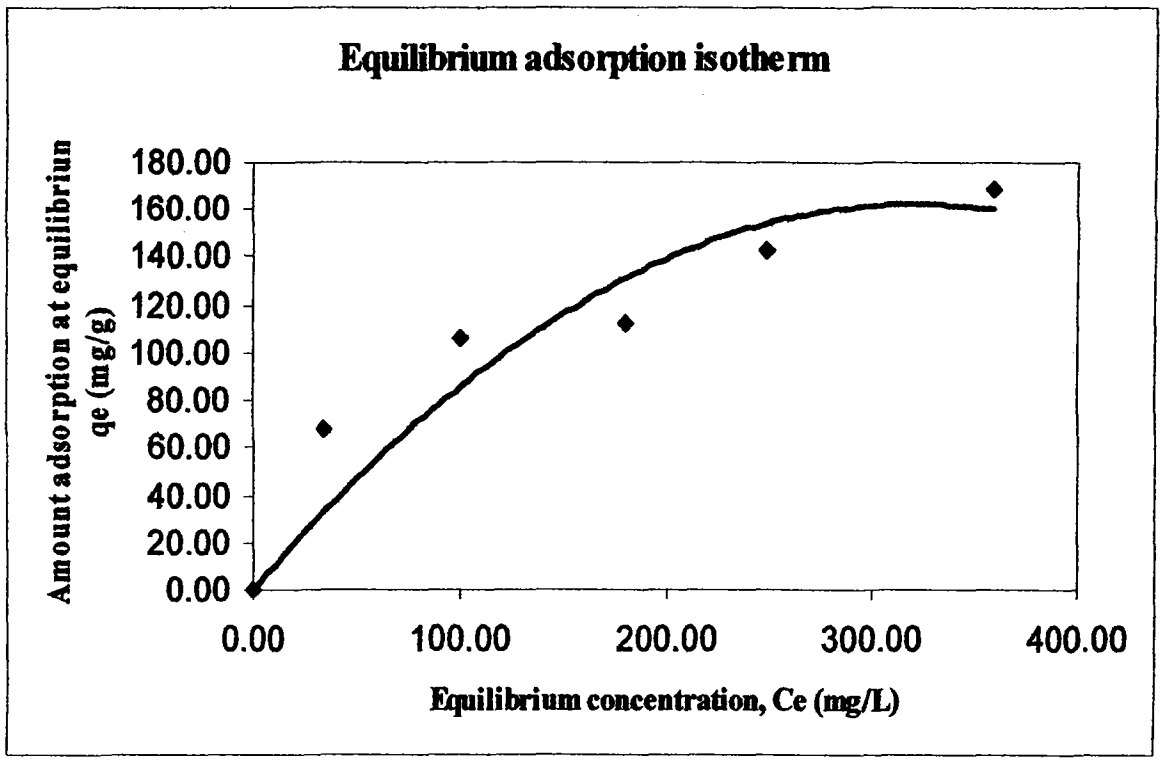

Figure 5.13 : Equilibrium adsorption isotherm of phenol onto AC850(5)2.

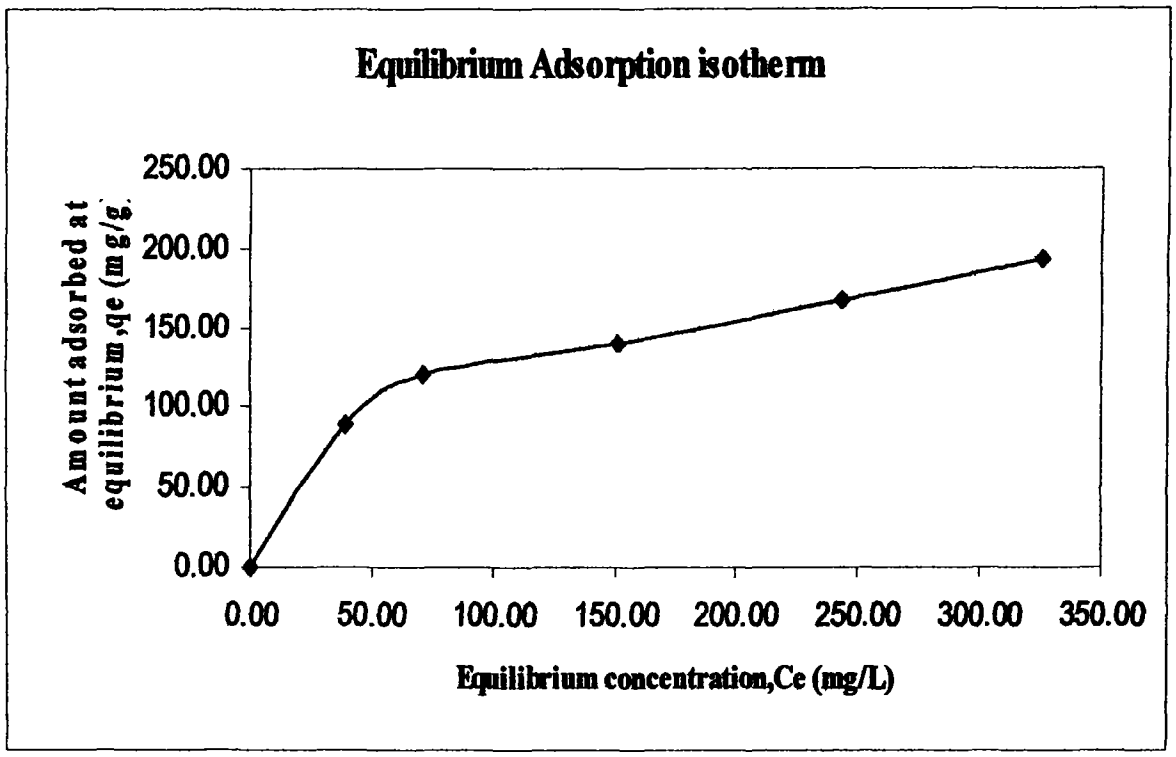

Figure 5.14 : Equilibrium adsorption isotherm of phenol onto commercial activated carbon.

5.3.4 Langmuir Isotherm

The linear form of Langmuir's isotherm model is given by equation below:

$$\frac{C_e}{q_e} = \frac{1}{Q_o b} + \left(\frac{1}{Q_o}\right) C_e \qquad (5)$$

where C_e is the adsorbate's concentration at equilibrium (mg/L), q_e is the amount of solute adsorbed per unit weight of adsorbent (mg/g) and Q_o and b are Langmuir constants related to adsorption capacity and rate of adsorption respectively.

When C_e/q_e was plotted versus C_e, a straight line can be achieved with slope $1/Q_o$. The value of Langmuir constants, Q_o and b can be calculated from the isotherm from the slope and intercept.

The essential characteristics of the Langmuir isotherm can be expressed in terms of a dimensionless equilibrium parameter, R_L which is:

$$R_L = \frac{1}{1+bC_o} \quad (6)$$

where b is Langmuir constant and C_o is the highest phenol concentration in mg/L. The value of R_L indicates the type of the isotherm to be either unfavorable ($R_L>1$), linear ($R_L=1$), favorable ($0<R_L<1$) or irreversible ($R_L=0$). Based on Table 5.5, for all the activated carbon produced, they are favorable as the value for R_L is between zero and one for adsorption of phenol under conditions used in this study.

Figure 5.15 and Figure 5.16 shows the trend of activated carbon AC850(5)2 and commercial activated carbon respectively for Langmuir model. Plots of Langmuir model is necessary to determine adsorption capacity, Q_o (mg/g).

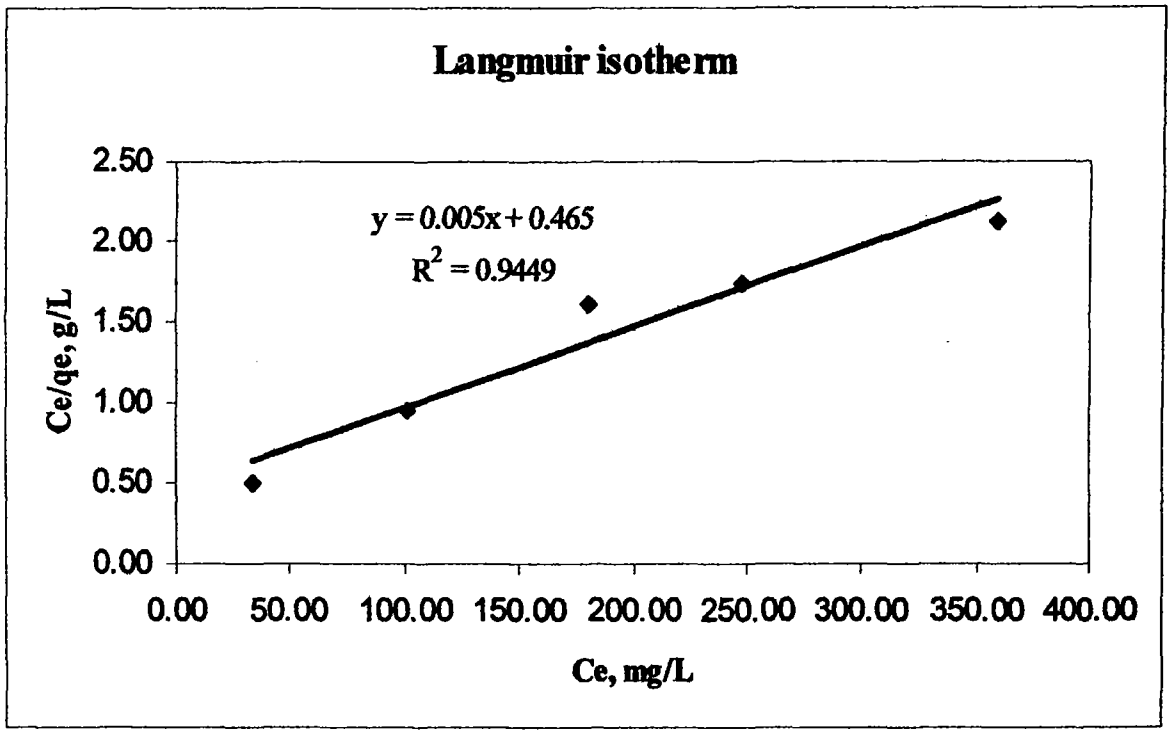

Figure 5.15 : Langmuir adsorption isotherm of phenol onto AC850(5)2.

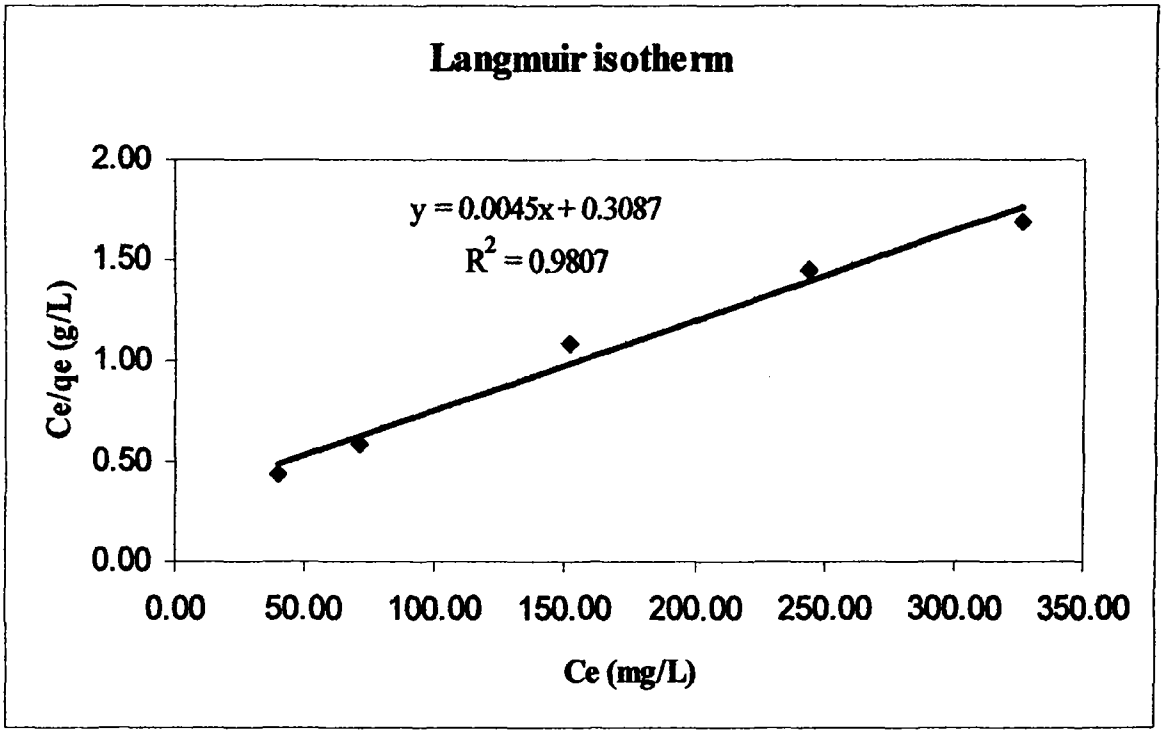

Figure 5.16 : Langmuir adsorption isotherm of phenol onto commercial activated carbon.

5.3.5 Freundlich Isotherm

The logarithmic form of Freundlich model is given by the equation below:

$$\log q_e = \log K_F + \left(\frac{1}{n}\right)\log C_e \qquad (7)$$

where q_e is the amount of solute adsorbed per unit weight of adsorbent at equlibrium (mg/g), C_e is the adsorbate's concentration at equilibrium (mg/L) and K_F and n are Freundlich constants. The value of K_F can be taken as a relative indicator of adsorption capacity or distribution coefficient and represents the quantity of dye adsorbed onto activated carbon adsorbent for a unit equilibrium concentration. Meanwhile, 1/n is indicative of the energy or intensity of the adsorption. The slope 1/n ranges between 0 and 1. The plot of log q_e versus log C_e gives straight line with slope 1/n which shows that the adsorption follows the Freundlich isotherm. Figure 5.17 and Figure 5.18 shows the trend of activated carbon AC850(5)2 and commercial activated carbon respectively for Frendlich model.

Table 5.5 and 5.6 shows the values of parameters of the two isotherms and the related correlation coefficients. For AC850(5)2, the Freundlich isotherm yields a better fit than Langmuir isotherm compared to AC800(5)2, AC850(4)2 and commercial activated carbon which is opposite based on the value of R^2 in Table 5.5 and 5.6.

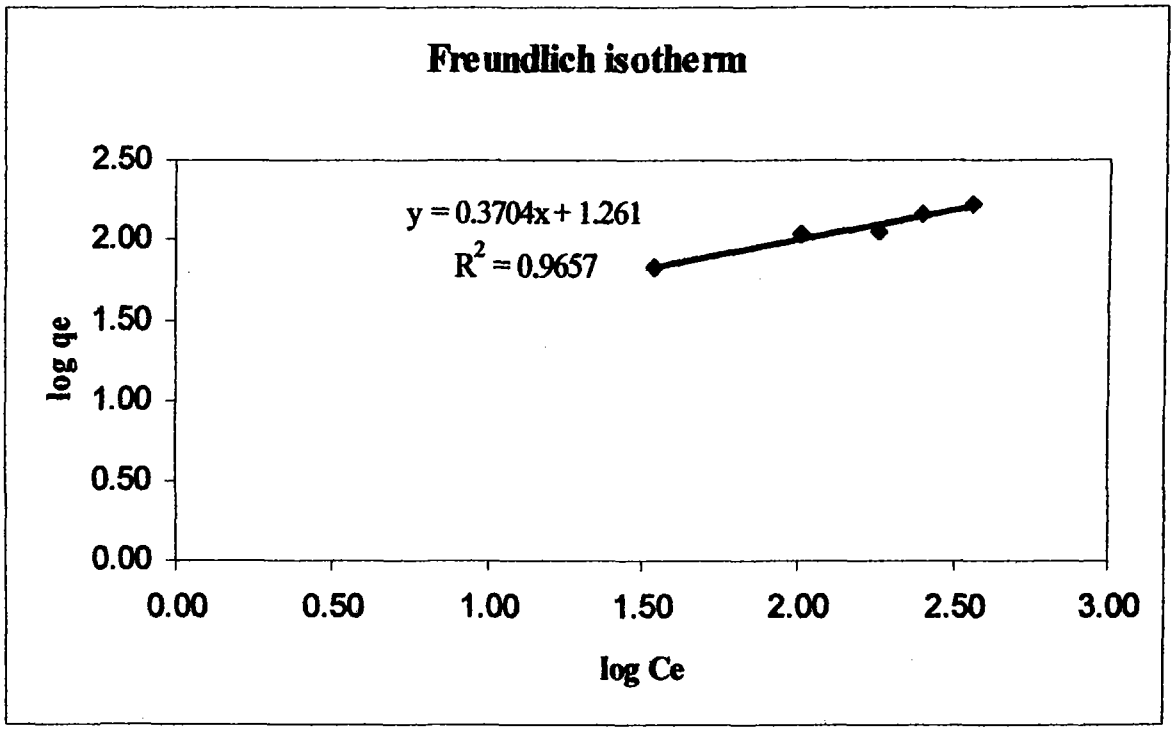

Figure 5.17 : Freundlich isotherm of phenol on AC850(5)2.

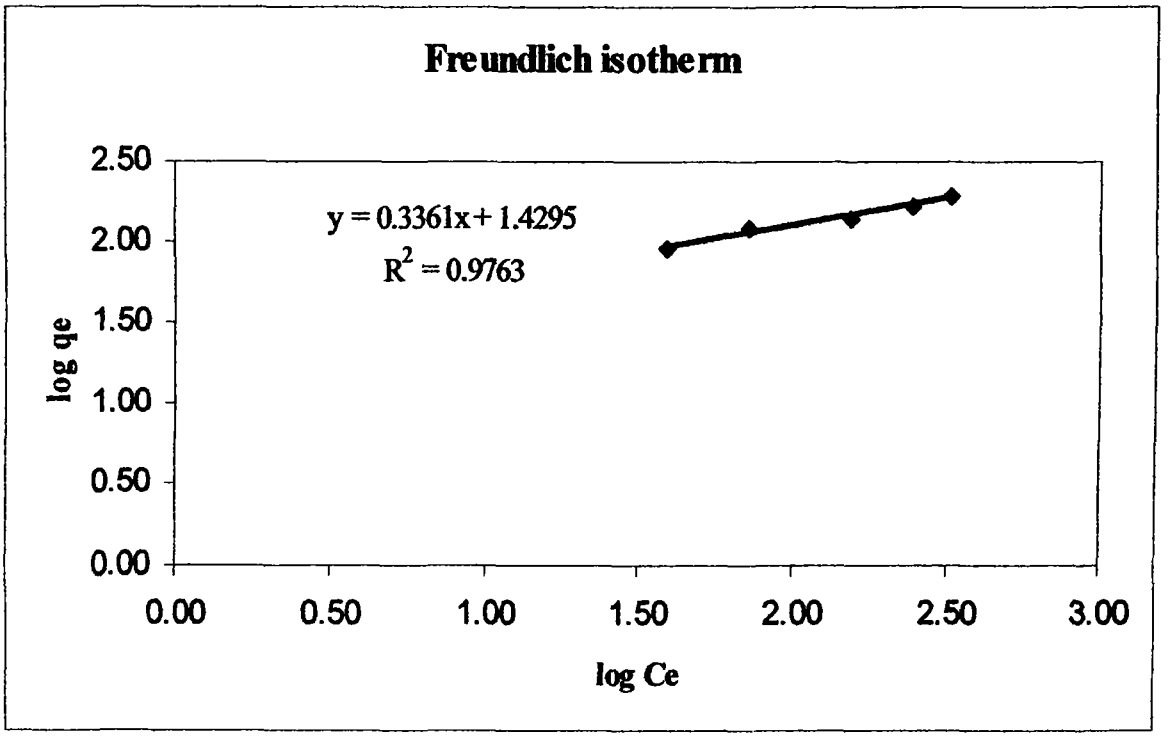

Figure 5.18 : Freundlich isotherm of phenol on commercial activated carbon.

The adsorption capacity, Q_o for every activated carbon is different because of the activation temperature, activation time and KOH to char ratio. According to Table 5.5, the value of adsorption capacity, Q_o (mg/g) for commercial activated carbon is comparable to AC850(5)2. The result achieved can be attributed to the high mesopore fraction. Mesopores have been shown to facilitate the adsorption of large adsorbates in the inner and narrow micropores [Lin and Teng, 2002].

Table 5.7 shows the comparison of maximum monolayer adsorption capacity of phenol for different activation method for activated carbon from waste tire. It shows that the adsorption capacity for this work using physiochemical activation for char produced from fluidized bed ractor is the highest compared to other works.

According to this study, as the activation temperature and KOH/char ratio increase the higher the adsorption capacity. Therefore, it can be proved that the activation temperature and KOH/char ratio contribute to adsorption capacity towards solute.

Table 5.5 : Langmuir isotherm constants of phenol for various activated carbon

Langmuir Isotherm	ACcommercial	AC850(5)2	AC800(5)2	AC850(4)2	AC850(3)2
Q_o (mg/g)	222.222	200	113.636	138.889	117.647
b (1/mg)	0.0146	0.0108	0.0460	0.079	0.0069
R^2	0.9807	0.9449	0.9865	0.8834	0.7716
R_L	0.1206	0.1568	0.0417	0.2011	0.2255

Table 5.6 : Freundlich isotherm constants of phenol for various activated carbon

Freundlich Isotherm	ACcommercial	AC850(5)2	AC800(5)2	AC850(4)2	AC850(3)2
n	2.9753	2.6998	5.9347	2.7917	2.6497
K_F	4.1760	3.5289	5.0068	2.9799	2.5948
R^2	0.9763	0.9657	0.8113	0.7811	0.7406

Table 5.7 : Comparison of maximum monolayer adsorption capacity, Qo of phenol for different activation method for activated carbon from waste tire.

Adsorbent	Activation	Activation Temperature (°C)	Maximum monolayer adsorption capacity, Q_o (mg/g)	References
Activated carbon	Physiochemical activation	850	200	Present
Activated carbon	Physical activation	950	99	Miguel et al., 2003
Activated carbon	Physical activation	900	32	Helleur et al., 2001
Activated carbon	Physical activation	900	43.06	Laszlo et al., 1997
Activated carbon	Physical activation	900	170	Bota et al., 1996

5.3.6 Adsorption Kinetics

5.3.6(a) Pseudo 1st Order Kinetic

The rate constant, k of adsorption can be determined either by first order equation or second order equation. The first order equation is given:

$$\log(q_e - q_t) = \log q_e - \frac{k_1 t}{2.303} \quad (8)$$

where q_e are the amounts of phenol adsorbed at equilibrium (mg/g), q_t are the amounts of phenol adsorbed at time t (hour) and k_1 is the rate constant of adsorption for first order (1/hr).

Values of k_1 were calculated from the plots of $\log(q_e-q_t)$ versus t (Figure 5.19 and Figure 5.20) for different concentrations of phenol.

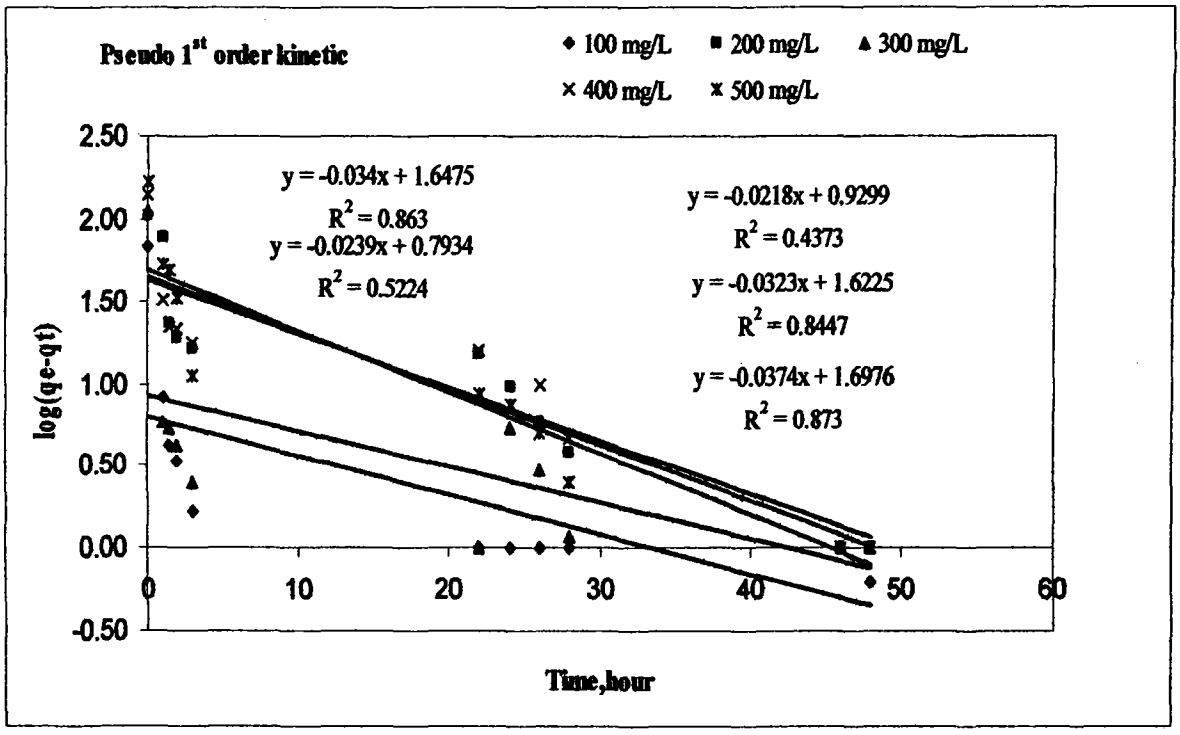

Figure 5.19 : Pseudo first order kinetic for adsorption of phenol on AC850(5)2.

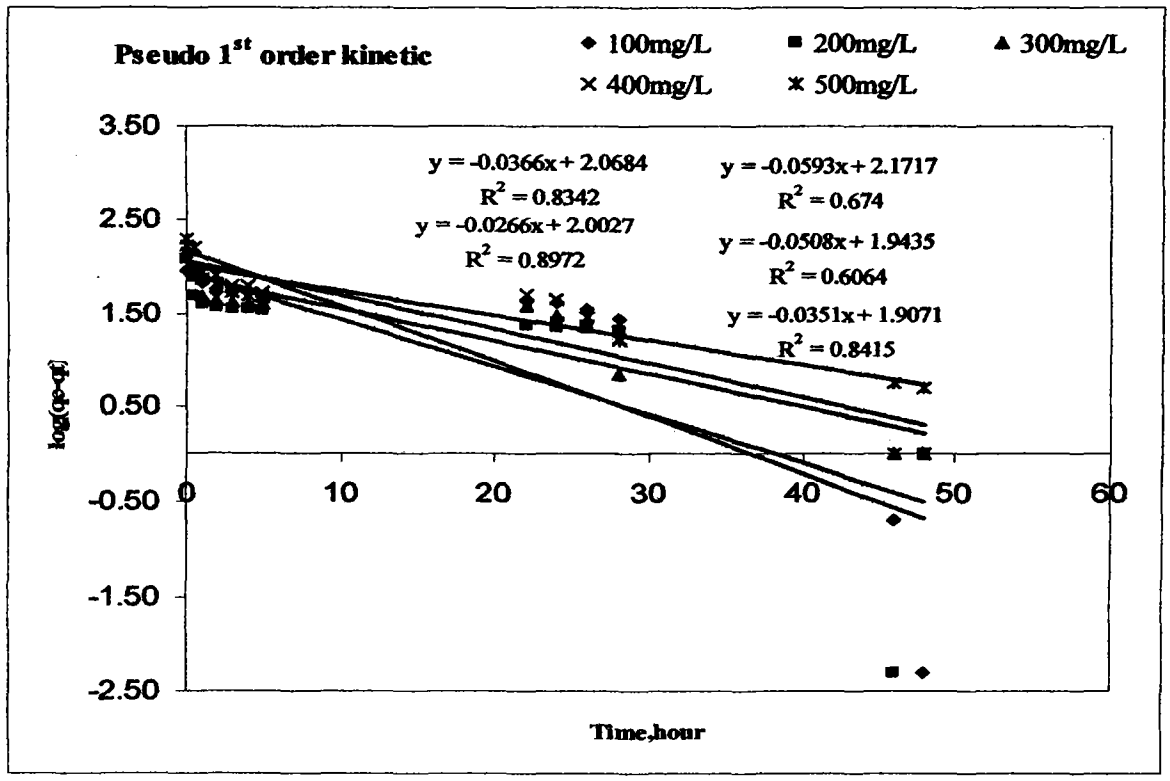

Figure 5.20 : Pseudo first order kinetic for adsorption of phenol on commercial activated carbon.

5.3.6(b) Pseudo 2nd Order Kinetic

Pseudo second order equation is expressed as:

$$\frac{t}{q_t} = \frac{1}{k_2 q_e^{\ 2}} + \left(\frac{1}{q_e}\right)t \qquad (9)$$

where k_2 is the rate constant of adsorption for second order (1/hr). If graph t/q_t versus t were plotted, a linear relationship will be shown. Therefore, the value of q_e and k_2 can be calculated based on the slope and intercept of the plot respectively (Figure 5.21 and Figure 5.22).

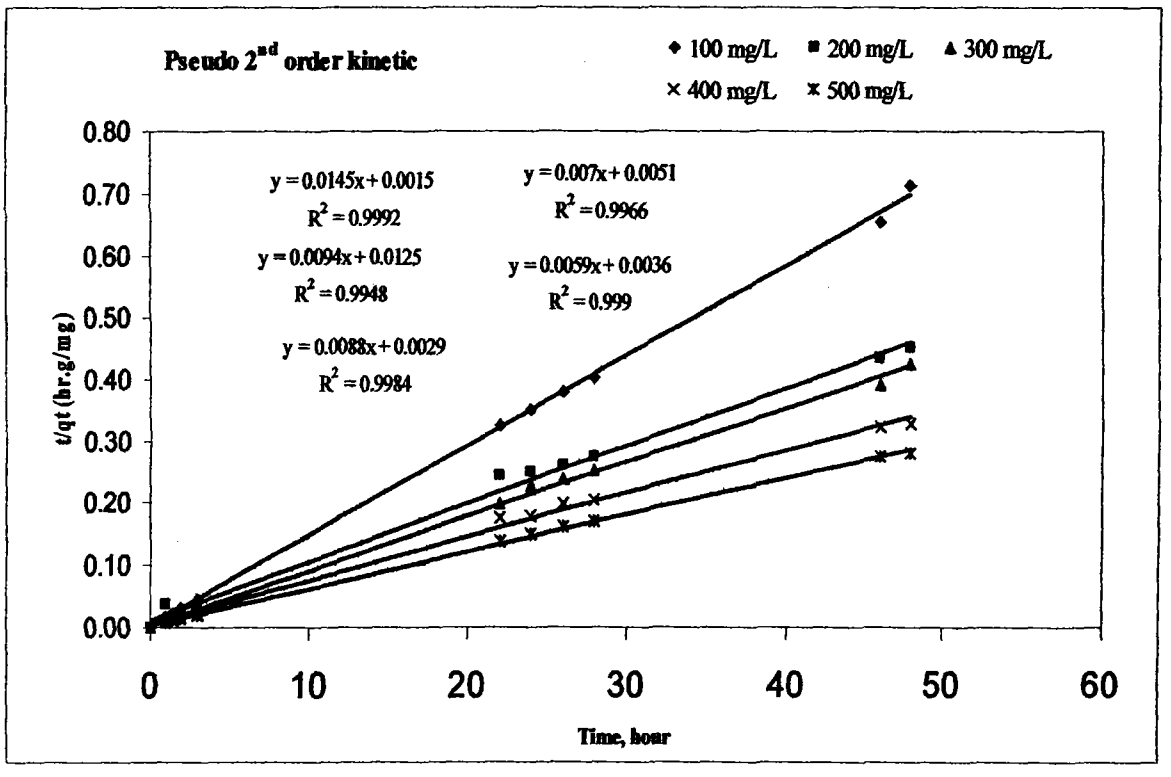

Figure 5.21 : Pseudo second order kinetic for adsorption of phenol on AC850(5)2

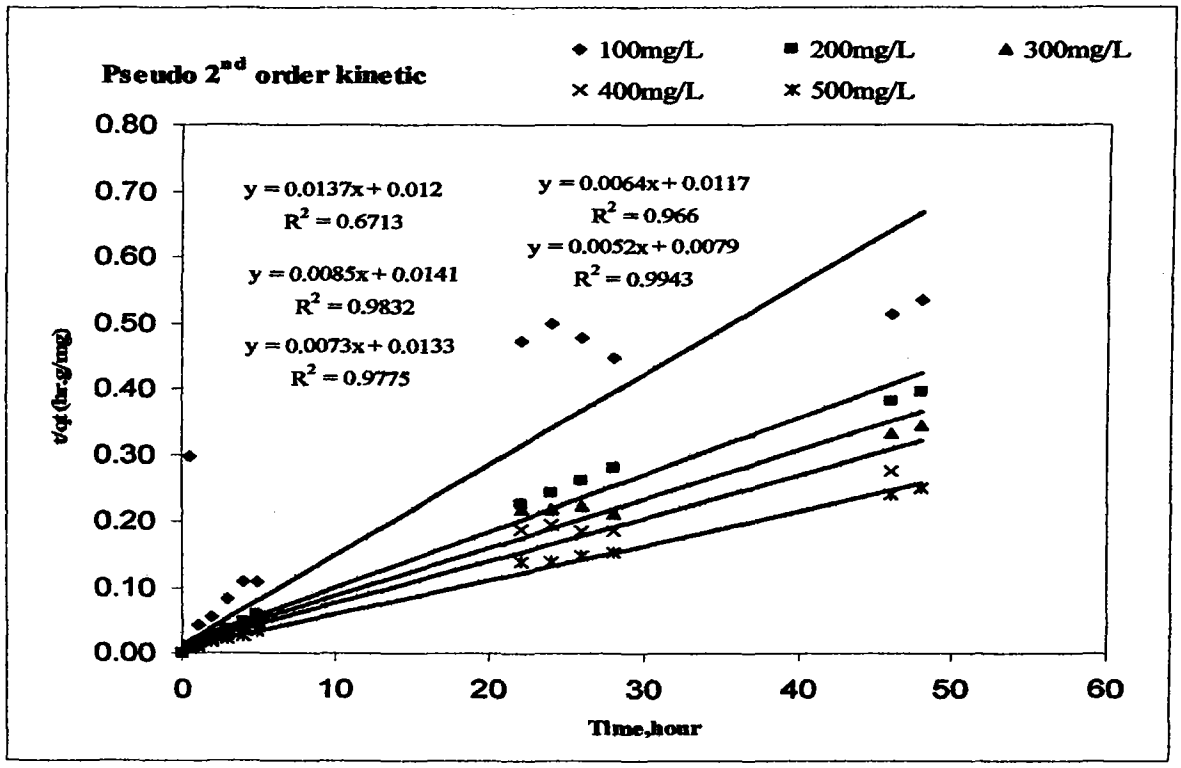

Figure 5.22 : Pseudo second order kinetic for adsorption of phenol on commercial activated carbon.

Referring to Table 5.8, the experimental amount of phenol adsorbed at equilibrium, q_e (mg/g) do not agree with the calculated one for pseudo first order kinetic obtained from the plots of $\log(q_e-q_t)$ versus t (Figure 5.19 and Figure 5.20). Therefore, the adsorption of phenol onto activated carbon is not a first order kinetic.

However, based on equation 9, the plots for t/q_t versus t (Figure 5.21 and Figure 5.22) show a good agreement between experimental and calculated q_e values (Table 5.8). The correlation coefficients for the second order kinetic model are greater than 0.99 indicating the applicability of this kinetic equation and the second order nature of the adsorption process of phenol on activated carbon. Table 5.9 shows the results of pseudo first order and

second order for commercial activated carbon for comparison purposes between AC850(5)2 and commercial activated carbon.

Table 5.8 : Comparison of the pseudo first order and second order adsorption rate constants, and calculated and experimental qe values for different initial phenol concentration of AC850(5)2.

C_0 (mg/L)	First order kinetic model				Second order kinetic model			SSE %	
	$q_{e,exp}$ (mg/g)	$q_{e,cal}$ (mg/g)	k_1 (1/hr)	R^2	$q_{e,cal}$ (mg/g)	k_2 (g/mg.hr)	R^2	1st	2nd
100	67.76	6.21	0.0550	0.5224	68.97	0.1402	0.9992	19.46	0.38
200	105.83	44.41	0.0783	0.863	106.38	0.0071	0.9948	19.42	0.17
300	112.10	8.51	0.0502	0.4373	113.64	0.0267	0.9984	32.76	0.49
400	142.63	41.93	0.0744	0.8447	142.86	0.0096	0.9966	31.84	0.07
500	168.14	49.84	0.0861	0.873	169.49	0.0097	0.9990	37.41	0.43

Table 5.9 : Comparison of the pseudo first order and second order adsorption rate constants, and calculated and experimental qe values for different initial phenol concentration of commercial activated carbon.

C_0 (mg/L)	First order kinetic model				Second order kinetic model			SSE %	
	$q_{e,exp}$ (mg/g)	$q_{e,cal}$ (mg/g)	k_1 (1/hr)	R^2	$q_{e,cal}$ (mg/g)	k_2 (g/mg.hr)	R^2	1st	2nd
100	89.74	148.49	0.1366	0.674	91.74	0.0156	0.7744	16.96	0.58
200	120.88	87.80	0.1170	0.6064	117.65	0.0051	0.9832	9.55	0.93
300	139.08	80.74	0.0808	0.8415	136.99	0.0040	0.9775	16.84	0.60
400	167.73	117.06	0.0843	0.8342	156.25	0.0035	0.9660	14.63	3.31
500	192.55	100.62	0.0613	0.8972	192.31	0.0034	0.9943	26.54	0.07

5.3.7 Test of kinetics models

In stead the value of correlation coefficient, R^2 the applicability of both kinetic models can be verified through the sum of error squares (SSE %).

The SSE equation is given by:

$$SSE\% = \sqrt{\frac{\sum\left(q_{e,exp} - q_{e,cal}\right)^2}{N}} \qquad (10)$$

where N is the number of data points. The best graph between the first and second order will be determined according to the value of R^2 and SSE. The higher the value of R^2 and the lower the value of SSE %, it will result the best fit [Hameed et al., 2006].

Based on the pseudo second order kinetic model (Table 5.8), the activated carbon at 850°C for 2 hour activation time, AC850(5)2 gave the value of correlation coefficients more than 0.99 and lower sum of error squares value, SSE%. Therefore, AC850(5)2 for pseudo second order kinetic model produce the best fit compared to pseudo first order kinetic model. Similar results have been achieved in the adsorption of methylene blue onto bamboo based activated carbon [Hameed et al., 2006].

Dr. Ridzuan Zakaria

UNIVERSITI SAINS MALAYSIA
SCHOOL OF CHEMICAL ENGINEERING
ENGINEERING CAMPUS

ADSORPTION PERFORMANCE OF ACTIVATED CARBON FROM WASTE TIRE

KONG CHIA SENG
Matric No.: **73132**

April 2007

ABSTRACT

Adsorption is a very important process in many application of industrial and activated carbon plays an important role in this application. Thus, many methods have been used to produce activated carbon. In this study, the performances of adsorption of activated carbon in different parameter are being investigated. In this study, activated carbons were produced from waste tires. Waste tire is used to produce a char in fixed bed. Chemical activation is done by using Potassium hydroxide (KOH) and gas N_2 with flow rate 100ml/minute at temperature of 760^0C. The activation time were 1 hour, 1.5 hours, and 2 hours. KOH per char rations are varies from 3, 4 and 5. The adsorption characteristics were determined by using methylene blue and phenol and its performance and characteristic were investigated. From the experiments that undergo, the adsorption capacity reaches its optimization when activated carbon produced in the 760^0C, KOH/char equal to 5 with the activation time 1.5 hours used. The best condition to produce the activated carbon with high potential in adsorption had been found through this thesis.

Keywords: Waste tire, KOH activation, pylorysis, activated carbon, fluidized bed, chemical activation, adsorption, methylene blue, phenol.

CHAPTER 4

RESULT AND DISCUSSION

Table 4.1: Adsorption data based on Langmuir and Freudlich isotherms model

Activated carbon	Langmuir isotherm			RL	Freundlich isotherm	KF	R^2
	Q0 (mg/g)	b (1/mg)	R^2		n	(mg/g)(L/mg)1/n	
760MB31	196.078	0.0916	0.996	0.0214	6.1652	6.6174	0.9440
760MB41	125	0.6452	0.994	0.0031	18.9753	7.2609	0.5321
760MB51	147.059	1.1333	0.9989	0.0018	10.1833	7.0442	0.7211
760MB31.5	126.582	0.0355	0.9631	0.0533	10.8696	6.1719	0.6426
760MB41.5	175.439	0.7403	0.9981	0.0027	7.0621	6.8654	0.8269
760MB51.5	200	0.1412	0.9967	0.014	6.7295	7.0203	0.9249
760MB32	158.73	0.0423	0.9655	0.0451	5.6948	5.6831	0.8227
760MB42	125	0.6452	0.994	0.0031	18.9753	7.2609	0.5321
760MB52	192.308	0.0239	0.9573	0.0772	4.6147	5.3618	0.9283

760PH31	227.273	0.0056	0.7971	0.2615	1.9164	2.3651	0.9358
760PH41	153.846	0.0075	0.9673	0.2111	2.264	2.5244	0.9746
760PH51	163.934	0.009	0.976	0.1812	2.1524	2.5487	0.9103
760Ph31.5	188.679	0.006	0.5582	0.2491	1.9142	2.2289	0.768
760PH41.5	232.558	0.0079	0.9671	0.2027	2.0141	2.7045	0.9859
760PH51.5	238.095	0.0062	0.7728	0.2438	2.1413	2.7896	0.9175
760PH32	158.730	0.0423	0.9655	0.0451	5.6948	5.6831	0.8227
760PH42	125.000	0.6452	0.994	0.0031	18.9753	7.2609	0.5321
760PH52	192.308	0.0239	0.9573	0.0772	4.6147	5.3618	0.9283

4.1 Effect of agitation time and concentration of methylene blue and phenol on adsorption

Adsorption will reach equilibrium after several hours. As a result, adsorption isotherms can be determined under equilibrium conditions. In this study, the adsorption experiment of methylene blue and phenol were done for about 48 hours continuously. This is to make sure that full equilibrium was attained and increase the accuracy of the adsorption process. The condition of the experiment were at 30 °C with different initial concentration from 100mg/l to 500mg/l. Figure 4.1 shows the contact time necessary for phenol to reach equilibrium while Figure 4.2 shows the adsorption equilibrium of methylene blue with the ratio of KOH/char is 5 and activation time is 1.5 hours.

Both Figures show an increase in time to reach the equilibrium. This means that the amount of the adsorbed phenol and methylene blue onto activated carbon increases with time until its adsorption limit when no more molecules of phenol and methylene blue can be adsorbed. In this case, equilibrium time can be defined as the time required attaining this state of equilibrium. Amount of methylene blue and phenol adsorbed at the equilibrium time reflects the maximum adsorption capacity of the adsorbent under those operating conditions. As shown by the Figure 4.1 and Figure 4.2, the adsorption capacity at equilibrium increases with an increase in the initial phenol and methylene blue concentration from 100 to 500 mg/l. This is due to increase in the driving force of the concentration gradient, as an increase in the initial dye concentration. However, for MB solutions with higher initial concentrations, longer equilibrium times were required.

Thus, it can be said that activated carbon prepared from waste tire is efficient in adsorbing phenol and methylene blue from aqueous solution. Three consecutive mass transport steps are associated with the adsorption of solute from solution by porous adsorbent. First, the adsorbate migrates through the solution, mostly known as film diffusion. After that, solute will move from particle surface into interior site by pore diffusion. The last step is adsorption of the adsorbate into the active sites at the interior of the adsorbent particle. Long contact time is needed to complete the mass transport and the adsorption process.

Figure 4.1 shows the contact time necessary for phenol with initial concentrations of 100-300 mg/l to reach equilibrium is 6 hours. For phenol with high initial concentration in the range of 400-500 mg/l, the time for it to reach the equilibrium was about 28 hours. As shown by the figure 1, the adsorption capacity at equilibrium increases with an increase in the initial dye concentration from 100 to 500 mg/l. Thus, activated carbon prepared from waste tire is efficient in adsorbing phenol from aqueous solution.

Fig. 2 shows the contact time necessary for methylene blue with initial concentrations of 100-300 mg/l to reach equilibrium is 6 hours. For phenol with high initial concentration rarely from 400-500 mg/l, the time for it to reach the equilibrium was longer and 26 hours are needed to reach the equilibrium. So, activated carbon prepared from waste tire is efficient in adsorbing phenol from aqueous solution.

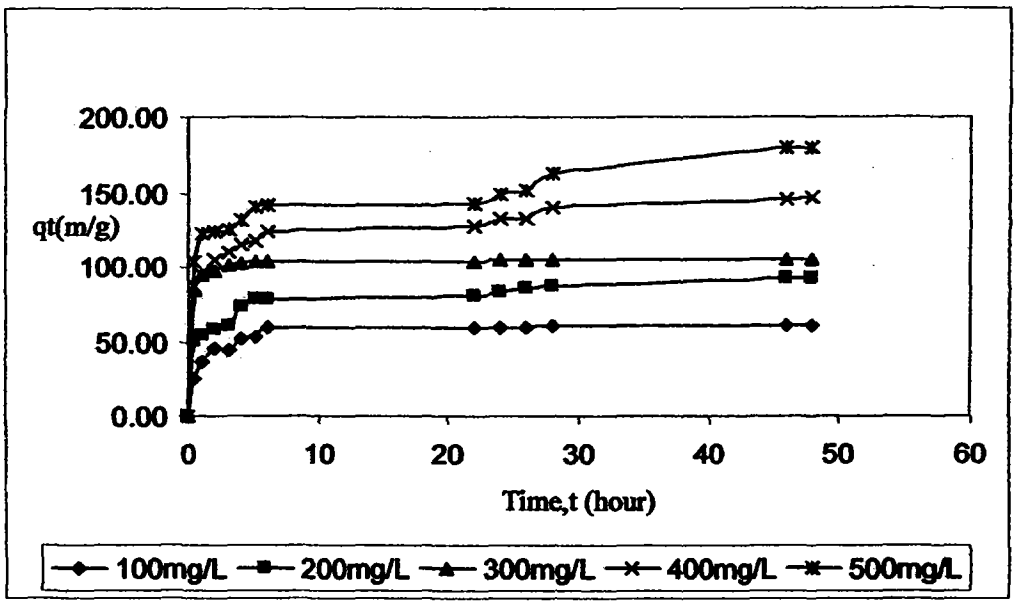

Figure 4.1: Adsorption capacity, qt (m/g) versus time, t (hour) for phenol (760PH51.5)

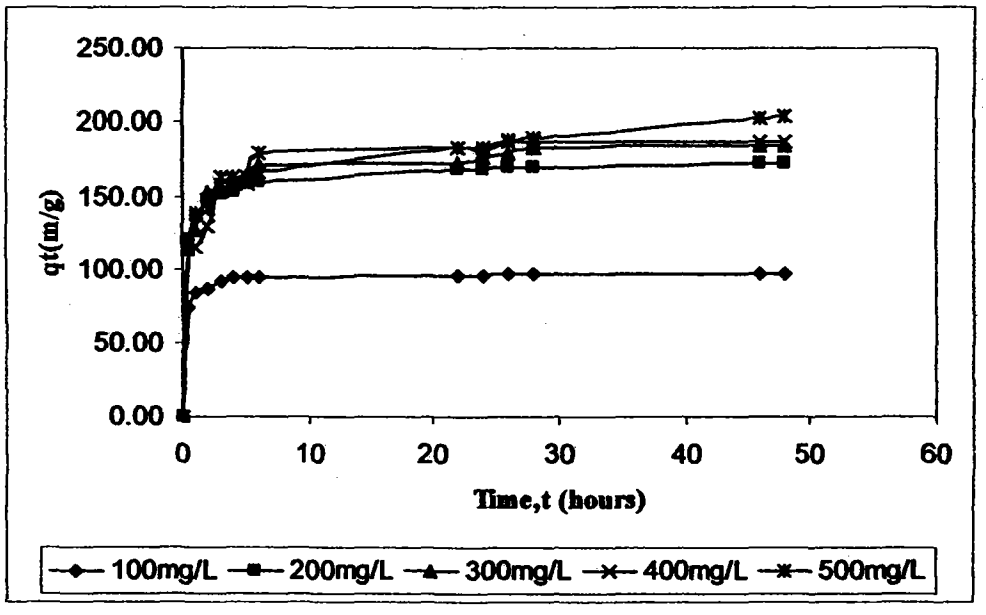

Figure 4.2: Adsorption capacity, qt (m/g) versus time, t (hour) for methylene blue (760MB51.5)

4.2. Adsorption isotherms

The way solutes interact with the adsorbents is a field that needs to be explored in order to know the adsorption's performance of the activated carbon. Thus, adsorption isotherm is method to describe how solutes interact with adsorbents. The study of adsorption isotherm enables the optimizing of quantity adsorbents. The adsorption isotherm indicates how the adsorption molecules distribute between the liquid phase and the solid phase when the adsorption process reaches an equilibrium state. By fitting the isotherm data in different isotherm models, suitable model can be found in order to produce the desired activated carbon.

Two well-known adsorption isotherms to be studied in this study are Langmuir and Freundlich isotherms. Langmuir isotherm assumes monolayer adsorption onto a surface containing a finite number of adsorption sites of uniform strategies of adsorption with no transmigration of adsorbate in the plane of surface. Meanwhile, Freundlich isotherm model assumes heterogeneous surface energies, in which the energy term in Langmuir equation varies as a function of the surface coverage.

In this work, both models were used to describe the relationship between the amount of phenol and methylene blue adsorbed and its equilibrium concentration. The amount of phenol and methylene blue adsorbed (q_e) has been plotted against the equilibrium concentration (C_e) as shown in Figure 4.3 and Figure 4.4. The equilibrium adsorption density, q_e increased with the increase in dye concentration. The applicability of the isotherm equation is compared by judging the correlation coefficients, R^2.

Figure 4.3 typically shows the adsorption isotherms of phenol at 30 °C on the activated carbon. Figure 4.4 shows the adsorption isotherms of methylene blue dye at 30 °C on the activated carbon.

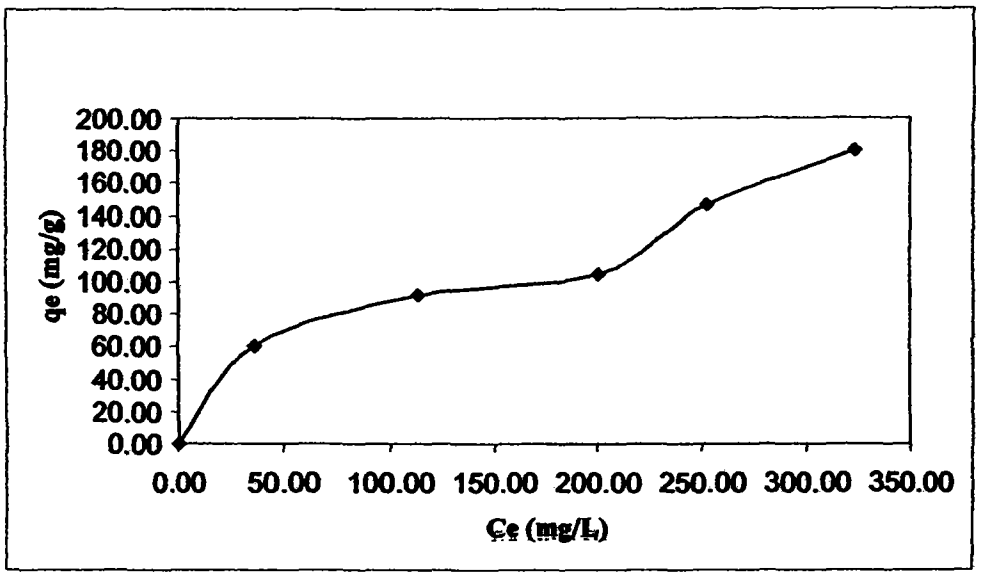

Figure 4.3: Adsorption isotherms, qe (mg/g) versus Ce (mg/L) for phenol (760PH51.5)

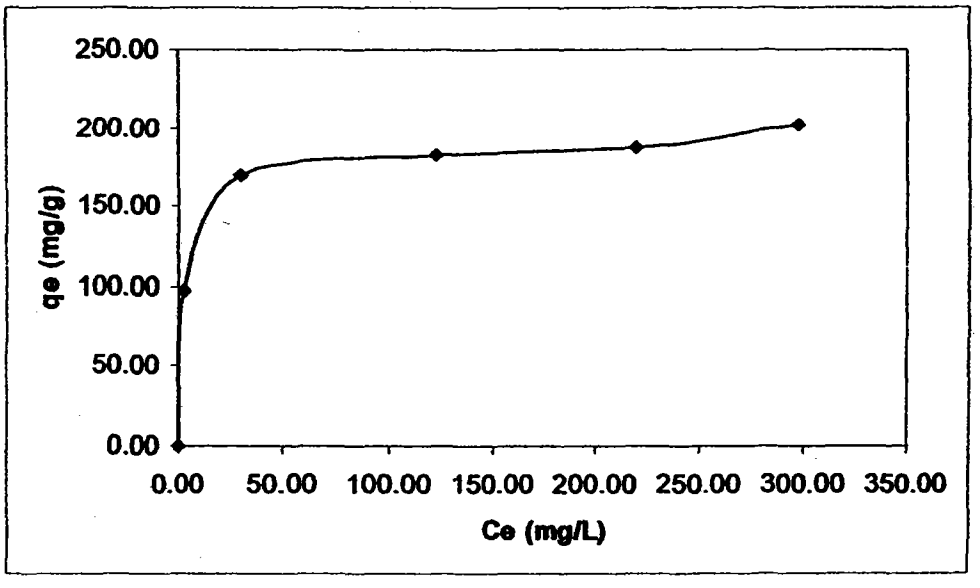

Figure 4.4: Adsorption isotherms, qe (mg/g) versus Ce (mg/L) for Methylene blue (760MB51.5)

4.2.1. Langmuir isotherm

The linear form of Langmuir's isotherm model is given by the following equation:

$$\frac{C_e}{q_e} = \frac{1}{Q_0 b} + \left(\frac{1}{Q_0}\right) C_e \quad \text{.....Equation 4.1}$$

Where *Ce* is the equilibrium concentration of the adsorbate (mg/l), *qe* the amount of adsorbate adsorbed per unit mass of adsorbate (mg/g), and*Qo* and *b* are Langmuir constants related to adsorption capacity and rate of adsorption respectively. Straight line with slope 1/*Qo* was obtained when *Ce*/*qe* was plotted against *Ce*. Both graphs for phenol and methylene blue as parameters are shown in Figure 4.5 and Figure 4.6. The straight line indicates that the adsorption of phenol and methylene blue on activated carbon obeys the Langmuir isotherm. The Langmuir constants '*b*' and '*Q*o' were calculated from this isotherm and their values are given in Table 4.1. The R_2 value of methylene blue is 0.9927 while is 0.7728 for phenol. This indicated that the adsorption data of methylene blue onto the activated carbon best fitted to the Langmuir isotherm model.

Application of the experimental data into Langmuir isotherm model shows the homogeneous nature of waste tire carbon surface. Formation of monolayer coverage of both phenol and methylene blue molecule can be demonstrated by using Langmuir isotherm model. A dimensionless equilibrium parameter (R_L) which indicates these essential characteristics of the Langmuir isotherm can be carried out. R_L can be defined by: $R_L = \frac{1}{1 + bC_0}$ .....Equation 4.2

Where *b* is the Langmuir constant and C_0 the highest dye concentration (mg/l). The value of R_L indicates the type of the isotherm to be either unfavorable ($R_L > 1$), linear

(R_L = 1), favorable (0 < R_L < 1) or irreversible (R_L = 0). Value of R_L was found to be 0.014 for methylene blue and 0.2438 for phenol and confirmed that the activated carbon is favorable for adsorption of Methylene blue and phenol under conditions used in this study.

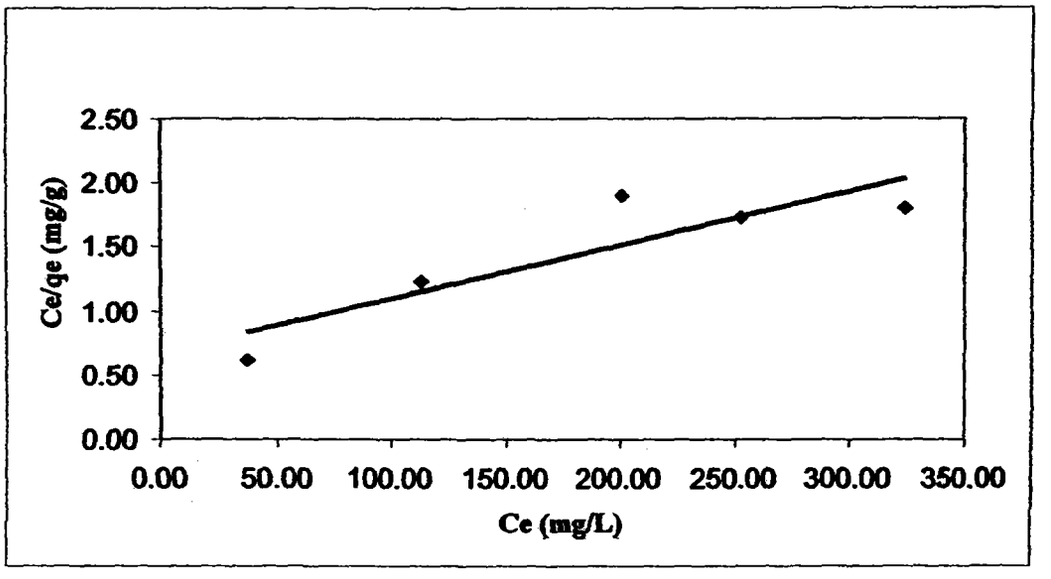

Figure 4.5: Langmuir isotherm, Ce/qe (mg/g) versus Ce (mg/L) for phenol (760PH51.5)

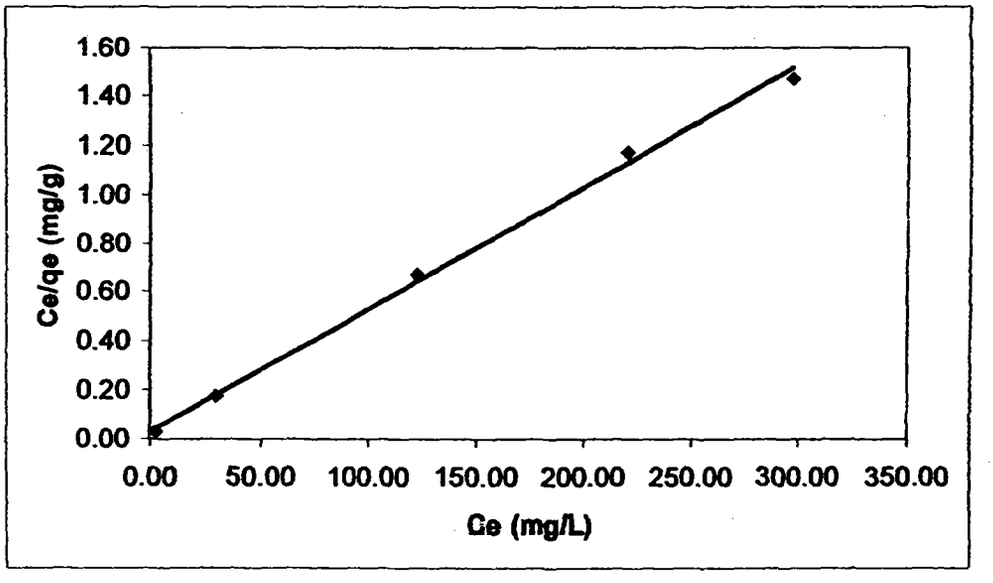

Figure 4.6: Langmuir isotherms, Ce/qe (mg/g) versus Ce (mg/L) for methylene blue (760MB51.5)

4.2.2. Freundlich isotherm

The Freundlich isotherm model in logarithmic form is given by the following equation:

$$\log q_e = \log K_F + \left(\frac{1}{n}\right)\log C_e \quad \text{.....Equation 4.3}$$

where q_e is the amount adsorbed at equilibrium (mg/g), C_e the equilibrium concentration of the adsorbate and K_F and n are Freundlich constants, n giving an indication of how favorable the adsorption process and K_F (mg/g (l/mg)$^{-n}$) is the adsorption capacity of the adsorbent. K_F can be defined as the adsorption or distribution coefficient and represents the quantity of dye adsorbed onto activated carbon adsorbent for a unit equilibrium concentration. The slope $1/n$ ranging between 0 and 1 is a measure of adsorption intensity or surface heterogeneity, becoming more heterogeneous as its value gets closer to zero. A value for $1/n$ below one indicates a normal Langmuir isotherm while $1/n$ above one is indicative of cooperative adsorption.

The plot of log q_e versus logC_e gives straight lines with slope '$1/n$',shown in figure 4.7 and Figure 4.8 which shows that the adsorption of MB also follows the Freundlich isotherm. Table 4.1 shows the values of the parameters of the two isotherms and the related correlation coefficients. As seen from Table 4.1, for phenol, R_2 for Langmuir isotherm is 0.7728 and 0.9175 in Freundlich isotherm. Meanwhile, R_2 for methylene blue in Langmuir isotherm is 0.9967 and 0.9249 in Frendlich isotherm. It shows that adsorption of phenol is better describe by using Frendlich isotherm while Langmuir isotherm is better to fit the adsorption of methylene blue as illustrated in Table 4.1, the value of $1/n$ is 0.268, which indicates favorable adsorption.

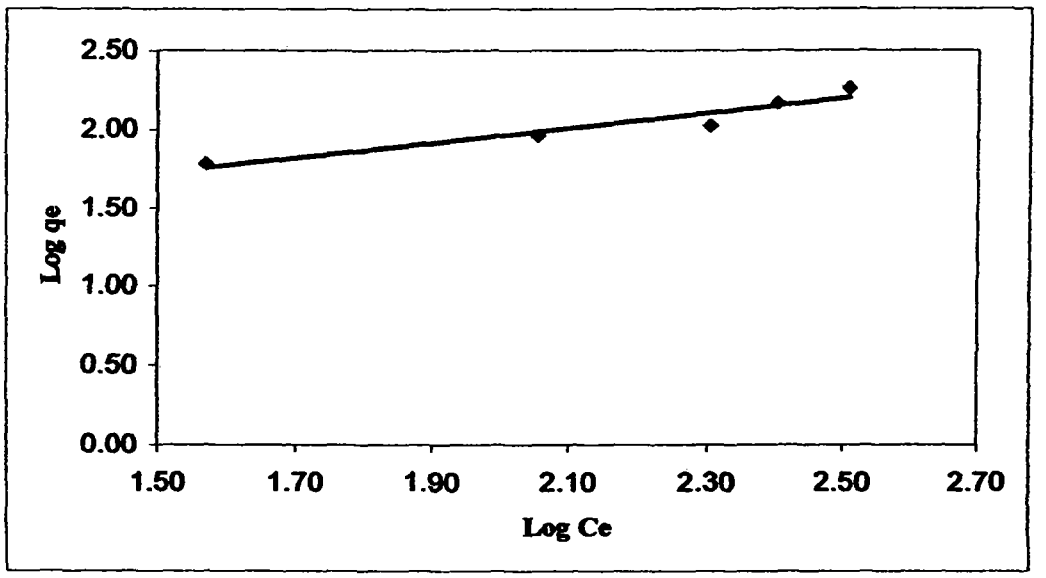

Figure 4.7: Freundlich isotherms, Log qe versus Log Ce for phenol (760PH51.5)

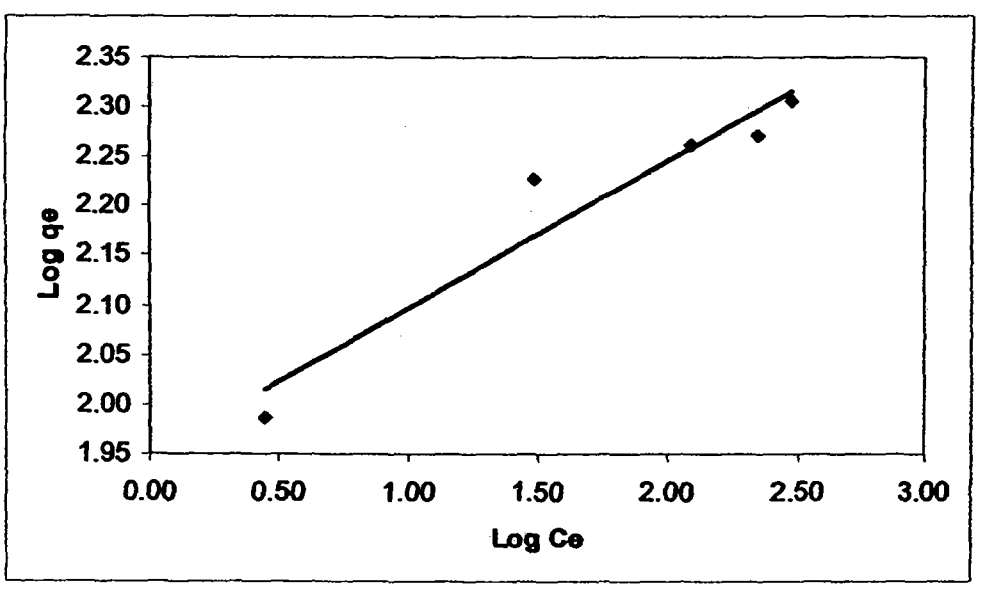

Figure 4.8: Freundlich isotherms, Log qe versus Log Ce for Methylene blue (760MB51.5)

4.3. Adsorption kinetics

The rate constant of adsorption is determined from the pseudo first-order equation given by Langergren and Svenska:

$$\ln(q_e - q_t) = \ln q_e - k_1 t \quad \text{.....Equation 4.4}$$

where q_e and q_t are the amounts of methylene blue and phenol adsorbed (mg/g) at equilibrium and at time t (min), respectively, and k_1 the rate constant adsorption (h^{-1}). Values of k_1 were calculated from the plots of ln ($q_e - q_t$) versus t (Figure 4.9, 4.10, 4.11 and 4.12) for different concentrations of methylene blue and phenol. Due to the plot from Figure 4.9 and figure 4.11, which negative slope obtained, although the linear plots showed, the adsorption of MB and phenol onto activated carbon is not a first-order kinetic.

First, the kinetics of adsorption is analyzed through the pseudo-first-order equation shown as

$$dq_t/dt = k_1(q_e - q_t) \quad \text{.....Equation 4.5}$$

where k_1 is the pseudo-first-order rate constant (1/min) and q_e denotes the amount of adsorption at equilibrium. After integration, by application of the conditions $q_t = 0$ at $t = 0$ and $q_t = qt$ at $t = t$, Equation (4.5) becomes

$$\log(q_e - q_t) = \log q_e - (\frac{k_1}{2.303})t \quad \text{.....Equation 4.6}$$

where the value of q_e must be obtained independently from the equilibrium experiments. The pseudo-second-order equation based on the adsorption capacity

$$dq_t/dt = k_2(q_e - q_t)^2 \quad \text{.....Equation 4.7}$$

where k_2 is the pseudo-second-order rate constant (kg/ (g min)). By integrating Equation 2, applying the initial conditions, an integration equation is obtained

$$\frac{t}{q_t} = \frac{1}{k_2 q_e^2} + \left(\frac{1}{q_e}\right)t$$ .....Equation 4.8

On the other hand, a pseudo second-order equation based on equilibrium adsorption is expressed as:

$$\frac{1}{q_t} = \frac{1}{k_2 q_e^2} + \left(\frac{1}{q_t}\right)t$$ .....Equation 4.9

Where k_2 (g/mg h) is the rates constant of second-order adsorption. If second-order kinetics is applicable, the plot of *t/q* versus *t* should show a linear relationship. There is no need to know any parameter beforehand and q_e and K_2 can be determined from the slope and intercept of the plot. Also, this procedure is more likely to predict the behavior over the whole range of adsorption. The linear plots of *t/q* versus *t* show a good agreement between experimental and calculated *q*e values. The correlation coefficients for the second-order kinetic model are greater than 0.90 indicating the applicability of this kinetic equation and the second-order nature of the adsorption process of MB on activated carbon.

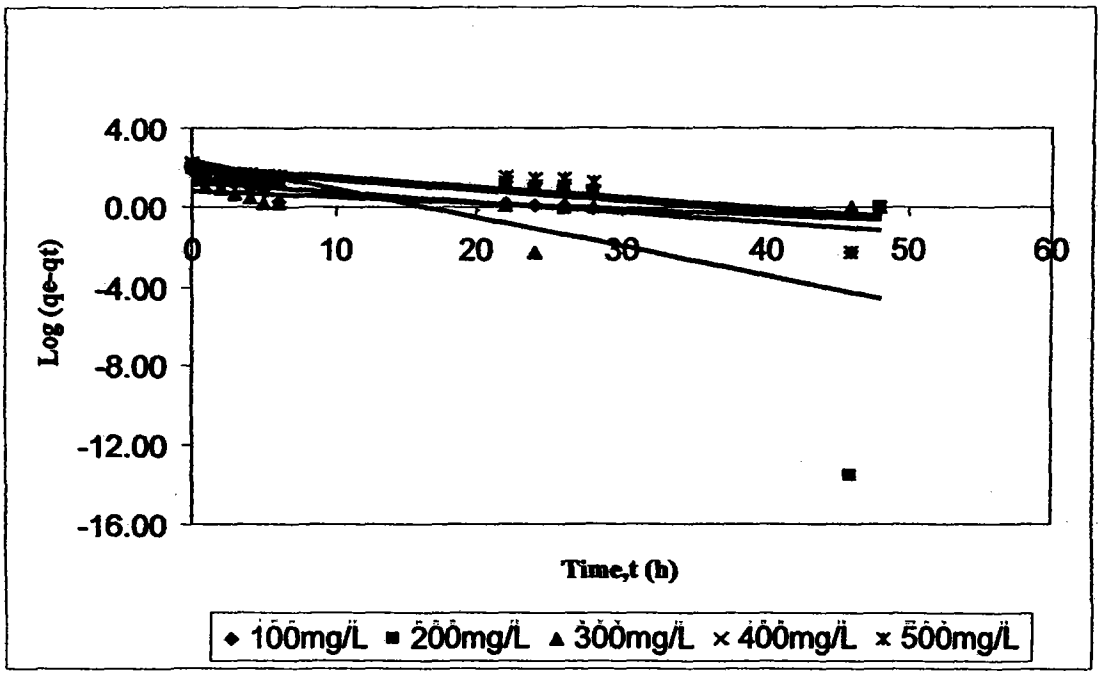

Figure 4.9: Pseudo first order, Log (qe-qt) versus Time, t (h) for phenol (760PH51.5)

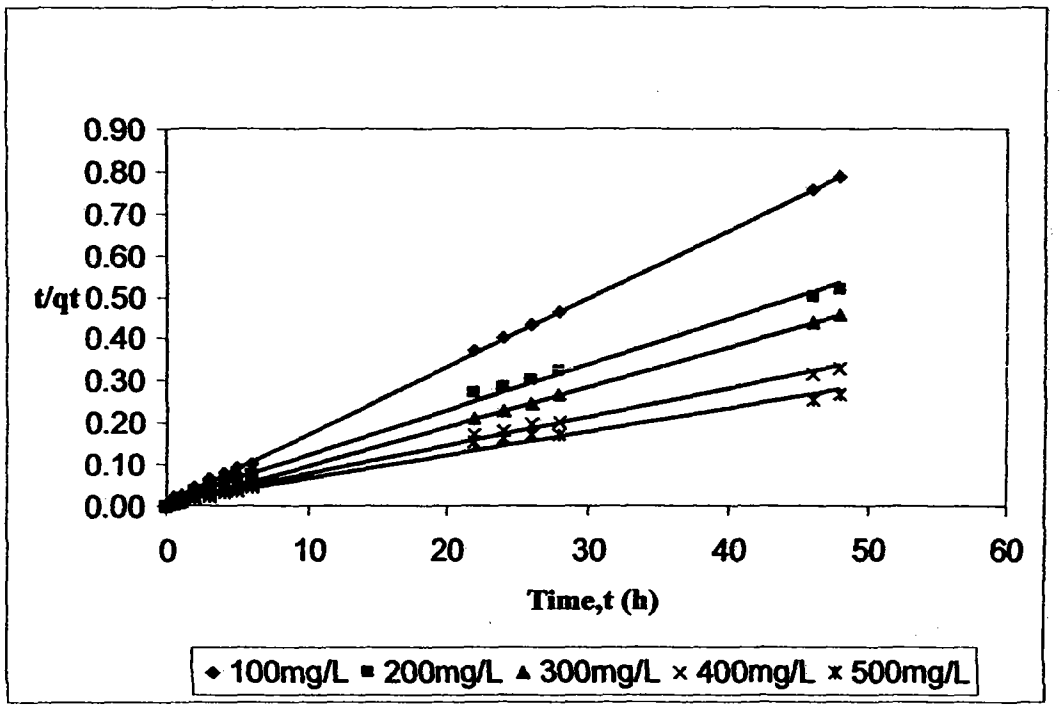

Figure 4.10: Pseudo second order, t/q_t versus time, t (h) for phenol (760PH51.5)

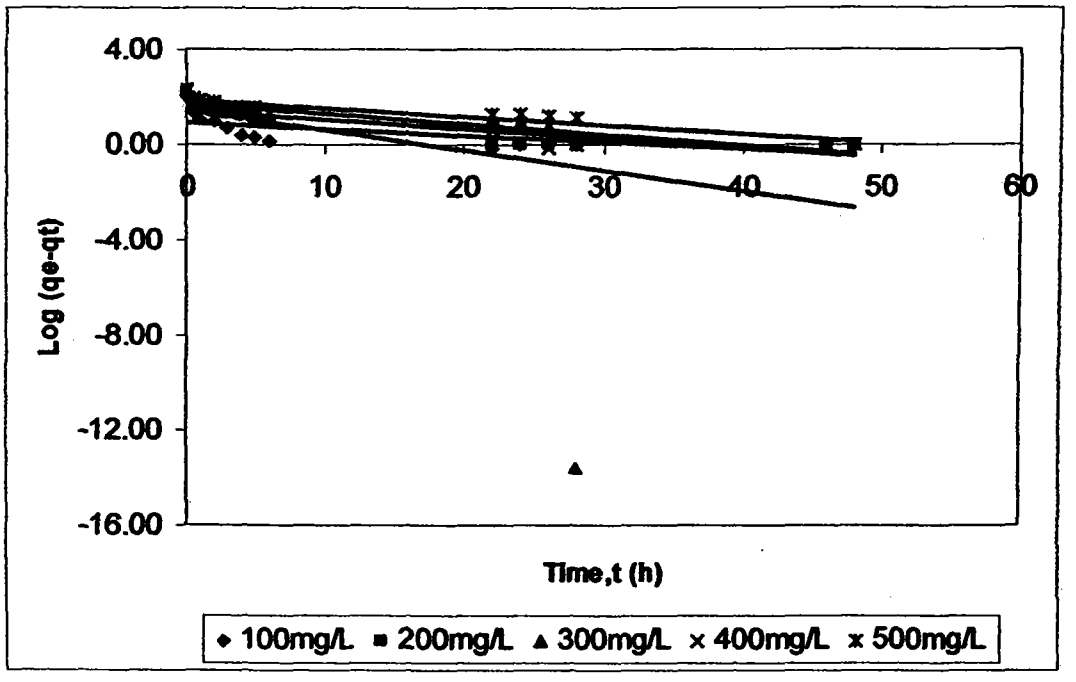

Figure 4.11: Pseudo first order, Log (qe-qt) versus Time, t (h) for methylene blue (760MB51.5)

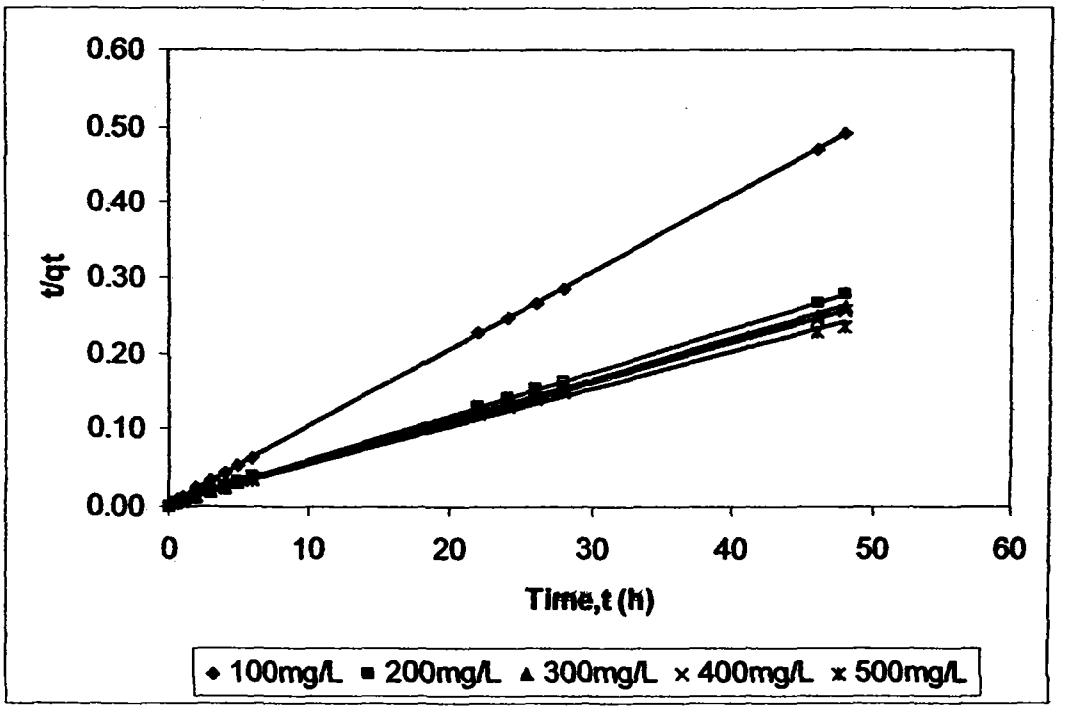

Figure 4.12: Pseudo second orders, t/q_t versus time, t (h) for methylene blue (760MB51.5)

4.4 Test of kinetics models

The value of R_2, the applicability of both kinetic models are verified through the sum of error squares (SSE, %). The adsorption kinetics of MB on AC was tested at different initial concentrations. The validity of each model was determined by the sum or error squares (SSE, %) given by:

$$SSE = \sqrt{\frac{\sum (qe,\exp - qe,cal)^2}{N}} \quad \text{.....Equation 4.10}$$

where N is the number of data points. The higher is the value of $R2$ and the lower is the value of SSEwith the best fit. Table 4.2 and table 4.3 lists the calculated results. It is found that the adsorption of methylene blue on AC can be best described by the second-order kinetic model. Similar phenomena processes have been observed in the adsorption of direct dyes on activated carbon prepared from saw dust and adsorption of Congo red dye on activated carbon from coir pith.

The adsorption kinetics for both phenols and methylene blue are suitably described by the pseudo-second order equation with R^2 almost equal to 1. This equation is based on the equilibrium chemical adsorption, which predicts the behavior over the whole range of studies, strongly supporting the validity, and agrees with chemisorption (chemical reaction) being rate-controlling. The reaction mechanism may mainly result from hydrogen binding between the hydroxyl groups of phenols and the functional groups, such as carboxylic, on the activated carbon surface.

Table 4.2: Sum or error square (SSE) for the adsorption of phenol (760PH51.5)

C0 (mg/L)	First order kinetic model		Second order kinetic model		SSE %	
	$q_{e,exp}$ (mg/g)	$q_{e,cal}$ (mg/g)	$q_{e,exp}$ (mg/g)	$q_{e,cal}$ (mg/g)	1st	2nd
100	61.04	20.21	61.04	61.73	11.33	0.19
200	92.04	216.87	92.04	92.59	34.62	0.15
300	105.23	6.04	105.23	105.26	27.51	0.01
400	146.19	81.28	146.19	147.06	18.00	0.24
500	180.08	123.71	180.08	175.44	15.63	1.29

Table 4.3: Sum or error square (SSE) for the adsorption of methylene blue (760PH51.5)

C0 (mg/L)	First order kinetic model		Second order kinetic model		SSE %	
	$q_{e,exp}$ (mg/g)	$q_{e,cal}$ (mg/g)	$q_{e,exp}$ (mg/g)	$q_{e,cal}$ (mg/g)	1st	2nd
100	97.04	3.92	97.04	101.01	25.83	1.10
200	169.06	62.20	169.06	153.85	29.64	4.22
300	183.19	66.40	183.19	156.25	32.39	7.47
400	187.11	35.88	187.11	147.06	41.94	11.11
500	202.28	32.28	202.28	149.25	47.15	14.71

Table 4.4: Result for adsorption performance of activated carbon using methylene blue and phenol based on pseudo first and second order. (KOH/char=5, Activation time 1.5hr)

Initial concentration (mg/l)	Methylene blue		Phenol	
	R^2		R^2	
	Pseudo fist order	Pseudo second order	Pseudo fist order	Pseudo second order
100	0.0983	0.9998	0.7179	0.9997
200	0.6904	0.9988	0.3781	0.9968
300	0.7268	0.9991	0.2817	1.0000
400	0.5200	0.9996	0.6932	0.9964
500	0.7896	0.9997	0.6352	0.9875